GPR40 EXPRESSION AND FUNCTION IN IMMUNE CELLS AND EXPERIMENTAL ARTHRITIS

Mrs Patricia Regina Soares de Souza

Submitted in partial fulfilment of the requirements of the Degree of Doctor of Philosophy

Centre for Biochemical Pharmacology
William Harvey Research Institute
Barts and the London School of Medicine and Dentistry
Queen Mary University of London
Charterhouse Square, London, EC1M 6BQ

I, Patricia Regina Soares de Souza, confirm that the research included within this thesis is my own.

I attest that I have exercised reasonable care to ensure that the work is original, and does not to the best of my knowledge break any UK law, infringe any third party's copyright or other intellectual Property Right, or contain any confidential material.

I accept that the College has the right to use plagiarism detection software to check the electronic version of the thesis.

I confirm that this thesis has not been previously submitted for the award of a degree by this or any other university.

Signed:

"The important thing is not to stop questioning.
Curiosity has its own reason for existing."

Albert Einstein

ABSTRACT

Omega-3 fatty acids (ω-3 FA, including eicosapentaenoic acid [EPA] and docosahexaenoic acid [DHA]), are essential polyunsaturated fatty acids which are correlated with lower incidence of chronic diseases. DHA and EPA can be enzymatically converted to resolvins, protectins and maresins, which play important roles in resolution of inflammation. Additionally, ω-3 FA can also directly activate surface receptors, namely the long-chain free fatty acid receptors GPR40 and GPR120, two GPCRs with poorly investigated biology.

Using real-time PCR analysis, GPR40 transcript in human neutrophils was detected; the protein expression was also confirmed by flow cytometry and image stream analysis. Expression of GPR40 protein was up-regulated after stimulation with platelet-activating factor (PAF, 10nM) or leukotriene B_4 (LTB_4, 10nM) for 10 minutes. I utilised the selective agonist GW9508 to investigate the biology of GPR40. Tested on human neutrophils, GW9508 elevated intracellular calcium when applied within the 0.1-10μM range. The up-regulation of GPR40 expression by pro-inflammatory stimuli suggested to us potential regulatory roles for this receptor during inflammation. I then showed that 1 and 10μM GW9508 increased neutrophil chemotaxis in response to the cytokine IL-8 (30ng/ml). In addition, GPR40 activation by GW9508 enhanced phagocytosis of *E. coli* by human neutrophils by approximately 50% when tested at 0.1 and 1μM. Moreover, GW9508-neutrophil stimulation augmented microvesicle release and delayed apoptosis after stimulation.

Finally, I demonstrated that GPR40 is expressed in inflammatory cells isolated from murine arthritic joints, such as neutrophils, macrophages and inflammatory monocytes. KBN-serum induced arthritic mice developed a more severe disease when treated prophylactically with GW9508 (10mg/kg, i.p. treated from day 0, daily), characterized by a higher clinical score and increased oedema when compared to

vehicle control mice. Therapeutic intervention with GW9508 at the peak of the disease (day 5) delayed the resolution of arthritis.

In summary, the data suggest that activation of GPR40 by GW9508 enhances neutrophil activation, up regulating the pro-inflammatory properties of this cell type, and therefore, exacerbating experimental inflammatory arthritis.

ACKNOWLEDGEMENTS

I gratefully acknowledge the opportunity, support and guidance of Prof Mauro Perretti. Without his thoughtful encouragement and careful supervision this thesis would never have taken shape. I am also grateful to my other supervisor Dr Lucy Norling for her continuous optimism, enthusiasm, encouragement and support.

My thanks also go out to the financial support provided by the program Science Without Borders of the Brazilian Government. To all staff members of the William Harvey Research Institute, especially for Martin Goss and Silvia Ayguade. I am thankful for the members of the Pathology Department, Flow Cytometry Department and Genome Center Departments. I would like to thank all members of the BSU in Chapterhouse Square and Whitechapel. I also would like to thank the midwives of The Royal London Hospital for kindly help us with the collections of umbilical cords. In addition, a big thanks to all the blood donors.

I also thank the examiners for accepting the invitation, their time spent analysing this thesis, and in advance, for the discussion and criticism that will be pointed during the Viva, I'm sure I'll learn a lot.

I am forever thankful to my colleagues at Biochemical Pharmacology Center for their friendship and support, and for creating a cordial and funny working environment, especially the old and new colleagues in the PhD Student's office Chiara, Hanna, Hazem, Hefin, Laura, Louise, Racheal, Sarah and Urszula. I thankfully acknowledge the contributions of Dr Dianne Cooper in several different situations. I would like to thank Dr Oliver Haworth for helping me with flow cytometry analysis. I would also like to thank Hefin Rhys with the help with Image Stream.

Finally, I extend my deepest thanks to my husband Simone for the cooked meals every night, his understanding in spending weekends at home, his patience and love. Thanks to my parents Valter and Aparecida for the support when their daughter decided to cross the ocean in search for another challenge. Thanks to my brother Adriano which inspired me as a scientist. And thank you to all my sisters Adriana, Ana Elisa and Debora for being always there. “Quando a saudade aperta, é a lembrança dos bons momentos juntos que me dá forças pra seguir em frente”.

TABLE OF CONTENTS

Abstract 4

Acknowledgements 6

Table of Contents 8

List of Figures 12

List of Tables 14

List of Abbreviations 15

CHAPTER 1: INTRODUCTION 21

1.1. The Inflammatory Response 22

1.1.1. General aspects of the inflammatory response 22

1.1.2. Mediators of inflammation 26

1.1.3. Major steps of the inflammatory response 30

1.2. Rheumatoid Arthritis 41

1.2.1. Introduction 41

1.2.2. Aetiology of RA 42

1.2.3. Pathogenesis of RA 43

1.2.4. Experimental models of Arthritis 45

1.3. Free Fatty Acid Receptors and Immune System 50

1.3.1. Introduction 50

1.3.2. Overview of FFAs and FFARs 50

1.3.3. A family of GPCRs for Free Fatty Acids 52

1.3.4. Fatty acids in Rheumatoid Arthritis 56

1.4. Scope of the thesis 58

1.4.1. Hypothesis 58

CHAPTER 2: MATERIAL AND METHODS 60

Materials 61

2.1. Cell Culture 61

2.2. Flow Cytometry 61
2.3. Molecular biology reagents 63
2.4. Other reagents and materials 63
2.5. Software and equipment 64
Methods 65
2.6. Isolation and culture of primary human umbilical vein endothelial cells (HUVEC) 65
2.7. Human blood leukocyte isolation 66
2.8. Collection of Exudated Human PMN 69
2.9. *In vitro* culture of chondrocytes 70
2.10. Modulation of GPR40 expression in neutrophils and macrophages 71
2.11. Gene expression analyses 72
2.12. Flow cytometry analysis 77
2.13. Imaging flow cytometry 81
2.14. Intracellular Calcium measurement 83
2.15. PMN chemotaxis assay 83
2.16. Flow chamber assay 85
2.17. Phagocytosis Assay 87
2.18. Measurement of apoptosis in neutrophils 87
2.19. Mice 91
2.20. K/BxN Serum Transfer Arthritis 91
2.21. Isolation of cells of the paws for flow cytometry analysis 93
2.22. GPR40 expression in cells from arthritic joints 93
2.23. Gene expression in cells isolated from arthritic joints 94
2.24. Histological staining and analysis 95
2.25. Statistical analyses 99
CHAPTER 3: RESULTS 100
Expression and Modulation of GPR40 101

3.1. Genomic expression of GPR40 101

3.2. Expression of GPR40 in human neutrophils 102

3.3. Expression of GPR40 in macrophages 109

Functionalities of GPR40 in Human Leukocytes 112

3.4. GPR40-induced intracellular calcium mobilization in neutrophils 112

3.5. Modulation of PMN adhesion molecules by GW9508 113

3.6. Effect of GW9508 on neutrophil-endothelial interactions under flow 115

3.7. Effect of GW9508 on neutrophil chemotaxis 117

3.8. Effects of GPR40 agonist GW9508 on phagocytosis of *E. coli* 118

3.9. Release of microvesicles induced by GW9508 in neutrophils 120

3.10. Effects of GW9508 induction on neutrophil apoptosis. 122

3.11. M1/M2 polarization of macrophages by GW9508 125

3.12. Effects of GW9508 stimulation in efferocytosis 126

Roles of GPR40 *In Vivo* 130

3.13. Expression of GPR40 in cells from murine arthritic joints 130

3.14. Effects of GW9508 in the initiation and progression of inflammatory arthritis 132

3.15. Effects of GW9508 treatment during the resolution phase of inflammatory arthritis 140

CHAPTER 4: DISCUSSION OF RESULTS 142

CHAPTER 5: CONCLUSION AND FUTURE PLAN 154

CHAPTER 6: REFERENCES 158

CHAPTER 7: ATTACHMENTS 173

Attachments 174

7.1. Implications for eicosapentaenoic acid- and docosahexaenoic acid-derived resolvins as therapeutics for arthritis 175

7.2. Neutrophil-derived microvesicles enter cartilage and protect the joint in inflammatory arthritis 184

7.3. Galectin-3-null mice display defective neutrophil clearance during acute inflammation 197

LIST OF FIGURES

Figure 1: Examples of common components of the inflammatory response. 23

Figure 2: Time-course of the inflammatory response. 26

Figure 3: Generalized pathway for the conversion of AA and EPA to eicosanoids. 29

Figure 4: Leukocyte recruitment cascade..... 31

Figure 5: Types of fatty acids. 51

Figure 6: Human blood leukocyte isolation..... 67

Figure 7: Illustration of grid counting in a Neubauer haemocytometer. 68

Figure 8: Phases of RNA extraction by TRIzol. 74

Figure 9: Chemotaxis assay. 84

Figure 10: Flow Chamber Assay. 86

Figure 11: Cytospin of neutrophils following overnight culture. 88

Figure 12: Measurement of apoptotic neutrophils by Annexin V staining. 89

Figure 13: Arthritis scoring procedure. 92

Figure 14: Split channels for cartilage damage evaluation by Image J. 97

Figure 15: Cartilage selection area for quantification in Image J as indicated by yellow line. 98

Figure 16: Expression of GPR40 mRNA in different cell types. 102

Figure 17: Expression of GPR40 in human neutrophils. 103

Figure 18: Modulation of GPR40 mRNA expression in neutrophils. 105

Figure 19: Modulation of GPR40 protein levels expression in human neutrophils. 106

Figure 20: Expression of GPR40 in exudate neutrophils. 108

Figure 21: GPR40 expression in macrophages. 109

Figure 22: Modulation of mRNA GPR40 expression in human macrophages. 111

Figure 23: Intracellular mobilization of calcium by GW9508 in human neutrophils. 112

Figure 24: Modulation of adhesion molecules by GW9508 in neutrophils. 114

Figure 25: Effects of GW9508 on neutrophils-endothelial interactions under flow. 116

Figure 26: Effect of GW9508 on neutrophil-endothelial interactions after LTB_4 stimulation under flow. 117

Figure 27: Effect of GW9508 treatment on the chemotaxis of neutrophils. 118

Figure 28: Enhanced E. coli phagocytosis by GW9508 in human neutrophils. 119

Figure 29: No effect of GW9508 on E. coli phagocytosis by human monocyte derived-macrophages. 120

Figure 30: Neutrophil-microvesicle release induced by GW9508. 121

Figure 31: GW9508 stimulation delays apoptosis of human neutrophils. 123

Figure 32: Measurement of neutrophil apoptosis by flow cytometry. 124

Figure 33: GW9508 does not affect M1/M2 polarization of human macrophages. 126

Figure 34: GW9508 impairs efferocytosis of neutrophils. 128

Figure 35: GW9508 do not modulate efferocytosis in stimulated mouse macrophages. 129

Figure 36: Expression of GPR40 in cells isolated from murine arthritic joints. 131

Figure 37: Characterization of arthritis severity following prophylactic treatment with GW9508..... 133

Figure 38: Expression of inflammatory mediators in murine arthritic joints. 135

Figure 39: Leukocyte infiltration in GW9508-treated arthritic mice. 138

Figure 40: GW9508 treatment does not affect cartilage degradation in arthritic mice. 140

Figure 41: Therapeutic administration of GW9508 at the peak of inflammatory arthritis delays resolution. 141

Figure 42: GW9508 induces a pro-inflammatory profile in neutrophils and increases severity of inflammatory arthritis. 157

LIST OF TABLES

Table 1: Main characteristics of some models of arthritis 48

Table 2: Antibody list 62

Table 3: Quantitec™ Primers used for analysis of mRNA expression 63

LIST OF ABBREVIATIONS

°C – Degree Celsius

AA – Arachidonic acid

ALA - α-linolenic acid

$AnxA_1$– Annexin A1

ATP – Adenosine triphosphate

Bak – Bcl-2 homologous antagonist/killer

Bax – Bcl-2-associated X protein

Bcl-2–B-cell lymphoma 2

BH-3 – Bcl-2 homology-3

Bid – BH-3-interacting domain death agonist

BMDMs – Bone-marrow-derived macrophages

BODIPY – Boron-dipyrromethene

BSA – Bovine albumin serum

C28/I2 – Immortalized chondrocyte cell line

C57Bl/6 – C57 black 6 mice

C5a – Complement factor 5a

cAMP – Cyclic adenosine monophosphate

CCL17 – Chemokine (C-C Motif) Ligand 17

CCL5 – Chemokine (C-C Motif) Ligand 5

CD – cluster of differentiation

CGRP – Calcitonin-related gene product

CIA – Collagen-induced arthritis

cm2 – square centimetre

COXs – Cyclooxygenases

CT – cycle threshold

CXCL10 – C-X-C motif chemokine 10

CXCL-8 – C-X-C motif chemokine 8

DHA – Docosahexaenoic acid

DHEA – Docosahexaenoyl ethanolamide

DMARDs – Disease-modifying anti-rheumatic drugs

DMEM – Dulbecco's Modified Eagle Medium

DMEM/F12 – DMEM/Nutrient Mixture F-12

DNA – Deoxyribonucleic acid

DNAse – Deoxyribonuclease

dNTP – Deoxyribonucleiotide triphosphate

DPBS – Dulbecco’s phosphate buffered saline

dT – Deoxythymine

DTT – Dithiothereitol

E. coli – *Escheria coli*

EDTA – Ethylenediaminetetraacetic acid

EPA – Eicosapentaenoic acid

ERK – Signal-regulated kinase

F4/80 – also known as EGF-like module-containing mucin-like hormone receptor-like 1

FABPs – Fatty acid binding proteins

FBS – Foetal bovine serum

FFARs – Free fatty acid receptors

FFAs – Free fatty acids

FSC – Forward Scatter

g – grams

g – gravitational acceleration

GAPDH – Glyceraldehyde 3-phosphate dehydrogenase

GCs – Glucocorticoids

GM-CSF – Granulocyte macrophage colony stimulating factor

GPCR – G-protein-coupled receptor

GW9508 – Selective G protein-coupled receptor 40 agonist

H&E – Haematoxylin and eosin

HBSS – Hank's Balanced Salt Solution

HEK293 – Human embryonic kidney 293 cells

HFD – High fat diet

HLA-DR –

hrTNF-α – Human recombinant tumour necrosis factor-α

HUVEC – Human umbilical vein endothelial cell

ICAM-1 – Intercellular adhesion molecule 1

IFNGRs – Interferon-γ receptors

IFN-γ – Interferon-γ

IL – Interleukin

ip – Intraperitoneal

IRF – Interferon regulatory factors

IRF – Interferon regulatory factors

Iso – Isotype control

ITS – Insulin transferrin selenium

JAK – Janus kinase

JAMS – Junctional adhesion molecules

LOs – Lipoxygenases

LPS – Lipopolysaccharides

LTB4 – Leukotriene B4

LXA_4 – Lipoxin A_4

Ly6C – Lymphocyte antigen 6 complex, locus C

Ly6G – Lymphocyte antigen 6 complex, locus G

M1 – Macrophages phenotype 1, pro-inflammatory

M199 – Medium 199 with Earle's Salts with L-glutamine

M2 – Macrophages phenotype 2, pro-resolution

mAb – monoclonal antibody

MaR1 – Maresin 1

Mcl-1 – Protein myeloid cell leukemia-1

MCP-1 – Monocyte chemoattractant protein-1

MCs – Melacortinocortins

M-CSF – Macrophage colony-stimulating factor

mg – Milligram

MHC-II – Major histocompatibility complex type II

ml – millilitres

MMPs – Matrix metalloproteinases

MRC1 – Mannose receptor

mRNA – Messenger RNA

MSH – α-Melanocyte-stimulating hormone

MUC1 – Mucin 1

MV – Microvesicle(s)

MW – Mouth wash

NO – Nitric oxide

NOS2 – Nitric oxide synthase 2

NSAID – Non-steroidal anti-inflammatory drugs

PAF – Platelet-activating factor

PBMC – Peripheral blood mononuclear cells

PBS – Phosphate buffered saline

PCR – Polymerase chain reaction

PD1 – Protectin D1

PECAM-1 – Platelet endothelial cell adhesion molecule 1

PFA – Paraformaldehyde

PG – Prostaglandins

PGE_2 – Prostaglandine E_2

pH – "power of hydrogen", numeric scale for the acidity or alkalinity

PI – Propidium Iodide

PI3K – Phosphoinositide-3 kinase

PICD – Phagocytosis-induced cell death

PLC – Phospholipase C

PMN – Polymorphonuclear cells

PMT – Photomultiplier tubes

PPARs – Peroxisome proliferator activated receptors

PS – Phosphatidylserine

PSGL-1 – P-selectin glycoprotein ligand-1

PTPR – Protein tyrosine phosphatase receptors

PUFAs – Polyunsaturated fatty acids

qPCR – Quantitative PCR, real-time PCR

RA – Rheumatoid arthritis

Rac1 – Ras-related C3 botulinum toxin substrate

RASF – Rheumatoid arthritis synovial fibroblasts

RPL13a – Ribosomal Protein L13a

RPMI – Roswell Park Memorial Institute medium 1640

ROS – Reactive oxygen species

Rvs – Resolvins

SEM – Standard error of the mean

SFM – Macrophage serum-free medium

SOCS1 – Suppressor of cytokine signalling 1

SSC – Side scatter

STAT1 – Signal transducers and activators of transcription 1

TAK1 – TGF-β-activated kinase 1

TGF-β – Transforming growth factor *beta*

TGM2 – Transglutaminase 2

THP-1 – Human monocytic cell line

TLR – Toll like receptor

TNF – Tumour necrosis factor

$TRPV_1$ – Transient Receptor Potential Cation Channel subfamily V member 1

U – units

ul – unlabelled

VAV - vav guanine nucleotide exchange factor

VCAM – Vascular cell adhesion molecule 1

VLA-4 – Very late antigen-4

µM – Micrometer

CHAPTER 1: INTRODUCTION

1.1. THE INFLAMMATORY RESPONSE

1.1.1. General aspects of the inflammatory response

Inflammation is a fundamental process that has been essential to humans since our origins. The cardinal signs of inflammation – rubor (redness), calor (heat), tumor (swelling) and dolor (pain) – were described in the 1st century AD by the Roman medical writer Aulus Cornelius Celsus. In addition, the fifth cardinal sign, loss of function, was described in the 19th century. Ever since, our knowledge of the inflammatory response has increased, but even after almost 20 centuries, we still do not have a full understanding of the multitude of molecular and cellular events that characterise this life-saving response of the host.

In the simplest definition, inflammation is an adaptive response that can be triggered by a variety of noxious stimuli, including infection and injury, that aims to restore homeostasis of the affected structures, and therefore has a crucial role in the physiology of mammalian organisms (Medzhitov, 2008). Inflammatory responses are highly heterogeneous in terms of cell types and molecular mediators involved. Inflammation also comes in different modalities that can be classified as acute versus chronic and local versus systemic. Despite this complexity, all inflammatory responses can be broken down into four common components that align in a universal configuration of the inflammatory pathway: inflammatory inducers, sensors, mediators, and effectors (Figure 1) (Medzhitov, 2010).

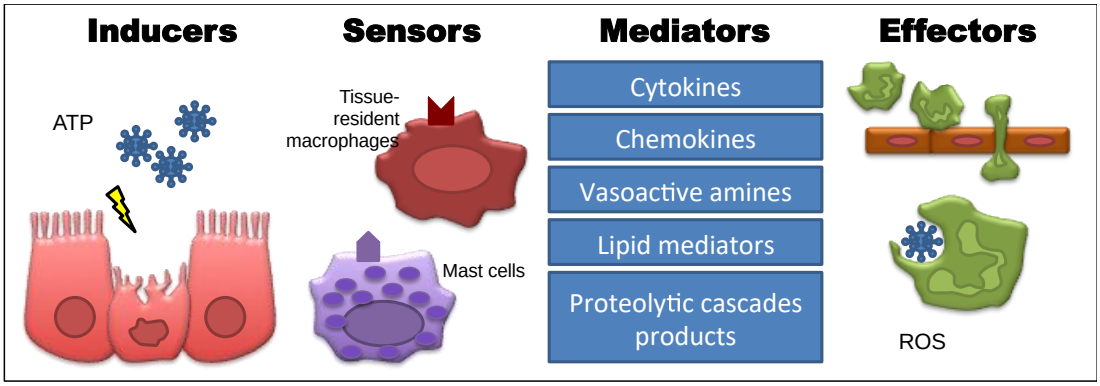

Figure 1: Examples of common components of the inflammatory response. The inflammatory response consists of inductors, sensors, mediators and effectors. Inducers initiate the response and are detected by the sensors. The sensors (receptors like Toll-like receptors) are expressed in specialized sentinel cells as tissue-resident macrophages, dendritic cells and mast cells. They induce the production of mediators, including cytokines, chemokines, vasoactive amines, lipid mediators and products of proteolytic cascades. These inflammatory mediators act on various target tissues to elicit changes in their functional states, favoring the migration of leukocytes from the blood to produce effector molecules (such as reactive radicals and proteases), thus facilitating the adaptation to deleterious condition in accordance with the inducer (tissue injury or infection) that elicited the inflammatory response (Medzhitov, 2010).

Inflammatory inducers can be exogenous signals (e.g. pathogens and toxins) or endogenous signals (e.g. ATP and urate crystals) that report on tissue stress, injury, or malfunction. Sensor cells, such as tissue-resident macrophages, dendritic cells and mast cells, detect inducers with specific receptors and respond by producing inflammatory mediators. Depending on the nature of the inducers, sensor cells produce different combinations and amounts of mediators (including cytokines, chemokines, vasoactive amines, lipid mediators and proteolytic cascades products), creating unique mediator signatures. Inflammatory mediators, in turn, act on target tissues triggering changes in the functional state thereof, favouring the migration of leukocytes from the blood and production of effector molecules (such as reactive radicals and proteases) (Okin and Medzhitov, 2012).

The development of an appropriate inflammatory response is essential for the host. Indeed, the activation and recruitment of leukocytes are required for the processing and presentation of antigens by leukocytes, and effector function of any immune response (Teixeira et al., 2001). However, inflammatory processes have the potential to cause damage to host tissues. Indeed, the effector molecules produced in this process do not discriminate if their targets are pathogens or structures of the

host, so the tissue damage is a potential side effect associated with any inflammatory response (Nathan, 2006, Medzhitov, 2008, Wink et al., 2011). Thus, this adaptive response is beneficial only if retained for a short duration. Indeed, chronic responses may lead to significant physiological changes. There is a wide list of human diseases associated with an inappropriate or uncontrolled inflammatory response that are triggered by known or unknown stimuli origin, this include rheumatoid arthritis, asthma, multiple sclerosis, chronic obstructive pulmonary disease and atherosclerosis (Libby, 2002, Weiner and Selkoe, 2002, Vilcek and Feldmann, 2004). Under these conditions, it is clear that tissue inflammation is deleterious. Therefore, an adequate control of inflammation is of fundamental importance for the restoration of the physiological conditions of the organism.

For years, it was believed that termination of acute inflammation was due to passive dilution of pro-inflammatory signals and effectors (Levy, 2010), in a process as simple as turning off the lights. Nowadays it is known that the resolution of inflammation is a tightly orchestrated and multifaceted host response. Indeed, the key steps in resolution of inflammation include 1) clearance of the inciting stimuli; 2) decrease of neutrophil and increase of monocyte recruitment; 3) apoptosis of recruited inflammatory cells; 4) efferocytosis of apoptotic cells by tissue and monocyte-derived macrophages; 5) switching from pro-inflammatory cell phenotypes and mediators to pro-resolution cell phenotypes and mediators; 6) either incorporation of myeloid cells into the local population or their recirculation via lymph or blood (Alessandri et al., 2013, Norling and Perretti, 2013, Buckley et al., 2014). Therefore, for resolution to occur an active and coordinated series of events must take place, likely involving multiple proresolving mediators and cellular processes.

Further, the understanding of the process of the resolution of inflammation gives hope for the treatment of a wide list of human diseases that are associated with chronic inflammatory responses. Diseases that are traditionally treated with anti-inflammatory therapies focus on strategies to decrease or neutralize the level of pro-

inflammatory mediators and/or inhibit the recruitment of leukocytes and their activation. Therapies including non-steroidal anti-inflammatory drugs (NSAID), glucocorticoids (GC) receptors agonists (synthetic GCs) and antibodies or inhibitors targeting specific pro-inflammatory cytokines, such as TNF-α and IL-1, have proven beneficial and have revolutionised the treatment of various diseases, yet a number of patients fail to respond to these therapies, or are subjected to side effects (Alessandri et al., 2013). For example, steroids can cause osteoporosis and impair wound healing, whereas novel selective inducible cyclooxygenase (COX)-2 inhibitors might reduce protective vascular prostacyclin synthesis, leading to an increase risk of thrombosis. Indeed, experience with TNF-α-neutralizing therapy has also revealed several complications (Lee, 2012). Therefore, pro-resolution-based strategies emerge as a new potential solution for the treatment of multiple inflammatory conditions.

Taking in mind the overview of the inflammatory response described above, a simplistic way of demonstrating the course of inflammation is shown in Figure 2. With inducers stimulating the initiation of acute inflammation, over time the inflammatory response reaches its peak, and after resolution steps have taken place, homeostasis is restored (blue line). However, when there is an exacerbated inflammatory response and a defective resolution, the inflammatory response persists, which could result in a range of chronic diseases (red line). In contrast, intervention with external pro-resolution mediators or drugs depicted on their structure or mimicking their biology could restore the balance of the inflammatory response (blue dashed line).

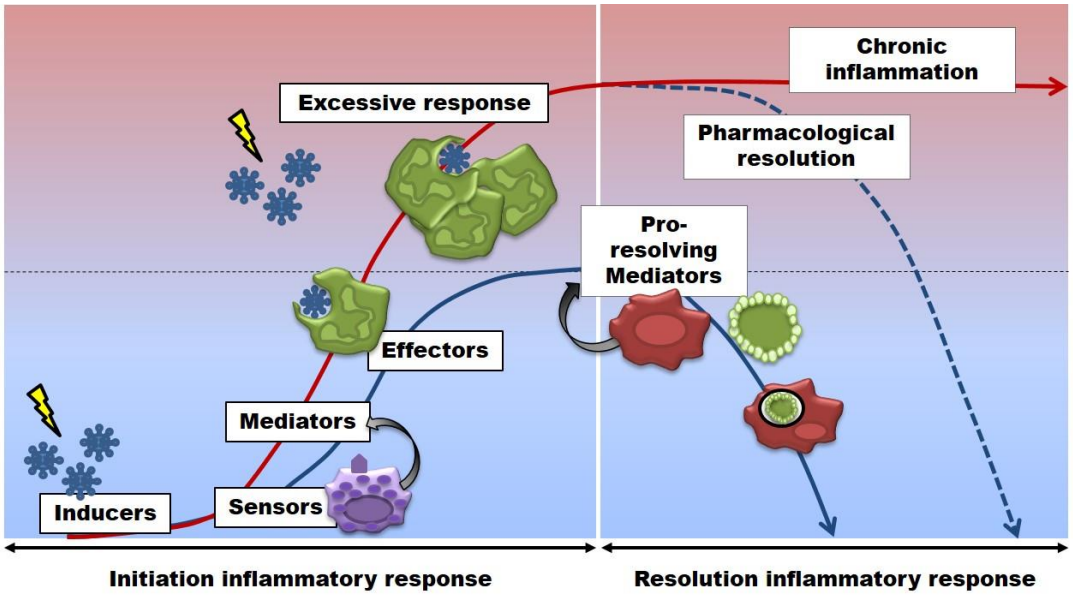

Figure 2: Time-course of the inflammatory response.
The inductors are detected by sensor cells, inducing the release of a number of different pro-inflammatory mediators, initiating the inflammatory response. Once effector cells are able to control or clear the inducers, cells with a pro-resolving profile start to produce mediators that control the inflammatory response. In a well-orchestrated response, the inflammatory process has its end (blue line). An excess of the initial inflammatory response results, in most cases, in a host's inability to control inflammation, leading to a chronic state (red line). However, the use of therapies that promote resolution of inflammation are believed to be a new intervention strategy capable of restoring tissue homeostasis (blue dashed line) Adapted from Perretti et al. (2015).

1.1.2. Mediators of inflammation

Mediators are substances released from injured or activated cells that co-ordinate the development of the inflammatory response. The Brazilian pharmacologist Rocha e Silva, 1978, defined that a chemical mediator should (i) be found in tissues in concentrations that can explain the observed symptoms or effects, (ii) be released by endogenous triggers which produces the response, (iii) have the same action in all species where the phenomenon occurs, (iv) be destroyed locally or systemically to avoid undue accumulation, and (v) be blocked (directly or indirectly) by inhibitors of inflammation (Rocha e Silva, 1978). Nowadays, inflammatory mediators are classified into several groups according to their biochemical properties, such as vasoactive amines, vasoactive peptides, fragments of complement components, lipid mediators, cytokines, chemokines and proteolytic enzymes.

Vasoactive amines (histamine and serotonin) are produced mainly by mast cells and platelets and are release after degranulation. They can cause an increase in vascular permeability and vasodilation, or vasoconstriction, depending on the context. Vasoactive peptides can also cause vasodilation and increased vascular permeability, however, they are usually stored in an active form in secretory vesicles or are generated by proteolytic processes of inactive precursors in the extracellular fluid. Another class of mediators, complement components, like C3a, C4a and C5a, are produced by several pathways of complement activation. They can promote granulocyte and monocyte recruitment, induce mast-cell degranulation and cell-killing membrane attack complex activation. Lipid mediators are derived from phospholipids, such as phosphatidylcholine, that are present in the inner leaflet of cellular membranes. They activate several processes that occur during the inflammatory response, including recruitment of leukocytes, vasodilation and vasoconstriction, increased vascular permeability and platelet activation. Recently, lipid mediators were also shown to be involved in the resolution phase of the inflammatory response (Serhan, 2014). Inflammatory cytokines are produced by many cell types, most importantly by macrophages and mast cells. They have several roles in the inflammatory response, including activation of the endothelium and leukocytes and induction of the acute-phase response. Chemokines are produced by many cell types in response to inducers of inflammation. They control leukocyte extravasation and chemotaxis towards the affected tissue. Finally, proteolytic enzymes are involved in many processes, including host defence, tissue remodelling and leukocyte migration (reviewed on (Medzhitov, 2008)).

As Rocha e Silva said, “it would be very unfortunate if any of the above mentioned mediators might constitute the final answer to the problem, because that would mean to shut our laboratories, or do something else!”. Indeed, although much is known about pro-inflammatory mediators, little is known about pro-resolving

mediators, and identification of new mediators (Serhan, 2014) shows us that much remains to be discovered.

1.1.2.1. Inflammatory mediators generated from polyunsaturated fatty acids

One of the most important classes of lipid mediators, eicosanoids (from the Greek *eicosa* = twenty; for twenty carbon fatty acid derivatives), was discovered after the observation that exclusion of fat from the diet were prejudicial in rats. Eicosanoids are generated from 20-carbon polyunsaturated fatty acids (PUFAs), and because inflammatory cells typically contain a high proportion of the omega-6 PUFA arachidonic acid (AA) and low proportions of other 20-carbon PUFAs, AA is usually the major substrate for eicosanoid synthesis. Eicosanoids, which include 2-series prostaglandins (PG), thromboxanes, 4-series leukotrienes (LTs), and other oxidized derivatives, are generated from AA (Calder, 2006) (Figure 3).

Eicosanoids are a large group of lipid mediators involved in modulating intensity and duration of the inflammatory response. They are produced from different cell sources upon application of several stimuli. Prostaglandins are formed by most cells in our bodies and act as autocrine and paracrine lipid mediators; they are synthesised de novo from membrane-released AA which is produced upon cell activation, with the second step involving COXs isozymes. It is important to mention that prostaglandin generation can be inhibited by NSAIDs, as discovered by John Vane and colleagues in 1971 (Vane, 1971). In contrast, leukotrienes are made predominantly by inflammatory cells like polymorphonuclear leukocytes, macrophages, and mast cells after stimulation by an inducer of the inflammatory response. In the case of leukotriene generation, one of the most important enzyme involved is 5-lipoxygenase (5-LO).

Functionally, eicosanoids frequently have opposing effects. Thus, the overall physiologic (or pathophysiologic) outcome will depend on the cells (plus hence enzymes) present, the nature of the stimulus, the timing of eicosanoid generation, the

concentrations of different eicosanoids generated, and the sensitivity of the target cells and tissues to the eicosanoid generated. For example, leukotrienes increase vascular permeability, enhance local blood flow, are chemotactic agents for leukocytes, induce release of lysosomal enzymes and ROS by granulocytes, and increase production of tumour necrosis factor (TNF)-α, interleukin (IL)-1β and IL-6 (Hammarstrom, 1983). Prostaglandins, such as PGE_2, are known to induce fever, increase vascular permeability and vasodilatation, cause pain, and increase production of IL-6 (Evans et al., 2015). Eicosanoids are also generated from PUFAs, such as EPA leading to the formation of 3-series PGs and 5-series LTs, for instance PGE_3 and LTB_5. The same enzymes are involved in the generation of eicosanoids from AA or EPA, resulting in a competition of the substrate. However, revealing the complexity and specificity of the inflammatory reaction, these autocrine mediators may exert anti-inflammatory effects, as shown by the effects of PGE_3 in inhibiting production of TNF and IL-1 (Miles et al., 2002) (Figure 3).

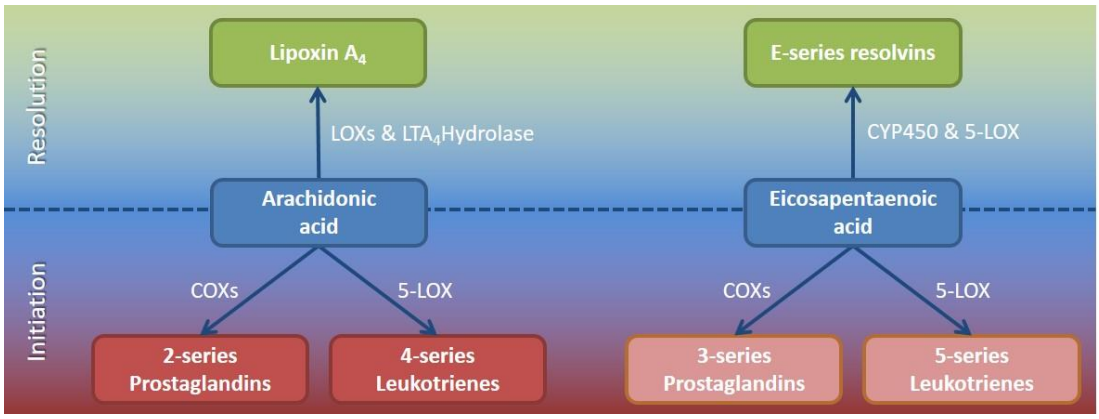

Figure 3: Generalized pathway for the conversion of AA and EPA to eicosanoids.
COX, cyclooxygenase; CYP450 cytochrome P450 enzymes, LOX, lipoxygenase. Adapted from Norling and Perretti (2013).

In addition to the production of mediators involved in the initialization of the inflammatory response, omega-3 and omega-6 PUFAs can also generate mediators involved in the resolution phase of inflammation. Firstly, it is important to define that pro-resolution mediators are not equivalent to anti-inflammatory mediators, which act

as a blocker of specific pathways or enzymes involved in the initiation of an anti-inflammatory response. Indeed, a pro-resolution mediator stimulates and activates endogenous pathways to regulate cellular trafficking, modulate myeloid cell lifespan and phenotype, and enhance tissue restoration to accelerate resolution (Norling and Perretti, 2013). These pro-resolving mediators include canonical mediators such as cortisol and adenosine as well as more recently identified lipid, protein and peptide agonists such as the lipoxins (LXs), resolvins (Rvs), annexin A_1 ($AnxA_1$) and melanocortins (MCs), amongst several others.

Even simplistically, the generalised description of the roles of lipid mediators shows the importance of fatty acids in the inflammatory response.

1.1.3. Major steps of the inflammatory response

The main and most immediate effect of the mediators produced by sensor cells is to elicit an inflammatory exudate locally: plasma proteins and leukocytes that are normally restricted to the blood vessels now gain access, through the postcapillary venules, to the extravascular tissues at the site of infection or injury.

1.1.3.1. The leukocyte recruitment cascade to the site of inflammation

The recruitment of leukocytes to the site of inflammation is a tightly regulated process characterized by the following stages: capture of leukocytes by the activated endothelium, rolling of leukocytes on the endothelium, activation of leukocytes by chemokines and other mediators, firm adhesion of leukocytes to the endothelium, crawling and transendothelial migration or diapedesis (Figure 4). There are several families of molecular regulators involved in the control of this process, which includes the selectins (glycoprotein adhesion molecules), integrins, chemokines, and additional junctional adhesion molecules (Ley et al., 2007, Chavakis et al., 2009).

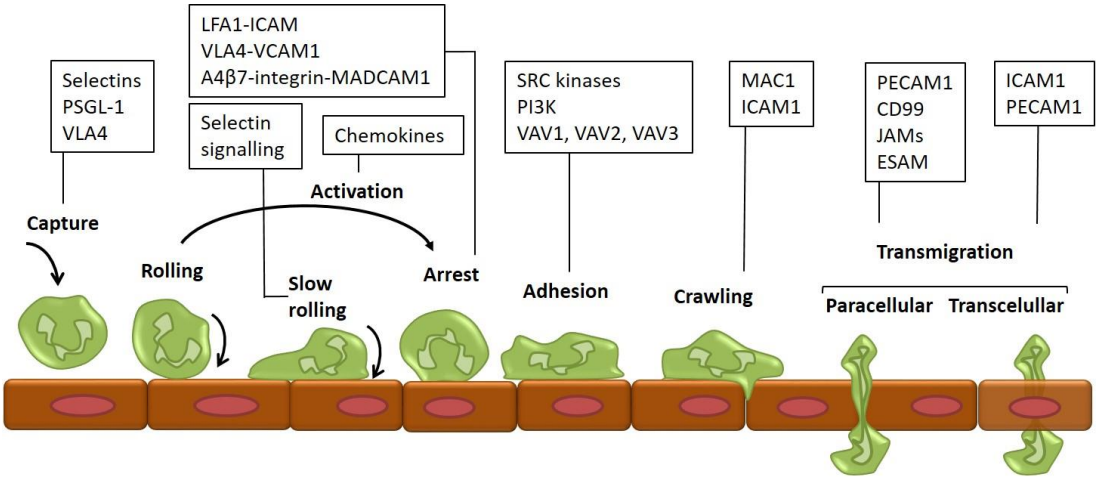

Figure 4: Leukocyte recruitment cascade.
All known steps for leukocytes recruitment are shown, including capture, which is mediated by selectins; activation which is mediated by chemokines; and adhesion which is mediated by integrins. Key molecules involved in each step are shown in boxes. ESAM: endothelial cell selective adhesion molecule; ICAM1: intracellular adhesion molecule 1; JAM: junctional adhesion molecule; LFA1: lymphocyte function-associated antigen 1 (also known as L 2 integrin); MAC1: macrophage 1 antigen; MADCAM1: Mucosal vascular addressin cell adhesion molecule-1; PSGL1: P-Selectin glycoprotein ligand 1; PECAM1: Platelet endothelial cell adhesion molecule-1; PI3K: phosphoinositol 3 kinase; VCAM1: vascular cell adhesion molecule 1; VLA4: very late antigen 4; VAV: vav guanine nucleotide exchange factor. Modified from Ley et al. (2007).

During the inflammatory response, selectins present on the surface of leukocytes interact with their respective receptors on endothelial cells in a transient and reversible interaction, promoting the first step of leukocyte recruitment, known as capture. Neutrophils (the first cells to arrive to the site of the infection) express L-selectin, while endothelial cells express P- and E-selectin (Bevilacqua, 1993). P-selectin is also expressed by activated platelets. A common ligand for all 3 selectins is P-selectin glycoprotein ligand-1 (PSGL-1). Although PSGL-1 is expressed in almost all leukocytes, it is only functional when properly glycosylated. The captured leukocytes then start to roll on the surface of the endothelial cells, which permits them to sense chemoattractant factors, including complement factor 5a (C5a), IL-8 (CXCL8), PAF, eotaxin/CCL11 and LTB_4, which reside on the luminal surface of the endothelium. The activation of relevant chemoattractant receptors on the rolling leukocytes provokes an increase in affinity (conformational changes) of integrins, promoting the arrest of leukocytes. This firm adhesion of leukocytes to endothelial cells is mediated by the interaction between integrins as VLA-4 (a4b1), α4β7 integrin,

Mac-1 (αMβ2) and LFA-1 (αLβ2) and their endothelial receptors of the superfamily of immunoglobulins, such as intercellular adhesion molecule (ICAM) and vascular cell adhesion molecule 1 (VCAM-1). While VCAM-1 interacts with VLA-4, β2 integrins (including LFA-1 and Mac-1) bind to ICAM1-5. ICAM-1 and ICAM-2 are extensively studied as binds to β2 integrin ligands on the endothelium. Other integrins includes ICAM-3, ICAM-4 and ICAM-5 that are expressed in white blood cells, red blood cells and brain neurons, respectively (Ley et al., 2007, Chavakis et al., 2009)

Following firm adherence, leukocytes move slowly on the surface of endothelial cells using their Mac-1 and LFA-1 integrin, in a process called crawling, to find an appropriate area for transmigration. The endothelial transmigration (also designated diapedesis) can happen on intercellular junctions, i.e., a paracellular way, or through the body of the endothelial cell, or a transcellular way. The preference of a track relative to another is not well understood and may depend on the levels of activation of endothelial cells (Chavakis et al., 2009). Migration into tissue relies on integrins and other cell adhesion molecules, including platelet endothelial cell adhesion molecule 1 (PECAM-1), and junctional adhesion molecules (JAMs) present in intercellular junctions (reviewed by Ley et al. (2007)).

Leukocyte recruitment to inflamed tissue forms the basis for any type of local immune response. Targeting this process remains an attractive possibility to either enhance immune defence or to suppress inflammation-induced tissue destruction. A wide range of pro-resolution mediators that decrease the recruitment of granulocytes have been discovered in the last few years. Including adenosine (Hasko et al., 2008), $AnxA_1$ and N-terminal peptide Ac2-26 (Perretti and D'Acquisto, 2009), docosahexaenoyl ethanolamide (DHEA) metabolites (Shinohara et al., 2012), PGE_2 (Levy et al., 2001), lipoxin (LX)A_4 (Fierro et al., 2003), maresin (MaR)1 (Hong, Gronert et al. 2003; Serhan, Yang et al. 2009), melanocyte-stimulating hormone (α-MSH and γ-MSH) (Leoni, Patel et al. 2008), protectin D1 (PD1) (Hong, Gronert et al. 2003), RvD series and RvE series (Serhan, Clish et al. 2000). These pro-resolution

mediators can act directly at endothelial cells or on leukocytes. For instance, activation of adenosine A2a receptors can inhibit the expression of E-selectin and VCAM-1 on endothelial cells (Hassanian et al., 2014).

1.1.3.2. Clearance of the inflammatory stimulus by phagocytosis

Once in the tissue, leukocytes can be further activated and become an important source of a range of substances, which include colony stimulating factors, cytokines, lipid mediators and reactive oxygen species (ROS) (Alessandri et al., 2013). In addition, neutrophils and macrophages, predominantly, will perform the phagocytosis of microorganisms in the site of infection, thereby promoting the elimination of injurious stimuli.

Three primary mechanisms are necessary in neutrophils when eliminating an invading pathogen: receptor-mediated uptake of the pathogen into a vacuole within the cell; production of highly toxic ROS in the pathogen-containing vacuole; and fusion of neutrophil granules, containing various antimicrobial mediators, to the vacuole. These steps may also contribute in the pathogenesis of sterile inflammation, as in autoimmune diseases, in which ligands are deposited on tissue components.

Phagocytosis of an opsonized inducer depends on engagement of opsonic receptors, such as FcγRs and C-type lectin receptors, which enclose the pathogen within a defined vacuole referred to as the phagosome. Uptake is followed by fusion of the phagocytic vacuole with preformed granules within the cell to form the phagosome, in a process referred to as phagosomal maturation. These granules contain hydrolytic enzymes and NAPDH oxidase subunits that initiate killing mechanisms. Phagocytosis in neutrophils differs from that in other professional phagocytes such as macrophages, in which both particle uptake and phagosome maturation are much slower (Vieira et al., 2002). Additionally, the fully mature neutrophil phagosome has a neutral pH, whereas in macrophages the phagosome is highly acidic (Jankowski et al., 2002). This difference may reflect the effects of the

oxidative burst, which is massive in neutrophils compared with macrophages, on vacuolar pH. Efficient phagosomal maturation in neutrophils also depends on cytosolic calcium, whereas in macrophages, fusion between lysosomes and the phagosome is calcium independent (reviewed in Mayadas et al. (2014)).

Recently, endogenous pro-resolving mediators were found to enhance phagocytosis by neutrophils and macrophages, including chemerin-derived peptides (Cash et al., 2010), LXA_4 (Maderna et al., 2005), MaR1 (Serhan et al., 2009), MSH (Montero-Melendez et al., 2011), and RvD and RvE series (Schwab et al., 2007, Norling et al., 2012).

The speed with which the neutrophil can engage, engulf, and kill pathogens is an obvious advantage in terms of host defence. However, phagocytosis and phagosomal maturation are not perfect processes, as granules may fuse with the phagosome before it is completely sealed. This leads to the release of cytolytic contents and oxidative products outside the neutrophil, where damage to other cells may occur. Neutrophil phagocytic receptors may also be engaged by immune complexes or complement deposited along large surfaces, such as the vascular endothelium, which the neutrophil cannot completely engulf. This so-called frustrated phagocytosis leads to the release of granule contents and oxidative products, causing extensive tissue injury (reviewed in (Mayadas et al., 2014). The importance of this process will be discussed further in the rheumatoid arthritis section (1.2.1).

1.1.3.3. Apoptosis of neutrophils

When the inflammatory response is effective and the initiator stimulus is cleared, the inflammatory process is switched off. As mentioned before, the ending of this process is complex and it involves a series of steps. One of these steps is the induction of neutrophil apoptosis.

Apoptosis is a process of programmed cell death in vertebrates, which was first reported in human neutrophils at end of the 80's by Savill and colleagues; until

that time, it was believed that neutrophils died by the classical mode of cell death, necrosis. Necrotic neutrophils present disruption of the plasma membrane, with consequence release of intracellular contents to the microenvironment in an irreversible mode. The release of intracellular contents of neutrophils in the tissue is associated with further damage and recruitment of more inflammatory cells into the damaged tissue. On the other hand, neutrophils undergoing apoptosis preserve their cytoplasmic granules intact, display a vacuolated cytoplasm and have a densely condensed nucleus (Savill et al., 1989). DNA fragmentation and loss of plasma membrane asymmetry, with accumulation of phosphatidylserine (PS) on the extracellular leaflet, are additional endpoints that can be used to quantify apoptosis kinetics.

Mature neutrophils are terminally differentiated cells and are recognized as one of the leukocytes with the shortest lifespan (8-20 hours) in the circulation (Tak et al., 2013). However, pro-survival signals, including granulocyte macrophage colony stimulating factor (GM-CSF) (Colotta et al., 1992), LTB_4 (Lee et al., 1999), C5a (Lee et al., 1993) as well as bacterial constituents lipopolysaccharides (LPS) (Lee et al., 1993, Colotta et al., 1992) and bacterial DNA (Jozsef et al., 2004) can increase the lifespan of neutrophils, which in some occasions, can reach up to 5.4 days (Pillay et al., 2010). A balance between survival and intracellular death pathways regulates neutrophils apoptosis. In the absence of extracellular stimuli, neutrophils undergo spontaneous apoptosis, however, under most conditions, neutrophils receive both pro-survival and pro-apoptosis cues, and the net effect is likely determined by the balance of these signals.

Three main apoptotic pathways have been described: an extrinsic pathway, that is activated by ligation of surface death receptors that bind Fas ligand, TNF-α or TRAIL; an intrinsic pathway, that is regulated at the level of mitochondria and is initiated by disruption of the outer mitochondrial membrane; and the phagocytosis-induced cell death (PICD) pathway (McCracken and Allen, 2014). In a general

overview, the extrinsic pathway is initiated by ligation and clustering of plasma membrane death receptors leading to activation of caspase-8, which mediates activation of the executioner caspase-3 to evoke many of the defining biochemical and biophysical changes that occur during apoptosis. The intrinsic apoptotic pathway is initiated when the relative abundance of the pro-apoptotic B-cell lymphoma 2 (Bcl-2) family members [Bcl-2-associated X protein (Bax) and Bcl-2 homologous antagonist/killer (Bak)] exceeds that of their anti-apoptotic counterparts [protein myeloid cell leukemia-1 (Mcl-1) and A1], which allows Bax and Bak to oligomerize and form pores in the outer mitochondrial membrane. This provokes the release of cytochrome C from the mitochondria into the cytosol, an essential signal for activation of caspase-9 upstream of caspase-3. On the other hand, the PICD pathway is driven by particle uptake and NADPH oxidase-derived ROS. Leakage of cathepsins from damaged azurophilic granules leads to death receptor-independent activation of caspase-8. In addition, cathepsin-driven activation of Bcl-2 homology-3 (BH-3)-interacting domain death agonist (Bid) and degradation of Mcl-1 favour mitochondrial disruption and intrinsic pathway activation [reviewed in McCracken and Allen (2014)]. Further, neutrophil apoptosis can be induced by $AnxA_1$ (Perretti and Solito, 2004), LXA_4 (Weinberger et al., 2008) and RvE1 (El Kebir et al., 2012) either directly or against an anti-apoptotic stimulus.

1.1.3.4. Clearance of apoptotic of neutrophils

In normal physiological conditions, apoptotic cells are rarely detected, and the presence of un-cleared apoptotic cells has been linked to several different diseases that involve infection, inflammation, autoimmunity and cancer. As such, efficient efferocytosis is essential for the resolution of inflammation; this process is a dynamic and rapid phenomenon to avoid secondary necrosis of the apoptotic neutrophil and perpetuation of tissue damage (Duffin et al., 2010).

Although efferocytosis resembles phagocytosis, it is a distinct process, highly regulated and mediated by specific receptors, bridging molecules, and downstream signalling pathways. Furthermore, at variance from phagocytosis, efferocytosis is a sort of silent process that inactivates the engulfing cell, instead of activating it. Work of Rossi and his team showed a lack of cytokine production from macrophages engulfing an apoptotic neutrophil as compared to cell phagocytosing bacteria (Liu et al., 1999). When an infected cell undergoes apoptosis during an inflammatory process, the inducer and its antigens are presumably packaged along with other intracellular contents into apoptotic bodies which have intact cellular membranes. During apoptosis, the dying cell produces “find me” signals, such as chemokines that recruit macrophages and other phagocytic cells to the site of the dying cell, along with the accumulation of PS on the exofacial leaflet of the cytoplasmic membrane (as mentioned in the previous sub-section). In the “catch me” phase, recruited macrophages express specific receptors and bridge molecules that bind to PS or other distinct ligands on the apoptotic cell. Binding between the apoptotic cell and the scavenger macrophages activates Ras-related C3 botulinum toxin substrate (Rac1), leading to actin reorganization and production of projections that surround the infected apoptotic cell, ultimately surrounding and engulfing the apoptotic cell in the efferosome. The efferosome undergoes step-wise maturation that includes fusion with lysosomes and endosomes, leading to rapid degradation of both the apoptotic cell and the intracellular pathogen [reviewed in (Martin et al., 2014)].

The following mediators have been shown to augment efferocytosis in macrophages: α-MSH (Montero-Melendez et al., 2011, Leoni et al., 2008), $AnxA_1$ and N-terminal peptide Ac2-26 (Maderna et al., 2005, Koroskenyi et al., 2011), chemerin-derived peptides (Cash et al., 2010), cortisol (Liu et al., 1999), DHEA metabolites (Shinohara et al., 2012), LXA_4 (Godson et al., 2000), MaR1 (Serhan et al., 2012), PD1 (Hong et al., 2003), as well as D and E series resolvins (Schwab et al., 2007).

1.1.3.5. Switch of cell phenotype

Phagocytosis of apoptotic bodies is not only important for the clearance, but also promotes a switch from a pro-inflammatory to a pro-resolution phenotype of the macrophage (and possibly other local resident cells) ultimately extinguishing the inflammatory response. This helps to contribute to a non-phlogistic environment that paves the way towards successful restoration of tissue function and physiology, hence homeostasis.

Macrophages presenting a pro-inflammatory phenotype are long known as M1 macrophages, while macrophages presenting a pro-resolution phenotype are known as M2 macrophages. This classification was proposed when a few markers were considered to establish differences and similarities in macrophage responses to stimuli. However, updated knowledge of cytokine signalling, the role of cytokines in the development of the hematopoietic system and in disease models with genetically modified mice and transcriptomic and proteomic analysis revealed a far more complex picture. Nowadays, the phenotypes of the macrophage are named according to the stimuli used (Murray et al., 2014).

The M1 stimuli are grouped according to their ability to induce pro-inflammatory responses and markers, but their source, role, receptors, and signalling pathways differ substantially. The main stimulus used to induce the pro-inflammatory M1 phenotype is interferon (IFN)-γ. When IFN-γ activates its receptors IFNGR-1 and IFNGR-2, Janus kinase (Jak)1 and Jak2 adaptors are recruited, activating STAT1 (signal transducers and activators of transcription 1) and interferon regulatory factors (IRF), such as IRF-1 and IRF-8. IFN-γ controls specific gene expression programs involving cytokine receptors (CSF2RB, IL15 receptor alpha [RA], IL2RA, and IL6R), cell activation markers (CD36, CD38, CD69, and CD97), and a number of cell adhesion molecules ICAM1, integrin alpha L [ITGAL], ITGA4, ITGbeta-7 [B7], mucin 1 [MUC1], and ST6 beta-galactosamide alpha-2,6-sialyltranferase 1 [SIAT1]). The major mediators of IFN-γ-induced signalling, STAT1, JAK2, and IRF1, and regulators

cytokine inducible SH2-containing protein (CISH), N-myc-interactor (NMI), protein tyrosine phosphatase receptor (PTPR) type -O and type -C, and suppressor of cytokine signalling 1 (SOCS1) are also under the control of the cytokine. Generally, IFN-γ stimulation is used in combination with LPS, to enhance the pro-inflammatory phenotype of the macrophages [reviewed in (Martinez and Gordon, 2014)].

The M2 group of stimuli arose from the initial IL-4 observations, and they are grouped mainly due to their ability to antagonize pro-inflammatory responses and markers. IL-4 is produced by Th2 cells, eosinophils, basophils, or macrophages themselves and is recognized by two different receptor pairs (IL-4Rα1 can pair with the common gamma chain (γc), and with the IL13Rα1 chain). Receptor binding of IL-4 activates JAK1 and JAK3, leading to activation STAT6. Other transcription factors involved include c-Myc and IRF4. IL-4 induces macrophage fusion and decreases phagocytosis. The IL-4 multispecies transcriptome includes transglutaminase 2 (TGM2), mannose receptor (MRC1), cholesterol hydroxylase (CH25H), and the prostaglandin-endoperoxide synthase PTGS1 (prostaglandin G/H synthase 1), the transcription factors IRF4, Krüppel-like factor 4 (KLF4), and the signalling modulators CISH and SOCS1 macrophages [reviewed in (Martinez and Gordon, 2014)].

It is important to mention that the pro-inflammatory or pro-resolution properties of M1 and M2 like macrophages can change between the type of the disease. For instance, in breast cancer, M2 like macrophages are immunosuppressive, contribute to the matrix-remodelling, and hence favour tumour growth (Mantovani et al., 2002). But as for most of the diseases the skewing from M1 to M2 results in protection, the use of adenosine and RvD1, that are known to promote such switching, could become an alternative for therapy (Titos et al., 2011).

1.1.3.6. Ending of the inflammatory response

Finally, the exudate tissue leukocytes that did not undergo apoptosis and those cleared by macrophages must leave the tissue by egressing into the draining

lymphatics or systemic re-circulation, restoring the homeostasis of the tissue. LXA_4, RvE1 and PD1 have been shown to enhance the traffic of leukocytes out of the inflamed – but resolving - tissue (Schwab et al., 2007).

Sometimes the damaged caused by the inflammatory response is irreversible after tissue leukocytes exudation. However, newly discovered mediators might play a role in tissue regeneration. Maresins (macrophage mediators in resolving inflammation) by definition are formed *via* 14-lipoxygenation of docosahexaenoic acid and promote resolution of acute inflammation and tissue regeneration (Dalli et al., 2014). Recently, a series of work by Serhan's group discovered new bioactive peptide-lipid conjugated mediators that are produced during the later stages of self-resolving infections (Dalli et al., 2014) that are also present in human sepsis patients (Dalli et al., 2015), named maresin conjugates in tissue regeneration (MCTR) because they regulate mechanisms in inflammation-resolution as well as tissue regeneration establishing links between local inflammatory exudates and tissue regeneration *via* novel chemical signals (Serhan, 2014). Specifically, Dalli and colleagues have very recently showed that three synthetic MCTR dose-dependently (1–100nM) accelerated tissue regeneration in planaria (Dalli et al., 2016).

1.2. RHEUMATOID ARTHRITIS

1.2.1. Introduction

Rheumatoid arthritis (RA) is a chronic inflammatory disorder that affects approximately 0.5-1% of the worldwide population, characterized by autoimmune reactivity and persistent active inflammation with concurrent tissue destruction. RA manifests as swelling, pain, functional impairment, and morning stiffness, severely affecting the quality of life of those suffering from this disease. Most commonly affected joints are within the feet, knees and hands, but any peripheral joint could be affected. If not appropriately treated, this can result in significantly higher incidence of cardiovascular diseases, and, consequently, enhanced mortality (Kollias et al., 2011, Klareskog et al., 2009, McInnes and Schett, 2007, Maradit-Kremers et al., 2005).

It is widely accepted that RA is a systemic autoimmune disease with a variety of etio-pathogenic determinants acting in concert to contribute to disease initiation, progression and chronicity. These factors include genetic susceptibility, environmental stimuli, physical stress and defective immune responses. While T and B cell-dependent pathways have been traditionally implicated in the development of RA, innate immune perturbations mediated mainly by neutrophils, macrophages and synovial fibroblasts have also gained momentum as major orchestrators of the unbalanced associated immune response. As a result of the molecular complexity that stems from the multifactorial nature of the disease, the clinical picture is highly heterogeneous with several different subsets of RA being manifested in patients (Kollias et al., 2011, Klareskog et al., 2009, McInnes and Schett, 2007). This complexity in the pathogenesis of human RA can also be visualized in mice, as nowadays a variety of experimental models have been created, reproducing different stages of the disease.

Two main therapeutic treatments are used: symptomatic treatment with

NSAIDs and disease-modifying anti-rheumatic drugs (DMARDs). NSAIDs only interfere with a small segment of the inflammatory cascade, mainly prostaglandin generation by inhibition of COXs (Smolen and Steiner, 2003). By contrast, DMARDs like methotrexate control disease activity, reduce joint erosions and improve quality of life as well as reduce cardiovascular morbidity associated with RA such as ischemic heart disease (van Halm et al., 2006). However, still a great number of patients do not response to the therapy, and those that respond, have to make use of this therapy life-long.

In the next subchapters, a general overview of the etiology, pathogenesis and known roles of the cells involved in the progression of arthritis will be given.

1.2.2. Aetiology of RA

The specific aetiological agent of RA has yet to be identified: it is accepted that RA is a systemic disease resulting from breach of tolerance leading to self-attack to several tissues (e.g. the joints) together with a clear systemic inflammatory component. In addition, the genetics of RA have been a focus of investigation for nearly 40 years, and genetic predisposition to the disease has now been refined to the level of individual amino acids. Previous studies have indicated that genetic factors contribute to approximately 60% of the variation in the liability of the disease. In addition, it is believed that, at least, five specific amino acids located in different HLA are associated with an increased risk of acquiring RA. However, genetic predisposition for RA is not only due to HLA genes. Actually, there are more than 30 loci outside of the MHC that are associated with an increased risk of developing RA, but some of these associations are not universal, being relevant in certain populations or ethnic groups (Okada et al., 2014).

Although RA clearly has a considerable genetic component, some environmental risks factors are also associated with the initiation of the disease, such as cigarette smoke (Silman et al., 1996, Klareskog et al., 2011). However, many other

environmental factors remain largely unknown and their contribution to RA aetiology is likely to be considerable.

Another factor that intrigues scientist is associated with the observed sex-bias (3:1 female to male ratio) in the incidence of RA. A wide range of hypotheses including potential roles for sex hormones is proposed by investigators as one of the reasons behind this gender bias (van Vollenhoven, 2009).

1.2.3. Pathogenesis of RA

The synovial joint is composed of two adjacent bony ends each covered with a layer of cartilage, separated by a joint space and surrounded by the synovial membrane and joint capsule. Only a few, if any, mononuclear cells are interspersed in the sublining connective tissue layer, which has considerable vascularity in a healthy individual. In contrast, RA is initially characterized by an inflammatory response of the synovial membrane (‘synovitis’) that is conveyed by a transendothelial influx and/or local activation of a variety of mononuclear cells, as well as by new blood vessel formation. The lining layer becomes hyperplastic and the synovial membrane expands and forms villi (Smolen and Steiner, 2003).

The inflammatory response of RA is characterized by infiltration of neutrophils, B and T lymphocytes and monocyte-derived macrophages in the arthritic joints. But the exact role of each cell type during RA pathogenesis is not completely understood. Neutrophils are the first immune cell to arrive at the site of inflammation. Within the synovial fluid, neutrophils phagocytose immune complexes and release powerful proteases and inflammatory mediators, which in turn recruit monocytes, T and B cells to the synovium. These cells then form discrete lymphoid aggregates, sometimes with ectopic germinal centers (Pitzalis et al., 2013), while macrophage-like and fibroblast-like synoviocytes accumulate in the intima causing hyperplasia and secreting degradative enzymes. Among the proteases and inflammatory mediators produced by neutrophils, TNF-α is associated with activation of other cell types and induction

of chemotactic factors, while reactive oxygen species are associated with tissue damage [reviewed in Cascao et al. (2010)].

In association with the increased infiltration of inflammatory cells to the joints, patients with arthritis have increased levels of adhesion molecules including E-selectin, VCAM-1, and ICAM-1, in the synovial endothelium and macrophage synovial tissue (Adams and Shaw, 1994, Bevilacqua et al., 1994). As the disease develops, the cells of the synovial lining proliferate, forming an invasive pannus. Together these processes can ultimately result in loss of cartilage, bone destruction and dramatic joint deformation with loss of function if uncontrolled. High concentrations of different cytokines and chemokines, including IL-1β, IL-6, IL-8, and TNF-α are found in synovial biopsies from patients with RA, which have been implicated in the development of the disease (Feldmann and Maini, 1999). In addition, PGE_2, LTB_4, 5-hydroxyeicosatretraenic acid and PAF are also found in the synovial fluid of patients with active RA (Sperling, 1995)

Large numbers of activated neutrophils are found within both RA synovial fluid and pannus (Wittkowski et al., 2007), and are associated with increased damage within RA joints. Indeed, a vast range of cytokines and chemokines are secreted by RA synovial fluid neutrophils, which are implicated in the activation of other cells. In addition, conditions within the synovial joint, such as hypoxia (Cross et al., 2006) and the presence of anti-apoptotic cytokines (Lally et al., 2005, Parsonage et al., 2008) increase neutrophil survival for up to several days (Raza et al., 2006, Weinmann et al., 2007).

However, neutrophils are not only responsible for the pathogenesis of the RA, but may also be important for protection. Recently we found that neutrophil-derived microvesicles (MVs) were increased in concentration in synovial fluid from RA patients compared to paired plasma (Headland et al., 2015). Interestingly, the synovial MVs overexpressed the pro-resolving protein $AnxA_1$. In vitro, exogenous neutrophil-derived $AnxA_1$-positive MVs activated anabolic gene expression in

chondrocytes via FPR2, leading to extracellular matrix accumulation and cartilage protection through the reduction in stress-adaptive homeostatic mediators IL-8 and PGE_2. In vivo, intra-articular injection of $AnxA_1$-positive MV lessened cartilage degradation caused by inflammatory arthritis (Headland et al., 2015). These findings are of extreme importance, as it could be used as a new therapeutic for RA.

Further, neutrophils are not the only subtype of cells with potential opposite roles in the development of the inflammation in RA. Indeed, many groups have shown that different subsets and/or polarized phenotypes of monocytes and macrophages may play distinct roles during the development and resolution of inflammation. Misharin and colleagues (2014) demonstrated in a murine model of RA that non-classical $Ly6C^-$ monocytes are required for the initiation and progression of sterile joint inflammation. Moreover, non-classical $Ly6C^-$ monocytes differentiate into inflammatory macrophages (M1), which drive disease pathogenesis and display plasticity during the resolution phase. But during the development of arthritis, these cells polarize toward an alternatively activated phenotype (M2), promoting – at this stage - the resolution of joint inflammation (Misharin et al., 2014).

1.2.4. Experimental models of Arthritis

Use of animal models have significantly increased our understanding of the pathogenesis of RA, despite the inherent limitations, contributing to several major advances in treatment. The most used model of arthritis is the collagen-induced arthritis (CIA) model, which shares many similarities with human RA. It was first described in rats, but quickly mouse models become available, with the use of type II heterologous collagen in complete Freund's adjuvant. Importantly, susceptibility in mice is linked to strains that have MHC Class II I-Aq haplotypes (Wooley et al., 1985, Brunsberg et al., 1994). CIA has also been used in non-human primates, a powerful instrument for the development of novel therapeutic targets (Hart et al., 1998).

For induction of arthritis with CIA, DBA/1 mice are the most widely used strain. Clinical signs of disease typically develop 21–25 days after the initial inoculation, which presents as a polyarthritis, which is most prominent in the limbs and characterized by synovial inflammatory infiltration, cartilage and bone erosion and synovial hyperplasia similar to human RA. The development of CIA is associated with both B- and T-lymphocyte responses with the production of anti-collagen type II antibodies and collagen-specific T cells. The auto-antibody response in CIA is predominated by the IgG2 subclass with high levels of both IgG2a and IgG2b present at the peak of arthritis. Disease severity is expected to peak at approximately day 35, after which DBA/1 mice enter remission, marked by increased concentrations of serum IL-10 and a subsequent decrease in pro-inflammatory Th1 cytokines (Mauri et al., 1996).

One disadvantage of this model is the challenge to use it for genetic modifications or targeted gene deletion, as most transgenic mice are on the C57BL/6 background, which is generally considered resistant to CIA. However, changes in the way CIA is induced (immunisation with chicken type II collagen), have recently allowed the use of CIA in C57BL/6 background (Inglis et al., 2007). The C57BL/6 strain develops arthritis ~4–7 days later compared with DBA/1 mice, eventually reaching severity at a level comparable to arthritis in DBA/1 mice (Inglis et al., 2007). The arthritis was associated with sustained levels of serum anti-collagen antibody titters, higher levels of T-cell proliferation and IFN-γ secretion in the late stage of disease. However, there are differences in the onset and progression of disease between the DBA/1 and C57BL/6, which may cause discrepancies when comparing studies between these two strains. The severity in the B6 strain is sustained, but incidence of disease is markedly lower than DBA/1 mice and more variable across different substrains of B6 mice. Therefore, while both strains of mice may be useful to study the pre-clinical development or prophylactic treatment of arthritis, the

C57BL/6 model requires further characterization in different B6 substrains (Asquith et al., 2009).

Recently another model of inflammatory arthritis has been developed. In this model, transgenic mice expressing the KRN receptor in T cells and the A(g7) MHC class II, once bred with the NOD mouse colony (often used for experiments on diabetes), spontaneously develop severe inflammatory arthritis. Sera are collected from 10-week old mice by cardiac puncture. Importantly, the serum from these animals induces arthritis when injected into recipient mice, a response mounted in a large number of mouse strains (Kouskoff et al., 1996, Matsumoto et al., 2002, Kyburz and Corr, 2003). In this model, the deposition of glucose-6-phosphate isomerase antibodies from the arthritogenic serum onto the surface of the cartilage initiates an innate immune response mainly mediated by complement and LTB_4 recruiting neutrophils (Kyburz and Corr, 2003, Chen et al., 2006). K/BxN serum transfer arthritis is an acute, aggressive polyarthritis with high disease penetrance, which can resolve over 28 days, depending on the volume of serum injected and the frequency of these injections.

Other models of arthritis include collagen-antibody-induced arthritis, zymosan-induced arthritis, and the methylated BSA model, and the genetically manipulated or spontaneous arthritis models such as the TNF-α-transgenic mouse, and the Skg mouse. Table 1 report comparative characteristics of the models discussed and/or mentioned here.

Table 1: Main characteristics of some models of arthritis

Model	Species	Characteristics	Similarities to RA	Differences from RA
Collagen-induced arthritis (CIA)	Mouse, rat, rabbit, non-human primate	Polyarthritis, only inducible in susceptible strains, antibody and T-cell response. Low incidence and variability of disease severity in C57BL/6 mice. Inoculation with homologous collagen induces relapsing/remitting arthritis but otherwise is self-limiting.	Symmetric joint involvement, peripheral joints affected, synovitis, cartilage and bone erosions, inflammatory cell infiltrate, pannus formation, erythema, oedema, genetically regulated by MHC and non MHC genes	Formation of antibodies to collagen, greater incidence in males, periostitis, poor responses to NSAIDs, not characterized by exacerbations and remissions
Collagen type II (CAIA)	Mouse	Self-limiting polyarthritis in 100% animals, onset within 48 h, macrophage and polymorphonuclear cell involvement, no T- and B-cell involvement. Can be induced in most strains of mice	Macrophage and PMN inflammatory cell infiltrate	Not associated with a T- and B-cell response
Zymosan-induced arthritis	Mouse, rat	Monoarthritis, develops 3 days after inoculation and subsides by day 7, but has shown to relapse after day 25. Needs a high degree of technical ability to perform intra-articular injection in mice. TLR 2 dependent and can be induced in multiple strains of mice	Proliferative inflammatory arthritis with mononuclear cell infiltration, synovial hypertrophy and pannus formation	Monoarthritis
Antigen-induced arthritis	Mouse, rat	Inoculation with antigen by intra-articular injection requires a high degree of technical ability and precludes analysis of the systemic component of disease	Symmetric joint involvement, inflammatory cell infiltrate, cartilage degradation, synovial hyperplasia, genetic linkage, T cell dependence	Damage to cartilage less severe than in RA, bone destruction more prominent; no rheumatoid factor produced, gastrointestinal tract and skin affected

K/BxN-Tg mice	Mouse	Generated by crossing the TCR transgenic KRN line with mice expressing the MHC class II molecule Ag7. K/BN mice develop severe and destructive inflammatory arthritis	Symmetrically affects small peripheral joints	Distal interphalangeal joints often affected, no systemic manifestations, no production of rheumatoid factor
Human TNF–Tg mice	Mouse	Chronic inflammatory erosive polyarthritis	Synovial hyperplasia, presence of an inflammatory cell infiltrate, pannus formation, cartilage destruction, and bone resorption	No production of rheumatoid factor

Reviewed in Bevaart et al. (2010) Asquith et al. (2009).

1.3. FREE FATTY ACID RECEPTORS AND IMMUNE SYSTEM

1.3.1. Introduction

Previously I discussed the effects and importance of some lipid mediators in the initiation and resolution phases of inflammation. However, there has been particular interest in free fatty acid (FFA) sensing and its association with the mode of signalling of a number of recently de-orphanised G protein-coupled receptors (GPCRs) as many of FFA can directly activate GPCRs. In addition, an epidemic increase of obesity and other chronic conditions has been visualised in western populations. The increased incidence of such conditions is associated with increased intake of high fat- and high sugar content foods (Thorburn et al., 2014). In the next subsection, it will describe some of the FFA and their receptors Next, it will be described some of these FFA and their receptors, and their association with inflammatory processes. In the next subchapters, an overview of free fatty acid and free fatty acid receptors will be given, focussing in the know literature for GPR40 and GPR120. The importance of fatty acids in rheumatoid arthritis will also be discussed.

1.3.2. Overview of FFAs and FFARs

A FFA is a carboxylic acid with a long aliphatic chain, which is either saturated (no double bonds between carbons atoms) or unsaturated (Figure 5). Unsaturated FFA can be further classified as monounsaturated fat acids, which have only one double bond between carbons atoms, or as polyunsaturated FFAs when more than two double bonds are present. In addition, unsaturated FFA can be classified as *cis* (when the two hydrogen atoms adjacent to the double bound stick out on the same side of the chain) or *trans* (when adjacent two hydrogen atoms lie on opposite sides of the chain).

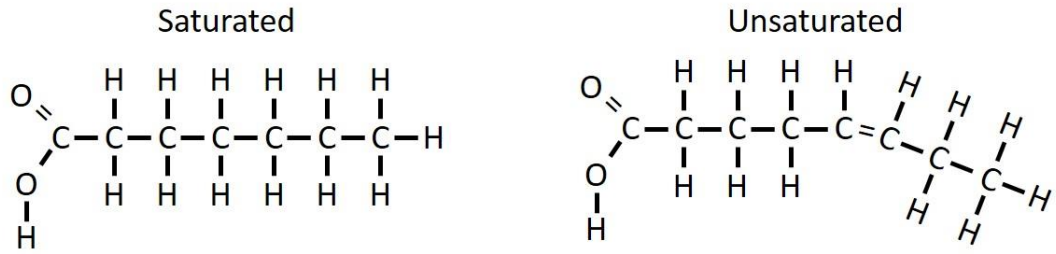

Figure 5: Types of fatty acids.

FA are also widely classified based on the length of their carbon chains and grouped into short chain fatty acids (2-6 carbon atoms long) such as butanoic acid; medium chain fatty acids (7-12 carbon atoms long) such as lauric acid; and long chain fatty acids (more than 12 carbon atoms long) such as palmitic acid (Alvarez-Curto and Milligan, 2016). Essential fatty acids, such as linoleic acid (18:2, n-6) or alpha-linolenic acid (18:3, n-3), which humans cannot synthesise directly, and other long and medium chain fatty acids, are generally obtained through the diet. Some other FFAs are obtained through the breakdown of fats (triglycerides) in adipose tissue and the liver. By contrast the vast majority of short chain fatty acids, including acetate and propionate are derived from the fermentation of fibres and breakdown of dietary carbohydrates by the bacteria present in the gut (Krishnan et al., 2015, Macfarlane et al., 2011).

As mentioned before, an important family of FFA are the omega-3 fatty acids, which are essential polyunsaturated fatty acids with a double bond between the third and fourth carbon atoms from the methyl end of the fatty acid carbon chain. Nutritionally important omega-3 fatty acids include α-linolenic acid (ALA), EPA and DHA. Although the health benefits of long-chain omega-3 fatty acids were discovered in the 1970s by researchers studying the Greenland Inuits, much more is now known of these benefits (O'Keefe and Harris, 2000). The Greenland Inuit people consumed large amounts of fat from seafood but experience lower incidences of cardiovascular diseases (Yates, Calder et al. 2014). Today omega-3 fatty acids are prescribed for hypertriglyceridemia and the prevention of myocardiac infarction (Ito, 2015).

Evidently, omega-3 fatty acids reduce blood triglyceride levels and regular intake may reduce the risk of a secondary or primary heart (He et al., 2004). However, PUFA can influence inflammatory cell function by the following mechanisms (Yates et al., 2014):

- PUFA intake can influence complex lipid, lipoprotein, metabolite and hormone concentrations that in turn influence inflammation;
- PUFAs can be oxidized and the oxidized derivatives can act directly on inflammatory cells via surface or intracellular receptors;
- PUFAs can be incorporated into the phospholipids of inflammatory cell membranes, which can influence the membrane order (fluidity) and lipid raft formation. The composition of the membrane phospholipids can also interfere in cell signalling pathways (composition of second messengers);
- Non-esterified PUFAs can act directly on inflammatory cells via surface or intracellular fatty acid receptors.

The last mechanism involves the activation of free fatty acid receptors, as detailed in the next section.

1.3.3. A family of GPCRs for Free Fatty Acids

G-Protein-coupled receptors constitute the most prosperous protein families for drug discovery, with 30–50% of all approved drugs acting by targeting GPCRs. The complexity of GPCRs is determined by the diversity of external stimuli they can respond to (including lipids, amino acids, proteins, hormones, nucleotides, neurotransmitters, light, etc.) and the variety of intracellular pathways they can engage, which depends in part by which particular Gα, Gβ, or Gγ proteins they are coupled to. GPCRs are characterized by 7 transmembrane segments, which based on sequence similarity, can be clustered into 5 families: the rhodopsin family (701 members), the adhesion family (24 members), the frizzled/taste family (24 members),

the glutamate family (15 members), and the secretin family (15 members) (Rosenbaum et al., 2009).

FFARs are members of the 'rhodopsin-like' GPCR family and currently four receptors have been classified and named as FFAR1 (GPR40), FFAR2 (GPR43), FFAR3 (GPR41) and FFAR4 (GPR120). GPR40, GPR43 and GPR41 are closely related in terms of sequence and are co-located on chromosome 19q13.12 in humans (Sawzdargo et al., 1997). Recently, a gene sequence between the coding regions for GPR41 and GPR40, which was initially considered a pseudogene, seems to be active in some individuals, and has been named GPR42 (Puhl et al., 2015). On the other hand, GPR120 is located on chromosome 10 (10q23.33) in humans and displays little overall homology with the other FFARs. GPR41 and GPR43 can be activated by short chain fatty acids, and display various potencies for the different ligands (Nilsson et al., 2003, Brown et al., 2003). In contrast both GPR40 and GPR120 are activated selectively by long chain fatty acids, as described below.

1.3.3.1. Free Fatty Acid Receptor 1 (GPR40)

GPR40, also known as the FFAR1, was originally isolated from a human DNA fragment (Sawzdargo et al., 1997). Three independent groups demonstrated that GPR40 functions as a receptor for medium- and long-chain saturated and unsaturated FFAs (Briscoe et al., 2003, Itoh et al., 2003, Nilsson et al., 2003). Arachidonic acid and the omega-3 PUFAs EPA and DHA can activate GPR40 (Briscoe et al., 2003), but it is not known if activation of this receptor by different ligands would result in different responses. In CHO cells with a stable expression of GPR40, FFAs induced an increase in intracellular calcium levels and activation of extracellular signal-regulated kinase (ERK) 1/2 (Itoh et al., 2003). A large rise in the intracellular calcium was also observed in pancreatic β-cells (Shapiro et al., 2005, Hara et al., 2009) and in primary pancreatic islet cells (Fujiwara et al., 2005). Therefore, GPR40 couples with a G protein α-subunit of the Gq family. Since no

changes were detected with respect to cAMP production, it seemed that GPR40 did not couple with Gs or Gi/Go in pancreatic β-cells (Briscoe et al., 2003, Welters et al., 2006). In human embryonic kidney 293 (HEK293) cells overexpressing GPR40, linoleic acid evoked activation of phospholipase C (PLC) through the Gq protein (Salehi et al., 2005). This identifies linoleic acid as an endogenous ligand for GPR40. The hydrolysis of inositol lipids by GPR40 activation has not been studied directly in β-cells, however the FFA-induced intracellular calcium rise in β-cells is consistent with the involvement of PLC. Through the use of reverse-transcription polymerase chain reaction, immunohistochemistry, and in situ hybridization, GPR40 was shown to be expressed in insulin-producing pancreatic islet cells (Itoh et al., 2003). The expression level of GPR40 in pancreatic islets was from two-fold to 100-fold higher than in whole pancreas (Briscoe et al., 2003) indicating a selective or restricted expression pattern for this receptor. However, GPR40 expression has also been detected in monocytes, brain and cell lines of breast cancer (Briscoe et al., 2003, Hardy et al., 2005). Many compounds showing either agonistic or antagonistic activity have been identified and their physiological and pharmacological effects have been examined using various experimental systems (Bharate et al., 2009). The first report identifying a series of novel GPR40 agonists based on 3-(4-[(N-alkyl) amino]phenyl) propanoic acid was from Garrido and colleagues (Garrido et al., 2006). These compounds showed a 100-fold increase in potency, and structure-activity relationships have been investigated for some of them. Furthermore, synthetic GPR40 antagonists have been identified and their antagonistic activities were examined via both in vitro and in vivo studies (Briscoe et al., 2003) (Humphries et al., 2009, Zhang et al., 2010). In particular, the physiological and pharmacological properties of GW9508 have been studied in detail because it has the potential as an agonist for not only GPR40, but also GPR120. However, GW9508 is approximately 100-fold more selective for GPR40 over GPR120. In addition, the small-molecule GW1100 inhibited (1μM) the intracellular calcium level elevation stimulated by GW9508 mediated by GPR40, but not that

mediated via GPR120, demonstrating that GW1100 was a selective antagonist of the GPR40 receptor (Briscoe et al., 2006). Besides the ability to increase the release of insulin only when glucose levels are elevated (Briscoe et al., 2003, Alquier et al., 2009), GPR40 is also involved in the suppression of CCL5, CCL17 and CXCL10 induced by TNF-α stimulation (Fujita et al., 2011), protection of bone loss by inhibiting osteoclast differentiation (Wauquier et al., 2013), inhibition of NLRP3 activation in macrophages (Yan et al., 2013), and in the suppression of inflammatory chronic pain (Nakamoto et al., 2013). Furthermore and in contrast to the succinctly described anti-inflammatory properties, a recent study showed that the long-chain FFAs palmitic acid and linoleic acid induce secretion of pro-inflammatory cytokine/chemokines, such as IL-6, IL-8 and MCP-1, in RA synovial fibroblasts (RASF) and production of IL-6 in palmitic acid, linoleic acid and oleic acid induced human chondrocytes, showing that FFA may also directly contribute to inflammation and joint degradation in inflammatory joint diseases (Frommer et al., 2015).

1.3.3.2. Free Fatty Acid Receptor 4 (GPR120)

GPR120 shares only 10% sequence homology with FFAR1, and is optimally activated by saturated FAs of chain length 14-18 and unsaturated FAs of chain length 16-22 carbons. GPR120 is expressed in adipose tissue, macrophages, the gastrointestinal tract, lung and pituitary. Long-chain FFAs induce a rise in cytosolic free calcium in HEK293 overexpressing GPR120, but they do not promote cAMP production. This suggested that GPR120 is coupled with Gq protein, as GPR40, but not with the Gs or Gi/o families (Hirasawa et al., 2005, Bharate et al., 2009). GPR120 can also induce the activation of ERK1/2 under certain conditions, and the activation of phosphoinositide (PI)-3-kinase and the serine/threonine protein kinase Akt in GPR120-expressing cells (Katsuma et al., 2005) but is unclear whether this response derives from the rise in intracellular calcium or whether an independent coupling mechanism is involved. Recently, GPR120 was found as a receptor for the omega-

3 fatty acids DHA and EPA, and stimulation of macrophages with these omega-3 FFAs caused broad anti-inflammatory effects, all abrogated by siRNA against GPR120 (Oh et al., 2010). Stimulation of GPR120 specifically inhibited TGF-β-activated kinase 1 (TAK1) phosphorylation and activation of both toll like receptor (TLR) and TNF-α signalling.

1.3.4. Fatty acids in Rheumatoid Arthritis

Numerous randomized, placebo-controlled, double-blinded studies using omega-3 polyunsaturated fatty acids in RA are reported. Almost all of these trials showed some benefit of fish oil, a source of these fatty acids. Such benefits include reduced duration of morning stiffness, reduced number of tender or swollen joints, decreased pain and time to fatigue, increased grip strength, and decreased use of non-steroidal anti-inflammatory drugs (reviewed in Calder (2008), and (Miles and Calder, 2012)). The dose range of omega-3 polyunsaturated fatty acids reported in these trials varied from 1.6 to 7.1 g/day and averaged 3.5 g/day (Calder, 2008, Miles and Calder, 2012). Thus, evidence-based reports implicate fish oil supplementation as an useful complementary therapy for RA. Alongside some of these studies, the authors also investigated inflammatory parameters that are modulated following omega-3 treatment, which include decreased LTB_4 production by neutrophils (Cleland et al., 1988, Kremer et al., 1987, Kremer et al., 1990, Sperling et al., 1987), reduced IL-1β production by macrophages (Kremer et al., 1990), and lower plasma levels of IL-11β (Espersen et al., 1992, Kremer et al., 1990). Thus, the mechanisms by which omega-3 PUFAs exert their beneficial effects are of mounting interest. These actions can be mediated, directly or indirectly, by EPA and DHA, the most prevalent omega-3 PUFAs found in fish oil.

One of the traditional hypothesis is that omega-3 PUFAs compete with the canonical omega-6 substrate AA to generate eicosanoids such as prostaglandins of the 3-series and leukotrienes of the 5-series that are thought to be more anti-

inflammatory than their AA-derived counterparts (reviewed by Calder (2015)). More recently, Serhan discovered that both EPA and DHA could be enzymatically converted *in vivo* to novel bioactive lipid mediators, termed resolvins, protectins and maresins (termed specialized pro-resolving mediators) that stimulate the resolution of inflammation and have proven to be log-orders more potent than their lipid precursors (reviewed in Serhan (2014)). Biosynthetic generation of these mediators may represent a potential molecular mechanism to explain the beneficial use of omega-3 fatty acids as nutraceuticals.

1.4. SCOPE OF THE THESIS

1.4.1. Hypothesis

Free Fatty Acids are newly described as extracellular signalling molecules, besides their nutritional and metabolic properties. Given the widespread expression of FFAR and the attributed health benefits of the PUFA omega 3 fatty acids in prevention of various diseases, it is hypothesized that GPR40 and GPR120, receptors for medium- and long-chain fatty acids, could have protective roles in inflammation and possibly in RA. Thus, the objective of this work consists of investigating functions and expression of GPR40 in cell types found within the joints in RA such as synovial fibroblasts, macrophages, monocytes, neutrophils, endothelial cells, lymphocytes, and chondrocytes. And then determine if GPR40 activation in human leukocytes could modulate the inflammatory response.

1.4.1.1. Aims

This hypothesis will be challenged by addressing the following specific aims:

- Evaluate the expression and modulation of GPR40:
    - Genomic expression will be evaluated in human cells, including leukocytes, endothelial cells and chondrocytes by polymerase chain reaction (PCR);
    - Protein expression will be verified by flow cytometry.
    - GPR40 modulation will be assessed after stimulation with pro-inflammatory mediators.
- Evaluate the functionality of GPR40 in leukocytes by using the agonist GW9508 to modulate:
    - Intracellular calcium flux;
    - The expression of neutrophils adhesion molecules;

- Neutrophil-endothelial interactions under flow;
- Neutrophil chemotaxis;
- The phagocytic ability of neutrophils and macrophages;
- Release of microvesicle in neutrophils;
- Apoptosis of neutrophils;
- The polarization of M1/M2 macrophages.

- To determine the expression and functional roles of GPR40 *in vivo* and *ex vivo*:
  - Evaluate if GPR40 is expressed in immune cells from arthritic joints by flow cytometry;
  - Assess whether prophylactic treatment with GW9508 modulates the initiation and progression of inflammatory arthritis by evaluating arthritic parameters, inflammatory mediators and leukocytes infiltration;
  - Assess whether therapeutic treatment with GW9508 modulates the resolution of inflammation in arthritic mice.

CHAPTER 2: MATERIAL AND METHODS

MATERIALS

2.1. Cell Culture

Dulbecco's phosphate buffered saline (DPBS) with calcium and magnesium and DPBS without calcium and magnesium, foetal bovine serum (FBS), Hank's Balanced Salt Solution (HBSS), human serum, Medium 199 with Earle's Salts with L-glutamine (M199), penicillin/streptomycin (100U/100mg/ml) and Roswell Park Memorial Institute medium 1640 (RPMI), acetic acid, crystal violet, dextran (molecular weight 450,000-650,000), gelatine type B from bovine skin, HBSS 10X, Histopaque 1077, phosphate buffered saline (PBS), sodium citrate, LPS, ionomycin, IL-8, Escherichia coli strain K12 and human recombinant tumour necrosis factor-α (hrTNF-α) were purchased from Sigma-Aldrich, Poole, Uk. Insulin transferrin selenium (ITS) supplement, non-heat inactivated FBS, Fungizone and trypsin/EDTA (0.25%/0.01%), Dulbecco's Modified Eagle Medium (DMEM), DMEM/Nutrient Mixture F-12 (DMEM/F12) (containing phenol red or phenol red free), RPMI and macrophage serum-free medium (SFM, 1X) were purchased from Gibco, Invitrogen, Paisley, UK. Type II collagenase was purchased from Worthington Biochemical Corporation, Lakewood, USA. Accutase was purchased from Millipore, Watford, UK. Macrophage colony-stimulating factor (M-CSF) and IL-4 were purchased from Peprotech, NJ, USA. IFN-γ was purchased from eBioscience, Hatfield, UK. BodyP 576/589 dye, Fura-2AM and pluronic acid were purchased from Life technologies, Eugene, OR, USA.

2.2. Flow Cytometry

Annexin V-FITC apoptosis detection kit was purchased from BD Pharmingen, Oxford, UK. Human Fc block was purchased from BD Bioscience, Abingdon, UK. Intracellular fixation and permeabilisation buffers were purchased from eBioscience, Hatfield, UK. Bovine serum albumin (BSA), paraformaldehyde (PFA), collagenase D, DNase and sodium chloride were purchased from Sigma-Aldrich, Poole, Uk. Zombie NIR™ was

purchased from BioLegend, San Diego, CA, USA. All antibody suppliers, clones and concentrations are listed below.

Table 2: Antibody list

Antibody (Species)	Clone, Host	Company	Fluorochrome	Class type	Final concentration
CD11b (Human)	ICRF44, Mouse	eBioscience	APC	IgG1κ	100ng/ml
CD16 (Human)	CB16, Mouse	eBioscience	PE	IgG1	300ng/ml
CD62L (Human)	DREG56, Mouse	eBioscience	PECy5	IgG1κ	100ng/ml
F4/80 (Mouse)	BM8, Rat	eBioscience	PE	IgG2a	250ng/ml
GPR40 (Human and mouse)	EP4632, Rabbit	Abcam	-	IgG	0.181μg/ml
Isotype CD11b	Mouse	eBioscience	APC	IgG1κ	100ng/ml
Isotype CD62L	Mouse	eBioscience	PECy5	IgG1κ	100ng/ml
Ly6C (Mouse)	HK1.4, Rat	eBioscience	PerCP-Cy5.5	IgG2c	200ng/ml
Ly6G (Mouse)	1A8, Rat	BD Pharmigen	APC	IgG2a	10μg/ml
Ly6G (Mouse)	1A8, Rat	BD Pharmigen	FITC	IgG2aκ	0.5μg/ml
2nd antibody (Rabbit)	Goat	Life Technologies	Alexa 488	IgG	5μg/ml
HLA-DR (Human)	Tü39, Mouse	BioLegend	FITC	IgG2aκ	10μg/ml
CD86 (Human)	IT2.2, Mouse	BioLegend	PE	IgG2bκ	1μg/ml
CD206 (Human)	15-2, Mouse	BioLegend	APC	IgG1κ	4μg/ml
CD14 (Human)	HCD14, Mouse	BioLegend	PE/Cy7	IgG1κ	2μg/ml
CD45 (Mouse)	30-F11, Rat	eBioscience	V450	IgG2bκ	2μg/ml
CD11b (Mouse)	M1/70, Rat	BioLegend	PE-Cy7	IgG2bκ	200ng/ml
I-A/I-E (Mouse)	M5/114.1 5.2, Rat	BioLegend	AF700	IgG2bκ	800ng/ml
CD64 (Mouse)	X54-5/7.1, Rat	BioLegend	Pacific Blue	IgG1κ	200ng/ml
Isotype GPR40	EPR25A	Abcam	-	IgG	0.181μg/ml

2.3. Molecular biology reagents

GelRed™ DNA dye was purchased from Biotium, Cambridge, UK. A 1-kilobase molecular weight DNA ladder buffer, deoxyribonucleiotide triphosphate (dNTP) and oligo$(DT)_{15}$ were purchased from Promega, Southampton, UK. Quantitec™ primers (listed in Table 3) and Qiagen mini-kit were purchased from Qiagen, Manchester, UK. Chloroform, 2-Propanolol, β-mercaptoethanol, RNAlater and molecular biology grade ethanol were purchased from Sigma-Aldrich, Poole, UK. ReddyMix PCR master-mix was purchased from Thermo-Scientific, St-Leon Rot, Germany. Power SYBRgreen mastermix, dithiothreitol (DTT) and TURBO DNA-free™ kit were purchased from Applied Biosystems Inc., CA, USA. Trizol®, agarose, RNase out, first strand buffer and SuperScript III were purchased from Invitrogen, Paisley, UK.

Table 3: Quantitec™ Primers used for analysis of mRNA expression

Gene code	Catalogue number	Detected transcript
Hs_GAPDH	QT01192646	NM_002046 (1401 bp)
Hs_RPL32	QT01668198	NM_000994 (1668 bp)
Hs_FFAR1_1_S	QT00211449	NM_005303 (923 bp)
Mm_Nos2_1_SG	QT00100275	NM_010927 (3990 bp)
Mm_Tnf_1_SG	QT00104006	NM_013693 (1653 bp) NM_001278601 (1605 bp)
Mm_Rpl13a_1_SG	QT00267197	NM_009438 (1039 bp) XR_105101 (1039 bp) XR_105102 (1039 bp) XR_107897 (1039 bp)
Mm_Il1b_2_SG	QT01048355	NM_008361 (1328 bp) XM_006498795 (2137 bp)
Mm_Il4_1_SG	QT00160678	NM_021283 (605 bp)
Mm_Il6_1_SG	QT00098875	NM_031168 (1087 bp)
Mm_Il10_1_SG	QT00106169	NM_010548 (1306 bp)

2.4. Other reagents and materials

Isoflurane inhalable gas anaesthetic was purchased from Baxter, Norfolk, UK. Haematoxylin, DPX slide mountant and methanol were purchased from Sigma-Aldrich, Poole, UK. Eosin was purchased from VWR, Leicestershire, UK. Polystyrene

ultracentrifuge tubes were purchased from Beckman Coulter, High Wycombe, UK. Neubauer Chamber was purchased from Celeromics, Valencia, Spain. Histoclear was purchased from Fisher Scientific, Loughborough, Leistershire, UK. Neuroprobe ChemoTx™ 96-well plate, Receptor Technologies Ltd, U.K. Six channel µ-slides VI$^{0.4}$ was purchased from ibidi, Martinsried, Germany. Tabasco® sauce was purchased from McIlhenny Company, Louisiana, USA. Maldon sea salt was purchased from Maldon Crystal Salt Company Ltd, Essex, UK. Evian natural mineral water was purchased from Danone Waters, Evian, France. Precellys tubes were purchased from Peqlab, Germany. Syringes and needles were purchased from Terumo, Heverlee, Belgium. Glass microscope slides were purchased from Thermo Scientific, Leicestershire, UK. All cell culture flaks, plates and plastics not stated before were purchased from Corning Amsterdam, NL.

2.5. Software and equipment

Software packages utilised during this project were IDEAS and INSPIRE software, Amnis Corporation, Seattle, WA, USA; FLOWJO Software, FlowJo, Stanford, CA, USA; Lucia Imaging Software, Lucia Laboratory Imaging, Prague, CZ; ND 1000 software, NanoDrop Technologies, Wilmington, DE; ImageJ software, NIH, Bethesda, MD, USA; ImagePlus.

Analytical hardware included Imagestream^X mk. II, Amnis corporation, Seattle, WA, USA; ABI Prism 7900 real-time PCR system, Applied Biosystems Inc., CA, USA; BD LSR Fortessa and BD FACSCalibur, BD Bioscience, Abingdon, UK; Leica tissue processor and Leica microtome, Leica Microsystems, Milton Keynes, UK; NanoDrop Spectrophotometer, NanoDrop Technologies, Wilmington, DE; Nikon DXM1200 digital camera, Nikon, Melville, NY, USA; Olympus BH-2 light microscope, Olympus, Tokyo, Japan; FluorChem E digital darkroom, Protein Simple, Santa Clara, CA, USA; NOVOSTAR, BMG Labtech, Germany; and Abgene Thermal Cycler, ThermoScientific, Leicestershire, UK.

METHODS

IN VITRO METHODS

2.6. Isolation and culture of primary human umbilical vein endothelial cells (HUVEC)

All cell culture flasks/dishes were coated in 0.5% gelatin type B from bovine skin in DPBS without calcium and magnesium (DPBS -/-) for 20 minutes prior to use. Following this coating procedure, gelatin was aspirated before seeding cells.

Umbilical cords were kindly supplied by the midwifery staff of the Maternity Unit, Royal London Hospital (Ethicals Approval REC Reference Number: 06/Q0605/40). Cords were placed in cord buffer [HBSS containing penicillin/streptomycin (100U/100mg/ml) and fungizone (2.5µM/ml)] and stored at 4°C until endothelial isolation. Endothelial cells were isolated from umbilical cords by collagenase digestion of the interior of the umbilical vein (Jaffe et al., 1973). Briefly, a 21-gauge butterfly needle was introduced into the vein of the umbilical cord and clamped. The vein was perfused with approximately 30ml of DPBS -/- using a sterile syringe to wash out the residual blood. The other end of the cord was then clamped and approximately 20ml of 0.1% collagenase type II in serum free M199 containing penicillin/streptomycin (100U/100mg/ml) and fungizone (2.5µM/ml) was added. The cord was incubated in a humidified chamber in 5% CO_2 at 37°C for 15 minutes. Following incubation, the collagenase solution was collected into a 50ml centrifuge tube and the vein was flushed with 30ml of DPBS -/-, and once with air to remove endothelial cells. The cells were centrifuged at 300*g* for 5 minutes, supernatant removed, and the pellet was re-suspended in 12ml of complete medium [M199 containing penicillin/streptomycin (100U/100mg/ml), fungizone (2.5µM/ml) and 20% human serum] and transferred to a T75 flask (75cm^2). The cells were incubated in a humidified chamber in 5% CO_2 at 37°C, medium was replaced after 24h and changed every 48h thereafter.

Once the confluence of 95% was reached, cells were subcultured at a ratio of 1:3 in T75 flasks. Flasks were rinsed with DPBS -/- to remove any serum, and cells were detached with warm trypsin/EDTA (0.25%/0.01%). Once cells had rounded and detached, the trypsin was deactivated by the addition of complete medium. Cells were divided between T75 flasks kept in culture and used in subsequent experiments between passages 1-3.

2.7. Human blood leukocyte isolation

Human leukocytes were isolated from the peripheral blood of healthy volunteers (Ethicals Approval REC Reference Number: QMREC2014.61) using the dextran sedimentation method. Blood was collected from healthy volunteers with a 21-gauge butterfly needle into a 60ml syringe and transferred to a 50ml centrifuge tube containing 1/10 volume of 3.2% sodium citrate, to prevent clotting. The blood was centrifuged at 130*g* for 20 minutes at room temperature to sediment the cells. The upper layer (platelet rich plasma) was removed then 10ml DPBS -/- and 8ml dextran 6% (in DPBS -/-, molecular weight 450000-650000) was gently added on top. The tubes were inverted gently to mix the cell suspension with DPBS and dextran. Dextran causes red cells to form aggregates, which sink to the bottom of the tube, leaving a layer of DPBS/dextran enriched in blood leukocytes that is largely depleted of red blood cells. This process takes around 20 minutes. Following the incubation, the leukocyte rich layer was carefully collected without generating bubbles and layered over 10ml Histopaque® (10771 density) in a new 50ml centrifuge tube. The sample was centrifuged at 450*g* for 30 minutes at room temperature. This step allows the separation of peripheral blood mononuclear cells (PBMC) and polymorphonuclear cells (PMN) as shown in Figure 6 below:

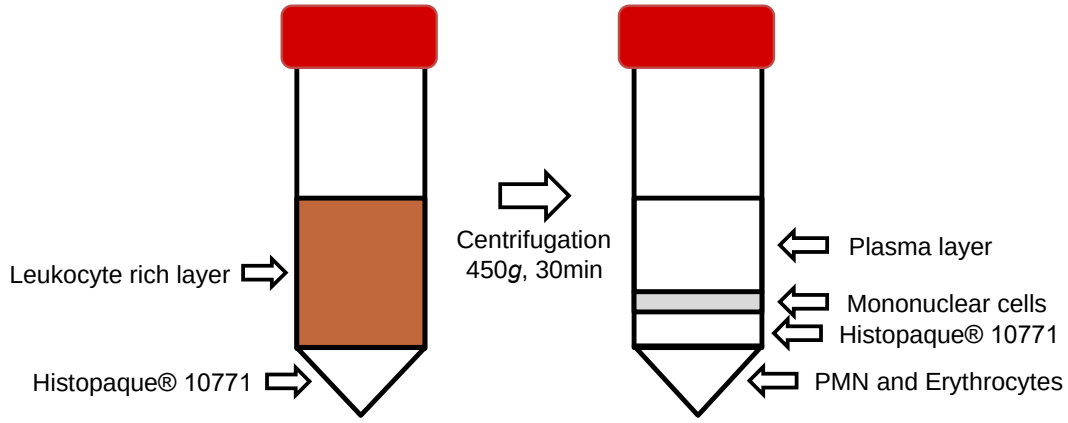

Figure 6: Human blood leukocyte isolation.

2.7.1. Preparation of human monocyte derived macrophages

PBMC were collected by using a Pasteur pipette and transferred into a new centrifuge tube. Cells were washed by adding up to 50ml of DPBS -/-, and centrifuged at 300*g* for 10 minutes at room temperature. Following the centrifugation, half of the supernatant was aspirated off, and up to 50ml of DPBS -/- was added for a second wash and centrifuged at 150*g* for 10 minutes at room temperature. This improves the number of the cells that are isolated as any Histopaque® in the solution could prevent the PBMC to reach the bottom of the tube; and also allows a better separation of the platelets. The supernatant was discarded and the cells were gently re-suspended in 2ml of DPBS -/- for counting by using Pasteur pipette. To count, 10μl of the cell suspension was added to 990μl Turk's stain (98ml distilled water, 2ml acetic acid and 2g crystal violet) in a 1.5ml microcentrifuge tube, then vortexed briefly to obtain a homogenous cell suspension with no clumps. Cells in Turk's dye were applied to a Neubauer counting chamber with coverslip. The cells were visualised with an Olympus BH-2 standard light microscope with X40 objective. Cells in the 4 larger outer squares were counted (marked in red in Figure 7), and divided by 4 to obtain the average. The total number of cells per ml was calculated according to the formula below:

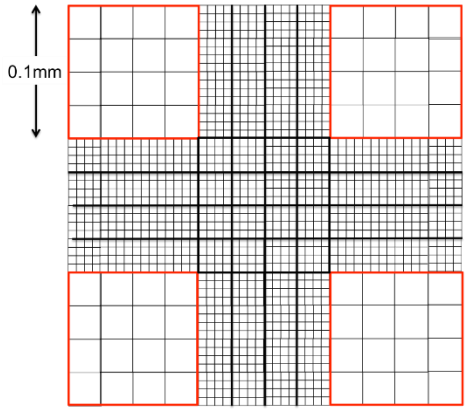

Average cell count per square x dilution factor x 10^4 = Cell count per ml.

Figure 7: Illustration of grid counting in a Neubauer haemocytometer. Cells were counted in the four outer squares marked in red and the average was calculated dividing the total value by four, and using the equation indicated.

Once counted, cells were re-suspended in incomplete media and left at 37ºC for 1h to allow monocytes to adhere. Non-adherent cells were washed off and monocyte-derived macrophages were obtained by incubating the cells for seven days at 37ºC in RPMI supplemented with 10% FBS and 50ng/ml M-CSF.

2.7.2. Isolation of peripheral blood neutrophils

After removal of PBMC, the remaining layers were removed leaving only the layer containing PMN and erythrocytes. The erythrocytes were lysed through hypotonic shock with 9ml ice-cold ultrapure distilled water. Isotonicity was quickly restored (after less than 20 seconds) by drawing up the cell/water suspension and transferring it to a new centrifuge tube containing 1ml 10X HBSS. New tubes were used for isotonicity restoration to prevent any mononuclear cells adherent to the plastic of the tube being washed into the granulocyte suspension. Cells were washed by adding up to 50ml of DPBS -/-, and centrifuged at 300*g* for 10 minutes at room temperature. The supernatant was discarded and pellet (containing the cells) were gently re-suspended using a Pasteur pipette in 2ml of DPBS -/- for counting. Cells were counted as described above for PBMC.

2.8. Collection of Exudated Human PMN

Activation of Transient Receptor Potential Cation Channel subfamily V member 1 ($TRPV_1$) receptors expressed at dorsal root ganglion by capsaicin can lead to neurogenic inflammation. Activation of those receptors results in the release of calcitonin-related gene product (CGRP) and substance P, neuropeptides that act on the local vasculature to promote inflammation (Helme and McKernan, 1985). Tabasco® Sauce contains high levels of capsaicin (0.33.g capsaicinoids/ml) as determined by high pressure chromatography (Gonzalez et al., 1998) and thus induces this effect when administered orally.

The local research committee approved experiments with healthy volunteers and informed consent was provided according to the declaration of Helsinki (Ethicals Approval REC Reference Number: QMREC2010/17). Volunteers were asked to rinse the buccal cavity three times with 20ml of 0.9% saline (prepared with Maldon sea salt as it contains low levels of impurities compared to other table salts and Evian still water) for 30 seconds and then a 10% Tabasco® solution in Evian water (20ml for 30 seconds). These were discarded and the volunteers were asked not to eat or drink anything for the following two hours. The volunteers were then asked to rinse the buccal cavity again three times with 20ml of 0.9% saline. The samples were collected and passed through a 70μm strainer and centrifuged at 300*g* for 10 minutes at room temperature to pellet the cells. The cells were resuspended with 50ml of DPBS-/- and passed through a 40μm strainer to separate epithelial cells and centrifuged at 300*g* for 10 minutes at room temperature to pellet the cells. The supernatant was discarded and the cells were gently re-suspended using a Pasteur pipette in 2ml of DPBS -/- for counting. Cells were counted as described above.

2.9. *In vitro* culture of chondrocytes

2.9.1. Culture of C28/I2 chondrocyte cell line

The C28/I2 cell line was used in this project for production of micromass culture. These cells express collagen type II, one of the most labile features of cultured (primary and immortalised) chondrocytes, and produce matrix that reacts with antibodies against collagen type II, large proteoglycan and sulphated glycosaminoglycans. They also exhibit decreased expression of collagen type II and increased expression of matrix metalloproteinases (MMPs) in response to IL-1β stimulation (Goldring et al., 1994), reminiscent of the true chondrocytic phenotype.

Cells were cultured DMEM/F12 complete medium [supplemented with 10% non-heat inactivated FBS, penicillin/streptomycin (100U/100mg/ml)] during monolayer culture. C28/I2 cells were cultured to confluence before subculture. Flasks were rinsed with DPBS to remove any serum, and cells were detached with warm trypsin/EDTA (0.25%/0.01%). Once cells had rounded shape and detached, the trypsin was deactivated by the addition of complete medium. Cells were re-suspended in 30ml complete medium and transferred to fresh flasks (10ml per flask) to achieve a 1:3 subculture. Cells were used between passage 3 and 20 for micromass culture.

2.9.2. Generation of C28/I2 chondrocyte micromass cultures

C28/I2 can be differentiated into matrix-producing chondrocytes when cultured in high density and serum free conditions (Greco et al., 2011). Briefly, confluent C28/I2 monolayers were rinsed with DPBS to remove any serum, and cells were detached with trypsin/EDTA (0.25%/0.01%). Once cells had rounded and detached, the trypsin was deactivated by the addition of complete medium, transferred to a tube, then centrifuged for 10 minutes at 400*g* before being re-suspended in 5ml complete medium for counting (see section 2.7). The cells were re-suspended to a volume of 2.5 x 10^7 cells/ml in complete medium. Using a reverse

displacement Gilson pipette, 20μl of the well-mixed cell suspension was placed into each well of a 48-well plate, so that the surface tension allowed a rounded drop to be formed on the bottom of the well. The peripheral wells of a 48-well plate were pre-filled with sterile DPBS to increase relative humidity to prevent evaporation of the medium. Plates were carefully transferred to an incubator without disrupting the pellets and cells were left to adhere for 3 hours at 37°C in 5% CO_2. After the 3 hour period, 2ml complete medium was added very slowly to each well, taking care not to dislodge the delicate cell pellet. After 24 hours the medium was replaced with 1ml chondrocyte differentiation medium [serum free, phenol-red free DMEM/F12 containing 1% insulin/transferrin/selenium (ITS) supplement]. After 24 hours, cells were considered ready to use.

2.10. Modulation of GPR40 expression in neutrophils and macrophages

Neutrophils and macrophages were isolated and prepared as described in section 2.7. To assess their pattern for GPR40 expression and potential function, neutrophils and macrophages were stimulated with different pro-inflammatory mediators involved in the initiation and progression of RA.

To assess the genomic modulation of GPR40, I personally decided to stimulated neutrophils for 4 and 6 hours, while macrophages were stimulated for 6 and 18 hours with TNF-α (10ng/ml) in 0.1% FBS RPMI. After stimulation, RNA was isolated and quantify as described in section 2.11. To assess protein modulation, neutrophils were stimulated with TNF-α (10ng/ml), IL-8 (10ng/ml), PAF (10nM) and LTB_4 (10nM) for 10 minutes in incomplete RPMI at 37°C (Norling et al., 2012, Krishnamoorthy et al., 2010). After stimulation, GPR40 expression was determined by flow cytometry analysis as described in section 2.12.1.

2.11. Gene expression analyses

In this project, two different types of Ribonucleic acid (RNA) isolation were used: a commercially available kit (Qiagen RNeasy® Plus Mini Kit) was used for RNA isolation from micromass, HUVEC, monocytes, lymphocytes and macrophages; while TRIzol® reagent was used to isolate RNA from neutrophils as it resulted in better recovery. Both methods are explained below:

2.11.1. RNA isolation using RNeasy® Plus Mini Kit

Total RNA was extracted using a commercially available kit (Qiagen RNeasy Mini Kit) following manufacturer's guidelines. Briefly, one million cells of micromass, HUVEC, monocytes, lymphocytes and macrophages samples were lysed in 600μl buffer RLT plus (containing 1:100 β-mercaptoethanol) and frozen at -80°C to increase RNA yield. The exact composition of Buffer RLT plus is confidential, but it is a lysis buffer for lysing cells and tissues before RNA or deoxyribonucleic acid (DNA) isolation. It contains a proprietary blend of detergents that allows efficient binding of DNA molecules to the gDNA Eliminator column. It also contains a high concentration of guanidine isothiocycanate, which supports the binding of RNA to the silica membrane. The β-mercaptoethanol is added to effectively inactivate RNases in the lysate. Samples were defrosted on ice before being homogenised by syringing 5 times through a 23-gauge needle. One volume of 70% molecular biology grade ethanol was added and samples were mixed well by pipetting before transferring the entire volume to the RNeasy kit columns. The ethanol creates conditions that promote selective binding of RNA to the RNeasy membrane. Samples were centrifuged at 10,000*g* for 15 seconds and flow-through discarded. Contaminants were washed by adding 700μl RW1 buffer to the columns and centrifuged at 10,000*g* for 15 seconds. The exact composition of Buffer RW1 is confidential, but it contains a guanidine salt, as well as ethanol, and is used as a stringent washing buffer that efficiently removes

biomolecules such as carbohydrates, proteins and fatty acids, that are non-specifically bound to the silica membrane. At the same time, RNA molecules larger than 200 bases remain bound to the column. Flow through was discarded before the addition of 500μl RPE and a further centrifugation step. The exact composition of Buffer RPE is confidential, but it is a mild washing buffer that removes traces of salts, which are still on the column due to buffers used earlier in the protocol. A second wash with 500μl RPE followed, and samples were centrifuged a further time at 10,000*g,* this time for 2 minutes. The collection tube was discarded and replaced with a new collection tube followed by a centrifugation at 12,000*g* for 1 minute to dry the membrane. Columns were placed into new collection microcentrifuge tube and 30μl RNase-free water was added directly to the membrane for RNA elution. Total RNA concentrations and purity was measured as described in section 2.11.3. The samples were stored at -80ºC until further use.

2.11.2. RNA isolation using TRIzol® reagent

To access specific messenger RNA (mRNA) levels, total cellular RNA was isolated using TRIzol® reagent (a solution of phenol and guanidine isothiocyanate). Neutrophils were lysed directly by adding 1ml of reagent to 5-10x10^6 cell pellet, and frozen at -80ºC to increase RNA yield. Samples were defrosted on ice before being homogenized by passing the lysate at least 5 times through a 23-gauge needle fitted to a RNase-free syringe to improve the homogenization. The homogenised samples were incubated for 15 minutes at room temperature to allow complete dissociation of nucleoprotein complexes, before addition of 200μl of chloroform (per ml of TRIzol®). Tubes were shaken vigorously by hand for 15 seconds, left at room temperature for 5 minutes before centrifuging at 12000*g* for 15 minutes at 4ºC. This procedure separates the solution into a colourless aqueous phase containing the RNA, an interphase and a lower organic phase (Figure 8). The aqueous phase was transferred

to new tube and the RNA was precipitated with 0.5ml of 2-propanol (per ml of TRIzol®). Samples were incubated for 10 minutes at room temperature, centrifuged at 12000*g* for 10 minutes at 4°C to pellet the RNA, supernatants were carefully aspirated off, and the pellet was washed with 1ml of 75% ethanol (per ml of TRIzol®). Samples were vortexed, centrifuged at 7500*g* for 5 minutes at 4°C, supernatants carefully aspirated and pellets briefly air-dried at 50°C, and the RNA was dissolved in 30µl of RNase-free water. Total RNA concentrations and purity were measured as described below. The samples were stored at -80°C until further use.

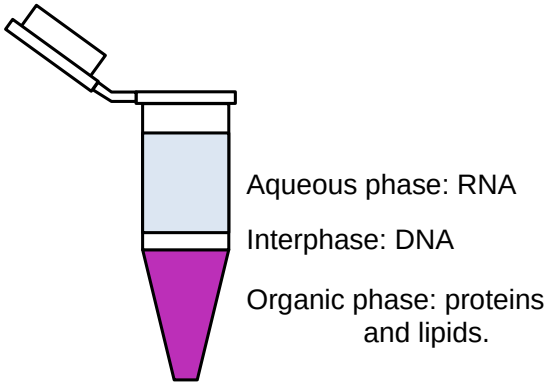

Figure 8: Phases of RNA extraction by TRIzol.

2.11.3. RNA quantification

RNA was quantified using a Nanodrop ND-1000 Spectrophotometer. With the sampling arm open, 1µl of RNase-free water was pipetted onto the lower measurement pedestal (to setup the machine), the sampling arm was closed and spectral measurement made using the ND 1000 software (NanoDrop Technologies); for RNA quantification, the nucleic acid option was selected. When the measurement was complete, the sampling arm was opened and wiped gently from both upper and lower pedestals using a soft tissue. All the samples were then measured by repeating this procedure. The concentration of RNA was measured in ng/µl from the absorbance at 260nm. The purity of RNA was considered satisfactory when the ratio of absorbance at 260 and 280nm was greater than 1.6.

2.11.4. cDNA Synthesis

Following RNA extraction, complementary DNA (cDNA) was obtained via reverse transcription of 0.5µg of the total RNA samples, using Superscript III reverse transcriptase system. Firstly, a mastermix *A* solution was created containing 1µl Oligo(dT)$_{15}$ primer, 1µl dNTP Mix and 4µl RNase free distilled water per sample. Oligo(dT) is a short single-stranded sequence of deoxythymine (dT) used for priming reactions catalysed by reverse transcriptase. The Oligo(dT) primer is first annealed to the poly(A) sequences universally present at the 3' end of nearly every mRNA by T:A base-pairing. The reverse transcriptase then extends from the annealed Oligo(dT) primer along the mRNA template, copying the mRNA sequence into the cDNA sequence. To a clean microcentrifuge tube, 6µl mastermix *A* was added and 0.5µg RNA sample (total 7µl volume) and incubated for 5 minutes at 65^{o}C to denature RNA secondary structure, followed by incubation on ice for 4 minutes to allow primers to anneal. A mastermix *B* solution was made by adding 4µl 5X First-Strand buffer, 1µl 1M DTT, 1µl RNaseOUT (a recombinant RNase inhibitor), and 1µl of Superscript™ III Reverse Transcriptase (200U/µl). Thereafter, 7µl of the mastermix *B* was added to the samples. Samples were then placed in the Abgene thermal cycler and incubated for 1 hour at 55°C for cDNA extension then heated at 70°C for 15 minutes to deactivate the enzyme and stop the reaction. Negative controls were samples run without Reverse Transcriptase enzyme to exclude the possibility of human genomic DNA contamination. The cDNA samples were stored at -20^{o}C until use.

2.11.5. Standard Polymerase Chain Reaction (PCR)

The resultant cDNA was analysed using the gene specific primers. The conventional PCR reaction was performed by adding 10µl ReddyMix PCR Master Mix® (that contains DNase polymerase, dNTPs, magnesium chloride and buffer), 1µl gene specific primer and 1µl cDNA. PCR tubes were placed in a MWG Biotech *Primus*

96 Plus thermal cycler and the following program was employed: 94ºC for 5 minutes, then 40 cycles of 94ºC for 30 seconds (denaturation), 55ºC for 30 seconds (annealing), and 72ºC for 30 seconds (elongation); and 72ºC for 10 minutes. The PCR product were loaded in 4% agarose gel with 1:10000 GelRed™ Nucleic Acid Gel Stain and migrated at approximately 100 volts for 80 minutes. The products were visualized using FluorChem E Digital Darkroom (Protein Simple™).

2.11.6. Real-Time Polymerase Chain Reaction

Real-Time PCR (qPCR) allows sensitive quantification of mRNA within cells by using SYBRgreen dye to visualise amplicon generation from a complimentary-DNA template. SYBRgreen dye binds to newly synthesised double-stranded DNA and emits fluorescent light in direct proportion to the number of amplicons generated in the reaction. A threshold of fluorescence detected above background was set in the exponential phase of amplification, and the cycle number at which the sample reached this level was referred to as the cycle threshold value (Ct), thus reflecting the relative abundance of the specific mRNA transcripts. To quantify the relative expression of each gene, Ct values were normalized with an endogenous housekeeping (reference) gene.

For the real-time (qPCR), a mastermix *C* solution was created adding 2µl of RNase free distilled water, 5µl of Power SYBR mastermix and 1µl of gene-specific primer, enough for each sample and corresponding gene. Primers were commercially available and used to probe for target mRNA. Two microliters cDNA was added to the appropriate mastermixes. Quantitative PCR was performed using the ABI Prism 7900 Real-Time PCR system, using the following amplification profile: 2 minutes at 50°C, 15 minutes at 95° followed by 40 cycles of 94°C for 15 seconds (denaturation), 55°C for 30 seconds (annealing), and 72°C for 30 seconds (elongation). A dissociation step of 95°C for 15 seconds, 60°C for 15 seconds and 95°C for 15 seconds was added after the PCR reaction to confirm the absence of non-specific

PCR products. The comparative Ct method (Pfaffl, 2001) was used to measure gene transcription in the samples. mRNA data were normalised relative to housekeeping gene mRNA and then used to calculate expression levels. Two housekeeping genes were run routinely to check variation in experiments with treatments. Results are expressed as $2^{-\Delta\Delta CT}$, which gives the relative amount of target gene normalised to the endogenous constitutive control. Negative controls were prepared without cDNA template.

2.12. Flow cytometry analysis

Flow cytometry is a well-characterised and useful tool that can simultaneously detect multiple parameters such as the size, granularity (internal complexity), surface topography and biochemical makeup of a population of cells in suspension. Ideally, cells guided in a hydrodynamically focussed stream pass one-by-one through a flow cell (any remained doublets were excluded during analysis). Fixed alignment lasers transmit light through the flow cell, and as the cell passes through the beam, an optical signal is generated. This optical signal reaches a detector, which translates the signal to an electronic one. Two types of detector are used in this system, photomultiplier tubes (PMT), used to detect weaker signals such as those generated by fluorescent labels and the side scatter (a measure of internal cellular complexity), and photodiodes, used to detect stronger forward scatter signals (a rough measure of cellular size). To allow accurate detection of different fluorescent signals, the signals pass though filters and mirrors arrayed around the flow cell. Long pass dichroic filters, placed in front of the PMT detectors transmit wavelengths that are longer than a specified value, steering shorter wavelengths of light to the next PMT so that progressively shorter wavelengths are detected by the last PMT. Band-pass filters are used to only transmit a narrow bandwidth of light to the detector. The digital signals generated using this system can be used to probe multiple parameters of cellular phenotype, and data generated are usually displayed in histograms of one

parameter, such as fluorescence intensity, or in 2-parameter scatter plots, such as forward/side scatter (showing size and complexity).

2.12.1. Expression of GPR40 on human leukocytes by flow cytometry

PMN and PBMC were isolated from healthy volunteers using dextran sedimentation followed by gradient centrifugation as described in section 2.7. Cells were washed twice with DPBS + 0.1% BSA and plated in a 96-well plate. Cells were fixed with 100µl of Fixation buffer (containing 1:4 Fixation/Permeabilization concentrate) for 20 minutes at room temperature. Following the incubation, 200µl of permeabilization buffer was added on top and the cells were left for another 20 minutes on ice. Cells were washed twice with permeabilization buffer and incubated with the GPR40 antibody (clone EP4632, 0.181µg/ml) for 30 minutes on ice. Following the incubation, cells were washed twice with permeabilization buffer. A 488-conjugated secondary antibody was added to allow the visualization by flow cytometry, as the GPR40 antibody was unconjugated. The secondary antibody (goat anti-rabbit, 5µg/ml) was incubated for 45 minutes on ice. Following the incubation, the cells were washed twice with permeabilization buffer and re-suspended in 200µl of DPBS + 0.1% BSA. The cells were transferred to clean microtubes and kept refrigerated until use. IgG isotype and unstained controls were also prepared for accurate calibration of the flow cytometry machine. GPR40 expression was recorded as MFI units in the FL1 channel of a BD FACSCalibur or in the B530/30 channel of a BD LSR Fortessa.

2.12.2. Assessment of adhesion molecule expression on PMN by flow cytometry

PMN were isolated from healthy volunteers using dextran sedimentation followed by gradient centrifugation as described in section 2.7. One million cells were incubated in DPBS +/+ with GW9508 (agonist of GPR40, 0.1µM, 1µM or 10µM) or

vehicle (0.1% ethanol) for 10 minutes at 37°C. Some of the cells were also stimulated with hrTNF-α (10ng/ml). Cells were washed twice with DPBS + 0.1% BSA and plated in a 96-well plate. Cells were then incubated with the following purified mouse anti-human monoclonal antibodies (mAb): CD11b (clone ICRF44, 100ng/ml, fluorochrome APC) and CD62L (clone DREG56, 100ng/ml, fluorochrome PE/Cy5) for 30 minutes on ice. Antibodies were diluted in DPBS-/- containing Fc block to prevent nonspecific binding of antibodies. Following the incubation, the cells were washed twice with DPBS-/- containing 0.1% BSA and re-suspended in 0.2ml of 1% paraformaldehyde (PFA). The cells were transferred to clean microtubes and kept refrigerated until use. Conjugated isotypes and unstained controls were also prepared for accurate calibration of the flow cytometry machine. Adhesion molecule expression CD11b and CD62L were recorded as MFI units in the R670/14 and YG670/30 channels, respectively, of a BD LSR Fortessa.

2.12.3. Leukocyte preparation using whole blood lysing reagents

Blood was collected from healthy volunteers (Ethicals Approval REC Reference Number: QMREC2014.61) with a 21-gauge butterfly needle into a 30ml syringe and transferred to a 50ml centrifuge tube containing 1/10 volume of 3.2% sodium citrate, to prevent clotting. One-hundred microliters of blood were them transferred to 15ml centrifuge tubes. Cells were fixed with 100µl of Fixation buffer (containing 1:4 Fixation/Permeabilization concentrate) for 20min at room temperature. Following the incubation, 200µl of permeabilization buffer was added on top and the cells were left for another 20min on ice. Cells were washed twice with permeabilization buffer and incubated with the GPR40 antibody (clone EP4632, 0.181µg/ml) for 30min on ice. Following the incubation, cells were washed twice with permeabilization buffer. A 488-conjugated secondary antibody was added to allow the visualization by flow cytometry, as the GPR40 antibody was unconjugated. The

secondary antibody (goat anti-rabbit, 5μg/ml) was incubated for 45min on ice. Following the incubation, the cells were washed twice with permeabilization buffer and re-suspended in 200μl of DPBS + 0.1% BSA. Cells were then incubated with the following purified mouse anti-human monoclonal antibodies (mAb): CD11b (clone ICRF44, 100ng/ml, fluorochrome APC) and CD62L (clone DREG56, 100ng/ml, fluorochrome PE/Cy5) for 30 minutes on ice. Antibodies were diluted in DPBS -/- containing Fc block to prevent nonspecific binding of antibodies. Following the incubation, the cells were washed twice with DPBS -/- containing 0.1% BSA. After staining, red cells were lysing by adding 1ml of Immune-Lyse working solution to each tube and vortex vigorously. Tubes were allowed to sit for no more than 30 seconds, and no longer than 2 minutes before adding 250μl of Fixative. Tubes were them vortexed vigorously. Cells were washed twice with PBS and centrifuged at 400*g* for 3 minutes at room temperature. Supernatant was discarded and cells were re-suspended in 0.2ml of PBS. The cells were transferred to clean microtubes and kept refrigerated until use. GPR40 and adhesion molecules expression were recorded as MFI units in the B530/30, R670/14 and YG670/30 channels, respectively, of a BD LSR Fortessa.

2.12.4. Determination of pro-inflammatory and pro-resolution polarization of macrophages by flow cytometry

PBMC were isolated from healthy volunteers using dextran sedimentation followed by gradient centrifugation and the monocytes were induced into macrophages in culture as described above. On the seventh day, cells were washed with DPBS -/- and treated for 24h in macrophages SFM media with GW9508 (0.1 μM, 1 μM, 10μM) at 37ºC. Without washing, cells were then stimulated with IFN-γ (10ng/ml) and LPS (50ng/ml) to induce into pro-inflammatory macrophages or stimulated with IL-4 (10ng/ml) to induce into pro-resolution macrophages for 24 hours at 37ºC. Concentrations of INF-γ, LPS and IL-4 used to induce polarization of

macrophages were chosen in accordance with personal experience by other members of the group in Biochemical Pharmacology. Un-stimulated macrophages were also used to measure basal levels of specific markers. Following incubation, cells were de-attached using accutase/EDTA (0.01%/0.5mM) and washed twice with DPBS + 0.1% BSA and plated in a 96-well plate. Cells were incubated with the following purified mouse anti-human monoclonal antibodies (mAb): CD14 (clone HCD14, 100µg/ml, fluorochrome PE/Cy7), CD86 (clone IT2.2, 100µg/ml, fluorochrome PE), CD206 (clone 15-2, 100µg/ml, fluorochrome APC), and HLA-DR (MHC-II, clone T39, 100µg/ml, fluorochrome FITC) pre-diluted in Fc block to prevent nonspecific binding of antibodies for 30 minutes on ice. Following the incubation, the cells were washed twice with DPBS + 0.1% BSA and re-suspended in 0.2ml of 1% PFA. The cells were transferred to clean microtubes and kept refrigerated until use. Conjugated isotypes and unstained controls were also prepared for accurate calibration of the flow cytometry machine. The specific markers CD14, CD86, CD206 and HLA-DR expression were recorded as MFI units in YG780/60, YG582/15, R670/14 and B530/30 channels, respectively, using a BD LSR Fortessa.

2.13. Imaging flow cytometry

Amnis Imagestream^X mk. II (ISX), an imaging flow cytometry, uses charge-coupled devices instead of PMTs and captures up to 12 images of each event as it passes through the flow cell. The machine was designed to allow the co-localisation of subcellular particles within cells and is equipped with a X60 objective in order to do this. Acquisition parameters can be determined by a large variety of physical parameters rather than just size, complexity and fluorescence intensity, as in the standard flow cytometry. Each event recorded is paired with a bank of images generated for each single event. Dot plots and image galleries are therefore searchable and can be used to corroborate event identity. Furthermore, multicolour staining can be used for accurate identification of various subpopulations.

2.13.1. GPR40 expression by imaging flow cytometry

PMN were isolated from healthy volunteers using dextran sedimentation followed by gradient centrifugation as described in section 2.7. Cells were tripled stained for GPR40, CD11b and CD62L using the same protocol used in the standard flow cytometry. Following staining, the cells were transferred to a clean 1.5ml tube for acquisition.

The INSPIRE instrument and software were configured as follows: channel 01 (brightfield), channel 02 (Alexa 488), channel 05 (PE-Cy5) and channel 12 (APC) were activated in addition to any other fluorescence channels required. Sixty times magnification, providing a pixel size of 0.3μm^2 was chosen, and flow rate was set to low speed/high sensitivity and alignment stream was always adjusted as necessary. A minimum of 10000 events were acquired, which were subsequently analysed for the expression of the labelled antibodies by gating the population of PMN using the area and intensity profiles.

2.13.2. Assessment of microvesicle release by imaging flow cytometry

PMN were isolated from healthy volunteers using dextran sedimentation followed by gradient centrifugation as described as described in section 2.7. After counting, cells were re-suspended to 5x10^6 cells/ml in incomplete RPMI (phenol red free). Five million cells were stimulated with GW9508 (10μM) for 15 minutes at 37°C. A positive control was prepared by stimulating the cells with hrTNF-α (10ng/ml) for 15 minutes at 37°C. Vehicle control (0.01% ethanol) was also used to measure basal levels of microvesicle release. After stimulation, cells were centrifuged at 4400*g* for 15 minutes at 4°C to pellet cells. Following centrifugation, supernatant was collected in new microcentrifuge tubes and centrifuged at 13000*g* for 2 minutes at 4°C to pellet platelets. Following centrifugation, supernatant was transferred to new high speed microtubes and centrifuged for a last time at 20000*g* for 30 minutes at 4°C to pellet

microvesicle. The supernatant was discarded, and the microvesicle were re-suspended in 50μl of DPBS containing 1:100 BODIPY. Following staining, microvesicle were kept at 4°C until acquisition.

The INSPIRE instrument and software were configured as follows: channels 01 and 09 (brightfield), channel 02 (FITC) were activated in addition to any other fluorescence channels required. Sixty times magnification, providing a pixel size of 0.3μm^2 was chosen, and flow rate was set to low speed/high sensitivity and alignment stream was always adjusted as necessary. A minimum of 10000 events was acquired, which were subsequently analysed for the presence of microvesicle labelled with the dye by gating the specific population using the intensity profiles as described by Headland (2014).

2.14. Intracellular Calcium measurement

PMN were isolated from healthy volunteers using dextran sedimentation followed by gradient centrifugation as described in section 2.7. One million cells were added per well in a 96 black-well plate. The cells were washed twice with DPBS -/- and 100μL of loading buffer (containing 2μM Fura-2AM and 1μM pluronic acid in DPBS -/-) was added per well. The cells were incubated for 1 hour in a humidified chamber in 5% CO_2 at 37°C. Subsequently, the cells were washed twice with DPBS -/- and 50μL HBSS was added per well. Mobilization of intracellular calcium was measured by recording the ratio of fluorescence emission at 510nm after sequential excitation at 340nm and 380nm. Fluorescence was determined using a plate reader. The results were compared to ionomycin (1μM) used as a positive control. The results are expressed as percentage of the positive control or as delta of time “zero”.

2.15. PMN chemotaxis assay

The commercially available Neuroprobe ChemoTx^{TM} 96-well plate with polycarbonate membrane filters and 3μm membrane pores was utilised as described

previously (Frevert et al., 1998) to assess the chemotaxis of PMN. PMN were stimulated with GW9508 (0.1µM, 1µM or 10µM,) or vehicle for 10 minutes at 37°C in RPMI medium containing 0.1% FBS. The chemotaxis assay was performed using interleukin-8 (IL-8 or CXCL8; 30ng/ml) as the chemotactic stimulus (concentration chosen from preliminary studies, in order to obtain around 80% to 90% of the maximal response). IL-8 or medium was added to the bottom wells (28µl), the filter was placed on top and 25µl of the PMN cell suspension (previously diluted to $4x10^6$ cells/ml) were placed above the membrane (Figure 9). Plates were incubated for 60 minutes in a humidified incubator at 37°C with 5% CO_2. Cells remaining on top of the filter were absorbed off using cotton buds and the surface was washed with 25µl of RPMI per well and absorbed off again using cotton buds.

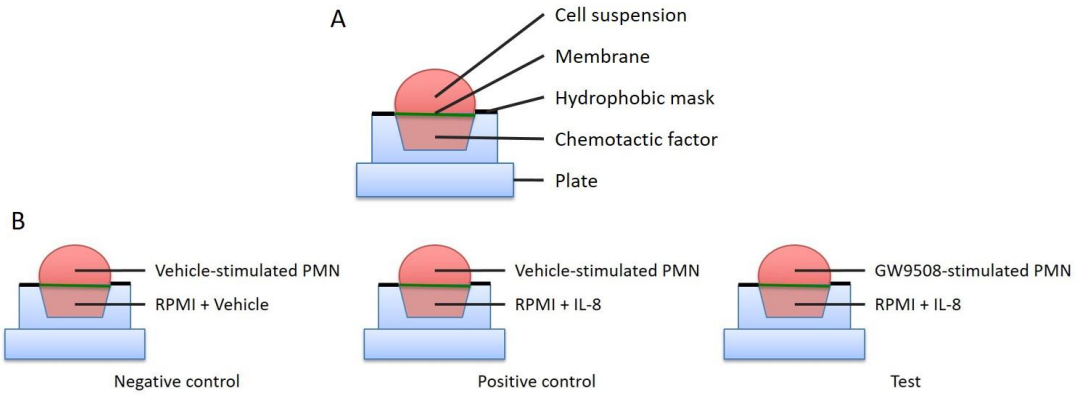

Figure 9: Chemotaxis assay.
(A) Cross-section of one well of the 96-well chemotaxis chamber. (B) Experimental setup of the chemotaxis assay.

The plate was centrifuged at 312*g* for 1 minute, and then the filter was removed and the pelleted cells re-suspended. An aliquot of 20µl was transferred and mixed with 30µl of PrestoBlue® (pre-diluted 1:6 in DPBS) in a 96-well plate and incubated at 37°C with 5%CO_2 for 4 hours. PrestoBlue® is a ready to use cell permeable resazurin-based solution that functions as a cell viability indicator by using the reducing power of living cells to quantitatively measure cell metabolism. When added to cells, the PrestoBlue® reagent is modified by the reducing environment of

the viable cell and turns red in colour, becoming highly fluorescent. A standard curve was constructed using 0-4x10^6 PMN, and adding known cell numbers in 20µl to the wells, then transferring them to the 96-well plate for PrestoBlue addition, as above. Plates were then read at 530-560nm excitation wavelength and 590nm emission wavelength for fluorescence values. Fluorescence was determined using a plate reader. All stimulations were performed in quadruplicate. Unknown values were interpolated using the standard curve constructed with known PMN numbers. Average of each group was subtracted by the average of negative control group to give the total number of cells chemotactic to IL-8.

2.16. Flow chamber assay

To assess the interactions between neutrophils and endothelial cells, flow chamber assay was used, as described before (Norling et al., 2012). Briefly, HUVEC were plated on µ-slides VI$^{0.4}$ and confluent monolayers were stimulated with hrTNF-α (10ng/ml) for 4 hours to up-regulate adhesion molecules such as CD62E, ICAM-1 and VCAM-1. PMN were isolated from healthy volunteers using dextran sedimentation followed by gradient centrifugation as in section 2.7. Immediately prior to flow over HUVEC, PMN were suspended at 1x10^6/ml in DPBS supplemented with calcium and magnesium (DPBS +/+) containing 0.1% BSA (as integrins on the PMN require these divalent cations for their adhesive function), and stimulated with GW9508 (1µM or 10µM) for 10 min at 37°C. In a second set of experiments, neutrophils were pre-stimulated with LTB4 (10nM) for 10 minutes, followed by 10min stimulation with 1µM GW9508. PMN were perfused over the HUVEC monolayer at 1 dyne/cm^2 using a programmable syringe pump (Stoelting, Germany) for 8 minutes, then 100 sequences of six fields per treatment were randomly capture, for 10 seconds each. The number of PMN interacting with the HUVEC monolayer was measured as captured and also classified as adherent or rolling (if stationary for the period of 10

seconds), the transmigrated motility cells were characterized by the appearance of a dark phase and motility under the HUVEC monolayer (Figure 10).

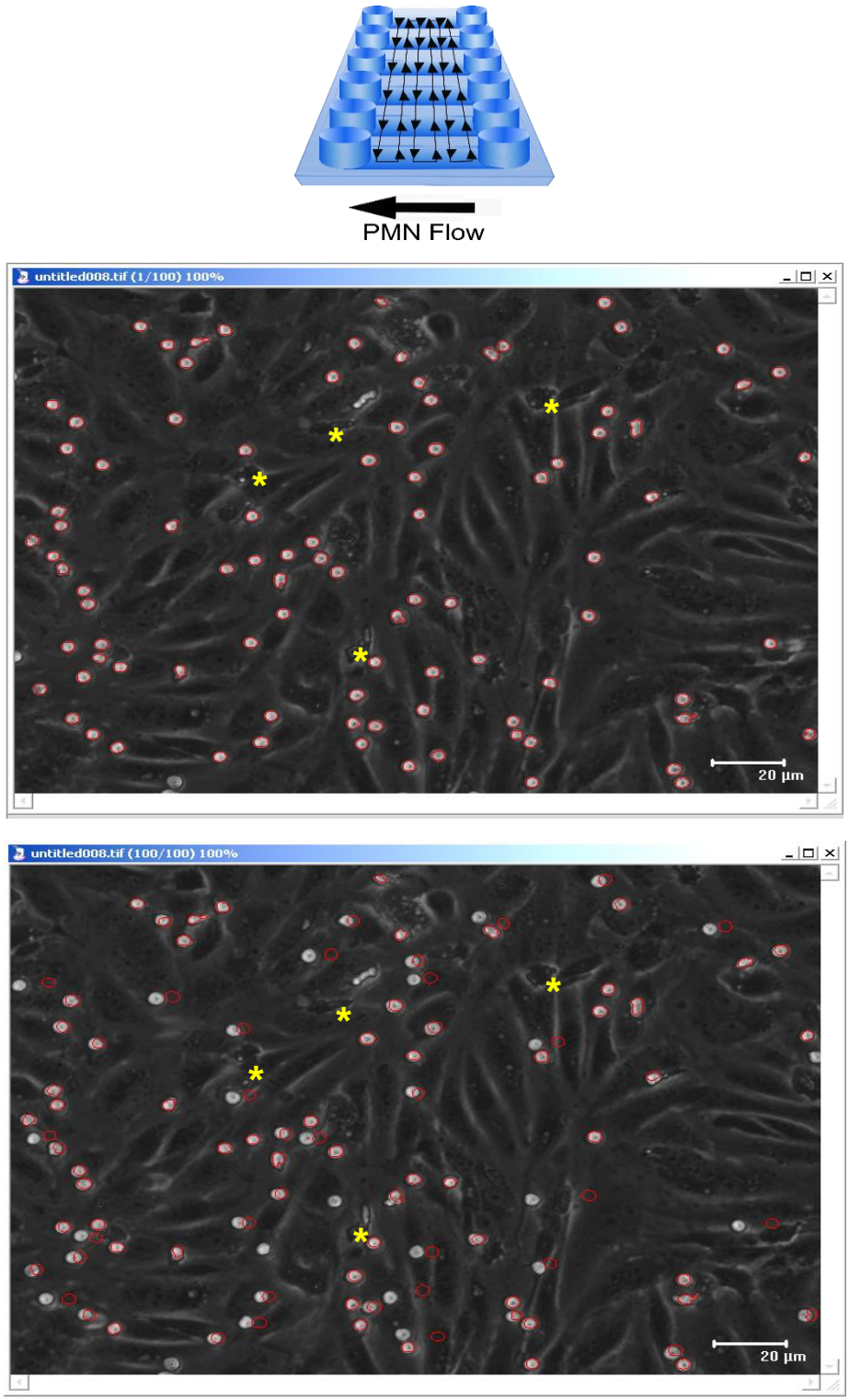

Figure 10: Flow Chamber Assay. Diagram represents a flow chamber slide, showing the way the photos were taken, and the direction of the PMN flow. The top image shows the first photo of the sequence of photos taken to analyse the movement of PMN, while the bottom image is the last photo taken in the same sequence from the same frame. PMN (white circle cells) is counted as adherent if in the last photo of the sequence the same cell from frame 1 is inside the red circle. On the other hand, if the cell is outside the red circle, is counted as rolling. Yellow stars represent transmigrated PMN.

2.17. Phagocytosis Assay

PMN were isolated from healthy volunteers using dextran sedimentation followed by gradient centrifugation as described in section 2.7. One million PMN were stimulated with GW9508 (0.1μM, 1μM or 10μM) for 10 minutes at 37°C in medium RPMI containing 0.1% FBS. After the treatments, *E. coli* (final concentration 1mg/ml) labelled with BODIPY 576/589 (final concentration 1μM) was added. The cells were incubated at 37°C, 5% CO_2 for 30 minutes to allow the phagocytosis of the bacteria by the neutrophils. After 30 minutes, the cells were washed three times with cold DPBS to stop the process. The rate of the phagocytosis was determined using a fluorescence plate reader. The results are expressed in intensity of fluorescence or as the percentage of the positive control.

Monocyte-derived macrophages were obtained from healthy volunteers using dextran sedimentation followed by gradient centrifugation as described in section 2.7. Half million macrophages were stimulated with GW9508 (0.1μM, 1μM or 10μM) for 18 hours at 37°C in macrophage serum-free medium. After the treatments, *E. coli* (final concentration 1mg/ml) labelled with BODIPY 576/589 (final concentration 1μM) was added. The cells were incubated at 37°C, 5% CO_2 for 1 hour to allow the phagocytosis of the bacteria by the macrophages. Following incubation, cells were washed three times with cold DPBS to stop the process. The rate of phagocytosis was determined using a fluorescence plate reader. The results are expressed in intensity of fluorescence or as percentage of the positive control.

2.18. Measurement of apoptosis in neutrophils

2.18.1. By Morphology in Light Microscopy

PMN were isolated from healthy volunteers using dextran sedimentation followed by gradient centrifugation as described in section 2.7. PMN were plated at $4x10^6$ cells/ml in a 6-well plate in RPMI 0.1%FBS. The cells were stimulated with GW9508 (10μM) and vehicle and incubated at 37ºC in a 5% CO_2 incubator for 24

hours. After 2, 8, 18 and 24 hours of incubation, 100µl of aged neutrophils suspension were loaded in cytospin chambers. Cells were cytocentrifuged at 300*g* for 3 minutes. Cells were then left to air-dry for 5 minutes. Once dried, cells were fixed in methanol for 1 minute and stained with eosin (1 minute) and haematoxylin (1 minute). Cells were rinsed with water to wash off the excess dye. The slides were left to dry overnight. Using a light microscope, 200 cells per slide were counted with x100 objective. Viable neutrophils (arrowhead, Figure 11) can be readily differentiated from apoptotic neutrophils (black arrow, Figure 11) by their characteristic condensation of nuclear material, prominent nucleoli, and frequent vacuolization of the cytoplasm.

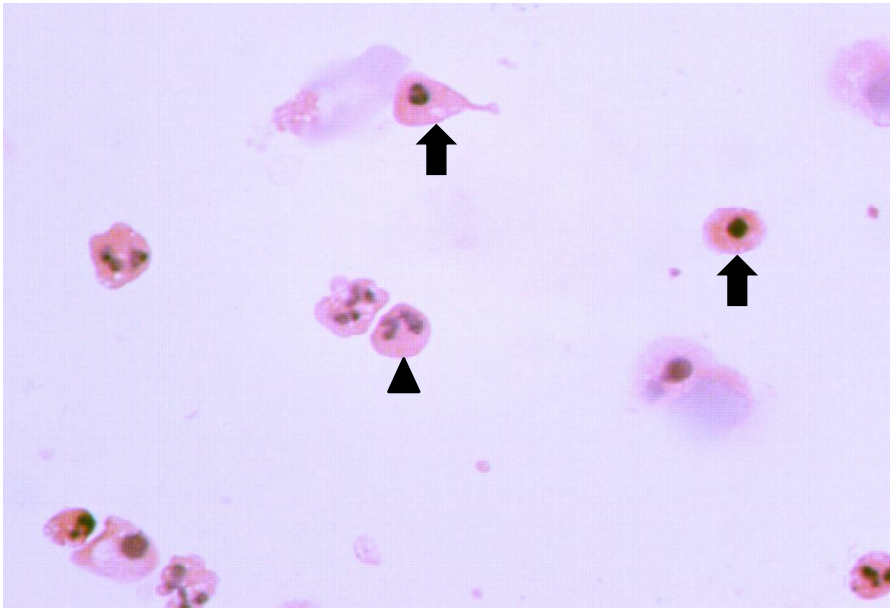

Figure 11: Cytospin of neutrophils following overnight culture.
Apoptotic neutrophils are indicated by arrows, whereas a viable neutrophil is indicated by the arrowhead. x100 magnification.

2.18.2. Annexin V apoptosis detection

For quantification of apoptotic neutrophils, FITC Annexin V Apoptosis Detection Kit was used. FITC Annexin V is used to quantitatively determine the percentage of cells within a population that are actively undergoing apoptosis. It relies on the property of cells to lose membrane asymmetry in the early phases of apoptosis. In apoptotic cells, the membrane phospholipid phosphatidylserine (PS) is translocated from the inner leaflet of the plasma membrane to the outer leaflet,

thereby exposing PS to the external environment. Annexin V is a calcium-dependent phospholipid-binding protein that has a high affinity for PS, and is useful for identifying apoptotic cells with exposed PS. Propidium Iodide (PI) is a standard flow cytometric viability probe and is used to distinguish viable from nonviable cells. Viable cells with intact membranes exclude PI, whereas the membranes of dead and damaged cells are permeable to PI. Cells that stain positive for FITC Annexin V and negative for PI are undergoing apoptosis. Cells that stain positive for both FITC Annexin V and PI are either in the end stage of apoptosis, are undergoing necrosis, or are already dead. Cells that stain negative for both FITC Annexin V and PI are alive and not undergoing measurable apoptosis (Figure 12).

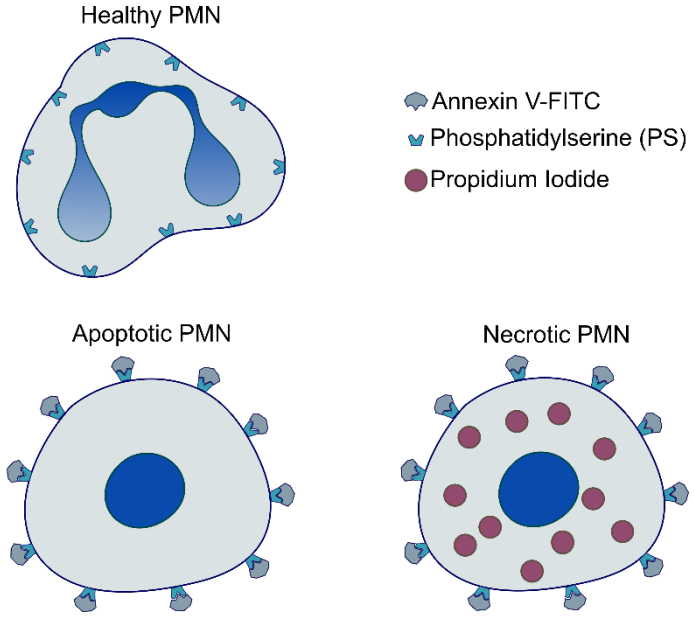

Figure 12: Measurement of apoptotic neutrophils by Annexin V staining. Healthy PMN have polymorphonuclear aspect, while apoptotic neutrophil presents a round nuclei, and superficial exposition of phosphatidylserine (PS) that bind to annexin V. In addition to PS exposition, necrotic PMN present damage in the cytoplasmic membrane, which allows the penetration of propidium iodide into the cytoplasm.

PMN were isolated from healthy volunteers using dextran sedimentation followed by gradient centrifugation as described in section 2.7. PMN were plated at $4x10^6$ cells/ml in a 6-well plate in RPMI 0.1%FBS. The cells were stimulated with GW9508 (10μM) and vehicle and incubated at 37ºC in a 5% CO_2 incubator for 18 hours. After incubation, cells were washed twice with cold DPBS and then re-suspend

in 1X Binding Buffer at a concentration of $1x10^6$ cells/ml. A hundred microliters of the solution ($1x10^5$ cells) were transferred to a 96-well plate. Ten microliters of staining solution containing 5µl FITC Annexin V and 5µl PI was added per sample. The cells were gently vortexed and incubated for 15 minutes at room temperature in the dark. After incubation, cells were transferred to 3ml tubes containing 400µl of 1X Binding Buffer to each tube. The cells were analysed by flow cytometry within 1 hour. FITC Annexin V and PI expression were recorded as MFI units in B530/30 and YG610/20 channels respectively, using a BD LSR Fortessa.

2.18.3. Efferocytosis assay

To quantify the clearance of apoptotic neutrophils by macrophages *in vitro*, a plate-based myeloperoxidase (MPO) assay was performed as previously described (Taylor et al., 2000). To perform this experiment, peritoneal macrophages were recruited by injecting 1ml 2% polyacrylamide beads (in sterile PBS) in C57Bl/6 (ip). After 4 days, the peritoneum was washed twice with 4ml EDTA (30µM in PBS). Cells were washed twice by centrifugation for 10 min at 300*g* and filtered through a 70µM cell strainer to remove biogel beads. Macrophages were counted as described before (section 2.7.1) and plated at a density of 0.5×10^6 cells per well in 24-well plate in SFM medium. Meanwhile, human neutrophils were isolated as described before (section 2.7.2) and left to apoptose for 18 hours in RPMI serum free medium. Two set of experiments were performed. First neutrophils were stimulated with vehicle (0.01% ethanol) or GW9508 (0.1, 1 and 10µM) for 18 hours in RPMI serum free medium. In a second set of experiments, macrophages were stimulated with vehicle (0.01% ethanol) or GW9508 (0.1, 1 and 10µM) for 18 hours in SFM medium. In both cases, after stimulation, cells were washed twice. Apoptotic neutrophils were counted and added at a ratio of 1:2 (macrophage:neutrophil). After 1 hour incubation, cells were washed with cold PBS and were fixed for 30 minutes in 2.5% glutaraldehyde. Cells were then rinsed with PBS, and the MPO assay was performed by adding 0.1 mg/mL

of dimethoxybenzidine and 0.03% (v/v) hydrogen peroxide. Cells were washed with PBS 1 hour later and were analysed by light microscopy, with four random fields being acquired per well (*n* = 2 wells per treatment). More than 400 cells were counted per treatment point.

IN VIVO METHODS

2.19. Mice

All experiments were approved and performed under the guidelines of the Ethical Committee for the Use of Animals, Barts and The London School of Medicine and Home Office regulations (Scientific Procedures Act, 1986). All experiments strictly followed UK Home Office regulations (Guidance on the Operation of Animals, Scientific Procedures Act, 1986). C57BL/6 mice were purchased from Charles River (London, United Kingdom). In all experiments age and sex-matched controls were used. Mice were fed standard laboratory chow and water *ad libitum* and were maintained on a 12-hour light-dark cycle under specific pathogen-free conditions.

2.20. K/BxN Serum Transfer Arthritis

Ten to twelve-week old male C57BL/6 mice were injected intraperitoneally (ip) with 100μl arthritogenic serum (generated in-house by crossing KRN TCR transgenic mice and NOD mice, and diluted 1:2 in PBS) on day 0 and day 2. Arthritic parameters were recorded everyday including clinical score, where any digits, wrists, ankles or pads on each limb were swollen, for a total score out of a possible twelve (Figure 13); weight loss (cachexia) and water displacement plethysmometry was performed to determine paw volume. The incidence of arthritis was also monitored.

Figure 13: Arthritis scoring procedure.
A scoring system was used to monitor the progression of the disease throughout the experiment as follows: each limb was inspected for signs of swelling and given a score based on the part of the paw which was swollen. Each paw can receive a total score of three, giving a maximum of 12 for each mouse. 0, No signal of arthritis. 1, Just one sign of swelling (digit, wrist, ankle or pad). 2, Combination of two swollen areas (more than one digit count as 1). 3, Swollen wrist or ankle AND pad AND any digit (Patel et al., 2012).

2.20.1. Treatment of K/BxN arthritic mice with GW9508

Ten to twelve-week old male C57Bl6 mice were administered 100µl K/BxN serum intraperitoneally day 0 and day 2. To assess the effects of GW0805 in the progression and pathogenesis of inflammatory arthritis, two protocols of treatments were used. First, arthritic mice received vehicle (0,1% ethanol, 100µl) and GW9508 (100µl, 10mg/kg) intraperitoneally from day 0 to day 6 to assess the effects of GW9508 during the initiation and progression of the inflammatory response. In a second set of experiments, arthritic mice received vehicle (0,1% ethanol, 100µl) and

GW9508 (100µl, 10mg/kg) intraperitoneally from day 5 to day 10 to assess the effects of this agonist in the resolution phase of the inflammatory response.

EX VIVO METHODS

2.21. Isolation of cells of the paws for flow cytometry analysis

C57Bl/6 mice received K/BxN serum for induction of arthritis as described in section 2.20. On day 8, cells from arthritic paws were isolated by collagenase digestion. Briefly, joints were collected by dissecting the paws of skin and cutting between digits, taking care to not break the bones. The paws were then transferred to an Erlenmeyer flask containing 15ml of digestion solution [collagenase D (0.5ng/ml) and DNAse (40ng/ml) in serum free RPMI]. The paws were incubated at 37^{o}C for 30 min whilst mixing at a medium speed on a magnetic stirrer. Following incubation, the digestion solution was collected into a 50ml centrifuge tube by passing the solution through a 70µm strainer, and kept on ice. Another 15ml of the digestion solution was added to the paws and incubated in a shaking chamber at 37^{o}C for 30 min on medium speed for a second time. The digest solution was collected by passing the solution through a 70µm strainer. The cells were centrifuged at 450*g* for 10 min at room temperature. Following centrifugation, the supernatant was discarded, and the cells were re-suspended in DPBS-/- for counting. The cells were stained for flow cytometry analysis.

2.22. GPR40 expression in cells from arthritic joints

C57Bl/6 mice received K/BxN serum for induction of arthritis as described in section 2.20. On day 6, cells from arthritic paws were isolated by collagenase digestion as described above. After counting, cells were transferred to a 96-well plate. Cells were then incubated with Zombie NIR^{TM} dye diluted 1:1000 in DPBS-/- for 20 minutes on ice and protected from the light. Zombie dye allows the separation between live and dead cells. Following incubation, cells were washed twice with flow

buffer (DPBS-/- containing 0.1% BSA) and anti-mouse Fc block diluted 1:5 in DPBS + 0.1% BSA was added to prevent nonspecific binding of antibodies. Following incubation, cells were washed twice with flow buffer. The following purified anti-mouse mAb were added to the cells for staining: CD45 (clone 30-F11, 2µg/ml, fluorochrome V450), CD11b (clone M1/70, 200ng/ml, fluorochrome Pe-Cy7), Ly6G (clone 1A8, 10µg/ml, fluorochrome APC), F4/80 (clone BM8, 250ng/ml, fluorochrome PE) and Ly6C (clone HK1.4, 200ng/ml, fluorochrome PerCP-Cy5.5) for 30 minutes on ice. Following the incubation, the cells were washed twice with DPBS + 0.1% BSA and re-suspended in 0.2ml of 1% PFA. Cells were transferred to clean microtubes and kept refrigerated until use. IgG isotype and unstained controls were also prepared for accurate calibration of the flow cytometry machine. Expression of CD45, CD11b, Ly6G, F4/80 and Ly6C were recorded as MFI units in the V450/50, YG780/60, R670/14, YG582/15 and B695/40 channels, respectively, of a BD LSR Fortessa. The same protocol described for GPR40 intracellular staining (section 2.12.1) was then followed to access the expression of GPR40 in the specific populations.

2.23. Gene expression in cells isolated from arthritic joints

C57Bl/6 mice received K/BxN serum for induction of arthritis as described in section 2.20 and treated with GW9508 as described previously. On the 6th day after the first injection, front paws were collected by dissecting the paws of skin and cutting between digits and stored in RNAlater® for RNA stabilization and protection and RNase inactivation and stored at -80^{o}C until use. About 30-50mg of the tissue was used for RNA extraction. Weighed tissue was transferred for 2ml Precellys tubes containing 600µl buffer RLT plus (containing 1:100 β-mercaptoethanol). Tissue was homogenised with a Precellys 24 machine (Bertin technologies) at 6500rpm for 30 seconds and left on ice for 5 minutes. This process was repeated 3 times. The lysate was then centrifuged for 3 minutes at 10000*g*. The supernatant was collected and

transferred for a gDNA Eliminator column. The protocol for RNA isolation described in section 2.11.1 was used. To eliminate any residue of DNA, purified RNA was treated with TURBO DNA-free™ kit. Thirty microliters of purified RNA were transferred to a clean 0.5ml microtube. To each sample, 3μl of 10X TURBO DNAse buffer and 2μl of TURBO DNase were added, which were then gently mixed. Samples were incubated at 37ºC for 20 minutes. After incubation, 7μl of DNase Inactivation Reagent was added to the sample, and mixed. Samples were incubated at room temperature for 2 minutes, mixing the samples every 30 seconds. Samples were centrifuged at 10000*g* for 90 seconds and transferred to a new tube. RNA was quantified as described in section 2.11.3. After RNA isolation, cDNA and qPCR were performed as in sections 2.11.4 and 2.11.6.

mRNA expression was analysed using the gene specific primers (Qiagen Quantitec Primer Assay®) for the following human genes: IL-1β, IL-4, IL-6, IL-10, NOS2 and TNF-α. The comparative Ct method (Pfaffl, 2001) was used to measure gene transcription in the samples. mRNA data were normalised relative to housekeeping gene mRNA (RPL13a) and then used to calculate expression levels. Results are expressed as $2^{-\Delta\Delta CT}$, which gives the relative amount of target gene normalised to the endogenous constitutive control. Negative controls were PCR without cDNA template

2.24. Histological staining and analysis

C57Bl/6 mice received K/BxN serum for induction of arthritis as described in section 2.20. On the 6th day after the first injection, joints were collected. The entire hind limbs with skin removed were fixed for 48 hours in neutral buffered formalin (40X the volume of the limb, around 50ml each; 10% neutral buffered formalin containing 0.4% sodium phosphate monobase and 0.65% sodium phosphate dibasic) before decalcification in 10% formic acid for 24 hours. To determine full decalcification, a fine

needle was used to test the softness of the bones. Once decalcification was complete, tissue was dissected into knee tissues and paw tissues and placed in labelled tissue cassettes for embedding separately. Cassettes were placed in running tap water for one hour, then left in tap water overnight to help remove the formic acid. Samples were then placed in 70% ethanol and processed for wax infusion in a Leica Tissue Processor. Finally, knee samples were embedded in molten paraffin wax using small molds. Knees were embedded coronally, so that the knee joint faced the front of the block with the femur and tibia perpendicular to each other. Embedded sample blocks were left to harden on a cold plate (-4^{o}C) before being removed from their molds. Blocks were taken kept at -20^{o}C degrees to harden for cutting. Sections (7μm) were cut using a Leica microtome, and placed on lukewarm water to remove wrinkles. Sections were transferred to charged glass microscope slides and left to dry.

Before staining, dried slides were placed in a 65^{o}C oven to soften the wax, which was removed by two 5 minutes incubations of Histoclear® (xylene replacement). Sections were rehydrated by moving from 100% ethanol from 5 minutes to 95% ethanol for 5 minutes followed by distilled water for 2 minutes before proceeding to staining.

2.24.1. Toluidine Blue Staining and cartilage quantification

Rehydrated slides were placed in 1% toluidine blue dye for 10 minutes before being washed with tap water for 5 minutes (or until the water was clear). Slides were air dried before mounting in DPX slide mountant and left to harden for 24 hours.

Percentage toluidine blue positive area was measured using ImageJ imaging software. Six-representative images per joint were obtained using an Olympus BH-2 light microscope with Nikon DXM1200 digital camera attached. Colour images were split into their individual red/green/blue channels and the channel which best represented the positive and negative staining was used for quantification (Figure 14).

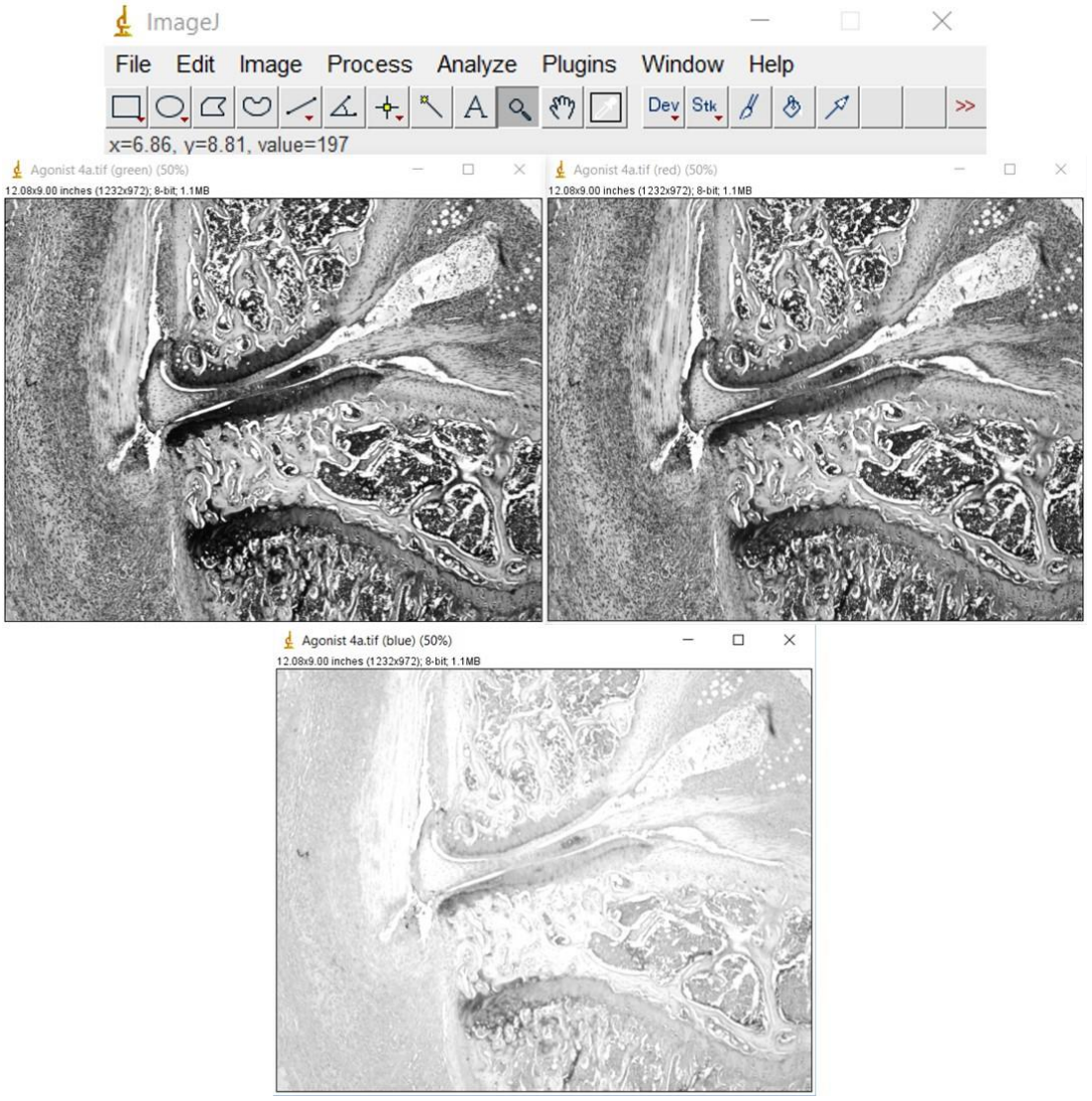

Figure 14: Split channels for cartilage damage evaluation by Image J.

The cartilage area was selected with the free hand tool. A positive threshold was applied by eye using positive and negative controls from the experiment and checked against the original colour image. With a free hand tool, the entire cartilage area was traced. The threshold mask was then measured over the selected area (Figure 15).

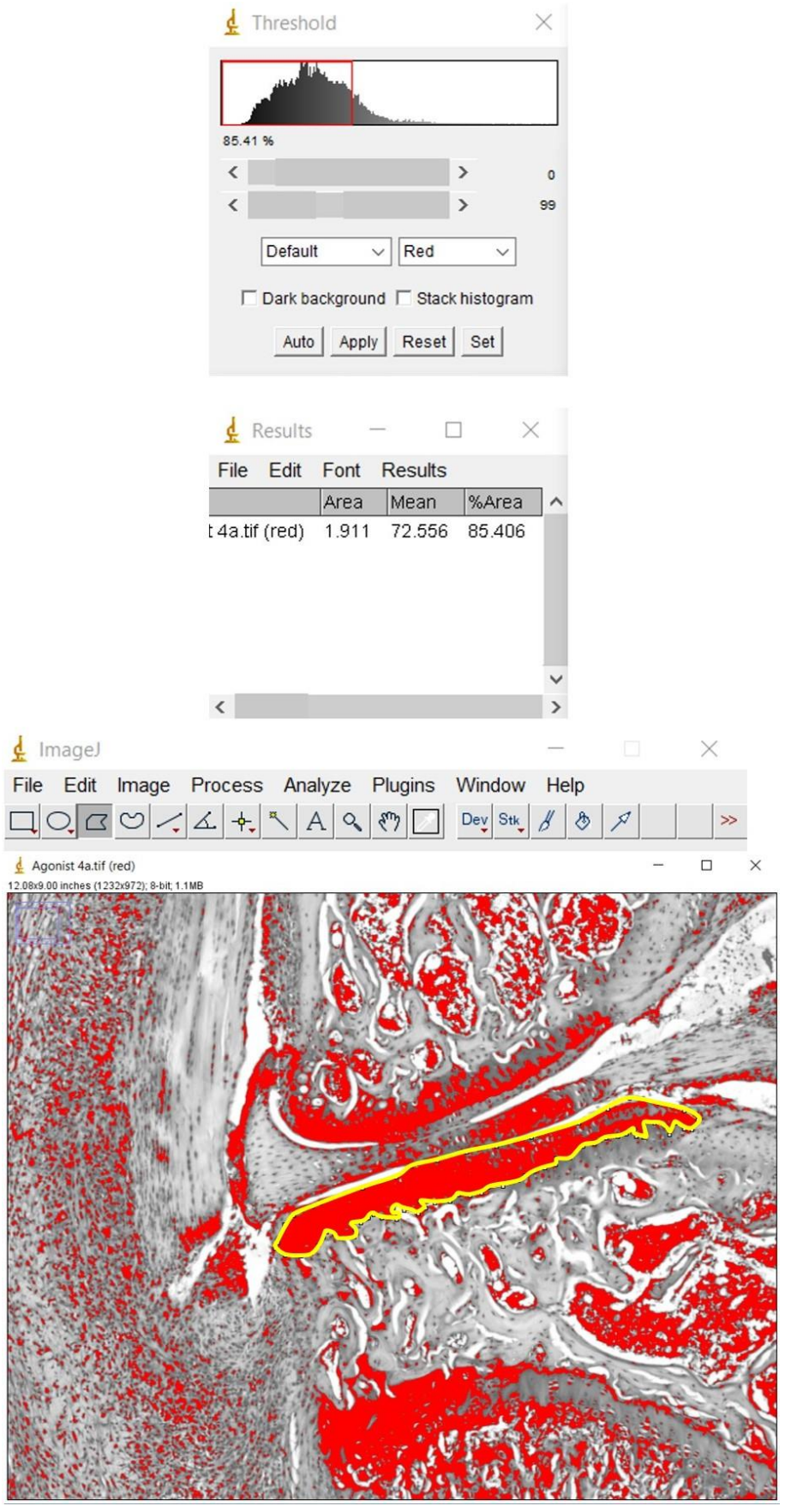

Figure 15: Cartilage selection area for quantification in Image J as indicated by yellow line.

2.24.2. Haematoxylin and Eosin (H&E) Staining and damage quantification

De-waxed and rehydrated slides were incubated in haematoxylin for 2 minutes then rinsed in tap water for 5 minutes to remove excess stain but also to blue the nuclei by introducing a more alkali pH. Slides were then stained for 1 minute in eosin before another wash in tap water. Slides were then dehydrated with 5 minutes each in graded ethanol (70%, 90% and 100% ethanol) followed by clearing twice in Histoclear® for 5 minutes. Slides were left to dry completely before mounting in DPX slide mounting solution and left to harden for 24 hours. Images were captures using an Olympus BH-2 microscope (Tokyo, Japan) and NIKON DXM1200 digital camera (New York, USA).

H&E sections were analysed and scored by two blinded scorers: 0 = normal, non-arthritic joint; 1 = moderate arthritis, minimal synovitis without cartilage/bone erosions; 2 = moderate arthritis, synovitis and erosions but joint architecture maintained; 3 = severe arthritis, erosions and loss of joint integrity. Results are expressed as the average from both scorers to each animal.

2.25. Statistical analyses

Statistical significance was assessed using GraphPad Prism 5 software. Data are expressed as mean ± standard error of the mean (SEM) of n experiments. Data were analysed using either 2-tailed paired or unpaired Student's *t* test, 1-way or 2-way ANOVA with appropriate post hoc analysis, Mann-Whitney *t* test, or 2-way ANOVA with repeated measures where appropriate. In all cases, $p < 0.05$ was considered significant to reject the null hypothesis.

CHAPTER 3: RESULTS

EXPRESSION AND MODULATION OF GPR40

3.1. Genomic expression of GPR40

The initial aim of my thesis was to evaluate the expression of GPR40 in cell types relevant to the inflamed joint, such as monocytes, macrophages, neutrophils, endothelial cells, lymphocytes and chondrocytes. I first assessed the basal expression of GPR40 in human primary immune cells isolated from blood, endothelium obtained from human umbilical cords and from the chondrocyte C28/I2 cell line grown in a 3D micromass (that augments the chondrocyte-like features) by using PCR. First, RNA integrity was checked by running 200ng of total RNA in a 0.8% agarose gel. A representative extraction from two different neutrophil samples is shown (Figure 16A). Only two bands were visualized in the gel, representing the 18s and 28s RNA, meaning that the RNA was intact (Figure 16A). After confirming the quality of RNA, conventional PCR was performed in all RNA isolates. As shown below, GPR40 mRNA was expressed in all the cell types tested (Figure 16B), including neutrophils and macrophages. There was some variation in levels of expression of the receptor in the different preparations of cells that may reflect the activation status of the cell. The expression of GPR40 in monocytes, macrophages, lymphocytes, HUVEC and chondrocytes was shown previously (Briscoe et al., 2003, Wauquier et al., 2013), but this is the first time that expression of GPR40 is reported in human neutrophils, an expression which appeared to be quite abundant.

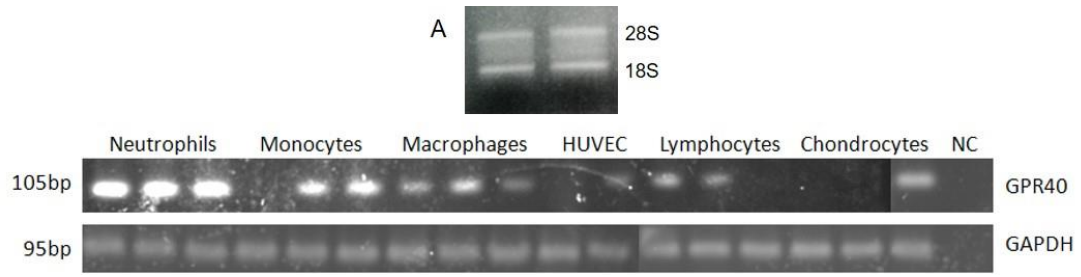

Figure 16: Expression of GPR40 mRNA in different cell types.
RNA was extracted from 1x10^6 cells using Trizol (PMN) or RNeasy mini kit, and GPR40 and GAPDH assessed using gene specific primers. (A) RNA integrity for neutrophil samples. (B) mRNA expression in neutrophils, monocytes, macrophages, HUVEC, lymphocytes and chondrocytes. NC, negative control was made by adding water in place of cDNA. bp, base pare. GAPDH, Glyceraldehyde 3-phosphate dehydrogenase.

3.2. Expression of GPR40 in human neutrophils

The next step was to demonstrate the protein expression of GPR40. Here, I focused on the first line of host defence, the neutrophils, that play important roles in inflammation and resolution. To do this, flow cytometry analysis was used to titrate a mouse IgG isotype control and anti-GPR40 antibodies. After serial dilutions of the antibody, a concentration of 0.181ng/ml was selected for the subsequent experiments, as this gave the biggest difference between the isotype and specific stain of GPR40, corresponding to a 1:100 dilution. (Figure 17A). The expression of GPR40 in neutrophils was also visualized by imaging flow cytometry (Figure 17B). The activation status of neutrophils was assessed by the levels of adhesion molecules L-selectin and CD11b. As expected, non-activated neutrophils present low CD11b and high L-selectin levels (Figure 17B).

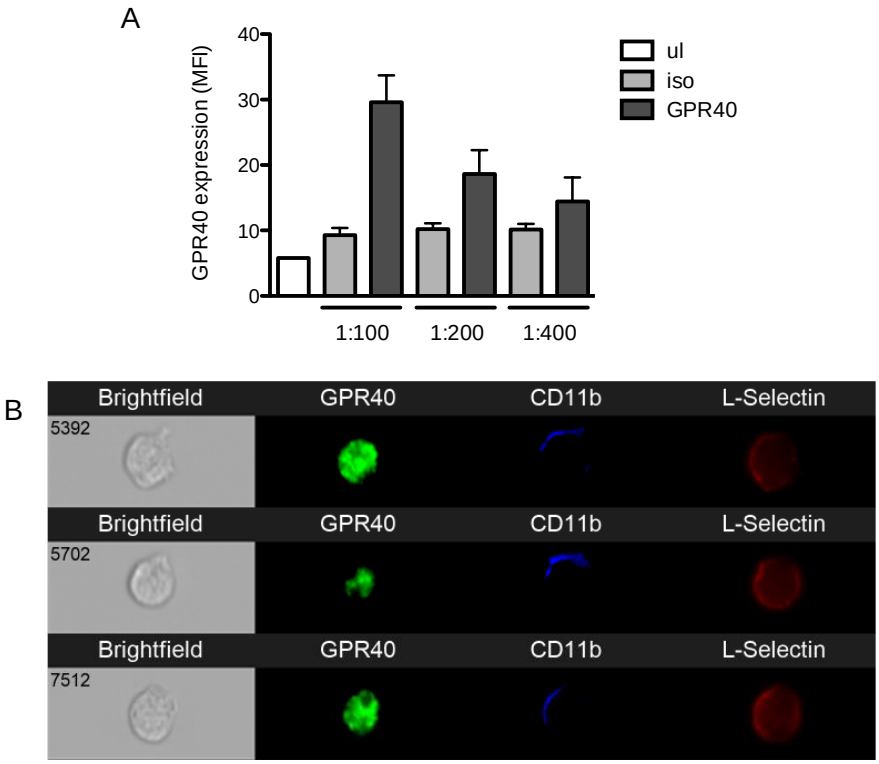

Figure 17: Expression of GPR40 in human neutrophils.
GPR40 levels in neutrophils isolated from healthy volunteers. (A) Titration of GPR40 antibody by flow cytometry. Each bar represents the mean ± SEM of 4 different experiments. (B) Expression of GPR40 and adhesion molecules in neutrophils by imaging flow cytometry (60x). ul, unlabeled cells. iso, IgG isotype control. MFI, median fluorescence intensity.

After demonstrating the expression of GPR40 in neutrophils, it was important to determine whether GPR40 gene expression was modulated or whether GPR40 is rapidly mobilized from granular stores after a short stimulation with inflamogens or trafficking to the inflammatory site. I therefore used a key cytokine involved in the pathogenesis of rheumatoid arthritis to test whether this receptor was transcriptionally controlled. Firstly, neutrophils were stimulated with TNF-α (10ng/ml, 4 and 6 hours), and the mRNA levels of GPR40 were assessed by real-time PCR. The amplification plot (Figure 18A and Figure 18C) and dissociation curve (Figure 18B and Figure 18D) for *gapdh* and *gpr40* are shown, respectively. As expected, the first cycle threshold for *gapdh* (Figure 18A) appears before the first cycle threshold for *gpr40* (Figure 18C). This is because GAPDH (Glyceraldehyde 3-phosphate dehydrogenase) is an enzyme involved in the glycolysis process, breaking down glucose for energy and carbon molecules. So, GAPDH is produced and highly expressed in all live cells at all times. The dissociation curves for *gapdh* (Figure 18B) and for *gpr40* (Figure 18D) are also shown, and illustrate, in both cases, the unique pattern of the melting curve for each reaction, in other words, all PCR products for the same primer pair has the same melting temperature, indicating that there is no contamination, mispriming (PCR products made due to annealing of the primers to complementary, or partially complementary sequences on non-target DNAs), primer-dimer artifacts (primers can sometimes anneal to themselves and create small templates for PCR amplification) or some other problem in the reaction. However, as shown on Figure 18E, the expression of GPR40 mRNA levels was not modulated by TNF-α (10ng/ml) in the chosen time-points

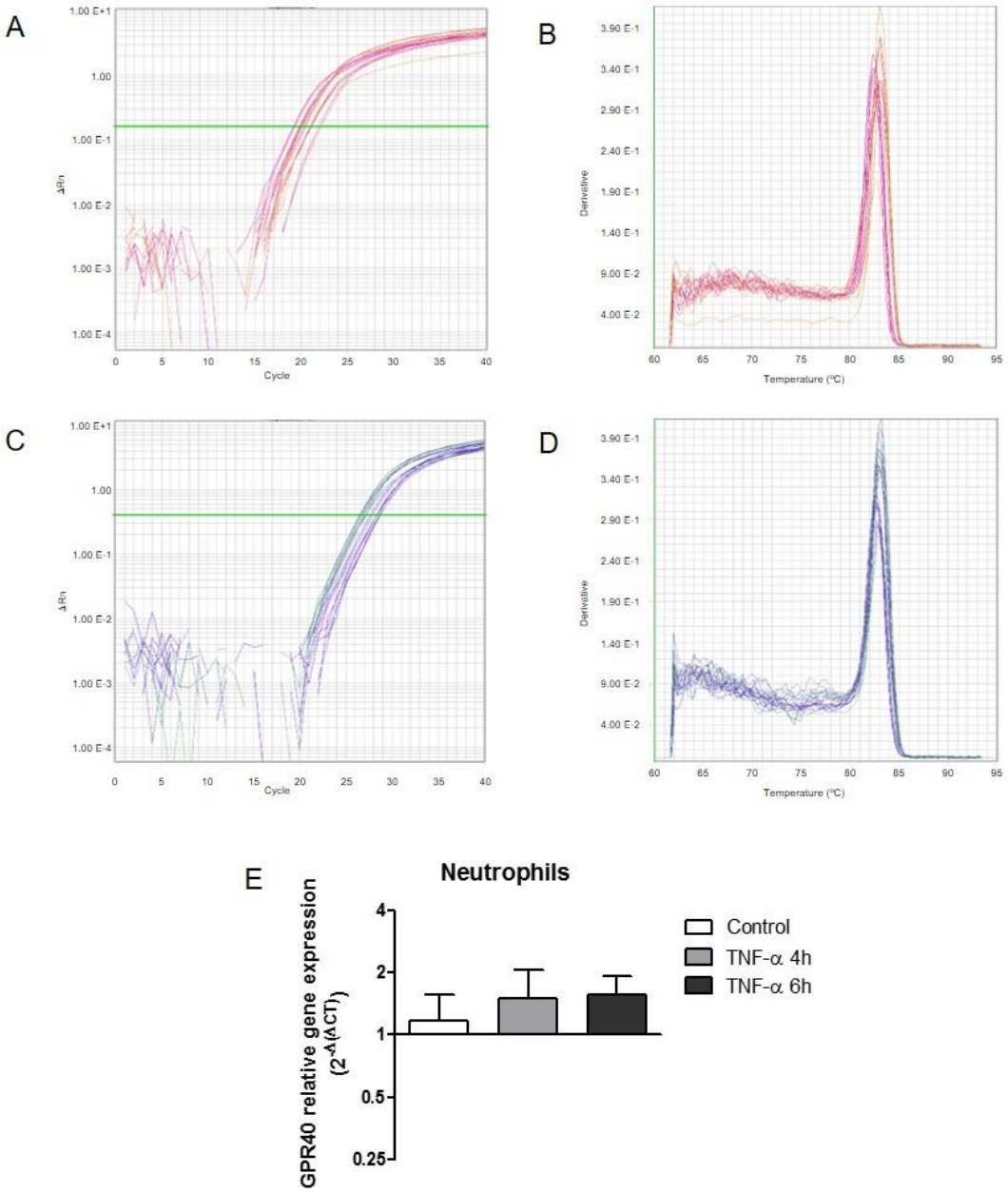

Figure 18: Modulation of GPR40 mRNA expression in neutrophils. Amplification plot and dissociation curve for *gapdh* (A and B, respectively) and *gpr40* (C and D, respectively). E, Levels of GPR40 mRNA expression in neutrophils after stimulation with TNF-α (10ng/ml) for 4 or 6 hours in 0.1% FBS RPMI. The relative expression of each gene, cycle threshold values, were normalized to a housekeeping gene (GAPDH) and expression quantified using $2^{-\Delta\Delta CT}$ with control unstimulated cells set as 1. Each bar represents the mean ± SEM of three different donors.

In another set of experiments, neutrophils were stimulated with TNF-α, IL-8 (a chemokine involved in the process of in vivo trafficking), PAF (a chemotactic agent capable of inducing enzyme release in neutrophils) and LTB_4 (a powerful chemotactic agent, which also induces the formation of reactive oxygen species and the release of enzymes in neutrophils). Protein expression of GPR40 was then analysed by flow

cytometry. To confirm the expression of GPR40 expression, some samples were not labelled with the antibody (UL). Rabbit IgG isotype control was also used to distinguish false positive staining (ISO). As shown below, the expression of GPR40 was not significantly modulated by TNF-α (10ng/ml) or IL-8 (10ng/ml) after 10 minutes (Figure 19A) when compared to vehicle (0.1% ethanol) stimulated cells (CT). On the other hand, PAF (10nM) and LTB_4 (10nM) stimulation increased the protein levels of GPR40 in neutrophils at the same time point. Figure 19B is an exemplification of the histogram overlay for GPR40 expression by flow cytometry, showing that after the stimulation with the selected mediators, intensity of fluorescence is shifted to the right.

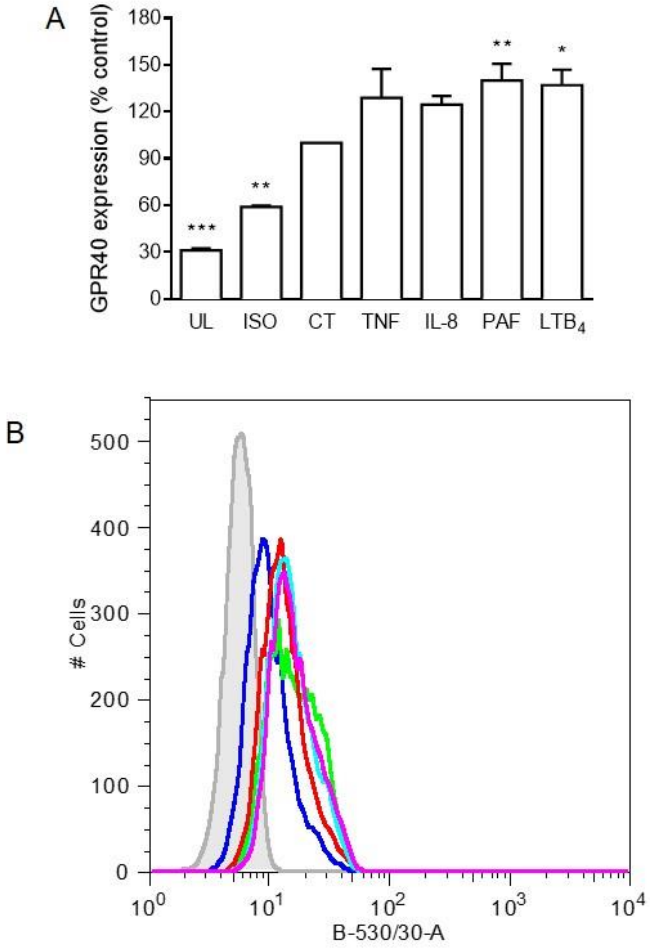

Figure 19: Modulation of GPR40 protein levels expression in human neutrophils.
Neutrophils isolated from healthy volunteers. (A) Levels of GPR40 protein expression after 10 minutes stimulation with TNF-α (10ng/ml), IL-8 (10ng/ml), PAF (10nM) and LTB_4 (10nM) at 37ºC. (B) Histogram overlay of the expression of GPR40 protein analysed by flow cytometry (Grey, isotype; blue control; green TNF-α; red IL-8; aqua, LTB_4 and pink, PAF). Each bar represents the mean ± SEM of three different donors. UL, unlabeled. ISO, isotype control, CT, control. MFI, mean fluorescence intensity. * $p<0.05$, ** $p<0.01$ and *** $p<0.001$ compared to control. 1-way ANOVA, followed by Dunnett's post-test.

It is well known that neutrophil recruitment to the site of inflammation results in an activation of those cells. The sensing of chemokines, and the physical contact with endothelial cells promotes a change in neutrophil profile, with substantial alterations in cellular composition, due to degranulation of a number of vesicles. To evaluate if this important step of the inflammatory response (the recruitment of cells) could modulate the expression of GPR40, human exudate neutrophils were isolated from the buccal cavity using a tabasco mouth wash in healthy volunteers (as described in section 2.8). Cells from whole blood were isolated as described in section 2.12.3. After isolation, cells were stained with antibodies to allow visualization by flow cytometry. Neutrophils were selected by size (FSC-A) and granularity (SSC-A) as represented in Figure 20A (whole blood sample) and Figure 20C (mouth wash sample) followed by selection of single cells (Figure 20B and D, representing samples from whole blood and mouth wash respectively). The activation level of neutrophils was assessed by measuring the levels of the adhesion molecules CD11b and L-selectin. As expected, neutrophils isolated from whole blood (red population Figure 20E) had a basal expression of CD11b, however, during the process to getting to the site of inflammation, in this case, promoted by tabasco mouth wash (blue population Figure 20F), a rapid increase in the expression of CD11b is seen in exudate neutrophils (Figure 20G). On the other hand, inactivated neutrophils showed high levels of L-selectin in the whole blood, expression that is lost during recruitment (Figure 20E and G). In addition, exudate neutrophils had a higher expression of GPR40 when compared to neutrophils isolated from peripheral blood in the same individual (Figure 20H and I).

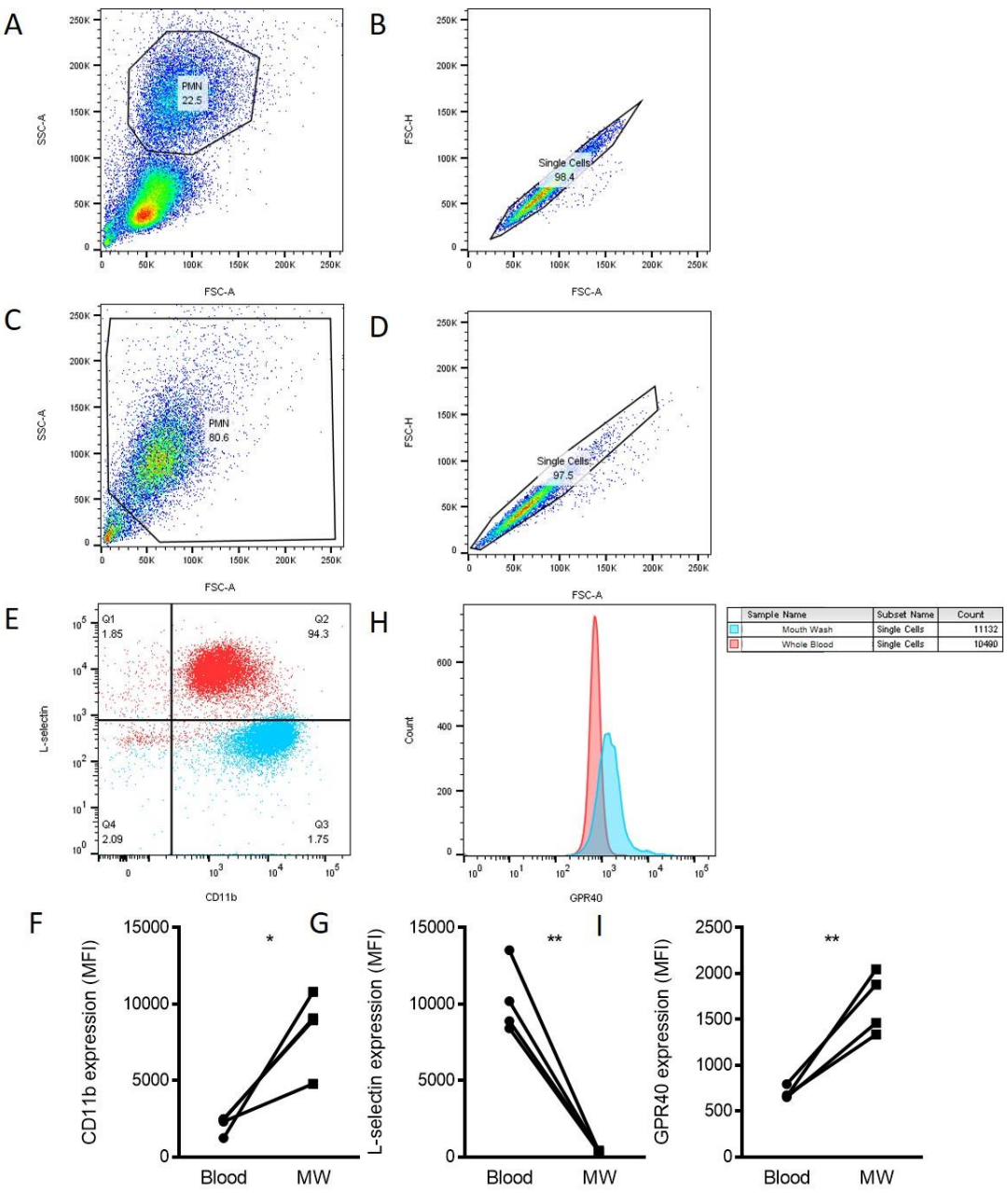

Figure 20: Expression of GPR40 in exudate neutrophils.
Blood was collected from healthy individuals and diluted to 1/10 volume of 3.2% sodium citrate. Red blood cells were lysed using a commercial kit. Neutrophils from the buccal cavity were isolated after mouth wash with Tabasco™ (MW). After antibody staining, PMN population from whole blood (A) and mouth wash (C) was selected by size (FSC-H) and granularity (SSC-H), followed by single cells selection (B and D, whole blood and mouth wash respectively) in flow cytometry. (E) Representative samples from whole blood (red population) and mouth wash (blue population) showing double staining of CD11b and L-selectin. (F) Expression of CD11b and (G) expression of L-selectin. (H) Representative histogram with expression of GPR40. (I) Expression of GPR40. Results are mean ± SEM, n=4. * p<0.05, **p,0.01 compared to control. Paired T-test**.**

3.3. Expression of GPR40 in macrophages

After showing expression and modulation of GPR40 in human neutrophils, I then decided to evaluate the expression of this receptor in macrophages, which are essential for clearance of cellular debris and the return of tissue homeostasis during the inflammatory process.

Expression of GPR40 in macrophages was previously demonstrated, however, most of those results used the THP-1 cell line or bone-marrow-derived macrophages (BMDMs) (Yan et al., 2013). I therefore evaluated the expression of GPR40 in primary human macrophages derived from blood monocytes with M-CSF (50ng/ml) for seven days (section 2.7.1). The protein expression of GPR40 in macrophages was determined by flow cytometry using the same concentration of the antibody used during assessment of the expression of this receptor in neutrophils. Positive expression of GPR40 was determined when compared to use of IgG isotype control (Figure 21).

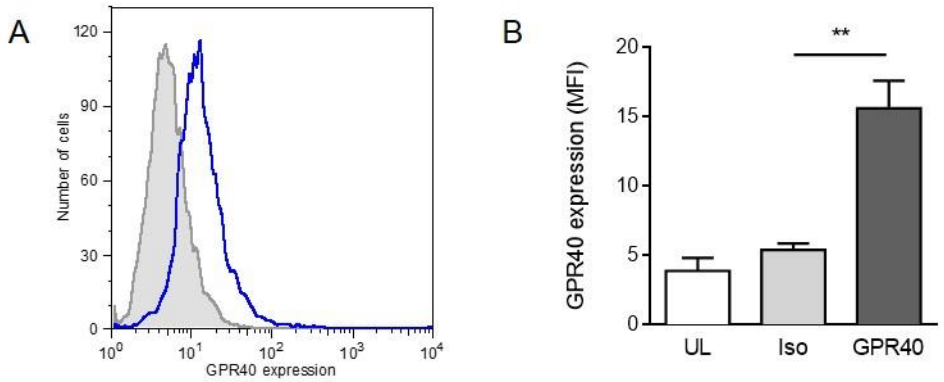

Figure 21: GPR40 expression in macrophages.
Monocytes were isolated from peripheral blood of healthy volunteers. Monocytes were separated from other PBMC by 1h adherence at 37ºC in RPMI medium without serum followed by seven days at 37ºC in RPMI supplemented with 10% FBS and 50ng/ml M-CSF. (A) Histogram overlay of the expression of GPR40 protein analysed by flow cytometry (Grey, isotype; blue GPR40). (B) MFI expression of GPR40. Each bar represents the mean ± SEM of four different donors. UL, unlabeled. Iso, isotype control. MFI, median fluorescence intensity.

Levels of mRNA for GPR40 were also assessed in macrophages stimulated with TNF-α (10ng/ml). As macrophages are longer lived cells compared to neutrophils, later time-points (6 and 18h stimulation) were chosen. The amplification plot (Figure 22A and Figure 22C) and dissociation curve (Figure 22B and Figure 22D) for *gapdh* and *gpr40* are shown, respectively. Again, expression of *gapdh* (Figure 22A) appears before the expression of *gpr40* (Figure 22C) at the amplification plots. Three samples showed lower levels of *gapdh* expression that could be due the quality of the RNA isolation or a human error during the preparation of real-time PCR assay. On the other hand, the dissociation curves for both primers tested were considered acceptable (Figure 22B and D). Figure 22E shows the expression of mRNA of GPR40 in the different times-points, but as can be visualised, TNF-α did not modulate the expression of this receptor after 6 or 18 hours of stimulation. Interestingly, CT values comparing neutrophils and macrophages indicated lower level of expression in macrophages, which corresponds to levels of mRNA expression by PCR (Figure 16) and protein expression by flow cytometry (Figure 21).

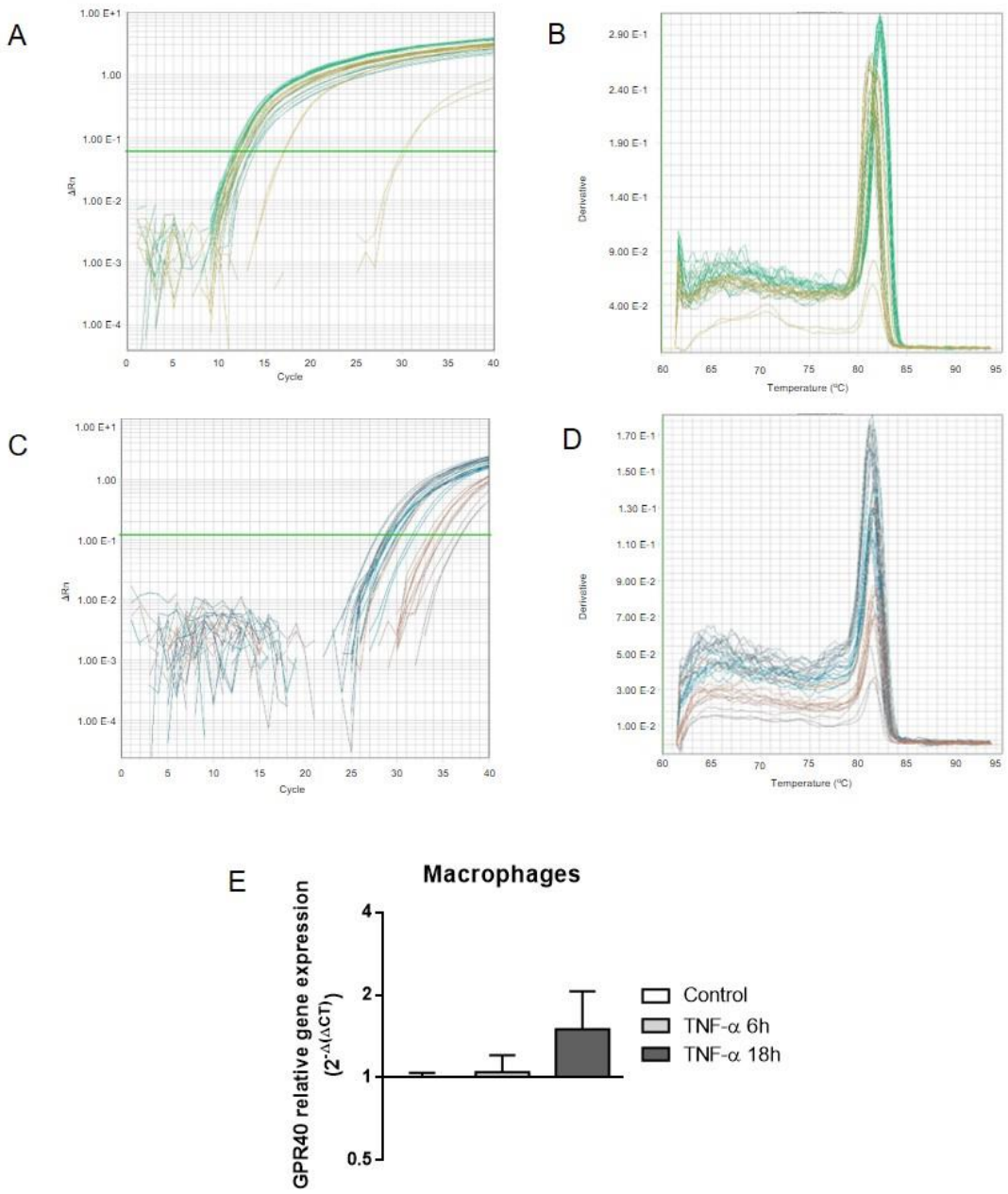

Figure 22: Modulation of mRNA GPR40 expression in human macrophages.
Amplification plot and dissociation curve for *gapdh* (A and B, respectively) and *gpr40* (C and D, respectively). E, Levels of GPR40 mRNA expression in macrophages after stimulation with TNF-α (10ng/ml) for 6 or 18 hours in 0.1% FBS RPMI. The relative expression of each gene, cycle threshold values, were normalized to a housekeeping gene (GAPDH) and expression quantified using $2^{-\Delta\Delta CT}$ with control unstimulated cells set as 1. Each bar represents the mean ± SEM of three different donors.

FUNCTIONALITIES OF GPR40 IN HUMAN LEUKOCYTES

3.4. GPR40-induced intracellular calcium mobilization in neutrophils

GPR40 is coupled to the α subunit of the Gq family of G proteins, and its activation in pancreatic islets is known to induce the activity of PLC, followed by hydrolysis of inositol lipids and an increase of intracellular calcium levels (Figure 23A) (Salehi et al., 2005). Because I demonstrated for the first time GPR40 expression in neutrophils, the next step was therefore to evaluate whether GW9508, a GPR40 selective agonist (Briscoe et al., 2006), was able to mobilise intracellular calcium in this cell type. As shown below, the concentrations of 0.1µM, 1µM and 10µM GW9508 promoted an intracellular calcium flux in neutrophils when compared to the vehicle control (Figure 23B). The time profiles for the changes in intracellular calcium levels at 0.1µM, 1µM and 10µM concentrations of GW9508 are also shown (Figure 23C).

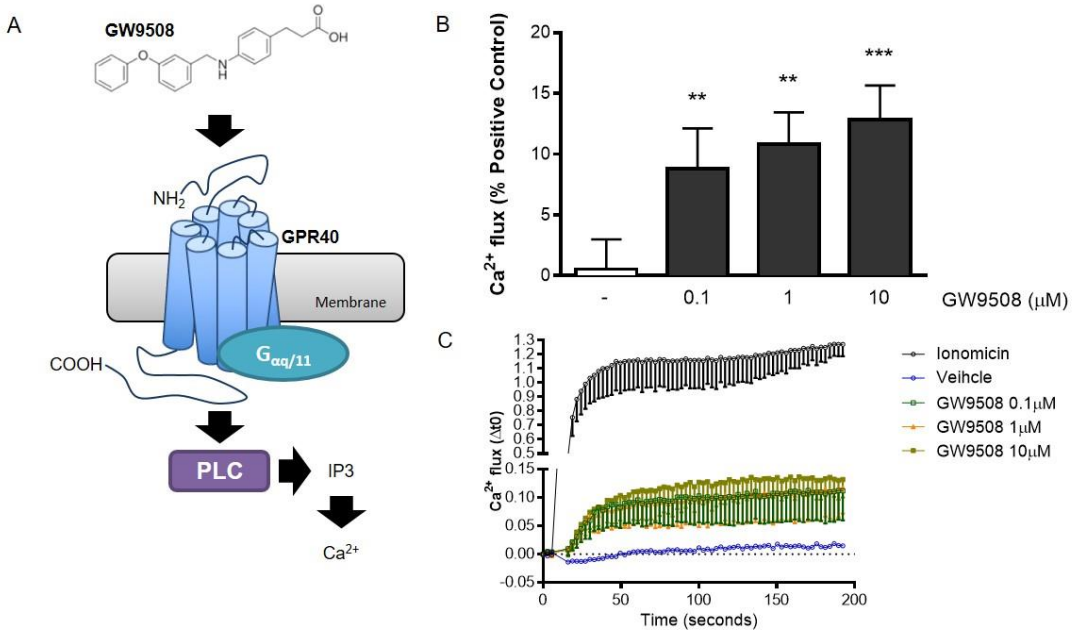

Figure 23: Intracellular mobilization of calcium by GW9508 in human neutrophils.
Neutrophils isolated from healthy volunteers were treated with Fura 2-AM and incubated with vehicle or GW9508 (0.1, 1 and 10µM final concentration). The intracellular calcium levels were recorded in a spectrophotometer. (A) Schematic of the cascade following activation of GPR40 by GW9508 resulting in intracellular calcium mobilization. (B) Intracellular calcium flux of GW9508 in neutrophils expressed as a percentage of the maximal response induced by the ionomycin positive control. (C) GW9508-induced calcium flux in neutrophils over time. Results are expressed as mean ± SEM from four independent experiments. ** p <0.01 and *** p <0.001 compared to vehicle (0.1% Ethanol); 1-way ANOVA, followed by Bonferroni post-test.

3.5. Modulation of PMN adhesion molecules by GW9508

Neutrophils are among the first cells to be recruited to the site of inflammation. Through a well-regulated cascade of events, neutrophils are capable of interacting with endothelial cells to migrate to the site of inflammation. One of the characteristics of this process is the change in adhesion molecule expression on both leukocytes and endothelial cells. Therefore, I assessed whether GPR40 activation leads to the modulation of adhesion molecules expression on neutrophils. L-selectin is involved in neutrophil tethering, the first step of recruitment, and it is expressed in higher levels in non-activated neutrophils. GW9508 did not modulate the expression of L-selectin with the concentrations chosen (Figure 24A). CD11b, is an integrin that is important during the adhesion step of recruitment. Expression of CD11b was also not modulated by treatment with GW9508 (Figure 24B). A tendency for an increase of CD11b expression could be visualised, but it did not reach statistical significance. In another set of experiments, neutrophils were pre-incubated with GW9508 followed by stimulation with TNF-α (a key cytokine involved in the pathogenesis of RA). TNF-α stimulation, as expected, promoted L-selectin shedding (Figure 24C). Whereas pre-incubation of neutrophils with GW9508 did not alter the modulation caused by TNF-α stimulation in neutrophils (Figure 24C). Also as expected, CD11b expression was increased after 10 minutes TNF-α stimulation. However, GW9508 pre-incubation did not alter the upregulation of CD11b induced by the cytokine TNF-α (Figure 24D).

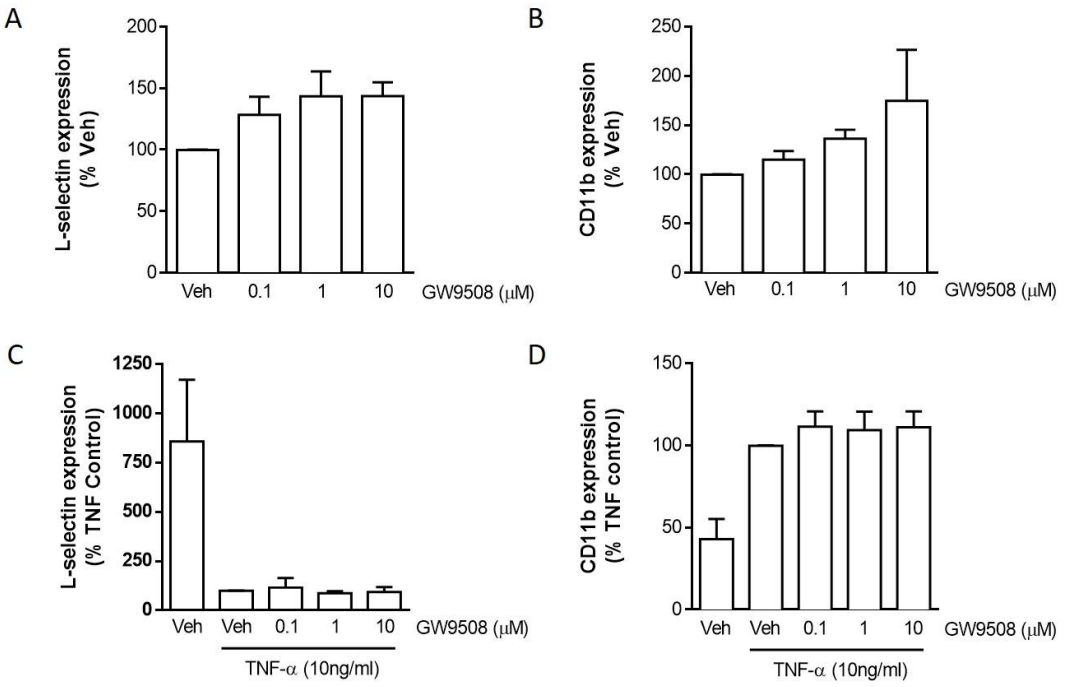

Figure 24: Modulation of adhesion molecules by GW9508 in neutrophils.
PMN isolated from the peripheral blood of healthy volunteers were treated GW9508 (0.1μM, 1μM and 10μM) for 10min at 37ºC. Expression of L-selectin and CD-11b in neutrophils without (A and C, respectly) or with TNF-α stimulation (10ng/ml) (B and D, respectly). Results are expressed as mean ± SEM from four independent experiments. One-way ANOVA, followed by Bonferroni post-test. Veh, vehicle (ethanol).

3.6. Effect of GW9508 on neutrophil-endothelial interactions under flow

The next step was to investigate the effect of GW9508 on neutrophil recruitment onto the endothelium under flow conditions. HUVEC were used in these assays due to the availability of the umbilical cords, ease of isolation and the essential advantage of using of primary endothelial cells. HUVEC express low levels of adhesion molecules, such as E-selectin, required to promote neutrophil rolling on the endothelium. Thus, monolayers of HUVEC were stimulated with the cytokine TNF-α for 4h to increase the levels of expression of ICAM-1, E-selectin and VCAM-1 (Mackay et al., 1993). As expected, the activation of monolayers of HUVEC caused a modest capture of the neutrophils, a prerequisite for further interactions, and hence both rolling and adherent neutrophils were visualised. However, GW9508 (1µM and 10µM) stimulation did not alter the number of neutrophils captured (Figure 25A), rolling (Figure 25B), adherent (Figure 25C) or transmigrated (Figure 25D) when compared to the vehicle control group. Nevertheless, the absence of induction of recruitment induced by GW9508 is in agreement with the lack of effect of GW9508 stimulation in modulating adhesion molecules on neutrophils (Figure 24).

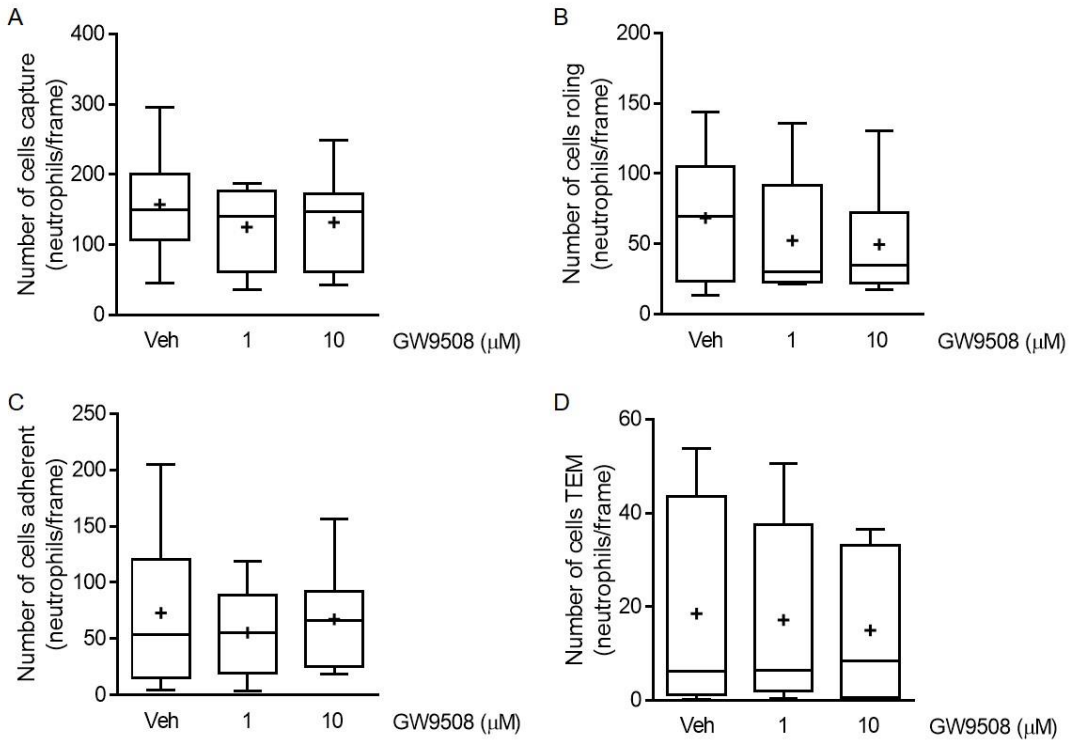

Figure 25: Effects of GW9508 on neutrophils-endothelial interactions under flow.
Neutrophils isolated from healthy volunteers were incubated with GW9508 for 10min at 37ºC. Number of neutrophils captured (A), rolling (B), adherent (C) and transmigrated (D) under flow. HUVEC were pre-incubated for 4h with TNF-α stimulation (10ng/ml), prior to the perfusion of neutrophils at 1dyne/cm^2. Interactions were quantified form 6 random fields/treatment. Results are expressed as max and min from eight independent experiments. + represents mean. TEM, trans-endothelial migrated. 1-way ANOVA followed by Bonferroni post-test. Veh, vehicle (0.1% ethanol).

It was then hypothesized that the level of GPR40 were not high enough to generate a modulation of the interaction of neutrophils-endothelial cells under flow. To test this hypothesis, neutrophils were pre-stimulated with LTB_4 (10nM) in $DPBS^{+/+}$ prior to stimulation with GW9508, as I demonstrated previously that this pro-inflammatory mediator can upregulate GPR40 in neutrophils (Figure 19A). The concentration of 1μM GW9508, which induced calcium flux in neutrophils (Figure 23C), was chosen for this assay. In agreement with results shown in Figure 25, GW9508 (1μM, 10 minutes) stimulation did not modulate capture (Figure 26A), rolling (Figure 26B), adherence (C) or transmigration (Figure 26C) of neutrophils under flow. Whereas LTB_4 stimulation promoted a decrease in the number of neutrophils rolling, and a tendency to increase adhesion and transmigration. Similarly, pre-stimulation with LTB_4 followed by GW9508 stimulation also decreased the number of neutrophils

rolling (Figure 26B), however, no modulation was observed in capture (Figure 26A), adherence (Figure 26C) or transmigration (Figure 26D). In general, these results show that treatment of neutrophils with GW9508 had little effect on their recruitment.

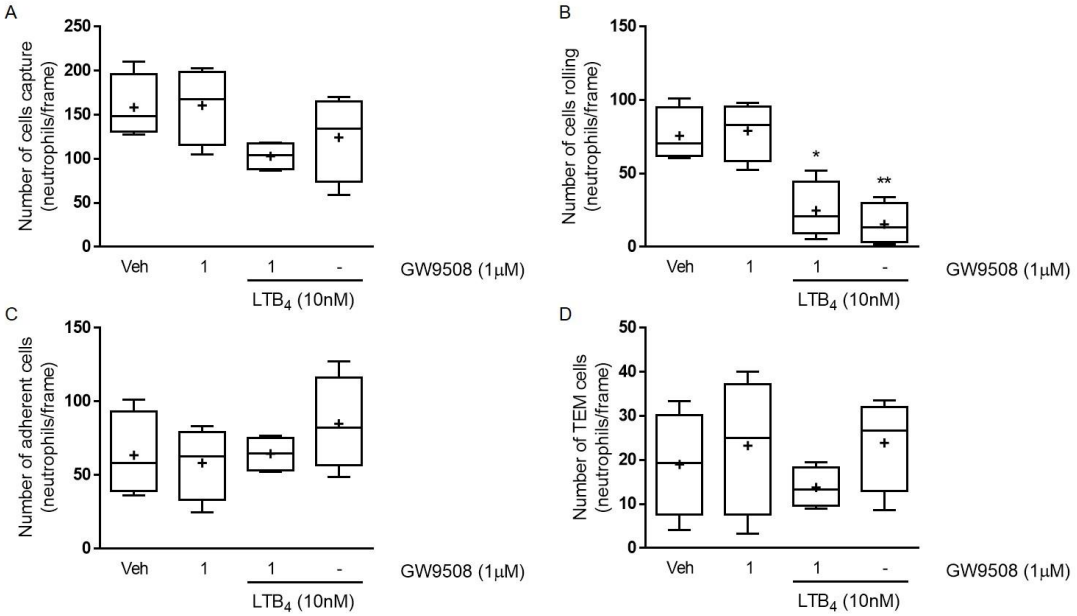

Figure 26: Effect of GW9508 on neutrophil-endothelial interactions after LTB_4 stimulation under flow.
Neutrophils isolated from healthy volunteers were pre-treated with LTB_4 (10nM) followed by treatment with GW9508 (1μM) for 10min at 37ºC. HUVEC were pre-incubated for 4h with TNF-α stimulation (10ng/ml), prior to the perfusion of neutrophils at 1dyne/cm^2. Number of neutrophils captured (A), rolling (B), adherent (C) and transmigrated (D) under flow. Interactions were quantified form 6 random fields/treatment. Results are expressed as max and min from four independent experiments. + represents mean. TEM, trans-endothelial migrated. * $p<0.05$ and ** $p<0.01$ when compared to Veh. 1-way ANOVA followed by Bonferroni post-test. Veh, vehicle (0.1% ethanol).

3.7. Effect of GW9508 on neutrophil chemotaxis

Chemokines play a key role in the process of leukocyte recruitment; their chief function is to direct cell migration. Thus, I next investigated the effects of GW9508 on neutrophil chemotaxis in response to the chemokine IL-8. Isolated human neutrophils were incubated with vehicle (0.1% ethanol) or pre-incubated with different concentrations of GW9508 (0.1, 1 and 10μM) in RPMI 0.1% FBS for 10 minutes, and the response to IL-8 tested. As shown below (Figure 27), incubation of neutrophils with GW9508 promoted a higher chemotactic response compared with vehicle alone. This effect was concentration-dependent, with the highest concentration of 10μM

evoking a cellular response over 80% higher than that quantified after application of IL-8 alone.

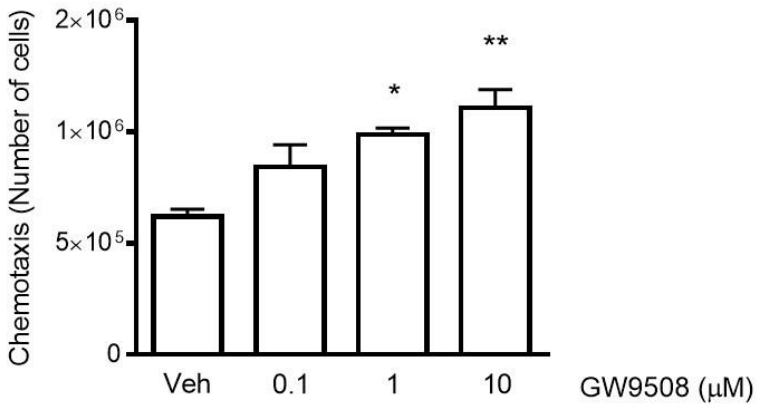

Figure 27: Effect of GW9508 treatment on the chemotaxis of neutrophils.
Neutrophils isolated from healthy volunteers were treated with GW9508 (0.1-10μM) or vehicle (0.1% ethanol) for 10min at 37ºC. Chemotactic response to IL-8 (30ng/ml) was assessed after 1 hour. Results are expressed as mean ± SEM from four independent experiments. 1-way ANOVA, followed by Bonferroni post-test. Veh, vehicle.

3.8. Effects of GPR40 agonist GW9508 on phagocytosis of *E. coli*

Different stimuli can trigger the inflammatory response, and bacterial infection is a very frequent cause of inflammation. Even in sterile inflammation, the phagocytosis of a variety of irritant particles, including crystals, minerals, and protein aggregates can damage the inflamed tissue. Phagocytic clearance of bacteria or cellular debris is one of the key steps for the resolution of inflammation. So, next I investigated whether GW9508 could alter the phagocytic ability of neutrophils and macrophages, key phagocytic cells. Phagocytosis was determined after incubation with labelled *Escherichia coli*. Figure 28A shows representative images of pre-stimulated human neutrophils with GW9508 (0.1-10μM) or vehicle (ethanol 0.1%) after 30min incubation with *E. coli*. Vehicle-stimulated neutrophils perform phagocytosis of *E. coli.* When neutrophils were stimulated with GW9508 the capacity of phagocytosis performance was increased, which was confirmed by the amount of intracellular *E. coli*. Indeed, 0.1μM GW9508 increased the phagocytosis by about 50% when compared to vehicle. The optimal concentration of GW9508 was 1μM,

leading to enhanced phagocytosis of 60% over vehicle stimulation. GW9508 was also effective at 10µM yet to a lesser extent when compared to lower concentrations (Figure 28B).

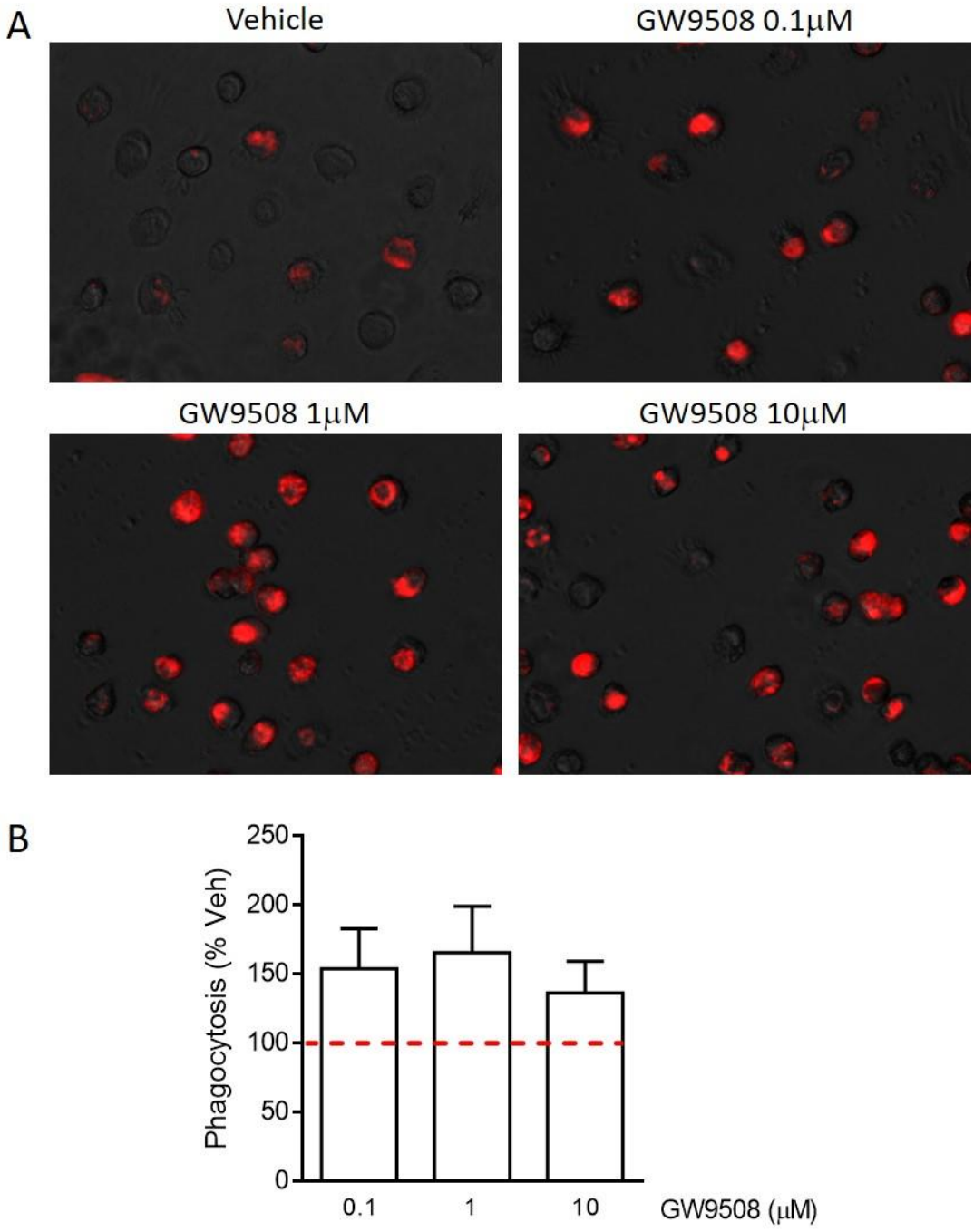

Figure 28: Enhanced *E. coli* phagocytosis by GW9508 in human neutrophils.
PMN isolated from the peripheral blood of healthy volunteers were stimulated with GW9508, 0.1µM, 1µM and 10µM) for 10min at 37ºC. Followed by incubation with BODYPI-labelled *E. coli* at 37°C for 30 minutes. After washing, the phagocytic level was recorded in a spectrophotometer. (A) Shows representative images of labelled E. coli in human neutrophils following treatment with GW9508. (B) Quantification of phagocytosis at 594 excitation spectra. Results are expressed as mean ± SEM from five independent experiments. 1-way ANOVA, followed by Bonferroni post-test. Veh, vehicle (0.1% ethanol).

In addition, phagocytic levels were also evaluated in human monocyte derived-macrophages after GW9508 stimulation. In this case, macrophages were incubated with *E. coli* for 1 hour. However, no modulation of the phagocytic response was visualised in any of the three concentrations of GW9508 tested (Figure 29).

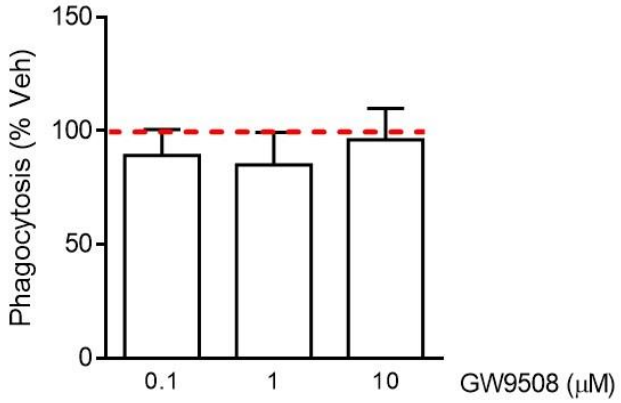

Figure 29: No effect of GW9508 on *E. coli* phagocytosis by human monocyte derived-macrophages.
PBMC were isolated from peripheral blood of healthy volunteers. Monocytes were induced into macrophages by culturing for 7 days in 10% FBS RPMI containing 50ng/ml M-CSF. Monocyte derived-macrophages were stimulated with GW9508 (0.1μM, 1μM and 10μM) for 18h at 37ºC. Followed by incubation with BODYPI-labelled *E. coli* at 37°C for 1 hour. After washing, the phagocytic level was recorded in a spectrophotometer at 594 excitation. Results are expressed as mean ± SEM from three independent experiments. 1-way ANOVA, followed by Bonferroni post-test. Veh, vehicle (0.1% ethanol).

3.9. Release of microvesicles induced by GW9508 in neutrophils

Cells can communicate between each other by sending small packages of information; these are called microvesicles that contain a wide range of protein and genomic information. Microvesicles are generated from the plasma membrane of many cell types, with leukocytes being particularly efficient in producing these blebs, though platelets are also highly active in this respect. Thus, it was tested if GW9508 stimulation in neutrophils could modulate the release of microvesicles; following cell incubation, microvesicles were purified from cell suspensions by a series of centrifugations. After staining, microvesicles were acquired using INSPIRE Instrument, a flow cytometer with a microscope attached allowing direct visualization (Figure 30A). Selection of the microvesicle population was made by plotting samples in intensity of BODIPY (FITC) against intensity of brightfield (Figure 30B). A more

refined selection of microvesicle was made by changing the scale on axis X and Y for 10 and 100, respectively, to reflect the small size of these microstructures (Figure 30C). Stimulation of neutrophils with GW9508 (10μM) in serum-free RPMI induced an increase in the microvesicle release (Figure 30D), similar to that observed with the positive control, TNF-α, a known stimulant for microvesicle release from human neutrophils (Headland et al., 2015).

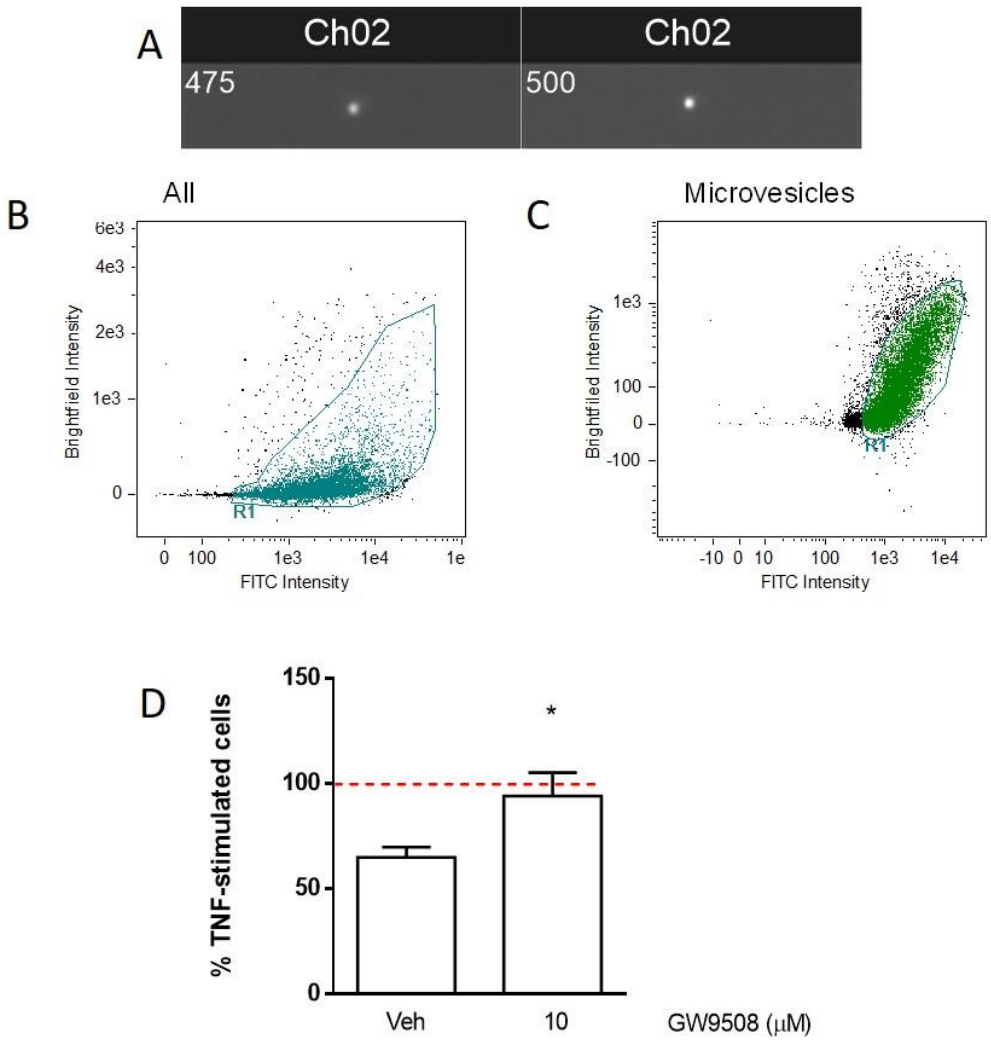

Figure 30: Neutrophil-microvesicle release induced by GW9508.
PMN isolated from the peripheral blood of healthy volunteers were stimulated with GW9508 (10μM) for 15min at 37ºC. After serial centrifugations, microvesicle were isolated. Microvesicle were stained with BODIPY and assessed by intensity in channel 2 of the INSPIRE Instrument. (A) Representative images of microvesicle. (B) Selection of microvesicle population. (C) Refined selection of microvesicle population. (D) Number of microvesicle released normalized to TNF-stimulated neutrophils. *<p 0.05. T-test. Veh, vehicle (0.1% ethanol). Dashed line represents TNF-α stimulated sample (10ng/ml, 15 minutes).

3.10. Effects of GW9508 induction on neutrophil apoptosis.

An important phase of the resolution of inflammation is neutrophil apoptosis, a process necessary for disposing these cells after they have killed pathogens and cleared debris. Otherwise, the continual release of mediators from the activated neutrophil into the tissue could lead to self-induced damage. The mode by which the neutrophil dies is also important: two main mechanisms can occur during neutrophil death, necrosis and apoptosis. Necrosis can cause tissue damage, by release of a range of mediators that are in the cytoplasm of neutrophils into the tissue by rupture of the cytoplasmic membrane. On the other hand, apoptosis preserves the membrane so those mediators will not be released into the tissue. As shown below, stimulation with GW8508 resulted in a delay of the natural apoptotic process when compared to vehicle (ethanol 0.1%) (Figure 31A). At later times points (8 and 18 hours), the difference between groups was reduced, and by 24 hours all cells were considered apoptotic (Figure 31A). Figure 31B shows representative images from neutrophils stimulated with vehicle (top) or GW9508 (bottom) for 2 hours.

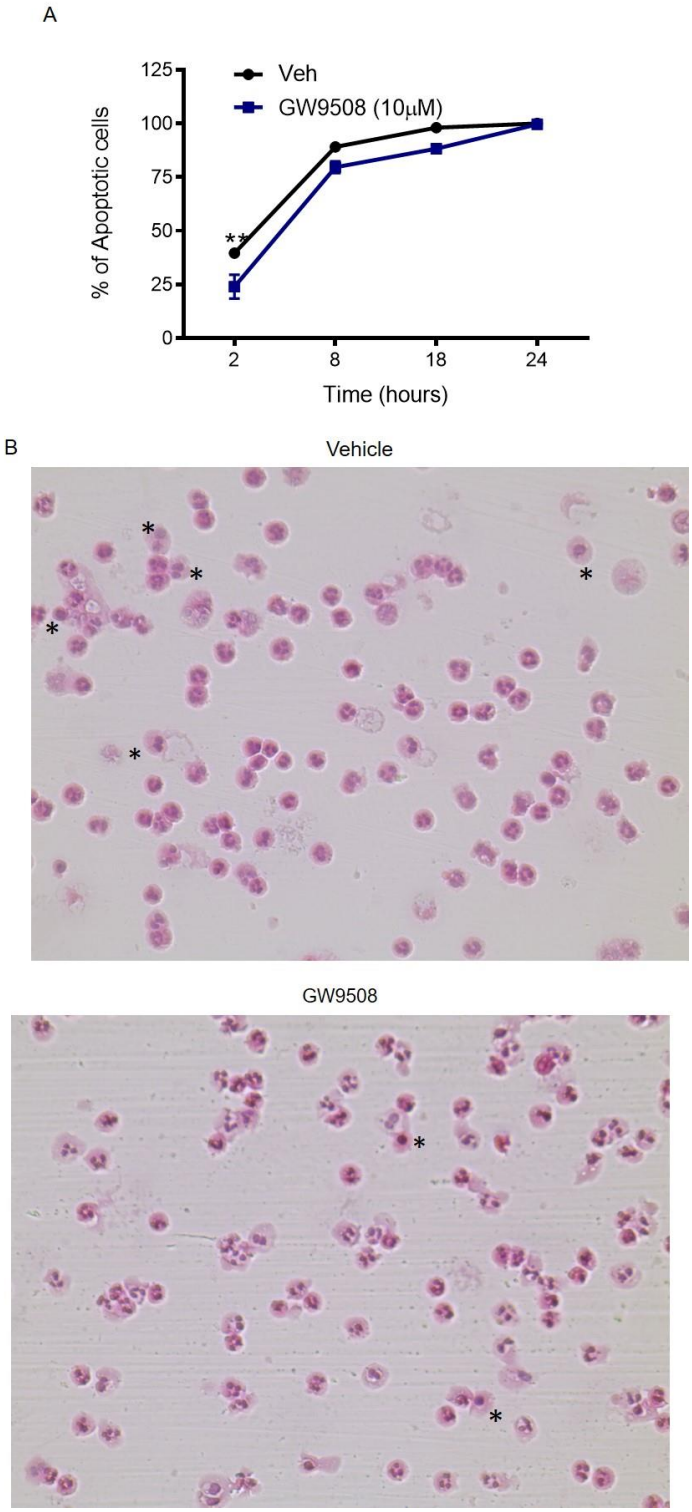

Figure 31: GW9508 stimulation delays apoptosis of human neutrophils.
PMN isolated from the peripheral blood of healthy volunteers were stimulated with GPR40 agonist (GW9508, 10μM). A, After 2, 8, 18 and 24 hours stimulation, 100μl of cells were transferred to a slide, stained with H&E and counted by light microscopy. Results are expressed as mean ± SEM from three independent experiments. **p<0.01 compared to Veh; 2-way ANOVA, followed by Bonferroni post-test. B, representative images from neutrophils stimulated for 2 hours with vehicle or GW9508 (x40 magnification). Stars represent apoptotic cells.

A second protocol was used as it has higher sensitivity. This time, neutrophil apoptosis was assessed by measuring the level of staining for annexin V and propidium iodide(PI). Neutrophils were stimulated with GW9508 (10µM) in RPMI 0.1% FBS for 18 hours. After stimulation, cells were stained with annexin V and PI. During apoptosis there is a loss of membrane asymmetry and PS is exposed on the cell surface, onto which annexin V binds. In addition, apoptotic cells can be differentiated from necrotic cells by the capacity of PI entry into the cytoplasm. Figure 32A and Figure 32B show representative images from vehicle-stimulated and GW0508-stmulated neutrophils, respectively. Once more, delay of apoptosis was visualised in the GW9508 stimulated-group, when compared to vehicle (0.1% ethanol) (Figure 32C). Interestingly, stimulation did not result in an increase of necrotic cells (Figure 32D), rather GW9508 increased the life-span of neutrophils (Figure 32E).

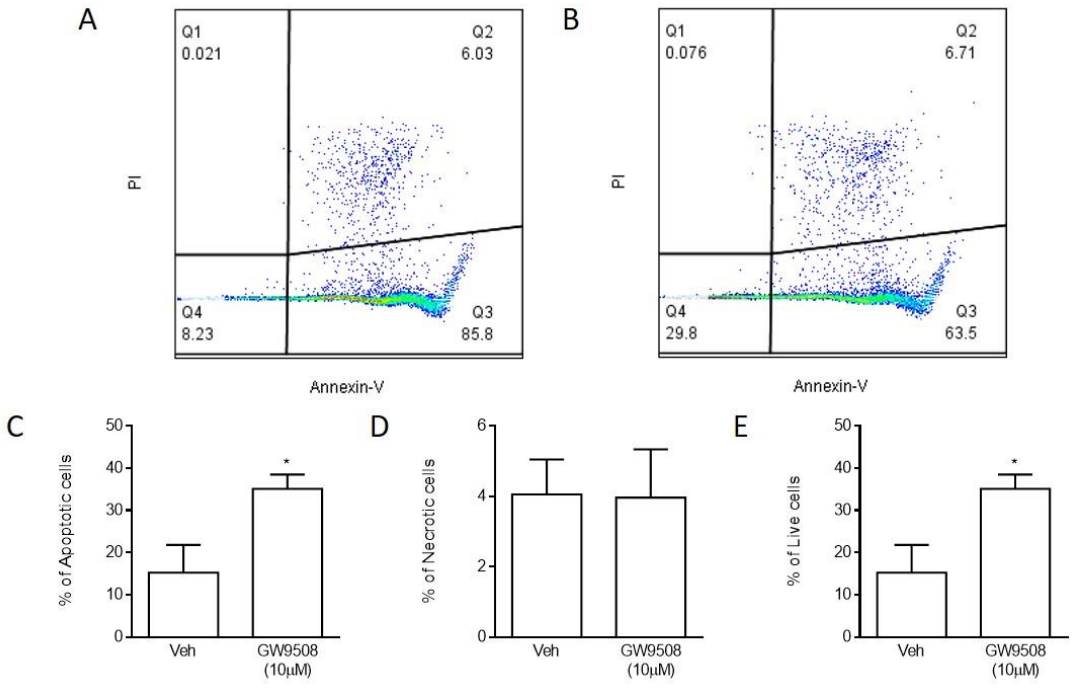

Figure 32: Measurement of neutrophil apoptosis by flow cytometry.
After 18 hours incubation at 37ºC with or without GW9508 (10µM), cells were washed and stained for annexin-V and PI and assessed by flow cytometry. (A) and (B) show representative image from vehicle- and GW9508-stimulated neutrophils, respectively. Percentage of (C) apoptotic cells, (D), necrotic cells and (E) live cells. Results are expressed as mean ± SEM from three independent experiments. *p<0.05 compared to Veh; T-test. Veh, vehicle.

3.11. M1/M2 polarization of macrophages by GW9508

Another important step for the resolution of inflammation is the switching from pro-inflammatory to pro-resolution cell phenotypes and mediators. When macrophages are sampling and encounter a xenobiotic (be it a pathogen or damaged tissue), their receptors trigger a *decision* to fight (kill it) or fix (repair it). The fight profile is associated with M1 macrophages and is characterized by production of pro-inflammatory mediators (Italiani and Boraschi, 2014). While the fix profile is associated with M2 macrophages and characterized by production of pro-resolution mediators. Therefore, to test if activation of GPR40 could modulate macrophage phenotype, monocyte derived-macrophages were pre-treated with GW9508 (10μM) in macrophage SFM medium for 24 hours and stimulated with IFN-γ/LPS (10ng/ml/50ng/ml) for 24 hours, to induce a M1 phenotype, or with IL-4 (10ng/ml) to induce a M2 phenotype. Cultures of macrophages were then analysed by flow cytometry. As shown below, cells were selected by size (FSC-H) and granularity (SSC-H) (Figure 33A) and macrophages selected by expressing low intensity of CD14 (Figure 33B). The profile of polarization was measured by levels of expression of CD86 and MHC-II for M1 macrophages and CD206 for M2 macrophages. Stimulation of macrophages with GW0508 did not significantly alter the expression of the M1 markers CD86 (Figure 33C) or MHC-II (Figure 33D), although the results showed a tendency to increase CD86 expression after GW9508 stimulation in IFN-γ/LPS-stimulated cells. Activation of GPR40 also did not modulate the basal expression of the M2 marker CD206 (Figure 33E) nor following IL-4 stimulation.

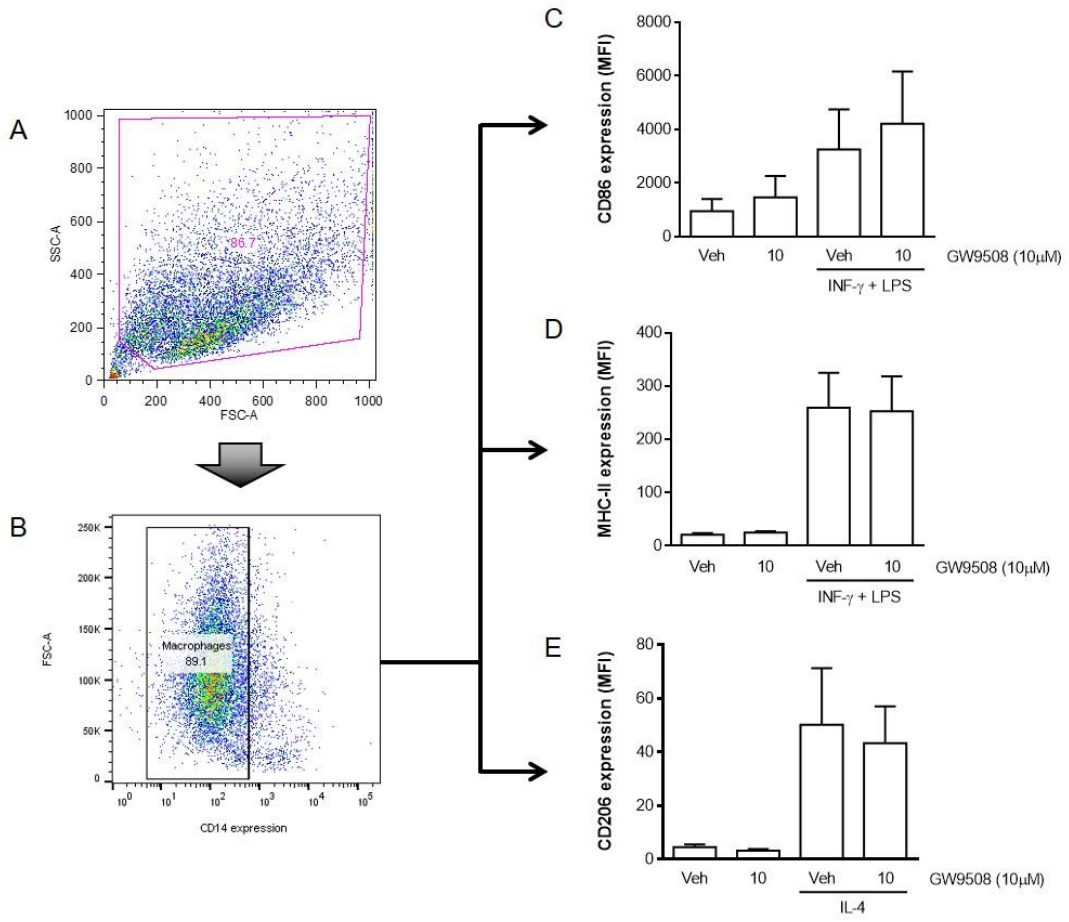

Figure 33: GW9508 does not affect M1/M2 polarization of human macrophages.
PBMC were isolated from peripheral blood by density gradient centrifugation. Monocytes were separated from other PBMC by 1h adhesion at 37ºC followed by differentiation over 7-day culture in 10% FBS RPMI containing 50ng/ml M-CSF. Monocytes derived-macrophages were treated with GW9508 (10µM) for 24h at 37ºC in MSF media. Without removing compounds, IFN-γ (10ng/ml) and LPS (50ng/ml) or IL-4 (10ng/ml) was added and incubated at 37°C for 24h. After washing, cells were stained and expression was determined by flow cytometry. (A) Selection of cells by size (FSC-H) and granularity (SSC-H). (B) Selection of macrophages ($CD14^{Low}$). Expression of (C) CD86, (D) MHC-II, and (E) CD206. Results are expressed as mean ± SEM from three independent experiments. 1-way ANOVA, followed by Bonferroni post-test. MFI, median fluorescence intensity. Veh, vehicle (0.1% ethanol).

3.12. Effects of GW9508 stimulation in efferocytosis

As mentioned in the Introduction chapter, efferocytosis is the process where apoptotic cells are phagocytosed by macrophages. This process is of fundamental importance as it prevents secondary necrosis of the apoptotic neutrophil thus avoiding perpetuation of tissue damage. Above, I showed that GW9508 stimulation delayed neutrophils apoptosis (Figure 31). At this stage, to evaluate if efferocytosis was also modulated by GW9508, two sets of experiments were performed. Firstly, I treated

neutrophils with GW9508 and secondly macrophages. In both cases, apoptotic human neutrophils and peritoneal mouse macrophages were utilised. Mouse macrophages were isolated after injection of 2% Bio-gel polyacrylamide beads in PBS (i.p.): Bio-Gel-elicited macrophages are free of intracellular debris because Bio-Gel beads cannot be phagocytosed by macrophages, making these cells more suitable for the studies pertaining to phagocytosis. Mouse macrophages were chosen for this assay as it was more precise to count the mature macrophages than plate human monocytes and induce into macrophages, which could result in different numbers between repetitions.

In the first set of experiments, human neutrophils were stimulated for 18 hours with vehicle or GW9508 (0.1, 1 and 10μM) in RPMI serum-free overnight. Following stimulation, neutrophils were washed twice in DPBS-/- and apoptotic neutrophils were added to the macrophages at a ratio of 1:2 (macrophage:neutrophils). Cells were incubated for 1h. After incubation, non-ingested neutrophils were removed and MPO assay was performed to selectively stain intracellular neutrophils. Macrophages containing ingested neutrophils could be differentiated by the presence of brown areas, as visualised in Figure 34A. As expected, vehicle-stimulated macrophages have the ability to ingest apoptotic neutrophils. Interestingly, the ability to recognise and ingest apoptotic neutrophils was impaired after GW9508 stimulation at all three concentrations tested (Figure 34B).

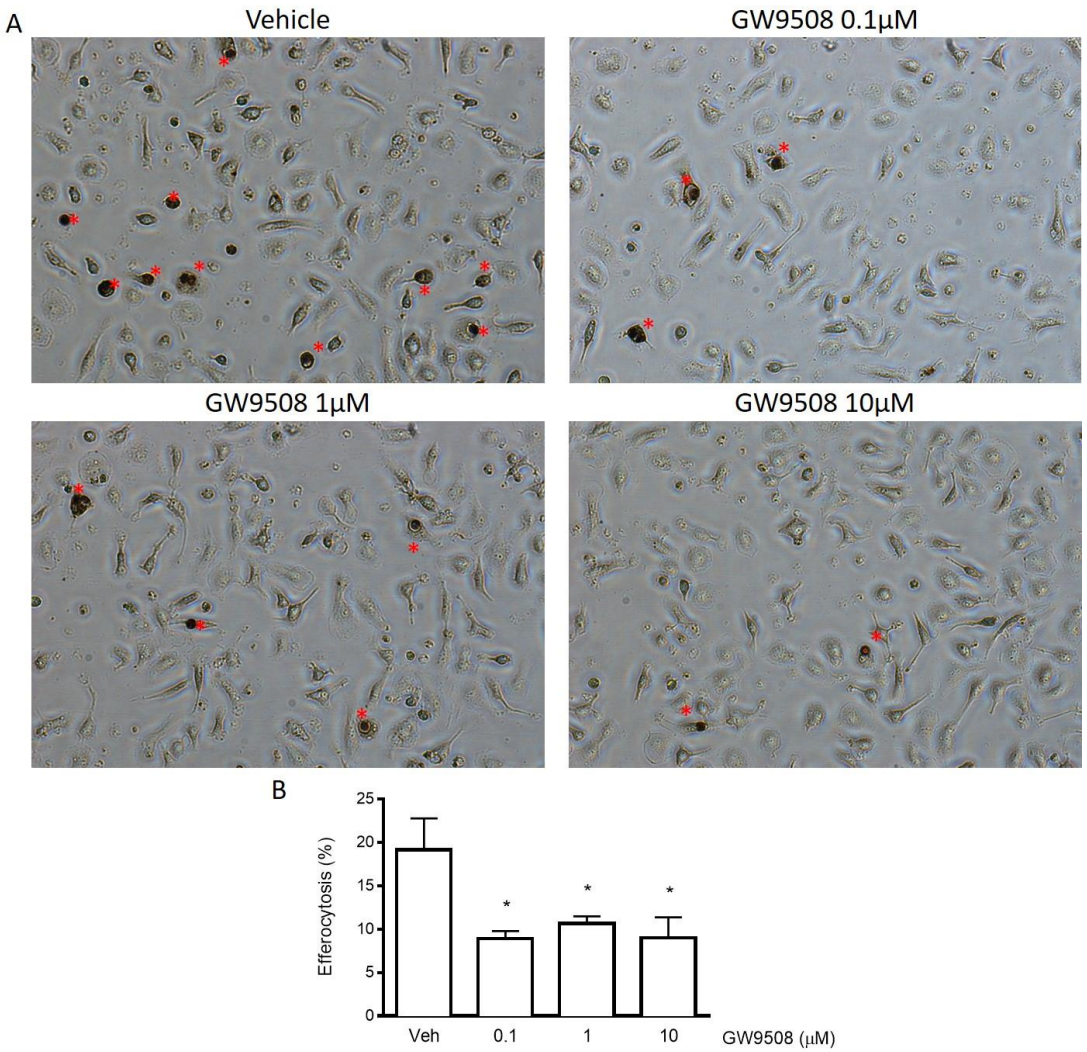

Figure 34: GW9508 impairs efferocytosis of neutrophils.
Human neutrophils were stimulated with vehicle or GW9508 (0.1-10µM) in FBS- free RPMI for 18 hours. Apoptotic neutrophils were then added to Bio-Gel–elicited macrophages (obtained from C57/Bl6 mice) at a ratio of 1:2 (macrophage:neutrophils) for 1 hour. Cells were then washed to remove non-ingested neutrophils, and the MPO assay was performed to selectively stain intracellular neutrophils. Images were acquired by light microscopy assessing more than 400 cells per treatment. (A) Representative images of macrophages after the MPO assay was performed. Red stars identify macrophages that have internalised an apoptotic neutrophil. (B) Percentage of positive macrophages. Results are expressed as mean ± SEM from four independent experiments. $p<0.05$ compared to vehicle. 1-way ANOVA, followed by Bonferroni post-test. Veh, vehicle (0.1% ethanol).

In the second set of experiments, macrophages were stimulated with the GPR40 agonist for 18 hours. Meanwhile, human neutrophils were left to die in RPMI serum-free overnight. Following stimulation, macrophages were washed twice in DPBS-/- and apoptotic neutrophils at ratio of 1:2 (macrophage:neutrophils) were added. Cells were incubated for 1h. After incubation, non-ingested neutrophils were removed and MPO assay was performed to selectively stain intracellular neutrophils.

Macrophages containing ingested neutrophils were counted (Figure 35A). As expected, vehicle-stimulated macrophages have the ability to ingest apoptotic neutrophils, however GW9508 failed to modulate this cellular response at any of the concentrations (Figure 35B).

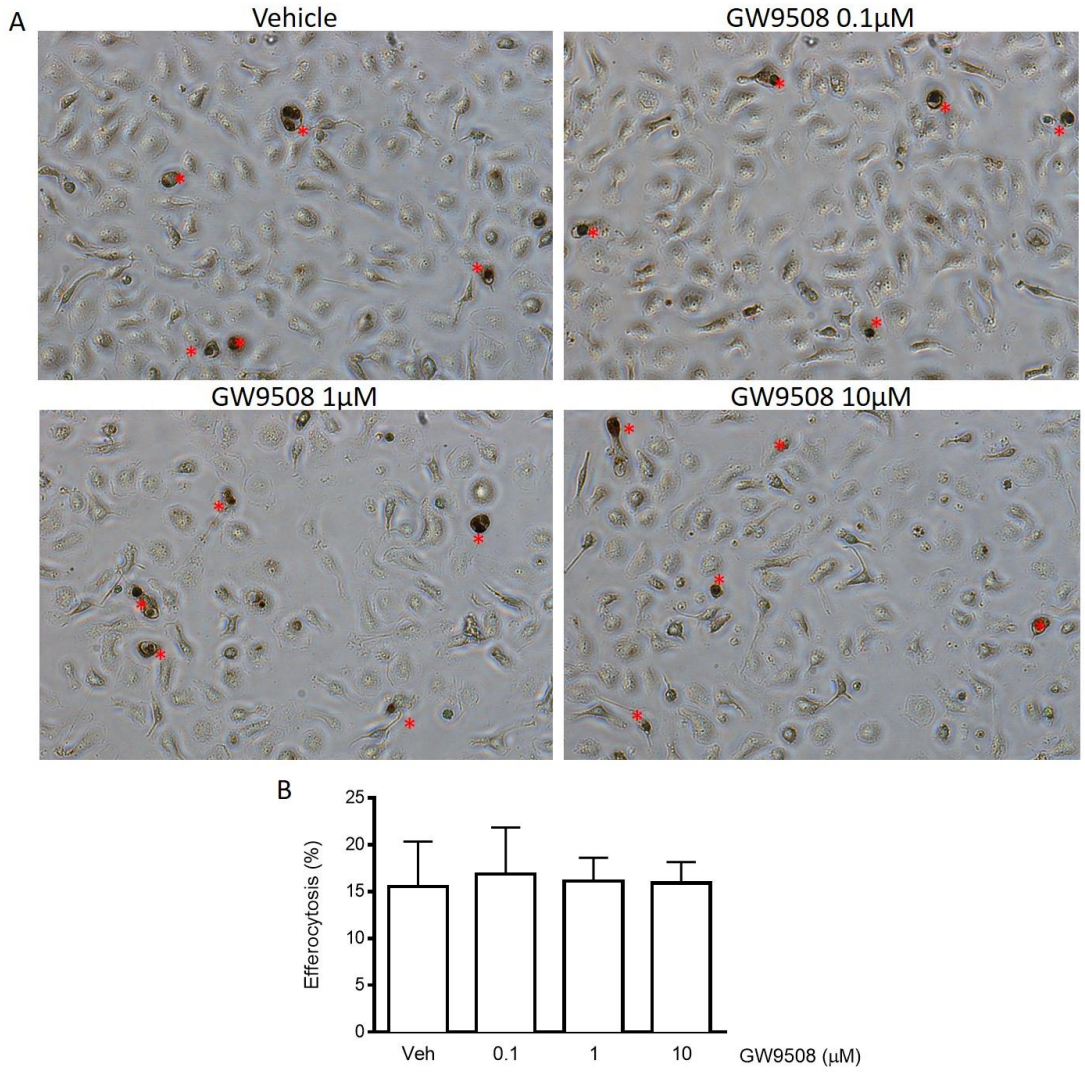

Figure 35: GW9508 do not modulate efferocytosis in stimulated mouse macrophages.
Human apoptotic neutrophils were added to Bio-Gel–elicited macrophages (obtained from C57Bl/6 mice) previously pretreated with vehicle or GW9508 at a ratio of 1:2 (macrophage/neutrophils) and were incubated for 1 hour. Cells were then washed to remove non-ingested neutrophils, and the MPO assay was performed to selectively stain intracellular neutrophils. Images were acquired by light microscopy assessing more than 400 cells per treatment. (A) Representative images of WT cells after the MPO assay was performed. Red Star identify macrophages that have internalised an apoptotic neutrophil. (B) Percentage of positive macrophages. Results are expressed as mean ± SEM from three independent experiments. 1-way ANOVA, followed by Bonferroni post-test. Veh, vehicle (0.1% ethanol).

ROLES OF GPR40 *IN VIVO*

3.13. Expression of GPR40 in cells from murine arthritic joints

After demonstrating expression of GPR40 in human cells, and evaluating the potential roles of this receptor by using a selection of cell assays, the next aim was to evaluate the expression of this receptor in an experimental model of arthritis, allowing a better understanding of the roles of this receptor in a more complex environment.

My *in vitro* results suggested that GW9508 activates neutrophils and has few or non-effect in monocyte derived macrophages (with the concentrations tested). So, a model where neutrophils plays a key role, was essential to text the effects f this compound in a more complex environment. K/BxN model of arthritis is initiated by an innate immune response mainly mediated by complement and LTB_4 recruiting neutrophils (Chen et al., 2006). The unique characteristics of this model are ideal for analysing the effects of GW9508 in inflammatory arthritis. In my *in vitro* data, I have shown that LTB_4 increases the expression of GPR40 in human neutrophils (Figure 19).

Arthritis was induced in mice by injecting 100µl K/BxN serum (i.p.) in C57/B6 mice on days 0 and 2. On day 8, animals were sacrificed and paws were collected. Cells were isolated by digestion with collagenase/DNase (0.5ng/ml and 40ng/ml) followed by staining with antibodies to allow visualization by flow cytometry. As the protocol used for isolation results in some cell death, I first gated the population of live cells by labelling with Zombie dye (an amine-reactive fluorescent dye that can differentiate dead cells from live cells) (Figure 38A), followed by selection of cells by size (FSC-A) and granularity (SSC-A) (Figure 38B). Subsequently, haematopoietic cells were selected by expression of high fluorescence of CD45 (Figure 38C). From this point onward, cells were subdivided into:

1. $CD11b^{+}/Ly6G^{high}$ (neutrophils, Figure 38D);
2. $CD11b^{+}/F4/80^{high}$ (macrophages, Figure 38E);

3. CD11b^{+}/Ly6C^{high} (inflammatory monocytes, Figure 38F).

As shown in Figure 38G, all three cells types expressed GPR40 when compared to isotype control.

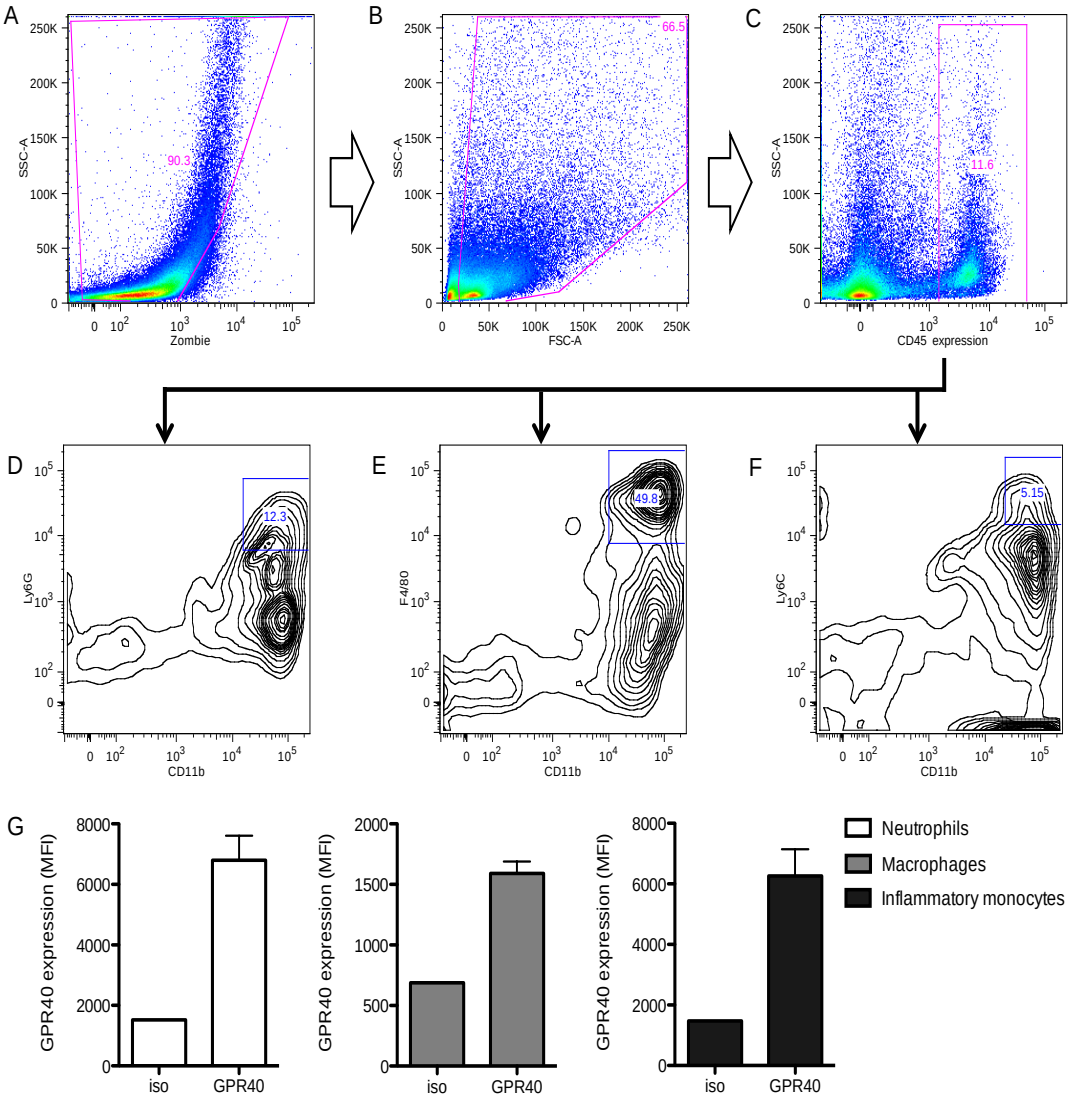

Figure 36: Expression of GPR40 in cells isolated from murine arthritic joints.
C57/Bl6 animals received 100µl (ip) of K/BxN serum on days 0 and 2. On day 8, the animals were sacrificed and their front and hind paws were removed. Cells were isolated by digestion with collagenase/DNase and labeled with the following antibodies to allow identification of cell types by flow cytometry. Selection of (A) live cells. (B) cells by size (FSC-H) and granularity (SSC-H) (C) hematopoietic cells expressing CD45 (D) neutrophils (CD11b^{+}/Ly6G^{high}). (E) macrophages (CD11b^{+}/F4/80^{high}) (F) monocytes (CD11b^{+}/Ly6C^{high}) and (G) GPR40 expression in selected cell types. Results are expressed as mean ± SEM. n=6. iso, isotype control. MFI, median fluorescence intensity.

3.14. Effects of GW9508 in the initiation and progression of inflammatory arthritis

After showing the expression of GPR40 in immune cells present within arthritic joints, the effects of GW9508 treatment was evaluated. Therefore, arthritis was induced in mice by injecting 100µl K/BxN serum (i.p.) in C57/Bl6 mice on days 0 and 2. Animals then received 100µl GW9508 (10mg/kg, i.p.) or vehicle (0.1% ethanol in PBS) from day 0 to 6. Arthritic parameters were recorded everyday including clinical score (section 2.20), weight loss and water displacement plethysmometry (oedema). On day 6, animals were euthanized, and paws collected for subsequent analysis. As shown below, both groups presented maximal disease incidence by day two (Figure 37A). Treatment with GW9508 daily exacerbated the severity of disease, characterized by higher clinical score on days 2-6 when compared to mice that received vehicle daily (Figure 37B). No statistical differences were visualized when comparing hind paw oedema associated with arthritis between vehicle and GW9508-treated groups (Figure 37C) despite the clear tendency in increased oedema GW9508-treated group. In addition, treatment of mice with GW9508 increased weight loss on days 4 and 5 when compared to the vehicle control group (Figure 37D).

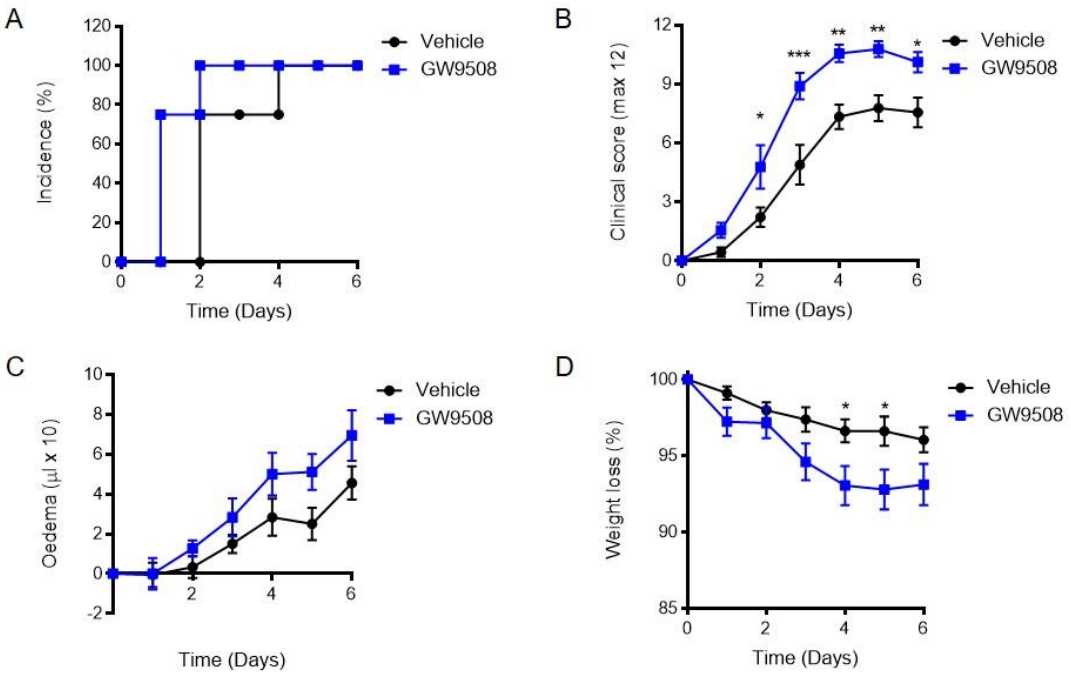

Figure 37: Characterization of arthritis severity following prophylactic treatment with GW9508. C57/Bl6 animals received 100µl (i.p) of K/BxN serum on days 0 and 2 and 100µl of GW9508 (100µl, 10mg/kg, ip) or vehicle (100µl, 0.1% ethanol in PBS) daily. Arthritic parameters were recorded everyday including (A) disease incidence, (B) clinical score, (C edema) water displacement plethysmometry, and (D) weight loss. Results are expressed as mean ± SEM. n=9. 2-way ANOVA, *p<0.05, **p<0.01, **p<0.001 compared to vehicle control (0.1% ethanol in PBS).

3.14.1. Expression of inflammatory mediators in GW9508-treated arthritic mice

Cytokines are implicated in each phase of the pathogenesis of rheumatoid arthritis, by promoting autoimmunity, by maintaining chronic inflammatory synovitis and by driving the destruction of the joint tissue (McInnes and Schett, 2007). Due to the importance of the pro-inflammatory cytokines in the pathogenesis of rheumatoid arthritis in humans, therapeutic strategies have been developed with the aim to neutralize these mediators. TNF-α- and IL-1R- but not IL-6-deficient mice are resistant to disease induction by KBxN serum, but TNF receptor-1- and TNF receptor-2-deficient mice are susceptible. I analysed the expression of these cytokines in the tissue from arthritic joints, but did not observe any differences between vehicle and GW9508 treated mice for TNF-α (Figure 38A), IL-1β (Figure 38B) or IL-6 (Figure 38C).

In animal models, the profile of cytokines can vary depending of the model used to induce arthritis. For instance, the development of arthritis in the KBN serum transfer model is critically dependent on IL-4 (Ohmura et al., 2005). I analysed the expression of IL-4 in cells of arthritic joints and my results showed a higher expression of IL-4 in mice treated with GW9508 in comparison with control group (Figure 38D). A result that could provide one possible explanation of why the disease manifested more severely in this animal group.

It has also been shown that neutrophils from RA patients have increased nitric oxide synthase type 2 (NOS2) protein expression and enhanced formation of nitric oxide (NO) that correlates with disease activity (St Clair et al., 1996). Accordingly, studies in experimental animal models of arthritis have suggested that excessive levels of NO can promote tissue injury and contribute to progression of the disease (Clancy et al., 1998). I also analysed expression of NOS2 mRNA in cells from arthritic joints, showing that in the group of mice treated with GW9508 there was increased expression of this protein in comparison to control group (Figure 38E). Additionally, I analysed the expression of the anti-inflammatory cytokine IL-10, and showed that

mRNA level of this cytokine was significantly decreased in GW9508-treated mice when compared to vehicle control group (Figure 38F).

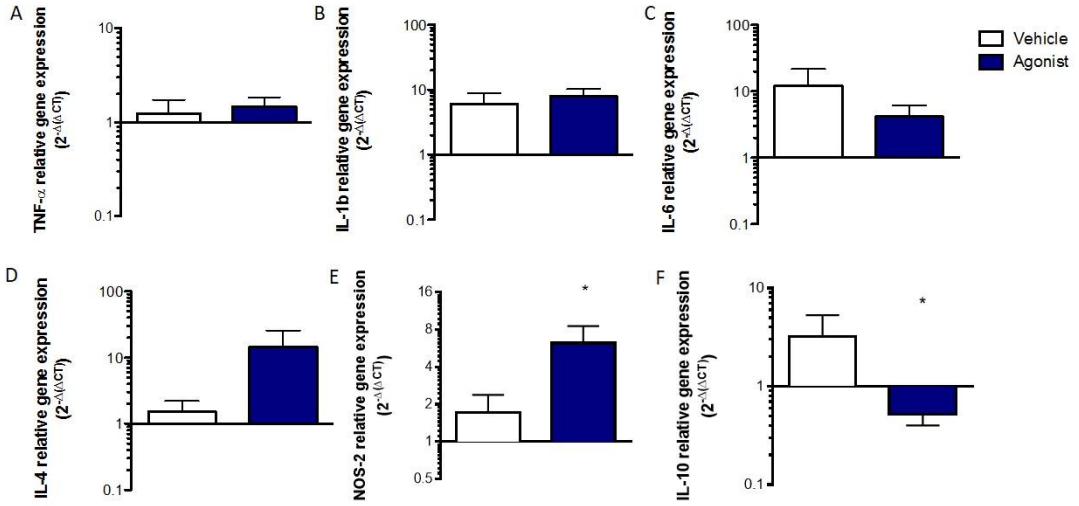

Figure 38: Expression of inflammatory mediators in murine arthritic joints.
Levels of (A) TNF-α, (B) IL-1β, (C) IL-6, (D) IL-4, (E) NOS2 and (F) IL-10 mRNA expression in arthritic joints. Cells were isolated from paws by RNeasy kit Qiagen® on day 6 after induction of arthritis by KBxN-serum transfer. The relative expression of each gene, cycle threshold values were normalized to a housekeeping gene (Rpl13a) and expression quantified using $2^{-\Delta\Delta CT}$. Results are expressed as mean ± SEM (n=5). Non parametric unpaired T-Test followed by Mann Whitney post-test, *p<0.05 compared to vehicle control (0.1% ethanol in PBS).

3.14.2. Histological analysis of arthritic knees

To evaluate the histological characteristics of the joint, knees were collected on day 6 decalcified and embedded in paraffin wax. Sections of knees were then stained with haematoxylin and eosin. Arthritis severity was scored as described in section 2.24.2. In both vehicle- and GW9508-treated arthritic mice pannus formation and leukocyte infiltration were visualised, which are characteristic of the inflammatory response that occurs during arthritis (Figure 39A). However, a wider pannus formation, stronger cellular infiltration and loss of joint architecture was visualized in the GW9508 treated mice (Figure 39A). In agreement, after analysis by two blinded scorers, GW9508 treated mice showed a higher score in joint damage (Figure 39B), when compared to vehicle control group.

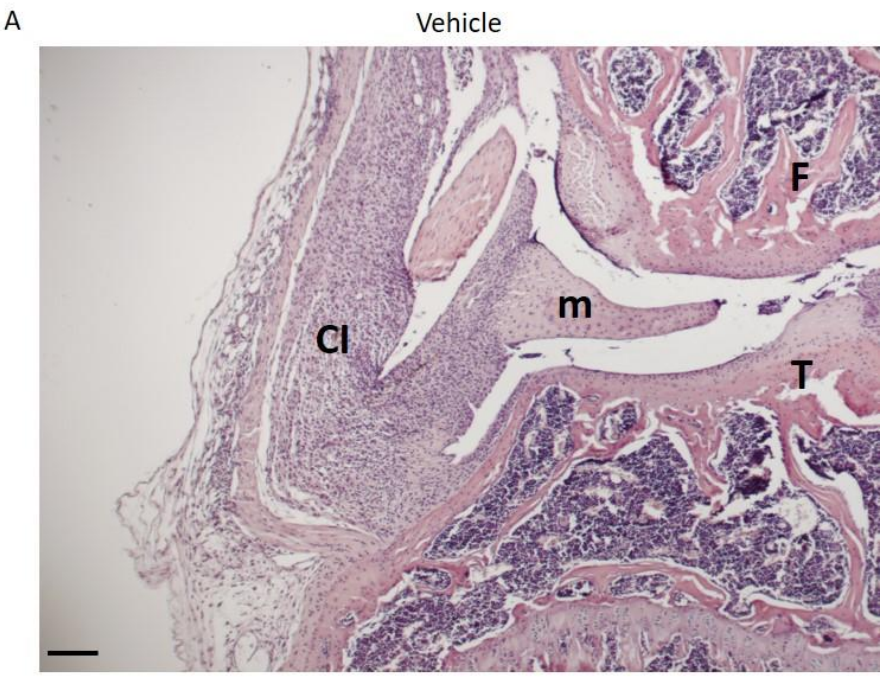
A
Vehicle
F
m
Cl
T

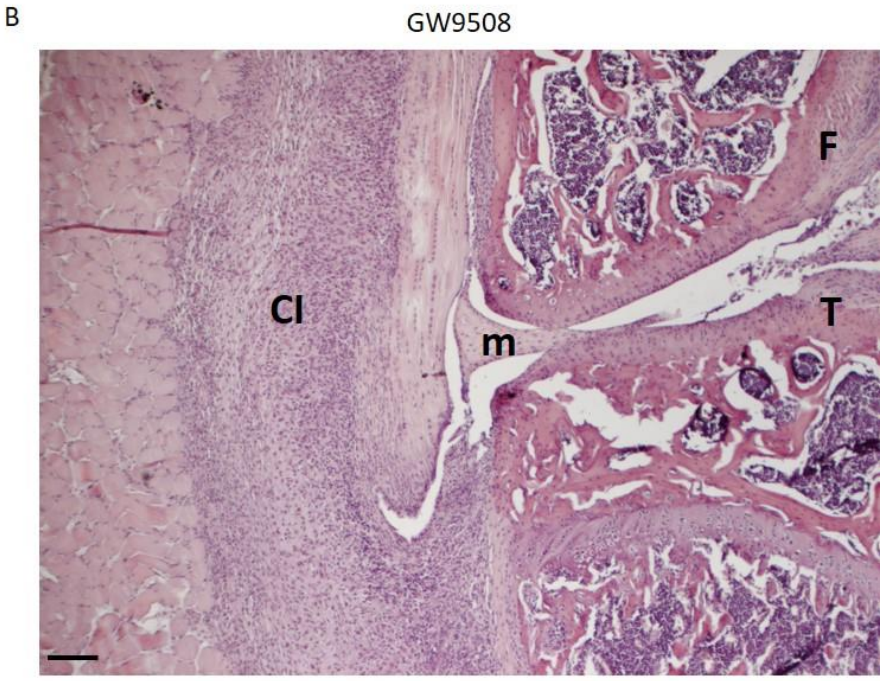
B
GW9508
F
Cl
m
T

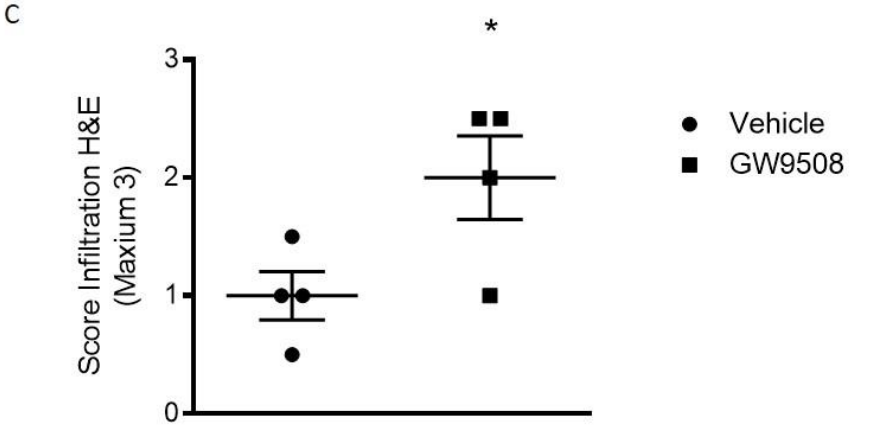
C
*
Score Infiltration H&E
(Maxium 3)
3
2
1
0
Vehicle
GW9508

Figure 39: Leukocyte infiltration in GW9508-treated arthritic mice. Twelve-week old male C57Bl6 mice were administered 100µl K/BxN serum intraperitoneally day 0 and day 2. Five K/BxN mice received intraperitoneally saline (100µl) and 5 K/BxN mice received GW9508 (100µl, 10mg/kg) intraperitoneally from day 0 to day 6. Knee joints were collected for histology on day 6. Hematoxylin and eosin (H&E) sections were analysed and scored by two blinded scorers. (A-B) Panel representing histological features joint from arthritic joint in vehicle control group (A) and GW9508 treated mice (B), x4 magnification. Scale bars: 200 µm. F, femur; T, tibia; m, meniscus; CI, cellular infiltration. (B) Mean histological scores were calculated from two sections for each animal. Results are expressed as mean ± SEM (n=4). T test, *p<0.05 compared to vehicle (0.1% ethanol in PBS).

Enzymes secreted by neutrophils, synoviocytes and chondrocytes are believed to be responsible for cartilage degradation. Previous results suggested an increased number of neutrophils present in the arthritic joints of GW9508-treated mice when compared to control group. Next I evaluated if this correlated with a higher degradation of cartilage in this group. A characteristic of arthritis is cartilage degradation. In agreement, knee sections of vehicle- (Figure 40A, left) and GW9508-treated mice (Figure 40A, right) stained with Toluidine blue confirmed cartilage degradation in both groups. However, no significant difference was visualised between GW9508 and vehicle treated group, as analysed by percentage of area stained with Toluidine Blue (Figure 40B).

A

Vehicle

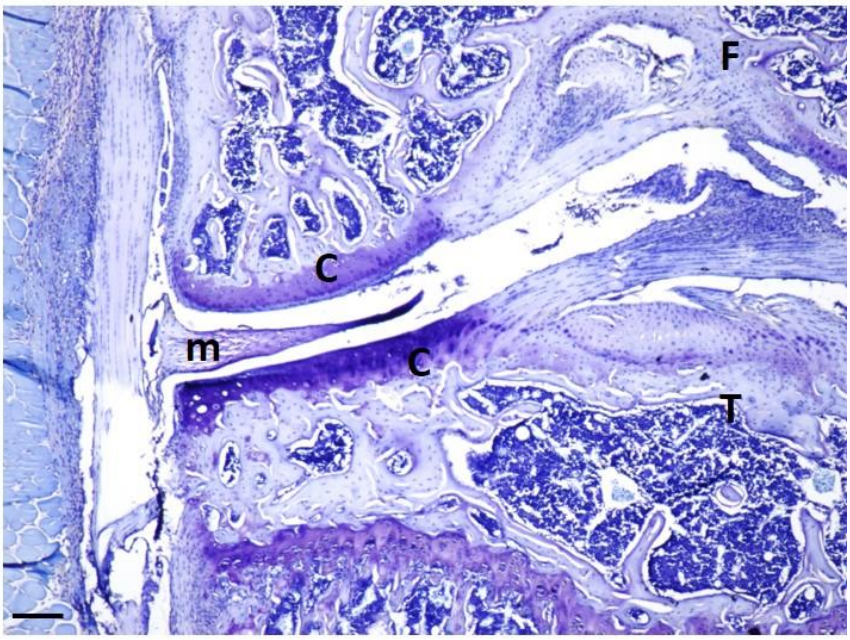

B

GW9508

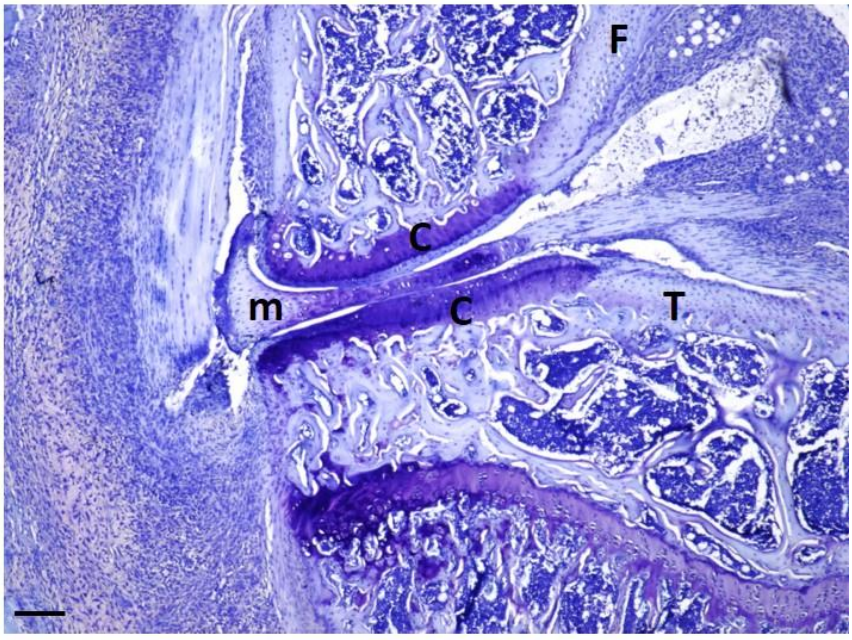

C

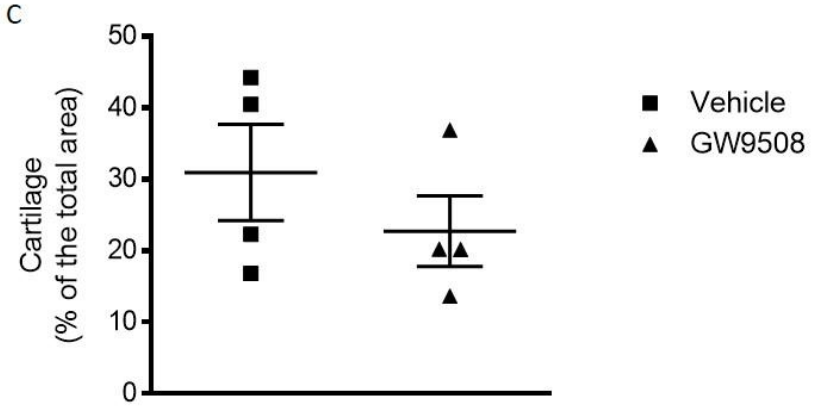

Figure 40: GW9508 treatment does not affect cartilage degradation in arthritic mice.
Twelve-week old male C57Bl6 mice were administered 100µl K/BxN serum intraperitoneally day 0 and day 2. Five K/BxN mice received intraperitoneal saline (100µl) and 5 K/BxN mice received GW9508 (100µl, 10mg/kg) intraperitoneally from day 0 to day 6. Knee joints were collected for histology on day 6. Toluidine Blue stained sections were analysed using ImageJ to determine extracellular matrix integrity. (A-B) Representative micrographs of Vehicle treated mice (A) and GW9505 treated mice (B). Scale bars: 200 µm. F, femur; T, tibia; m, meniscus; C, cartilage, 4x magnification. (C) Data shown are percentage area of articular cartilage stained positively for Toluidine Blue, quantified from at least six 20X magnification micrographs per section of 3 sections from each knee. Results are expressed as mean ± SEM (n=4). T-test.

3.15. Effects of GW9508 treatment during the resolution phase of inflammatory arthritis

Finally, the effects of GPR40 activation on the resolution of inflammation *in vivo* were addressed by treating arthritic mice with GW9508 at the peak of the disease (day 5, Figure 37). Arthritic parameters were assessed daily to evaluate the progression of the disease. As expected, all mice developed arthritis by day 2 and no differences were visualised between groups before the initiation of treatments (Figure 41A). Treatment with GW9508 (100µl, 10mg/kg, ip) or vehicle (100µl, 0.1% ethanol in PBS) started on day 5 and continued daily until day 10, when mice were euthanized. The vehicle control group showed peak of arthritis on day 5, and then began to gradually go into remission (Figure 41B, black line), while treatment with GW9508 prolonged the arthritis (Figure 41B, blue line). This effect was also reflected by the weight loss, as by day 7 the control group started to gain weight (Figure 41C, black line) while the GW9508-treated group continued to lose weight (Figure 41C, blue line). This trend was also observed for hind paw oedema, where vehicle group showed peak oedema on day 7 (Figure 41D, black line), but GW9508-treated still exhibited swollen paws on day 10 (Figure 41D, blue line).

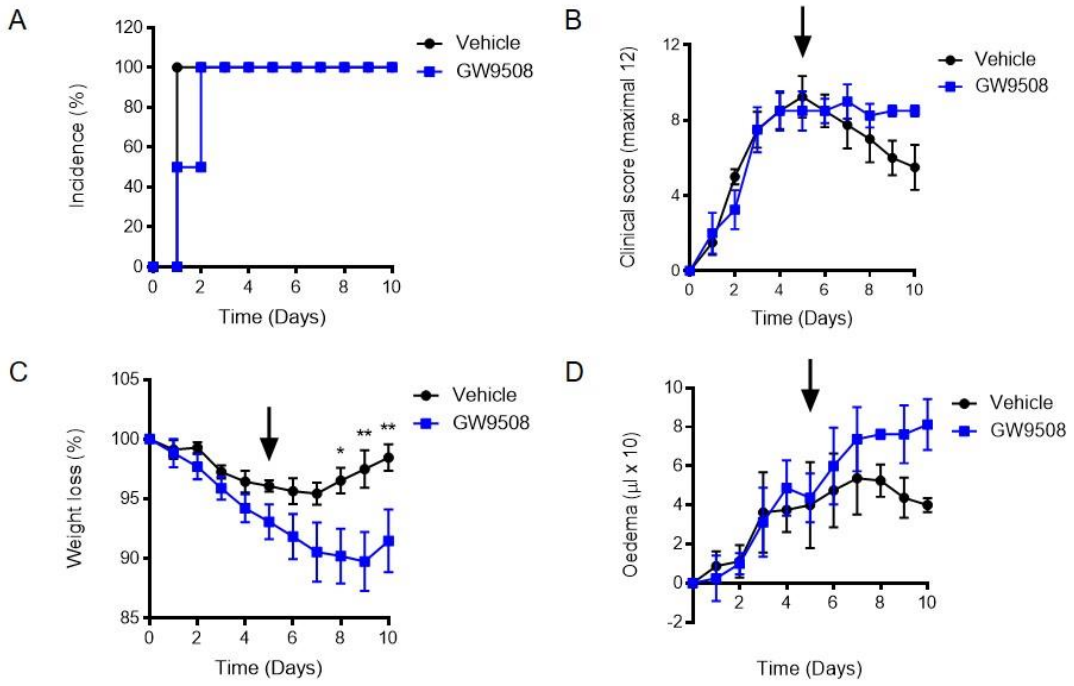

Figure 41: Therapeutic administration of GW9508 at the peak of inflammatory arthritis delays resolution.
C57/Bl6 animals received 100µl (i.p.) of K/BxN serum on days 0 and 2. After day 5, mice received GW9508 (100µl, 10mg/kg, ip) or vehicle (100µl, 0.1% ethanol in PBS) daily. Arthritic parameters were recorded everyday including (A) disease incidence, (B) clinical score, (C edema) water displacement plethysmometry, and (D) weight loss. Results are expressed as mean ± SEM. n=4. 2-way ANOVA, *p<0.05, *p<0.01 compared to vehicle control.

CHAPTER 4: DISCUSSION OF RESULTS

For a long time, fatty acids were considered the “bad boys” of our diet, and for many years we tried to decrease their consumption, however, it did not make us healthier. Nowadays, we know there are essential fatty acids necessary not only for development, but also to regulate our immune system. Two main categories of fatty acids are the omega-3 and the omega-6 fatty acids. Arachidonic acid (AA), one of the most studied omega-6 fatty acids, is known for its ability to induce the inflammatory response. In addition, AA can also be metabolized into other mediators, such as lipoxins that have anti-inflammatory and pro-resolution responses. On the other hand, omega-3 fatty acids are more widely known for their ability to decrease inflammation, due to the actions of their derivatives resolvins, maresins and protectins, which were identified at the start of the century (Serhan et al., 2002). Taking into account that omega-6 fatty acids have opposite effects on the time-course of inflammation, it is natural to believe that omega-3 fatty acids can also have contradictory effects depending on the pathways that they directly or indirectly activate. Indeed, omega-3 fatty acids can also be converted to 3-series prostaglandins and 5-series leukotrienes that are known to have pro-inflammatory properties, even if in lower magnitude when compared to prostaglandins and leukotrienes derived from AA. Therefore, to understand the mechanisms involved in the direct activation of long-chain free fatty acid receptors in the time-course of the inflammatory response, this work focused to evaluate expression and function of downstream activation of GPR40 in immune cells and an inflammatory model of arthritis by using GW9508, an agonist of GPR40.

Initially, this work was directed to the definition of GPR40 expression in different cell types involved in the inflammatory process, focusing on neutrophils (first cell of host defence). We were able to demonstrate, for the first time, gene and protein expression of GPR40 in human neutrophils. Later, we demonstrated expression of this receptor in monocytes as well as in human monocyte derived macrophages. Concurrently, and for translational purposes, we demonstrated the expression of this receptor in neutrophils, inflammatory monocytes and macrophages harvested from

the arthritic joints of mice. This indicates to us potential modulation of GPR40 expression by pro-inflammatory mediators, which are in inflammatory settings, and also a potential biological functions in the context of ongoing joint inflammation. Both these aspects have been addressed in subsequent experiments (*vide infra*).

As the expression of GPR40 had not been demonstrated in human neutrophils before, we used a variety of techniques to confirm the expression of GPR40 in this cell type. Initially, the expression of GPR40 was assessed by measuring gene expression by real-time and standard PCR. Following this, we showed protein expression by basic imaging and flow cytometry. Subsequently, we evaluated if mediators of the inflammatory response, such as TNFα, IL-8, LTB_4 and PAF, could modulate GPR40 expression. The focus was on mediators that are important in the inflammatory process by promoting the activation of neutrophils, and also induce the chemotaxis of neutrophils to the site of inflammation. Here we showed that LTB_4 (10nM) and PAF (10nM) could modulate the expression of GPR40 in neutrophils as early as after 10 minutes of stimulation. We also showed that the expression of this receptor was increased by approximately 30% after stimulation with TNF-α and IL-8, though this did not reach statistical significance. How could this expression be modulated so rapidly? PMN have a vast selection of functionally important molecules that are stored in cytoplasmic granules and vesicles. Upon stimulation, these intracellular granules are mobilized to the plasma membrane, increasing the quantity of specific receptors, cell adhesion molecules and proteases, that are involved in different activities, such as PMN adhesion, diapedesis and killing of bacteria (Hager et al., 2010). The swift upregulation of GPR40 by LTB_4 and PAF could be related to mobilization of GPR40 present in such cytoplasmic features, showing that GPR40 may have an important role in the inflammatory response. Another way to address the importance of GPR40 expression in ongoing inflammatory processes was to check the expression of this receptor in exudate neutrophils induced by Tabasco in

mouth cavity. In this case, we showed that exudate human neutrophils have higher levels of expression of GPR40 when compared to matched blood donor samples. Neutrophils are terminally differentiated cells with a short life-span due to constitutive apoptosis. Because of these characteristics, genetic manipulation of neutrophils has been difficult, although it is highly desired given the importance of neutrophils in the immune system (Geering et al., 2011). The effect of LTB_4 in increasing the expression of GPR40 in human neutrophils, makes the use of this cytokine an useful tool for studying the neutrophil biology. I made use of it when I pre-stimulated neutrophils with LTB_4 followed by GW9508 stimulation during flow chamber assay *in vitro*. In addition, I have choose a *in vivo* model where LTB_4 plays an important role, the K/BnX model (Chen et al., 2006).

To address the roles of GPR40 in neutrophils, the next aim was to identify a tool capable to activate this receptor. GW9508 is shown to stimulate intracellular Ca^{2+} mobilization in human embryonic kidney (HEK) 293 cells expressing GPR40 (pEC_{50} values of 7.32±0.03) (Briscoe et al., 2006). In our experimental settings, GW9508 did induce intracellular calcium mobilization in neutrophils, alongside a concentration dependent curve of the agonist. Therefore, after showing that this molecule activated neutrophil responses, we decided to address the effects of GW9508 stimulation in human immune cells, focusing on specific bioactions that are relevant both to the pro-inflammatory and resolving-phase of inflammation. As mentioned before, the resolution of inflammation is a tightly orchestrated and multifaceted host response, characterized by at least six key steps: 1) clearance of the inciting stimuli; 2) decrease of PMN and increase of monocyte recruitment; 3) apoptosis of recruited inflammatory cells; 4) efferocytosis of apoptotic cells by tissue and monocyte-derived macrophages; 5) switching from pro-inflammatory cell phenotypes and mediators to pro-resolution cell phenotypes and mediators; 6) either incorporation of myeloid cells into the local population or recirculation via lymph or blood (Alessandri et al., 2013, Norling and Perretti, 2013, Buckley et al., 2014). To

address if GPR40 was involved in the clearance of the inciting stimuli, I tested if GW9508 could modulate the level of *E. coli* phagocytosis by neutrophils *in vitro*. Indeed, at 10µM, GW9508 increased the phagocytic ability of neutrophils, when compared to the control treatment. Following this, another key step of the resolution of inflammation was investigated, that is the recruitment of neutrophils. Firstly, we addressed if GW9508 could modulate the expression of adhesion molecules in neutrophils. A concentration range (10-100µM) of GW9508 did not alter the expression of CD11b or L-selectin in neutrophils isolated from healthy volunteers indicating that the agonist itself did not cause neutrophil activation. It is known that TNF-α activation of neutrophils induces CD11b expression and L-selectin shedding (Hafezi-Moghadam et al., 2001), which I also observed, however, pre-stimulation of neutrophils with GW9508 was also not able to modulate the effects of TNF-α stimulation. There was also a lack of effect of GW9508 on the interactions of human neutrophils with endothelial cells under flow. I previously showed that 10 minutes LTB_4 stimulation could upregulate GPR40 expression, thus another set of experiments were performed to check if with higher surface levels of GPR40, GW9508 could have an effect on neutrophil-endothelial cells interactions. Indeed, fewer cells were observed rolling when compared to vehicle when neutrophils were stimulated with 10ng/ml LTB_4 for 10 minutes followed by a 10 minute stimulation with 1µM GW9508. I also assessed the chemotaxis of neutrophils induced by IL-8. IL-8, also known as neutrophil chemotactic factor, has two primary functions. It induces chemotaxis of neutrophils, causing them to migrate toward the site of infection, and also induces phagocytosis once neutrophils have arrived at the site of infection (Harada et al., 1994). Treatment with different concentration of GW9508 led to an increase of almost 50% of the chemotaxis of neutrophils, despite this it did not reach statistical significance. GW9508 stimulation has been shown to induce IL-8 release from bovine neutrophils. Thus, as IL-8 is known to induce actin conformation and redistribution to promote chemotaxis of neutrophils, GW9508 could increase

chemotaxis via this mechanism (Mena et al., 2016).

Taking in account the phagocytosis and chemotaxis results, is possible to hypothesise that GW9508 might have beneficial roles in another inflammatory condition. For instance, in an infection, like sepsis, the use of GW9508 could induce an increase of neutrophils into the site of the infection (Figure 27) and an increase in the phagocytosis rate (Figure 28). Which could result in a faster clearance of the bacteria.

Next, we studied the effects of GW9508-stimulation on release of neutrophil microvesicles. Microvesicles are fragments of plasma membrane ranging from 100 nm to 1000 nm shed from almost all cell types. This readout was chosen because vesicles are emerging as a new mechanism of intercellular communication by transferring cellular lipid and protein components to target cells (Camussi et al., 2010). Over a 15 minute incubation period, at 10 μM, GPR40 activation significantly increased the release of microvesicles. Interestingly, despite microvesicle release being a normal feature of any cell type, the proteomic profile of microvesicles may vary depending on the stimulus. Stimulation of human neutrophils, either in suspension or adherent to an endothelial monolayer, led to the production of microvesicles containing >400 distinct proteins with only 223 being shared by the two subsets. For instance, post-adherent microvesicles are enriched in alpha-2 macroglobulin and ceruloplasmin, whereas microparticles produced by neutrophils in suspension are abundant in heat shock 70 kDa protein 1 (Dalli et al., 2013). It would be interesting to assess the proteome profile of these microvesicles but due to time constraints I was unable to pursue this line of research.

Finally, I assessed the effects of GW9508 stimulation in the settings of neutrophil apoptosis. Apoptosis is a process of programmed cell death in vertebrates, essential to prevent release of intracellular contents of neutrophils in the tissue, which could lead to further damage and recruitment of more inflammatory cells into the damaged tissue (Savill et al., 1989). Here I showed that 10μM GW9508 neutrophil

stimulation delayed neutrophil apoptosis, increasing the number of viable cells. In an inflammatory process, many pro-inflammatory mediators, such as GM-CSF (Colotta et al., 1992), LTB_4 (Lee et al., 1999) and C5a (Lee et al., 1993), are associated with increasing the life span of neutrophils. On the other hand, usually pro-resolution mediators are associated with inducing apoptosis of neutrophils, such as AnxA1 (Perretti and Solito, 2004), LXA_4 (Weinberger et al., 2008) and RvE1 (El Kebir et al., 2012). Delayed neutrophil apoptosis contributes to the pathology of many inflammatory and autoimmune diseases. This is perhaps best exemplified by the phenotype of people with chronic granulomatous disease who are at risk of life-threatening infections because of inherited defects in the phagocyte NADPH oxidase, yet also develop granulomas that obstruct the liver, lungs, and gastrointestinal tract secondary to defects in PMN turnover and clearance (Fernandez-Boyanapalli et al., 2009, Kobayashi et al., 2004). Neutrophils from patients with acute arterial occlusions also exhibit delayed apoptosis (Garlichs et al., 2004) and the number of circulating neutrophils correlates with mortality subsequent to cardiovascular events (Guasti et al., 2011). In rheumatoid arthritis, it is hypothesized that an accumulation of neutrophils contributes to the presentation and persistence of autoantigens (Harper et al., 2001). In agreement with this, disease severity correlates with exceptionally high numbers of apoptotic neutrophils in circulation (Courtney et al., 1999). Altogether, these data lend further support to the notion that delayed neutrophil apoptosis contributes to the pathology of chronic inflammatory disorders (McCracken and Allen, 2014). Accordingly, my *in vitro* results, where I showed that GW9508 induces delay in neutrophil apoptosis, could be one of the factors in which severity of arthritis were increase in mice treated with GW9508.

After assessing the functions of GPR40 activation in human neutrophils, we evaluated the functions of this long-chain free fatty acid receptor in human macrophages. First, we showed expression of this receptor in monocyte-derived macrophages by real time PCR and flow cytometry. While basally expressed, we

were not able to establish any significant modulation of the level for GPR40 expression by TNF-α stimulation. Phagocytosis, a major effector function of macrophages, is of vital importance in the host immune defence. The multi-step process encompasses particle recognition by TLR and NOD receptors, followed by binding, regulated ingestion, and finally the destruction of internalized particles. The ability of macrophages to bind, engulf, and kill bacteria defines the bactericidal activity of the immune cells (Adolph et al., 2012). Long-chain free fatty acids DHA and EPA and their products (such as RvD- and RvE- resolvins) have been associated with an increase of the phagocytic activity of macrophages (Hong et al., 2008, Adolph et al., 2012, Rogerio et al., 2012, Hjorth et al., 2013). However, we were not able to demonstrate a modulation of the phagocytic ability of macrophages after application of GW9508. At this point, this set of experiments indicate that the modulation of phagocytosis by long-chain fatty acid may be more associated with an active remodelling of the plasma membrane structure (fluidity of the lipid bilayer) rather than the activation of the long-chain free fatty acid receptor GPR40 itself.

Another process involving engulfment is efferocytosis, or clearance of apoptotic cells. There is little direct evidence that human inflammatory arthritis is caused by defects in cell adherence (Kenyon et al., 2011, Hurst et al., 1983), however, it is known that extracellular debris, including oxidized lipids and intracellular components such as histone H3 and histone H4, can decrease efferocytosis at sites of inflammation (Friggeri et al., 2012). In this work, I evaluated if GPR40 activation could modulate efferocytosis of macrophages using two approaches. First, stimulating human neutrophils with GW9508 and second stimulating mouse macrophages with GPR40 agonist. When macrophages were stimulated with GW9508 it had no effect on apoptotic neutrophil clearance. This set of data matches the finding in the phagocytosis assay and indicates that GPR40 does not modulate any aspect of the engulfment process enacted by macrophages. On the other hand, when neutrophils were stimulated with GW9508, a decrease in efferocytosis was

visualised. This result corresponds with the finding that GW9508 delays neutrophil apoptosis. It is interesting to hypothesise that “find me” signals produced by apoptotic neutrophils, such as chemokines that recruit phagocytes, along with the accumulation of PS on the exofacial leaflet of the cytoplasmic membrane are modulated by GW9508. However, the “catch me” phase, which involves expression of specific receptors on macrophages that recognizes distinct ligands on the apoptotic cell were not modulated by GW9508 stimulation. Together these findings suggest that GW9508 has a direct effect on neutrophil lifespan and hence clearance rather than modulation of macrophage phenotype and function. These findings make me hypnotize that the lack of response induced by GW9508 in human macrophages and, most important, the decrease of efferocytosis when human neutrophils are stimulated with GW9508 is one of the factors by which a more severe disease was observed in the arthritic mice treated with the agonist of GPR40. As dying neutrophils, will become necrotic, losing the architecture of the plasma membrane, with consequence release of intracellular contents to the microenvironment in an irreversible mode. The release of these intracellular contents of neutrophils in the tissue is associated with further damage and recruitment of more inflammatory cells into the damaged tissue (Savill et al., 1989).

Another important step in the resolution of the inflammation is the switching from pro-inflammatory to pro-resolution cell phenotypes and mediators. To assess whether GPR40 activation in macrophages was associated with the polarization of macrophages into pro-inflammatory (M1) or pro-resolutive (M2) profiles, we measured the expression of different clusters of differentiation after treatment with GW9508 and stimulation with INF-γ/LPS or IL-4. We could conclude that GPR40 does not modulate the polarization of macrophages into M1 or M2 phenotype in vitro. In an obese model induced by high fat diet (HFD), administration of RvD1 and DHA increased the percentage of M2 adipose tissue macrophages, showing that the long-chain free fatty acid DHA may have a role in the switching from pro-inflammatory to

pro-resolution cell phenotypes (Titos et al., 2011). However, the lack of results when using macrophages could be due to insufficient expression of GPR40 in this cell type. Indeed, if we focus on the MFI and CT values in assays of flow cytometry and real-time PCR preformed in this work, we can observe that the expression of this receptor is very low.

When I started work on this project, I hypothesized that GPR40 activation by GW9508 would result in anti-inflammatory or pro-resolution effects. We know that GPR40 is activated by omega-3 fatty acids, and we also know that positive effects using DHA supplementation are observed in models of arthritis when very high doses are used. For instance, therapeutic oral or intraarticular administration of DHA (10 mg/kg daily and 20 µg/knee) reduced pain-related behaviors and knee edema in arthritis induced by complete Freund's adjuvant (CFA) (Torres-Guzman et al., 2014). In other work, prophylactic DHA treatment (1g/kg and 2.5g/kg daily for 4 weeks before induction of CFA arthritis) was able to significantly decrease clinical score and incidence of arthritis. The higher dose of DHA (2.5g/kg) had more marked and consistent effects on all arthritic parameters measured: clinical arthritis scores, disease incidence, histopathology, anti-collagen antibodies, and *ex vivo* cytokine production (Olson et al., 2013). Olson et al. (2013) suggested that doses of >2 g/day of DHA may be required to reduce disease in humans. Which is in agreement with doses of fish oils used in human trials (1.6–7.1 g/day and averaged 3.5 g/day) that showed improvement in reducing duration of morning stiffness, number of tender or swollen joints, decreasing pain and time to fatigue, increasing grip strength, and decreasing the use of non-steroidal anti-inflammatory drugs (reviewed in Calder (2008) and Miles and Calder (2012)). In this work, we found that activation of GPR40 by GW9508 results in a more severe disease, characterized by higher clinical score and increase of oedema associated with arthritis in K/BxN serum transfer induced arthritis when compared to the control group. This was associated with an increased number of leukocytes in the arthritic joints. We believe that most of the protective

effects induced by omega-3 FAs are indeed due to the effects of their metabolic mediators, such as RvD1 as recently shown (Norling et al., 2016). But we also speculate that GPR40 activation by GW9508 may set in motion a cascade of events that are different from when this receptor is activated by natural omega-3 FAs. Indeed, GPCRs are known to produce different types of responses depending on the activator, for example FPR2/ALX, which has a variety of different protein/peptide and lipid agonists that either induce or protect from inflammation (Cooray et al., 2013).

An interesting and surprising result was that despite GW9508 exacerbating arthritis it did not cause an increase in cartilage damage. We believe that two factors could be involved in this phenomenon, the direct effect of GPR40 activation in chondrocytes; and the number of microvesicles released in response to GW9508 stimulation of neutrophils. First, Monfoulet and colleagues have demonstrated that IL-1β-treated GPR40 deficient chondrocytes secrete more inflammatory mediators (such as nitric oxide, IL-6, PGE_2) and active catabolic enzymes (such as metalloproteinase-1, and metalloproteinase-9), and showed decreased anabolism compared to GPR40 positive chondrocytes (Monfoulet et al., 2015). Second, we have shown that GW9508-stimulation increases microvesicle release by neutrophils. Previously, we have shown that mice lacking the putative phospholipid scramblase TMEM16F, a lipid scramblase required for microvesicle release, exhibited exacerbated cartilage damage when subjected to inflammatory arthritis, despite no differences in the clinical scores when compared to wild-type mice after induction of arthritis (Headland et al., 2015). Accordingly, when we gave microvesicles derived from neutrophils to arthritic mice, we saw a decrease in cartilage damage when compared to vehicle mice (Headland et al., 2015). We therefore hypothesise that despite the increased number of leukocytes in the joints and hence an increase in inflammatory mediators, cartilage in GW9508 treated mice is protected by the effects of activation of GPR40 in chondrocytes and the protective effects of neutrophil-derived microvesicles in the cartilage.

Importantly, G-coupled protein receptors are quite promiscuous both in terms of agonist activation as well as interaction with binding partners. In this work, we focused on the use of GW9508, a compound that is currently in phase II clinical trials for the treatment of diabetes. However, as mentioned before, GPR40 can be activated by medium and long chain free fatty acid receptors. Despite the pro-inflammatory effects of GPR40 activation evoked in neutrophils by GW9508, it is possible that this same receptor can produce another type of response if activated by another agonist or compound.

Despite the interesting results found, some considerations must be taken into account. First, here it was chosen GW9058 as an activator for GPR40 (pEC50=7.32 ±0.03) (Briscoe et al., 2006). However, this agonist can also activate GPR120 (see Introduction), another long-chain free fatty acid receptor, but in higher concentrations (pEC50=5.46 ±0.09) (Briscoe et al., 2006). With this in mind, it might be possible that the results obtained herein may not solely be due to activation of GPR40 only, but also be secondary to activation of GPR120. However, due to time constraints it proved difficult to further dissect the actions of GPR40 by using other techniques or genetically deficient mice. Attempts were made to block the actions of GW9508 via GPR40 to show specificity. However, this antagonist also seemed to act as a partial agonist as it caused a calcium flux at concentrations of 10 and 100μM.

CHAPTER 5: CONCLUSION AND FUTURE PLAN

Notwithstanding the importance of the results presented here, some questions were left answered. One of the limitations with using an agonist is potential off-target effects. It is known that GW9508 can also activate GPR120, at higher concentrations than I tested (Briscoe et al., 2006). It would however be useful to verify my findings in a setting where the target cell does not express GPR120, and also utilise cells overexpressing/knocked-down in GPR40 to confirm specific actions. To do this, I could use the leukocyte-like cell line HL-60 overexpressing GPR40. In addition, the role of GPR40 could be assessed by performing the K/BxN arthritis model in GPR40 knockout mice.

Despite showing that GW9508 increases calcium flux in neutrophils, the signalling cascade of GPR40 activation in human neutrophils was not addressed. It is known that GW9508 induces intracellular calcium mobilization and ERK2 phosphorylation in bovine neutrophils (Hidalgo et al., 2011). I would like to perform western blot analyses to evaluate if GW9508 also induces phosphorylation of ERK1/2 in human neutrophils.

In this work, I have shown that GW9508-stimulated neutrophils have delayed apoptosis. Three main apoptotic pathways have been described: an extrinsic pathway, that is activated by ligation of surface death receptors that bind Fas ligand, TNF-α or TRAIL; an intrinsic pathway, that is regulated at the level of mitochondria and is initiated by disruption of the outer mitochondrial membrane; and the phagocytosis induced cell death (PICD) pathway (McCracken and Allen, 2014). The extrinsic pathway is mediated by activation of caspase-3, while the intrinsic and PICD pathways are mediated by Bcl-2 and Mcl-1. I would therefore like to evaluate if such proteins are modulated by GW9508 stimulation.

Finally, I have shown that activation of GPR40 increased microvesicle release by neutrophils. Microvesicle release is a normal feature of any cell type, however, the proteomic profile of the microvesicle is crucial for the initiation, exacerbation or resolution of the inflammatory process. In RA patients, increased numbers of

circulating levels of platelet derived microvesicles are correlated to disease activity (Knijff-Dutmer et al., 2002, Umekita et al., 2009). In the synovial fluid, elevation of platelet MPs was found at a significantly higher concentration than circulating MPs which can act alone by promoting coagulation so contributing to fibrin deposits in the joints or by causing activation of synovial fibroblasts partly responsible of inflammatory phenomena or by secreting pro-inflammatory mediators (Boilard et al., 2010, Buzas et al., 2014). However, the proteomic profile of the microvesicle can also differ depending of the stimulus in the same cell type. For instance, Dalli and colleagues showed that stimulation of human neutrophils, either in suspension or adherent to an endothelial monolayer, led to the production of microvesicles containing >400 distinct proteins with only 223 being shared by the two subsets (Dalli et al., 2013). Recently, we have shown that TNF-α stimulated microvesicles derived from neutrophils can actually promote cartilage repair (Headland et al., 2015). With this in mind, I would like to evaluate the proteomic profile of GW9508-stimulated neutrophils.

In conclusion, we demonstrated expression of GPR40 in human (neutrophils and monocyte derived-macrophages) and murine (neutrophils, inflammatory monocytes and macrophages) immune cells. We have also demonstrated that GPR40 expression is up-regulated after stimulation with pro-inflammatory mediators, an effect evident also at the site of inflammation. In addition, we have shown that one agonist of GPR40 – compound GW9058 – can promote pro-inflammatory features in neutrophils (chemotaxis and phagocytosis) as well as delaying apoptosis and increasing microvesicle release. These *in vitro* actions are translated *in vivo* to an exacerbation of inflammatory arthritis with a delay of resolution (Figure 42). Therefore, GPR40 should be targeted through antagonists or biased agonists in order to inform therapeutic approaches based on this receptor target.

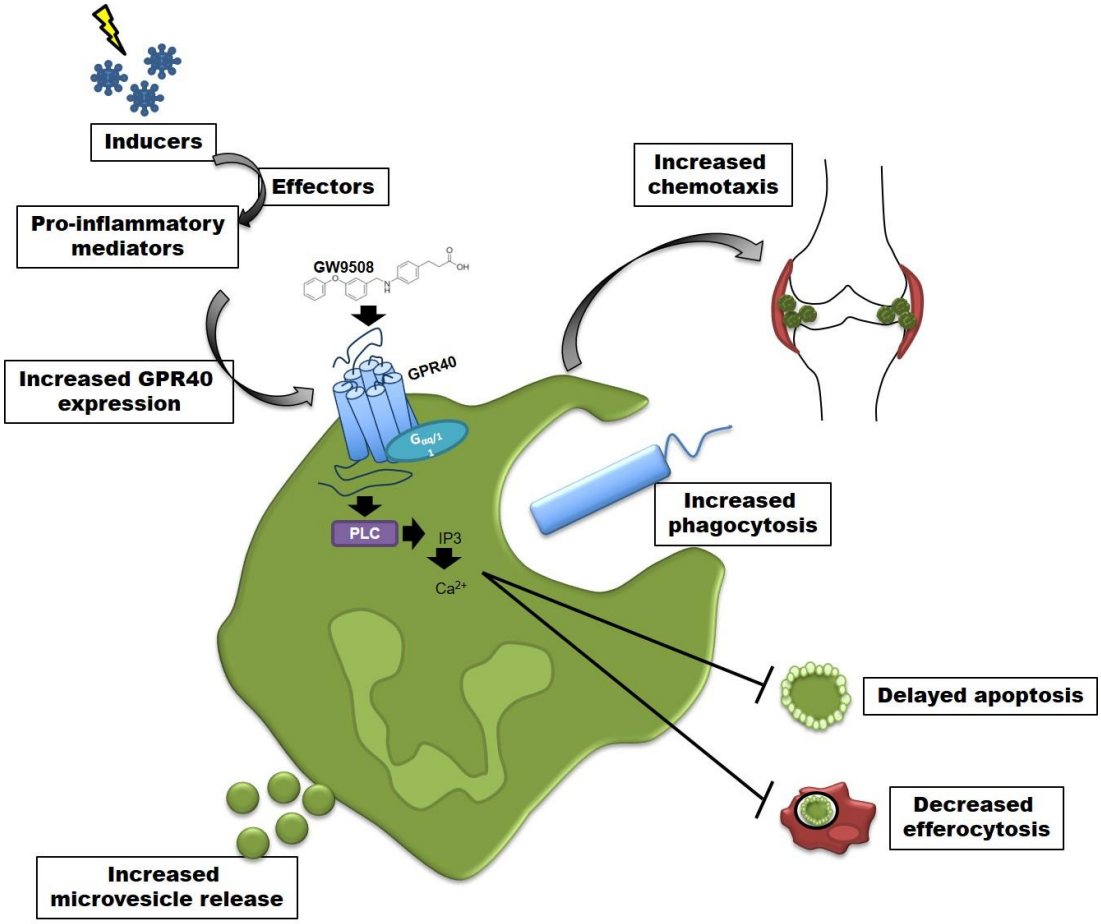

Figure 42: GW9508 induces a pro-inflammatory profile in neutrophils and increases severity of inflammatory arthritis.
Inducers are sensed by effector cells which will initiate the inflammatory response against the inducer. Pro-inflammatory mediators, such as LTB_4 and PAF, increase the expression of GPR40 in neutrophils, which when activated by GW9508, causes a calcium flux in these cells. Activation of GPR40 by its selective agonist promotes increased chemotaxis, phagocytosis and microvesicle release. On the other hand, GW9508 delays apoptosis of neutrophils and decreases efferocytosis by macrophages. The combination of such events results in the delay of the resolution of the inflammation as evidenced in a model of murine arthritis.

CHAPTER 6: REFERENCES

ADAMS, D. H. & SHAW, S. 1994. Leucocyte-endothelial interactions and regulation of leucocyte migration. *Lancet,* 343**,** 831-6.

ADOLPH, S., FUHRMANN, H. & SCHUMANN, J. 2012. Unsaturated fatty acids promote the phagocytosis of P. aeruginosa and R. equi by RAW264.7 macrophages. *Curr Microbiol,* 65**,** 649-55.

ALESSANDRI, A. L., SOUSA, L. P., LUCAS, C. D., ROSSI, A. G., PINHO, V. & TEIXEIRA, M. M. 2013. Resolution of inflammation: mechanisms and opportunity for drug development. *Pharmacol Ther,* 139**,** 189-212.

ALQUIER, T., PEYOT, M. L., LATOUR, M. G., KEBEDE, M., SORENSEN, C. M., GESTA, S., RONALD KAHN, C., SMITH, R. D., JETTON, T. L., METZ, T. O., PRENTKI, M. & POITOUT, V. 2009. Deletion of GPR40 impairs glucose-induced insulin secretion in vivo in mice without affecting intracellular fuel metabolism in islets. *Diabetes,* 58**,** 2607-15.

ALVAREZ-CURTO, E. & MILLIGAN, G. 2016. Metabolism meets immunity: The role of free fatty acid receptors in the immune system. *Biochem Pharmacol,* 114**,** 3-13.

ASQUITH, D. L., MILLER, A. M., MCINNES, I. B. & LIEW, F. Y. 2009. Animal models of rheumatoid arthritis. *Eur J Immunol,* 39**,** 2040-4.

BEVAART, L., VERVOORDELDONK, M. J. & TAK, P. P. 2010. Evaluation of therapeutic targets in animal models of arthritis: how does it relate to rheumatoid arthritis? *Arthritis Rheum,* 62**,** 2192-205.

BEVILACQUA, M. P. 1993. Endothelial-Leukocyte Adhesion Molecules. *Annual Review of Immunology,* 11**,** 767-804.

BEVILACQUA, M. P., NELSON, R. M., MANNORI, G. & CECCONI, O. 1994. Endothelial-leukocyte adhesion molecules in human disease. *Annu Rev Med,* 45**,** 361-78.

BHARATE, S. B., NEMMANI, K. V. & VISHWAKARMA, R. A. 2009. Progress in the discovery and development of small-molecule modulators of G-protein-coupled receptor 40 (GPR40/FFA1/FFAR1): an emerging target for type 2 diabetes. *Expert Opin Ther Pat,* 19**,** 237-64.

BOILARD, E., NIGROVIC, P. A., LARABEE, K., WATTS, G. F., COBLYN, J. S., WEINBLATT, M. E., MASSAROTTI, E. M., REMOLD-O'DONNELL, E., FARNDALE, R. W., WARE, J. & LEE, D. M. 2010. Platelets amplify inflammation in arthritis via collagen-dependent microparticle production. *Science,* 327**,** 580-3.

BRISCOE, C. P., PEAT, A. J., MCKEOWN, S. C., CORBETT, D. F., GOETZ, A. S., LITTLETON, T. R., MCCOY, D. C., KENAKIN, T. P., ANDREWS, J. L., AMMALA, C., FORNWALD, J. A., IGNAR, D. M. & JENKINSON, S. 2006. Pharmacological regulation of insulin secretion in MIN6 cells through the fatty acid receptor GPR40: identification of agonist and antagonist small molecules. *Br J Pharmacol,* 148**,** 619-28.

BRISCOE, C. P., TADAYYON, M., ANDREWS, J. L., BENSON, W. G., CHAMBERS, J. K., EILERT, M. M., ELLIS, C., ELSHOURBAGY, N. A., GOETZ, A. S., MINNICK, D. T., MURDOCK, P. R., SAULS, H. R., JR., SHABON, U., SPINAGE, L. D., STRUM, J. C., SZEKERES, P. G., TAN, K. B., WAY, J. M., IGNAR, D. M., WILSON, S. & MUIR, A. I. 2003. The orphan G protein-coupled receptor GPR40 is activated by medium and long chain fatty acids. *J Biol Chem,* 278**,** 11303-11.

BROWN, A. J., GOLDSWORTHY, S. M., BARNES, A. A., EILERT, M. M., TCHEANG, L., DANIELS, D., MUIR, A. I., WIGGLESWORTH, M. J., KINGHORN, I., FRASER, N. J., PIKE, N. B., STRUM, J. C., STEPLEWSKI, K. M., MURDOCK, P. R., HOLDER, J. C., MARSHALL, F. H., SZEKERES, P. G., WILSON, S., IGNAR, D. M., FOORD, S. M., WISE, A. & DOWELL, S. J. 2003. The Orphan G protein-coupled receptors GPR41 and GPR43 are activated by

propionate and other short chain carboxylic acids. *J Biol Chem,* 278**,** 11312-9.

BRUNSBERG, U., GUSTAFSSON, K., JANSSON, L., MICHAELSSON, E., AHRLUND-RICHTER, L., PETTERSSON, S., MATTSSON, R. & HOLMDAHL, R. 1994. Expression of a transgenic class II Ab gene confers susceptibility to collagen-induced arthritis. *Eur J Immunol,* 24**,** 1698-702.

BUCKLEY, C. D., GILROY, D. W. & SERHAN, C. N. 2014. Proresolving lipid mediators and mechanisms in the resolution of acute inflammation. *Immunity,* 40**,** 315-27.

BUZAS, E. I., GYORGY, B., NAGY, G., FALUS, A. & GAY, S. 2014. Emerging role of extracellular vesicles in inflammatory diseases. *Nat Rev Rheumatol,* 10**,** 356-64.

CALDER, P. C. 2006. Polyunsaturated fatty acids and inflammation. *Prostaglandins Leukot Essent Fatty Acids,* 75**,** 197-202.

CALDER, P. C. 2008. Session 3: Joint Nutrition Society and Irish Nutrition and Dietetic Institute Symposium on 'Nutrition and autoimmune disease' PUFA, inflammatory processes and rheumatoid arthritis. *Proc Nutr Soc,* 67**,** 409-18.

CALDER, P. C. 2015. Marine omega-3 fatty acids and inflammatory processes: Effects, mechanisms and clinical relevance. *Biochim Biophys Acta,* 1851**,** 469-84.

CAMUSSI, G., DEREGIBUS, M. C., BRUNO, S., CANTALUPPI, V. & BIANCONE, L. 2010. Exosomes/microvesicles as a mechanism of cell-to-cell communication. *Kidney Int,* 78**,** 838-48.

CASCAO, R., ROSARIO, H. S., SOUTO-CARNEIRO, M. M. & FONSECA, J. E. 2010. Neutrophils in rheumatoid arthritis: More than simple final effectors. *Autoimmun Rev,* 9**,** 531-5.

CASH, J. L., CHRISTIAN, A. R. & GREAVES, D. R. 2010. Chemerin peptides promote phagocytosis in a ChemR23- and Syk-dependent manner. *J Immunol,* 184**,** 5315-24.

CHAVAKIS, E., CHOI, E. Y. & CHAVAKIS, T. 2009. Novel aspects in the regulation of the leukocyte adhesion cascade. *Thromb Haemost,* 102**,** 191-7.

CHEN, M., LAM, B. K., KANAOKA, Y., NIGROVIC, P. A., AUDOLY, L. P., AUSTEN, K. F. & LEE, D. M. 2006. Neutrophil-derived leukotriene B4 is required for inflammatory arthritis. *J Exp Med,* 203**,** 837-42.

CLANCY, R. M., AMIN, A. R. & ABRAMSON, S. B. 1998. The role of nitric oxide in inflammation and immunity. *Arthritis Rheum,* 41**,** 1141-51.

CLELAND, L. G., FRENCH, J. K., BETTS, W. H., MURPHY, G. A. & ELLIOTT, M. J. 1988. Clinical and biochemical effects of dietary fish oil supplements in rheumatoid arthritis. *J Rheumatol,* 15**,** 1471-5.

COLOTTA, F., RE, F., POLENTARUTTI, N., SOZZANI, S. & MANTOVANI, A. 1992. Modulation of granulocyte survival and programmed cell death by cytokines and bacterial products. *Blood,* 80**,** 2012-20.

COORAY, S. N., GOBBETTI, T., MONTERO-MELENDEZ, T., MCARTHUR, S., THOMPSON, D., CLARK, A. J., FLOWER, R. J. & PERRETTI, M. 2013. Ligand-specific conformational change of the G-protein-coupled receptor ALX/FPR2 determines proresolving functional responses. *Proc Natl Acad Sci U S A,* 110**,** 18232-7.

COURTNEY, P. A., CROCKARD, A. D., WILLIAMSON, K., IRVINE, A. E., KENNEDY, R. J. & BELL, A. L. 1999. Increased apoptotic peripheral blood neutrophils in systemic lupus erythematosus: relations with disease activity, antibodies to double stranded DNA, and neutropenia. *Ann Rheum Dis,* 58**,** 309-14.

CROSS, A., BARNES, T., BUCKNALL, R. C., EDWARDS, S. W. & MOOTS, R. J. 2006. Neutrophil apoptosis in rheumatoid arthritis is regulated by local oxygen tensions within joints. *J Leukoc Biol,* 80**,** 521-8.

DALLI, J., CHIANG, N. & SERHAN, C. N. 2014. Identification of 14-series sulfido-conjugated mediators that promote resolution of infection and organ protection. *Proc Natl Acad Sci U S A,* 111**,** E4753-61.

DALLI, J., MONTERO-MELENDEZ, T., NORLING, L. V., YIN, X., HINDS, C., HASKARD, D., MAYR, M. & PERRETTI, M. 2013. Heterogeneity in neutrophil microparticles reveals distinct proteome and functional properties. *Mol Cell Proteomics,* 12**,** 2205-19.

DALLI, J., RAMON, S., NORRIS, P. C., COLAS, R. A. & SERHAN, C. N. 2015. Novel proresolving and tissue-regenerative resolvin and protectin sulfido-conjugated pathways. *FASEB J,* 29**,** 2120-36.

DALLI, J., SANGER, J. M., RODRIGUEZ, A. R., CHIANG, N., SPUR, B. W. & SERHAN, C. N. 2016. Identification and Actions of a Novel Third Maresin Conjugate in Tissue Regeneration: MCTR3. *PLoS One,* 11**,** e0149319.

DUFFIN, R., LEITCH, A. E., FOX, S., HASLETT, C. & ROSSI, A. G. 2010. Targeting granulocyte apoptosis: mechanisms, models, and therapies. *Immunol Rev,* 236**,** 28-40.

EL KEBIR, D., GJORSTRUP, P. & FILEP, J. G. 2012. Resolvin E1 promotes phagocytosis-induced neutrophil apoptosis and accelerates resolution of pulmonary inflammation. *Proc Natl Acad Sci U S A,* 109**,** 14983-8.

ESPERSEN, G. T., GRUNNET, N., LERVANG, H. H., NIELSEN, G. L., THOMSEN, B. S., FAARVANG, K. L., DYERBERG, J. & ERNST, E. 1992. Decreased interleukin-1 beta levels in plasma from rheumatoid arthritis patients after dietary supplementation with n-3 polyunsaturated fatty acids. *Clin Rheumatol,* 11**,** 393-5.

EVANS, S. S., REPASKY, E. A. & FISHER, D. T. 2015. Fever and the thermal regulation of immunity: the immune system feels the heat. *Nat Rev Immunol,* 15**,** 335-49.

FELDMANN, M. & MAINI, R. N. 1999. The role of cytokines in the pathogenesis of rheumatoid arthritis. *Rheumatology (Oxford),* 38 Suppl 2**,** 3-7.

FERNANDEZ-BOYANAPALLI, R. F., FRASCH, S. C., MCPHILLIPS, K., VANDIVIER, R. W., HARRY, B. L., RICHES, D. W., HENSON, P. M. & BRATTON, D. L. 2009. Impaired apoptotic cell clearance in CGD due to altered macrophage programming is reversed by phosphatidylserine-dependent production of IL-4. *Blood,* 113**,** 2047-55.

FIERRO, I. M., COLGAN, S. P., BERNASCONI, G., PETASIS, N. A., CLISH, C. B., ARITA, M. & SERHAN, C. N. 2003. Lipoxin A4 and aspirin-triggered 15-epi-lipoxin A4 inhibit human neutrophil migration: comparisons between synthetic 15 epimers in chemotaxis and transmigration with microvessel endothelial cells and epithelial cells. *J Immunol,* 170**,** 2688-94.

FREVERT, C. W., WONG, V. A., GOODMAN, R. B., GOODWIN, R. & MARTIN, T. R. 1998. Rapid fluorescence-based measurement of neutrophil migration in vitro. *J Immunol Methods,* 213**,** 41-52.

FRIGGERI, A., BANERJEE, S., XIE, N., CUI, H., DE FREITAS, A., ZERFAOUI, M., DUPONT, H., ABRAHAM, E. & LIU, G. 2012. Extracellular histones inhibit efferocytosis. *Mol Med,* 18**,** 825-33.

FROMMER, K. W., SCHAFFLER, A., REHART, S., LEHR, A., MULLER-LADNER, U. & NEUMANN, E. 2015. Free fatty acids: potential proinflammatory mediators in rheumatic diseases. *Ann Rheum Dis,* 74**,** 303-10.

FUJITA, T., MATSUOKA, T., HONDA, T., KABASHIMA, K., HIRATA, T. & NARUMIYA, S. 2011. A GPR40 agonist GW9508 suppresses CCL5, CCL17, and CXCL10 induction in keratinocytes and attenuates cutaneous immune inflammation. *J Invest Dermatol,* 131**,** 1660-7.

FUJIWARA, K., MAEKAWA, F. & YADA, T. 2005. Oleic acid interacts with GPR40 to induce Ca2+ signaling in rat islet beta-cells: mediation by PLC and L-type

Ca2+ channel and link to insulin release. *Am J Physiol Endocrinol Metab,* 289**,** E670-7.

GARLICHS, C. D., ESKAFI, S., CICHA, I., SCHMEISSER, A., WALZOG, B., RAAZ, D., STUMPF, C., YILMAZ, A., BREMER, J., LUDWIG, J. & DANIEL, W. G. 2004. Delay of neutrophil apoptosis in acute coronary syndromes. *J Leukoc Biol,* 75**,** 828-35.

GARRIDO, D. M., CORBETT, D. F., DWORNIK, K. A., GOETZ, A. S., LITTLETON, T. R., MCKEOWN, S. C., MILLS, W. Y., SMALLEY, T. L., JR., BRISCOE, C. P. & PEAT, A. J. 2006. Synthesis and activity of small molecule GPR40 agonists. *Bioorg Med Chem Lett,* 16**,** 1840-5.

GEERING, B., SCHMIDT-MENDE, J., FEDERZONI, E., STOECKLE, C. & SIMON, H. U. 2011. Protein overexpression following lentiviral infection of primary mature neutrophils is due to pseudotransduction. *J Immunol Methods,* 373**,** 209-18.

GODSON, C., MITCHELL, S., HARVEY, K., PETASIS, N. A., HOGG, N. & BRADY, H. R. 2000. Cutting edge: lipoxins rapidly stimulate nonphlogistic phagocytosis of apoptotic neutrophils by monocyte-derived macrophages. *J Immunol,* 164**,** 1663-7.

GOLDRING, M. B., BIRKHEAD, J. R., SUEN, L. F., YAMIN, R., MIZUNO, S., GLOWACKI, J., ARBISER, J. L. & APPERLEY, J. F. 1994. Interleukin-1 beta-modulated gene expression in immortalized human chondrocytes. *The Journal of clinical investigation,* 94**,** 2307-16.

GONZALEZ, R., DUNKEL, R., KOLETZKO, B., SCHUSDZIARRA, V. & ALLESCHER, H. D. 1998. Effect of capsaicin-containing red pepper sauce suspension on upper gastrointestinal motility in healthy volunteers. *Dig Dis Sci,* 43**,** 1165-71.

GRECO, K. V., IQBAL, A. J., RATTAZZI, L., NALESSO, G., MORADI-BIDHENDI, N., MOORE, A. R., GOLDRING, M. B., DELL'ACCIO, F. & PERRETTI, M. 2011. High density micromass cultures of a human chondrocyte cell line: a reliable assay system to reveal the modulatory functions of pharmacological agents. *Biochem Pharmacol,* 82**,** 1919-29.

GUASTI, L., DENTALI, F., CASTIGLIONI, L., MARONI, L., MARINO, F., SQUIZZATO, A., AGENO, W., GIANNI, M., GAUDIO, G., GRANDI, A. M., COSENTINO, M. & VENCO, A. 2011. Neutrophils and clinical outcomes in patients with acute coronary syndromes and/or cardiac revascularisation. A systematic review on more than 34,000 subjects. *Thromb Haemost,* 106**,** 591-9.

HAFEZI-MOGHADAM, A., THOMAS, K. L., PROROCK, A. J., HUO, Y. & LEY, K. 2001. L-selectin shedding regulates leukocyte recruitment. *J Exp Med,* 193**,** 863-72.

HAGER, M., COWLAND, J. B. & BORREGAARD, N. 2010. Neutrophil granules in health and disease. *J Intern Med,* 268**,** 25-34.

HAMMARSTROM, S. 1983. Leukotrienes. *Annu Rev Biochem,* 52**,** 355-77.

HARA, T., HIRASAWA, A., SUN, Q., SADAKANE, K., ITSUBO, C., IGA, T., ADACHI, T., KOSHIMIZU, T. A., HASHIMOTO, T., ASAKAWA, Y. & TSUJIMOTO, G. 2009. Novel selective ligands for free fatty acid receptors GPR120 and GPR40. *Naunyn Schmiedebergs Arch Pharmacol,* 380**,** 247-55.

HARADA, A., SEKIDO, N., AKAHOSHI, T., WADA, T., MUKAIDA, N. & MATSUSHIMA, K. 1994. Essential involvement of interleukin-8 (IL-8) in acute inflammation. *J Leukoc Biol,* 56**,** 559-64.

HARDY, S., ST-ONGE, G. G., JOLY, E., LANGELIER, Y. & PRENTKI, M. 2005. Oleate promotes the proliferation of breast cancer cells via the G protein-coupled receptor GPR40. *J Biol Chem,* 280**,** 13285-91.

HARPER, L., RADFORD, D., PLANT, T., DRAYSON, M., ADU, D. & SAVAGE, C. O. 2001. IgG from myeloperoxidase-antineutrophil cytoplasmic antibody-positive

patients stimulates greater activation of primed neutrophils than IgG from proteinase 3-antineutrophil cytosplasmic antibody-positive patients. *Arthritis Rheum,* 44**,** 921-30.

HART, B. A., BANK, R. A., DE ROOS, J. A., BROK, H., JONKER, M., THEUNS, H. M., HAKIMI, J. & TE KOPPELE, J. M. 1998. Collagen-induced arthritis in rhesus monkeys: evaluation of markers for inflammation and joint degradation. *Br J Rheumatol,* 37**,** 314-23.

HASKO, G., LINDEN, J., CRONSTEIN, B. & PACHER, P. 2008. Adenosine receptors: therapeutic aspects for inflammatory and immune diseases. *Nat Rev Drug Discov,* 7**,** 759-70.

HASSANIAN, S. M., DINARVAND, P. & REZAIE, A. R. 2014. Adenosine regulates the proinflammatory signaling function of thrombin in endothelial cells. *J Cell Physiol,* 229**,** 1292-300.

HE, K., SONG, Y., DAVIGLUS, M. L., LIU, K., VAN HORN, L., DYER, A. R., GOLDBOURT, U. & GREENLAND, P. 2004. Fish consumption and incidence of stroke: a meta-analysis of cohort studies. *Stroke,* 35**,** 1538-42.

HEADLAND, S. E., JONES, H. R., D'SA, A. S., PERRETTI, M. & NORLING, L. V. 2014. Cutting-edge analysis of extracellular microparticles using ImageStream(X) imaging flow cytometry. *Sci Rep,* 4**,** 5237.

HEADLAND, S. E., JONES, H. R., NORLING, L. V., KIM, A., SOUZA, P. R., CORSIERO, E., GIL, C. D., NERVIANI, A., DELL'ACCIO, F., PITZALIS, C., OLIANI, S. M., JAN, L. Y. & PERRETTI, M. 2015. Neutrophil-derived microvesicles enter cartilage and protect the joint in inflammatory arthritis. *Sci Transl Med,* 7**,** 315ra190.

HELME, R. D. & MCKERNAN, S. 1985. Neurogenic flare responses following topical application of capsaicin in humans. *Ann Neurol,* 18**,** 505-9.

HIDALGO, M. A., NAHUELPAN, C., MANOSALVA, C., JARA, E., CARRETTA, M. D., CONEJEROS, I., LOAIZA, A., CHIHUAILAF, R. & BURGOS, R. A. 2011. Oleic acid induces intracellular calcium mobilization, MAPK phosphorylation, superoxide production and granule release in bovine neutrophils. *Biochem Biophys Res Commun,* 409**,** 280-6.

HIRASAWA, A., TSUMAYA, K., AWAJI, T., KATSUMA, S., ADACHI, T., YAMADA, M., SUGIMOTO, Y., MIYAZAKI, S. & TSUJIMOTO, G. 2005. Free fatty acids regulate gut incretin glucagon-like peptide-1 secretion through GPR120. *Nat Med,* 11**,** 90-4.

HJORTH, E., ZHU, M., TORO, V. C., VEDIN, I., PALMBLAD, J., CEDERHOLM, T., FREUND-LEVI, Y., FAXEN-IRVING, G., WAHLUND, L. O., BASUN, H., ERIKSDOTTER, M. & SCHULTZBERG, M. 2013. Omega-3 fatty acids enhance phagocytosis of Alzheimer's disease-related amyloid-beta42 by human microglia and decrease inflammatory markers. *J Alzheimers Dis,* 35**,** 697-713.

HONG, S., GRONERT, K., DEVCHAND, P. R., MOUSSIGNAC, R. L. & SERHAN, C. N. 2003. Novel docosatrienes and 17S-resolvins generated from docosahexaenoic acid in murine brain, human blood, and glial cells. Autacoids in anti-inflammation. *J Biol Chem,* 278**,** 14677-87.

HONG, S., PORTER, T. F., LU, Y., OH, S. F., PILLAI, P. S. & SERHAN, C. N. 2008. Resolvin E1 metabolome in local inactivation during inflammation-resolution. *J Immunol,* 180**,** 3512-9.

HUMPHRIES, P. S., BENBOW, J. W., BONIN, P. D., BOYER, D., DORAN, S. D., FRISBIE, R. K., PIOTROWSKI, D. W., BALAN, G., BECHLE, B. M., CONN, E. L., DIRICO, K. J., OLIVER, R. M., SOELLER, W. C., SOUTHERS, J. A. & YANG, X. 2009. Synthesis and SAR of 1,2,3,4-tetrahydroisoquinolin-1-ones as novel G-protein-coupled receptor 40 (GPR40) antagonists. *Bioorg Med Chem Lett,* 19**,** 2400-3.

HURST, N. P., NUKI, G. & WALLINGTON, T. 1983. Functional defects of monocyte C3b receptor-mediated phagocytosis in rheumatoid arthritis (RA): evidence for an association with the appearance of a circulating population of non-specific esterase-negative mononuclear phagocytes. *Ann Rheum Dis,* 42**,** 487-93.

INGLIS, J. J., CRIADO, G., MEDGHALCHI, M., ANDREWS, M., SANDISON, A., FELDMANN, M. & WILLIAMS, R. O. 2007. Collagen-induced arthritis in C57BL/6 mice is associated with a robust and sustained T-cell response to type II collagen. *Arthritis Res Ther,* 9**,** R113.

ITALIANI, P. & BORASCHI, D. 2014. From Monocytes to M1/M2 Macrophages: Phenotypical vs. Functional Differentiation. *Front Immunol,* 5**,** 514.

ITO, M. K. 2015. A Comparative Overview of Prescription Omega-3 Fatty Acid Products. *P T,* 40**,** 826-57.

ITOH, Y., KAWAMATA, Y., HARADA, M., KOBAYASHI, M., FUJII, R., FUKUSUMI, S., OGI, K., HOSOYA, M., TANAKA, Y., UEJIMA, H., TANAKA, H., MARUYAMA, M., SATOH, R., OKUBO, S., KIZAWA, H., KOMATSU, H., MATSUMURA, F., NOGUCHI, Y., SHINOHARA, T., HINUMA, S., FUJISAWA, Y. & FUJINO, M. 2003. Free fatty acids regulate insulin secretion from pancreatic beta cells through GPR40. *Nature,* 422**,** 173-6.

JAFFE, E. A., NACHMAN, R. L., BECKER, C. G. & MINICK, C. R. 1973. Culture of human endothelial cells derived from umbilical veins. Identification by morphologic and immunologic criteria. *J Clin Invest,* 52**,** 2745-56.

JANKOWSKI, A., SCOTT, C. C. & GRINSTEIN, S. 2002. Determinants of the phagosomal pH in neutrophils. *J Biol Chem,* 277**,** 6059-66.

JOZSEF, L., KHREISS, T. & FILEP, J. G. 2004. CpG motifs in bacterial DNA delay apoptosis of neutrophil granulocytes. *FASEB J,* 18**,** 1776-8.

KATSUMA, S., HATAE, N., YANO, T., RUIKE, Y., KIMURA, M., HIRASAWA, A. & TSUJIMOTO, G. 2005. Free fatty acids inhibit serum deprivation-induced apoptosis through GPR120 in a murine enteroendocrine cell line STC-1. *J Biol Chem,* 280**,** 19507-15.

KENYON, K. D., COLE, C., CRAWFORD, F., KAPPLER, J. W., THURMAN, J. M., BRATTON, D. L., BOACKLE, S. A. & HENSON, P. M. 2011. IgG autoantibodies against deposited C3 inhibit macrophage-mediated apoptotic cell engulfment in systemic autoimmunity. *J Immunol,* 187**,** 2101-11.

KLARESKOG, L., CATRINA, A. I. & PAGET, S. 2009. Rheumatoid arthritis. *Lancet,* 373**,** 659-72.

KLARESKOG, L., MALMSTROM, V., LUNDBERG, K., PADYUKOV, L. & ALFREDSSON, L. 2011. Smoking, citrullination and genetic variability in the immunopathogenesis of rheumatoid arthritis. *Semin Immunol,* 23**,** 92-8.

KNIJFF-DUTMER, E. A., KOERTS, J., NIEUWLAND, R., KALSBEEK-BATENBURG, E. M. & VAN DE LAAR, M. A. 2002. Elevated levels of platelet microparticles are associated with disease activity in rheumatoid arthritis. *Arthritis Rheum,* 46**,** 1498-503.

KOBAYASHI, S. D., VOYICH, J. M., BRAUGHTON, K. R., WHITNEY, A. R., NAUSEEF, W. M., MALECH, H. L. & DELEO, F. R. 2004. Gene expression profiling provides insight into the pathophysiology of chronic granulomatous disease. *J Immunol,* 172**,** 636-43.

KOLLIAS, G., PAPADAKI, P., APPARAILLY, F., VERVOORDELDONK, M. J., HOLMDAHL, R., BAUMANS, V., DESAINTES, C., DI SANTO, J., DISTLER, J., GARSIDE, P., HEGEN, M., HUIZINGA, T. W., JUNGEL, A., KLARESKOG, L., MCINNES, I., RAGOUSSIS, I., SCHETT, G., HART, B., TAK, P. P., TOES, R., VAN DEN BERG, W., WURST, W. & GAY, S. 2011. Animal models for arthritis: innovative tools for prevention and treatment. *Ann Rheum Dis,* 70**,** 1357-62.

KOROSKENYI, K., DURO, E., PALLAI, A., SARANG, Z., KLOOR, D., UCKER, D. S., BECEIRO, S., CASTRILLO, A., CHAWLA, A., LEDENT, C. A., FESUS, L. & SZONDY, Z. 2011. Involvement of adenosine A2A receptors in engulfment-dependent apoptotic cell suppression of inflammation. *J Immunol,* 186**,** 7144-55.

KOUSKOFF, V., KORGANOW, A. S., DUCHATELLE, V., DEGOTT, C., BENOIST, C. & MATHIS, D. 1996. Organ-specific disease provoked by systemic autoimmunity. *Cell,* 87**,** 811-22.

KREMER, J. M., JUBIZ, W., MICHALEK, A., RYNES, R. I., BARTHOLOMEW, L. E., BIGAOUETTE, J., TIMCHALK, M., BEELER, D. & LININGER, L. 1987. Fish-oil fatty acid supplementation in active rheumatoid arthritis. A double-blinded, controlled, crossover study. *Ann Intern Med,* 106**,** 497-503.

KREMER, J. M., LAWRENCE, D. A., JUBIZ, W., DIGIACOMO, R., RYNES, R., BARTHOLOMEW, L. E. & SHERMAN, M. 1990. Dietary fish oil and olive oil supplementation in patients with rheumatoid arthritis. Clinical and immunologic effects. *Arthritis Rheum,* 33**,** 810-20.

KRISHNAMOORTHY, S., RECCHIUTI, A., CHIANG, N., YACOUBIAN, S., LEE, C. H., YANG, R., PETASIS, N. A. & SERHAN, C. N. 2010. Resolvin D1 binds human phagocytes with evidence for proresolving receptors. *Proc Natl Acad Sci U S A,* 107**,** 1660-5.

KRISHNAN, S., ALDEN, N. & LEE, K. 2015. Pathways and functions of gut microbiota metabolism impacting host physiology. *Curr Opin Biotechnol,* 36**,** 137-45.

KYBURZ, D. & CORR, M. 2003. The KRN mouse model of inflammatory arthritis. *Springer Semin Immunopathol,* 25**,** 79-90.

LALLY, F., SMITH, E., FILER, A., STONE, M. A., SHAW, J. S., NASH, G. B., BUCKLEY, C. D. & RAINGER, G. E. 2005. A novel mechanism of neutrophil recruitment in a coculture model of the rheumatoid synovium. *Arthritis Rheum,* 52**,** 3460-9.

LEE, A., WHYTE, M. K. & HASLETT, C. 1993. Inhibition of apoptosis and prolongation of neutrophil functional longevity by inflammatory mediators. *J Leukoc Biol,* 54**,** 283-8.

LEE, C. H. 2012. Resolvins as new fascinating drug candidates for inflammatory diseases. *Arch Pharm Res,* 35**,** 3-7.

LEE, E., LINDO, T., JACKSON, N., MENG-CHOONG, L., REYNOLDS, P., HILL, A., HASWELL, M., JACKSON, S. & KILFEATHER, S. 1999. Reversal of human neutrophil survival by leukotriene B(4) receptor blockade and 5-lipoxygenase and 5-lipoxygenase activating protein inhibitors. *Am J Respir Crit Care Med,* 160**,** 2079-85.

LEONI, G., PATEL, H. B., SAMPAIO, A. L., GAVINS, F. N., MURRAY, J. F., GRIECO, P., GETTING, S. J. & PERRETTI, M. 2008. Inflamed phenotype of the mesenteric microcirculation of melanocortin type 3 receptor-null mice after ischemia-reperfusion. *FASEB J,* 22**,** 4228-38.

LEVY, B. D. 2010. Resolvins and protectins: natural pharmacophores for resolution biology. *Prostaglandins Leukot Essent Fatty Acids,* 82**,** 327-32.

LEVY, B. D., CLISH, C. B., SCHMIDT, B., GRONERT, K. & SERHAN, C. N. 2001. Lipid mediator class switching during acute inflammation: signals in resolution. *Nat Immunol,* 2**,** 612-9.

LEY, K., LAUDANNA, C., CYBULSKY, M. I. & NOURSHARGH, S. 2007. Getting to the site of inflammation: the leukocyte adhesion cascade updated. *Nat Rev Immunol,* 7**,** 678-89.

LIBBY, P. 2002. Inflammation in atherosclerosis. *Nature,* 420**,** 868-74.

LIU, Y., COUSIN, J. M., HUGHES, J., VAN DAMME, J., SECKL, J. R., HASLETT, C., DRANSFIELD, I., SAVILL, J. & ROSSI, A. G. 1999. Glucocorticoids promote nonphlogistic phagocytosis of apoptotic leukocytes. *J Immunol,* 162**,** 3639-46.

MACFARLANE, S., BAHRAMI, B. & MACFARLANE, G. T. 2011. Mucosal biofilm communities in the human intestinal tract. *Adv Appl Microbiol,* 75**,** 111-43.

MACKAY, F., LOETSCHER, H., STUEBER, D., GEHR, G. & LESSLAUER, W. 1993. Tumor necrosis factor alpha (TNF-alpha)-induced cell adhesion to human endothelial cells is under dominant control of one TNF receptor type, TNF-R55. *J Exp Med,* 177**,** 1277-86.

MADERNA, P., YONA, S., PERRETTI, M. & GODSON, C. 2005. Modulation of phagocytosis of apoptotic neutrophils by supernatant from dexamethasone-treated macrophages and annexin-derived peptide Ac(2-26). *J Immunol,* 174**,** 3727-33.

MANTOVANI, A., SOZZANI, S., LOCATI, M., ALLAVENA, P. & SICA, A. 2002. Macrophage polarization: tumor-associated macrophages as a paradigm for polarized M2 mononuclear phagocytes. *Trends Immunol,* 23**,** 549-55.

MARADIT-KREMERS, H., CROWSON, C. S., NICOLA, P. J., BALLMAN, K. V., ROGER, V. L., JACOBSEN, S. J. & GABRIEL, S. E. 2005. Increased unrecognized coronary heart disease and sudden deaths in rheumatoid arthritis: a population-based cohort study. *Arthritis Rheum,* 52**,** 402-11.

MARTIN, C. J., PETERS, K. N. & BEHAR, S. M. 2014. Macrophages clean up: efferocytosis and microbial control. *Curr Opin Microbiol,* 17**,** 17-23.

MARTINEZ, F. O. & GORDON, S. 2014. The M1 and M2 paradigm of macrophage activation: time for reassessment. *F1000Prime Rep,* 6**,** 13.

MATSUMOTO, I., MACCIONI, M., LEE, D. M., MAURICE, M., SIMMONS, B., BRENNER, M., MATHIS, D. & BENOIST, C. 2002. How antibodies to a ubiquitous cytoplasmic enzyme may provoke joint-specific autoimmune disease. *Nat Immunol,* 3**,** 360-5.

MAURI, C., WILLIAMS, R. O., WALMSLEY, M. & FELDMANN, M. 1996. Relationship between Th1/Th2 cytokine patterns and the arthritogenic response in collagen-induced arthritis. *Eur J Immunol,* 26**,** 1511-8.

MAYADAS, T. N., CULLERE, X. & LOWELL, C. A. 2014. The multifaceted functions of neutrophils. *Annu Rev Pathol,* 9**,** 181-218.

MCCRACKEN, J. M. & ALLEN, L. A. 2014. Regulation of human neutrophil apoptosis and lifespan in health and disease. *J Cell Death,* 7**,** 15-23.

MCINNES, I. B. & SCHETT, G. 2007. Cytokines in the pathogenesis of rheumatoid arthritis. *Nat Rev Immunol,* 7**,** 429-42.

MEDZHITOV, R. 2008. Origin and physiological roles of inflammation. *Nature,* 454**,** 428-35.

MEDZHITOV, R. 2010. Inflammation 2010: new adventures of an old flame. *Cell,* 140**,** 771-6.

MENA, S. J., MANOSALVA, C., CARRETTA, M. D., TEUBER, S., OLMO, I., BURGOS, R. A. & HIDALGO, M. A. 2016. Differential free fatty acid receptor-1 (FFAR1/GPR40) signalling is associated with gene expression or gelatinase granule release in bovine neutrophils. *Innate Immun,* 22**,** 479-89.

MILES, E. A., ALLEN, E. & CALDER, P. C. 2002. In vitro effects of eicosanoids derived from different 20-carbon Fatty acids on production of monocyte-derived cytokines in human whole blood cultures. *Cytokine,* 20**,** 215-23.

MILES, E. A. & CALDER, P. C. 2012. Influence of marine n-3 polyunsaturated fatty acids on immune function and a systematic review of their effects on clinical outcomes in rheumatoid arthritis. *Br J Nutr,* 107 Suppl 2**,** S171-84.

MISHARIN, A. V., CUDA, C. M., SABER, R., TURNER, J. D., GIERUT, A. K., HAINES, G. K., 3RD, BERDNIKOVS, S., FILER, A., CLARK, A. R., BUCKLEY, C. D., MUTLU, G. M., BUDINGER, G. R. & PERLMAN, H. 2014. Nonclassical Ly6C(-) Monocytes Drive the Development of Inflammatory Arthritis in Mice. *Cell Rep,* 9**,** 591-604.

MONFOULET, L. E., PHILIPPE, C., MERCIER, S., COXAM, V. & WITTRANT, Y. 2015. Deficiency of G-protein coupled receptor 40, a lipid-activated receptor,

heightens in vitro- and in vivo-induced murine osteoarthritis. *Exp Biol Med (Maywood),* 240**,** 854-66.

MONTERO-MELENDEZ, T., PATEL, H. B., SEED, M., NIELSEN, S., JONASSEN, T. E. & PERRETTI, M. 2011. The melanocortin agonist AP214 exerts anti-inflammatory and proresolving properties. *Am J Pathol,* 179**,** 259-69.

MURRAY, P. J., ALLEN, J. E., BISWAS, S. K., FISHER, E. A., GILROY, D. W., GOERDT, S., GORDON, S., HAMILTON, J. A., IVASHKIV, L. B., LAWRENCE, T., LOCATI, M., MANTOVANI, A., MARTINEZ, F. O., MEGE, J. L., MOSSER, D. M., NATOLI, G., SAEIJ, J. P., SCHULTZE, J. L., SHIREY, K. A., SICA, A., SUTTLES, J., UDALOVA, I., VAN GINDERACHTER, J. A., VOGEL, S. N. & WYNN, T. A. 2014. Macrophage activation and polarization: nomenclature and experimental guidelines. *Immunity,* 41**,** 14-20.

NAKAMOTO, K., NISHINAKA, T., SATO, N., MANKURA, M., KOYAMA, Y., KASUYA, F. & TOKUYAMA, S. 2013. Hypothalamic GPR40 signaling activated by free long chain fatty acids suppresses CFA-induced inflammatory chronic pain. *PLoS One,* 8**,** e81563.

NATHAN, C. 2006. Neutrophils and immunity: challenges and opportunities. *Nat Rev Immunol,* 6**,** 173-82.

NILSSON, N. E., KOTARSKY, K., OWMAN, C. & OLDE, B. 2003. Identification of a free fatty acid receptor, FFA2R, expressed on leukocytes and activated by short-chain fatty acids. *Biochem Biophys Res Commun,* 303**,** 1047-52.

NORLING, L. V., DALLI, J., FLOWER, R. J., SERHAN, C. N. & PERRETTI, M. 2012. Resolvin D1 limits polymorphonuclear leukocyte recruitment to inflammatory loci: receptor-dependent actions. *Arterioscler Thromb Vasc Biol,* 32**,** 1970-8.

NORLING, L. V., HEADLAND, S. E., DALLI, J., ARNARDOTTIR, H. H., HAWORTH, O., JONES, H. R., IRIMIA, D., SERHAN, C. N. & PERRETTI, M. 2016. Proresolving and cartilage-protective actions of resolvin D1 in inflammatory arthritis. *JCI Insight,* 1**,** e85922.

NORLING, L. V. & PERRETTI, M. 2013. Control of myeloid cell trafficking in resolution. *J Innate Immun,* 5**,** 367-76.

O'KEEFE, J. H., JR. & HARRIS, W. S. 2000. From Inuit to implementation: omega-3 fatty acids come of age. *Mayo Clin Proc,* 75**,** 607-14.

OH, D. Y., TALUKDAR, S., BAE, E. J., IMAMURA, T., MORINAGA, H., FAN, W., LI, P., LU, W. J., WATKINS, S. M. & OLEFSKY, J. M. 2010. GPR120 is an omega-3 fatty acid receptor mediating potent anti-inflammatory and insulin-sensitizing effects. *Cell,* 142**,** 687-98.

OHMURA, K., NGUYEN, L. T., LOCKSLEY, R. M., MATHIS, D. & BENOIST, C. 2005. Interleukin-4 can be a key positive regulator of inflammatory arthritis. *Arthritis Rheum,* 52**,** 1866-75.

OKADA, Y., WU, D., TRYNKA, G., RAJ, T., TERAO, C., IKARI, K., KOCHI, Y., OHMURA, K., SUZUKI, A., YOSHIDA, S., GRAHAM, R. R., MANOHARAN, A., ORTMANN, W., BHANGALE, T., DENNY, J. C., CARROLL, R. J., EYLER, A. E., GREENBERG, J. D., KREMER, J. M., PAPPAS, D. A., JIANG, L., YIN, J., YE, L., SU, D. F., YANG, J., XIE, G., KEYSTONE, E., WESTRA, H. J., ESKO, T., METSPALU, A., ZHOU, X., GUPTA, N., MIREL, D., STAHL, E. A., DIOGO, D., CUI, J., LIAO, K., GUO, M. H., MYOUZEN, K., KAWAGUCHI, T., COENEN, M. J., VAN RIEL, P. L., VAN DE LAAR, M. A., GUCHELAAR, H. J., HUIZINGA, T. W., DIEUDE, P., MARIETTE, X., BRIDGES, S. L., JR., ZHERNAKOVA, A., TOES, R. E., TAK, P. P., MICELI-RICHARD, C., BANG, S. Y., LEE, H. S., MARTIN, J., GONZALEZ-GAY, M. A., RODRIGUEZ-RODRIGUEZ, L., RANTAPAA-DAHLQVIST, S., ARLESTIG, L., CHOI, H. K., KAMATANI, Y., GALAN, P., LATHROP, M., CONSORTIUM, R., CONSORTIUM, G., EYRE, S., BOWES, J., BARTON, A., DE VRIES, N., MORELAND, L. W., CRISWELL, L. A., KARLSON, E. W., TANIGUCHI, A., YAMADA, R., KUBO, M., LIU, J. S., BAE, S. C., WORTHINGTON, J.,

PADYUKOV, L., KLARESKOG, L., GREGERSEN, P. K., RAYCHAUDHURI, S., STRANGER, B. E., DE JAGER, P. L., FRANKE, L., VISSCHER, P. M., BROWN, M. A., YAMANAKA, H., MIMORI, T., TAKAHASHI, A., XU, H., BEHRENS, T. W., SIMINOVITCH, K. A., MOMOHARA, S., MATSUDA, F., YAMAMOTO, K. & PLENGE, R. M. 2014. Genetics of rheumatoid arthritis contributes to biology and drug discovery. *Nature,* 506**,** 376-81.

OKIN, D. & MEDZHITOV, R. 2012. Evolution of inflammatory diseases. *Curr Biol,* 22**,** R733-40.

OLSON, M. V., LIU, Y. C., DANGI, B., PAUL ZIMMER, J., SALEM, N., JR. & NAUROTH, J. M. 2013. Docosahexaenoic acid reduces inflammation and joint destruction in mice with collagen-induced arthritis. *Inflamm Res,* 62**,** 1003-13.

PARSONAGE, G., FILER, A., BIK, M., HARDIE, D., LAX, S., HOWLETT, K., CHURCH, L. D., RAZA, K., WONG, S. H., TREBILCOCK, E., SCHEEL-TOELLNER, D., SALMON, M., LORD, J. M. & BUCKLEY, C. D. 2008. Prolonged, granulocyte-macrophage colony-stimulating factor-dependent, neutrophil survival following rheumatoid synovial fibroblast activation by IL-17 and TNFalpha. *Arthritis Res Ther,* 10**,** R47.

PATEL, H. B., KORNERUP, K. N., SAMPAIO, A. L., D'ACQUISTO, F., SEED, M. P., GIROL, A. P., GRAY, M., PITZALIS, C., OLIANI, S. M. & PERRETTI, M. 2012. The impact of endogenous annexin A1 on glucocorticoid control of inflammatory arthritis. *Ann Rheum Dis,* 71**,** 1872-80.

PERRETTI, M. & D'ACQUISTO, F. 2009. Annexin A1 and glucocorticoids as effectors of the resolution of inflammation. *Nat Rev Immunol,* 9**,** 62-70.

PERRETTI, M., LEROY, X., BLAND, E. J. & MONTERO-MELENDEZ, T. 2015. Resolution Pharmacology: Opportunities for Therapeutic Innovation in Inflammation. *Trends Pharmacol Sci,* 36**,** 737-55.

PERRETTI, M. & SOLITO, E. 2004. Annexin 1 and neutrophil apoptosis. *Biochem Soc Trans,* 32**,** 507-10.

PFAFFL, M. W. 2001. A new mathematical model for relative quantification in real-time RT-PCR. *Nucleic Acids Res,* 29**,** e45.

PILLAY, J., DEN BRABER, I., VRISEKOOP, N., KWAST, L. M., DE BOER, R. J., BORGHANS, J. A., TESSELAAR, K. & KOENDERMAN, L. 2010. In vivo labeling with 2H2O reveals a human neutrophil lifespan of 5.4 days. *Blood,* 116**,** 625-7.

PITZALIS, C., KELLY, S. & HUMBY, F. 2013. New learnings on the pathophysiology of RA from synovial biopsies. *Curr Opin Rheumatol,* 25**,** 334-44.

PUHL, H. L., 3RD, WON, Y. J., LU, V. B. & IKEDA, S. R. 2015. Human GPR42 is a transcribed multisite variant that exhibits copy number polymorphism and is functional when heterologously expressed. *Sci Rep,* 5**,** 12880.

RAZA, K., SCHEEL-TOELLNER, D., LEE, C. Y., PILLING, D., CURNOW, S. J., FALCIANI, F., TREVINO, V., KUMAR, K., ASSI, L. K., LORD, J. M., GORDON, C., BUCKLEY, C. D. & SALMON, M. 2006. Synovial fluid leukocyte apoptosis is inhibited in patients with very early rheumatoid arthritis. *Arthritis Res Ther,* 8**,** R120.

ROCHA E SILVA, M. 1978. A brief survey of the history of inflammation. *Agents Actions,* 8**,** 45-9.

ROGERIO, A. P., HAWORTH, O., CROZE, R., OH, S. F., UDDIN, M., CARLO, T., PFEFFER, M. A., PRILUCK, R., SERHAN, C. N. & LEVY, B. D. 2012. Resolvin D1 and aspirin-triggered resolvin D1 promote resolution of allergic airways responses. *J Immunol,* 189**,** 1983-91.

ROSENBAUM, D. M., RASMUSSEN, S. G. & KOBILKA, B. K. 2009. The structure and function of G-protein-coupled receptors. *Nature,* 459**,** 356-63.

SALEHI, A., FLODGREN, E., NILSSON, N. E., JIMENEZ-FELTSTROM, J., MIYAZAKI, J., OWMAN, C. & OLDE, B. 2005. Free fatty acid receptor 1

(FFA(1)R/GPR40) and its involvement in fatty-acid-stimulated insulin secretion. *Cell Tissue Res,* 322**,** 207-15.

SAVILL, J. S., WYLLIE, A. H., HENSON, J. E., WALPORT, M. J., HENSON, P. M. & HASLETT, C. 1989. Macrophage phagocytosis of aging neutrophils in inflammation. Programmed cell death in the neutrophil leads to its recognition by macrophages. *J Clin Invest,* 83**,** 865-75.

SAWZDARGO, M., GEORGE, S. R., NGUYEN, T., XU, S., KOLAKOWSKI, L. F. & O'DOWD, B. F. 1997. A cluster of four novel human G protein-coupled receptor genes occurring in close proximity to CD22 gene on chromosome 19q13.1. *Biochem Biophys Res Commun,* 239**,** 543-7.

SCHWAB, J. M., CHIANG, N., ARITA, M. & SERHAN, C. N. 2007. Resolvin E1 and protectin D1 activate inflammation-resolution programmes. *Nature,* 447**,** 869-74.

SERHAN, C. N. 2014. Pro-resolving lipid mediators are leads for resolution physiology. *Nature,* 510**,** 92-101.

SERHAN, C. N., DALLI, J., KARAMNOV, S., CHOI, A., PARK, C. K., XU, Z. Z., JI, R. R., ZHU, M. & PETASIS, N. A. 2012. Macrophage proresolving mediator maresin 1 stimulates tissue regeneration and controls pain. *FASEB J,* 26**,** 1755-65.

SERHAN, C. N., HONG, S., GRONERT, K., COLGAN, S. P., DEVCHAND, P. R., MIRICK, G. & MOUSSIGNAC, R. L. 2002. Resolvins: a family of bioactive products of omega-3 fatty acid transformation circuits initiated by aspirin treatment that counter proinflammation signals. *J Exp Med,* 196**,** 1025-37.

SERHAN, C. N., YANG, R., MARTINOD, K., KASUGA, K., PILLAI, P. S., PORTER, T. F., OH, S. F. & SPITE, M. 2009. Maresins: novel macrophage mediators with potent antiinflammatory and proresolving actions. *J Exp Med,* 206**,** 15-23.

SHAPIRO, H., SHACHAR, S., SEKLER, I., HERSHFINKEL, M. & WALKER, M. D. 2005. Role of GPR40 in fatty acid action on the beta cell line INS-1E. *Biochem Biophys Res Commun,* 335**,** 97-104.

SHINOHARA, M., MIRAKAJ, V. & SERHAN, C. N. 2012. Functional Metabolomics Reveals Novel Active Products in the DHA Metabolome. *Front Immunol,* 3**,** 81.

SILMAN, A. J., NEWMAN, J. & MACGREGOR, A. J. 1996. Cigarette smoking increases the risk of rheumatoid arthritis. Results from a nationwide study of disease-discordant twins. *Arthritis Rheum,* 39**,** 732-5.

SMOLEN, J. S. & STEINER, G. 2003. Therapeutic strategies for rheumatoid arthritis. *Nat Rev Drug Discov,* 2**,** 473-88.

SPERLING, R. I. 1995. Eicosanoids in rheumatoid arthritis. *Rheum Dis Clin North Am,* 21**,** 741-58.

SPERLING, R. I., WEINBLATT, M., ROBIN, J. L., RAVALESE, J., 3RD, HOOVER, R. L., HOUSE, F., COBLYN, J. S., FRASER, P. A., SPUR, B. W., ROBINSON, D. R. & ET AL. 1987. Effects of dietary supplementation with marine fish oil on leukocyte lipid mediator generation and function in rheumatoid arthritis. *Arthritis Rheum,* 30**,** 988-97.

ST CLAIR, E. W., WILKINSON, W. E., LANG, T., SANDERS, L., MISUKONIS, M. A., GILKESON, G. S., PISETSKY, D. S., GRANGER, D. I. & WEINBERG, J. B. 1996. Increased expression of blood mononuclear cell nitric oxide synthase type 2 in rheumatoid arthritis patients. *J Exp Med,* 184**,** 1173-8.

TAK, T., TESSELAAR, K., PILLAY, J., BORGHANS, J. A. & KOENDERMAN, L. 2013. What's your age again? Determination of human neutrophil half-lives revisited. *J Leukoc Biol,* 94**,** 595-601.

TAYLOR, P. R., CARUGATI, A., FADOK, V. A., COOK, H. T., ANDREWS, M., CARROLL, M. C., SAVILL, J. S., HENSON, P. M., BOTTO, M. & WALPORT,

M. J. 2000. A hierarchical role for classical pathway complement proteins in the clearance of apoptotic cells in vivo. *J Exp Med,* 192**,** 359-66.

TEIXEIRA, M. M., CUNHA, F. Q. & FERREIRA, S. H. 2001. Response to an infectious insult (e.g., bacterial or fungal infection). *Braz J Med Biol Res,* 34**,** 1 p preceding 555.

THORBURN, A. N., MACIA, L. & MACKAY, C. R. 2014. Diet, metabolites, and "western-lifestyle" inflammatory diseases. *Immunity,* 40**,** 833-42.

TITOS, E., RIUS, B., GONZALEZ-PERIZ, A., LOPEZ-VICARIO, C., MORAN-SALVADOR, E., MARTINEZ-CLEMENTE, M., ARROYO, V. & CLARIA, J. 2011. Resolvin D1 and its precursor docosahexaenoic acid promote resolution of adipose tissue inflammation by eliciting macrophage polarization toward an M2-like phenotype. *J Immunol,* 187**,** 5408-18.

TORRES-GUZMAN, A. M., MORADO-URBINA, C. E., ALVARADO-VAZQUEZ, P. A., ACOSTA-GONZALEZ, R. I., CHAVEZ-PINA, A. E., MONTIEL-RUIZ, R. M. & JIMENEZ-ANDRADE, J. M. 2014. Chronic oral or intraarticular administration of docosahexaenoic acid reduces nociception and knee edema and improves functional outcomes in a mouse model of Complete Freund's Adjuvant-induced knee arthritis. *Arthritis Res Ther,* 16**,** R64.

UMEKITA, K., HIDAKA, T., UENO, S., TAKAJO, I., KAI, Y., NAGATOMO, Y., SAWAGUCHI, A., SUGANUMA, T. & OKAYAMA, A. 2009. Leukocytapheresis (LCAP) decreases the level of platelet-derived microparticles (MPs) and increases the level of granulocytes-derived MPs: a possible connection with the effect of LCAP on rheumatoid arthritis. *Mod Rheumatol,* 19**,** 265-72.

VAN HALM, V. P., NURMOHAMED, M. T., TWISK, J. W., DIJKMANS, B. A. & VOSKUYL, A. E. 2006. Disease-modifying antirheumatic drugs are associated with a reduced risk for cardiovascular disease in patients with rheumatoid arthritis: a case control study. *Arthritis Res Ther,* 8**,** R151.

VAN VOLLENHOVEN, R. F. 2009. Sex differences in rheumatoid arthritis: more than meets the eye. *BMC Med,* 7**,** 12.

VANE, J. R. 1971. Inhibition of prostaglandin synthesis as a mechanism of action for aspirin-like drugs. *Nat New Biol,* 231**,** 232-5.

VIEIRA, O. V., BOTELHO, R. J. & GRINSTEIN, S. 2002. Phagosome maturation: aging gracefully. *Biochem J,* 366**,** 689-704.

VILCEK, J. & FELDMANN, M. 2004. Historical review: Cytokines as therapeutics and targets of therapeutics. *Trends Pharmacol Sci,* 25**,** 201-9.

WAUQUIER, F., PHILIPPE, C., LEOTOING, L., MERCIER, S., DAVICCO, M. J., LEBECQUE, P., GUICHEUX, J., PILET, P., MIOT-NOIRAULT, E., POITOUT, V., ALQUIER, T., COXAM, V. & WITTRANT, Y. 2013. The free fatty acid receptor G protein-coupled receptor 40 (GPR40) protects from bone loss through inhibition of osteoclast differentiation. *J Biol Chem,* 288**,** 6542-51.

WEINBERGER, B., QUIZON, C., VETRANO, A. M., ARCHER, F., LASKIN, J. D. & LASKIN, D. L. 2008. Mechanisms mediating reduced responsiveness of neonatal neutrophils to lipoxin A4. *Pediatr Res,* 64**,** 393-8.

WEINER, H. L. & SELKOE, D. J. 2002. Inflammation and therapeutic vaccination in CNS diseases. *Nature,* 420**,** 879-84.

WEINMANN, P., MOURA, R. A., CAETANO-LOPES, J. R., PEREIRA, P. A., CANHAO, H., QUEIROZ, M. V. & FONSECA, J. E. 2007. Delayed neutrophil apoptosis in very early rheumatoid arthritis patients is abrogated by methotrexate therapy. *Clin Exp Rheumatol,* 25**,** 885-7.

WELTERS, H. J., DIAKOGIANNAKI, E., MORDUE, J. M., TADAYYON, M., SMITH, S. A. & MORGAN, N. G. 2006. Differential protective effects of palmitoleic acid and cAMP on caspase activation and cell viability in pancreatic beta-cells exposed to palmitate. *Apoptosis,* 11**,** 1231-8.

WINK, D. A., HINES, H. B., CHENG, R. Y., SWITZER, C. H., FLORES-SANTANA, W., VITEK, M. P., RIDNOUR, L. A. & COLTON, C. A. 2011. Nitric oxide and redox mechanisms in the immune response. *J Leukoc Biol,* 89**,** 873-91.

WITTKOWSKI, H., FOELL, D., AF KLINT, E., DE RYCKE, L., DE KEYSER, F., FROSCH, M., ULFGREN, A. K. & ROTH, J. 2007. Effects of intra-articular corticosteroids and anti-TNF therapy on neutrophil activation in rheumatoid arthritis. *Ann Rheum Dis,* 66**,** 1020-5.

WOOLEY, P. H., LUTHRA, H. S., GRIFFITHS, M. M., STUART, J. M., HUSE, A. & DAVID, C. S. 1985. Type II collagen-induced arthritis in mice. IV. Variations in immunogenetic regulation provide evidence for multiple arthritogenic epitopes on the collagen molecule. *J Immunol,* 135**,** 2443-51.

YAN, Y., JIANG, W., SPINETTI, T., TARDIVEL, A., CASTILLO, R., BOURQUIN, C., GUARDA, G., TIAN, Z., TSCHOPP, J. & ZHOU, R. 2013. Omega-3 fatty acids prevent inflammation and metabolic disorder through inhibition of NLRP3 inflammasome activation. *Immunity,* 38**,** 1154-63.

YATES, C. M., CALDER, P. C. & ED RAINGER, G. 2014. Pharmacology and therapeutics of omega-3 polyunsaturated fatty acids in chronic inflammatory disease. *Pharmacol Ther,* 141**,** 272-82.

ZHANG, X., YAN, G., LI, Y., ZHU, W. & WANG, H. 2010. DC260126, a small-molecule antagonist of GPR40, improves insulin tolerance but not glucose tolerance in obese Zucker rats. *Biomed Pharmacother,* 64**,** 647-51.

CHAPTER 7: ATTACHMENTS

ATTACHMENTS

1. Implications for eicosapentaenoic acid- and docosahexaenoic acid-derived resolvins as therapeutics for arthritis

   Patricia R Souza, Lucy V Norling

   Eur J Pharmacol. 2015 Jul 9. pii: S0014-2999(15)30148-5. doi: 10.1016/j.ejphar.2015. 05.072

2. Neutrophil-derived microvesicles enter cartilage and protect the joint in inflammatory arthritis

   Sarah E Headland, Hefin R Jones, Lucy V Norling, Andrew Kim, Patricia R Souza, Elisa Corsiero, Cristiane D GIL, A Nerviani, Francesco Dell'Accio, Constantino Pitzalis, Sonia M Oliani, Lily Y Jan, Mauro Perretti

   Sci Transl Med. 2015 Nov 25;7(315):315ra190. doi: 10.1126/scitranslmed.aac5608

3. Galectin-3–null mice display defective neutrophil clearance during acute inflammation

   Rachael D Wright, Patricia R Souza, Magdalena B Flak, Prasheetha Thedchanamoorthy, Lucy V Norling and Dianne Cooper

   Journal of Leukocyte Biology. Epub ahead of print October 12, 2016 - doi:10.1189/jlb.3A0116-026RR

7.1. Implications for eicosapentaenoic acid- and docosahexaenoic acid-derived resolvins as therapeutics for arthritis

European Journal of Pharmacology 785 (2016) 165–173

Contents lists available at ScienceDirect

European Journal of Pharmacology

journal homepage: www.elsevier.com/locate/ejphar

Implications for eicosapentaenoic acid- and docosahexaenoic acid-derived resolvins as therapeutics for arthritis

Patricia R. Souza, Lucy V. Norling *

The William Harvey Research Institute, Barts and The London School of Medicine and Dentistry, Charterhouse Square, London EC1M 6BQ, United Kingdom

ARTICLE INFO

Article history:
Received 30 January 2015
Received in revised form
16 April 2015
Accepted 11 May 2015
Available online 9 July 2015

Key Words:
Omega-3
Resolvins
Arthritis
Resolution
Inflammation

ABSTRACT

Omega-3 polyunsaturated fatty acids are essential for health and are known to possess anti-inflammatory properties, improving cardiovascular health as well as benefiting inflammatory diseases. Indeed, dietary supplementation with omega-3 polyunsaturated fatty acids has proved efficacious in reducing joint pain, morning stiffness and nonsteroidal anti-inflammatory drugs usage in rheumatoid arthritis patients. However, the mechanisms by which omega-3 polyunsaturated fatty acids exert their beneficial effects have not been fully explored. Seminal discoveries by Serhan and colleagues have unveiled a novel class of bioactive lipid mediators that are enzymatically biosynthesized in vivo from omega-3 eicosapentaenoic acid (EPA) and docosahexaenoic acid (DHA), termed resolvins, protectins and maresins. These bioactive pro-resolving lipid mediators provide further rationale for the beneficial effects of fish-oil enriched diets. These endogenous lipid mediators are spatiotemporally biosynthesized to actively regulate resolution by acting on specific G protein-coupled receptors (GPCRs) to initiate anti-inflammatory and pro-resolving signals that terminate inflammation. In this review, we will discuss the mechanism of actions of these molecules, including their analgesic and bone-sparing properties making them ideal therapeutic agonists for the treatment of inflammatory diseases such as rheumatoid arthritis.

1. Introduction

An observation made more than 40 years ago brought great interest to the field of omega-3 polyunsaturated fatty acids as a potential nutraceutical for human diseases. In the late 1970s, epidemiological studies revealed that Greenland Inuits had substantially lower frequency or absence of a vast number of diseases, including acute myocardial infarction, diabetes mellitus, thyrotoxicosis, bronchial asthma, multiple sclerosis and psoriasis, when compared with Western control subjects (Kromann and Green, 1980). These observations stimulated vast research into the mechanism of action of omega-3 fatty acids on human metabolism and health, as evidenced by the sheer number of research articles on this topic (more than 3400, search in the PubMed database). From epidemiology, cell culture and animal studies to randomized controlled trials, the cardioprotective effects of omega-3 polyunsaturated fatty acids are becoming increasingly recognized. Due to this observation, omega-3 polyunsaturated fatty acids are used to supplement the diet, and are also prescribed for hypertriglyceridemia and the prevention of myocardiac infarction (Bradberry and Hilleman, 2013). This encouraged researchers to investigate the anti-inflammatory properties ascribed to omega-3 polyunsaturated fatty acids for various chronic inflammatory diseases such as rheumatoid arthritis, inflammatory bowel disease, and asthma (discussed in recent review Calder (2015)).

Numerous randomized, placebo-controlled, double-blinded studies using omega-3 polyunsaturated fatty acids in rheumatoid arthritis are reported. Almost all of these trials showed some benefit of fish oil, a source of these fatty acids. Such benefits include reduced duration of morning stiffness, reduced number of tender or swollen joints, decreased pain and time to fatigue, increased grip strength, and decreased use of non-steroidal anti-inflammatory drugs (reviewed in Calder (2008), and Miles and Calder (2012)). The dose range of omega-3 polyunsaturated fatty acids reported in these trials varied from 1.6 to 7.1 g/day and averaged 3.5 g/day (Calder, 2008; Miles and Calder, 2012). Thus, evidence-based reports implicate fish oil supplementation as an useful complementary therapy for rheumatoid arthritis. Alongside some of these studies, the authors also investigated inflammatory parameters that are modulated following omega-3 treatment, which include decreased leukotriene B_4 production by neutrophils (Cleland et al., 1988; Kremer et al., 1987, 1990; Sperling et al., 1987), reduced interleukin 1β production by macrophages (Kremer et al., 1990), and lower plasma levels of interleukin 1β (Espersen et al., 1992; Kremer et al., 1995). Thus the mechanisms

*Correspondence to: Centre for Biochemical Pharmacology, William Harvey Research Institute, Barts and The London School of Medicine, Charterhouse Square, London EC1M 6BQ, United Kingdom.
E-mail address: l.v.norling@qmul.ac.uk (L.V. Norling).

http://dx.doi.org/10.1016/j.ejphar.2015.05.072
0014-2999/

by which omega-3 polyunsaturated fatty acids exert their beneficial effects are of mounting interest. These actions are thought to be mediated, directly or indirectly, by eicosapentaenoic acid (EPA) and docosahexaenoic acid (DHA), the most prevalent omega-3 polyunsaturated fatty acids found in fish oil. One of the traditional theories is that omega-3 polyunsaturated fatty acids compete with the canonical omega-6 substrate arachidonic acid to generate eicosanoids such as prostaglandins of the 3-series and leukotrienes of the 5-series that are thought to be more anti-inflammatory than their arachidonic acid-derived counterparts (reviewed by Calder (2015)). More recently, Serhan discovered that both EPA and DHA could be enzymatically converted *in vivo* to novel bioactive lipid mediators, termed resolvins, protectins and maresins (termed specialized pro-resolving mediators) that stimulate the resolution of inflammation and have proven to be log-orders more potent than their lipid precursors (reviewed in Serhan (2014)). These mediators may represent a potential molecular mechanism to explain the beneficial use of omega-3 fatty acids as nutraceuticals. In the next sections, we will present these newly discovered mediators, their known bioactions and how they can be harnessed therapeutically for the treatment of rheumatoid arthritis.

2. Ideal outcome – resolution of inflammation

In the simplest definition, inflammation is an adaptive response that can be triggered by a variety of noxious stimuli, including infection and injury, that aims to restore homeostasis of the affected tissues, and therefore has a crucial role in the physiology of mammalian organisms (Medzhitov, 2008). Inflammatory responses are highly heterogeneous in terms of the cell types and molecular mediators involved. Inflammation also comes in different modalities that can be classified as acute *versus* chronic and local *versus* systemic. Despite this complexity, all inflammatory responses can be broken down into four common components that align in a universal configuration of the inflammatory pathway: inflammatory inducers, sensors, mediators, and effectors (Medzhitov, 2010). Inflammatory inducers can be exogenous signals (*e.g.* pathogens and toxins) or endogenous signals (*e.g.* ATP or urate crystals) that report on tissue stress, injury, or malfunction. Sensor cells, such as tissue-resident macrophages, dendritic cells and mast cells, detect inducers with specific receptors and respond by producing inflammatory mediators. Depending on the nature of the inducers, sensor cells produce different combinations and amounts of mediators (including cytokines, chemokines, vasoactive amines, lipid mediators and proteolytic cascade products), creating unique mediator signatures. Inflammatory mediators, in turn, act on target tissues triggering changes in the functional state thereof, favouring the migration of leukocytes from the blood and production of effector molecules (such as reactive radicals and proteases), thereby leading to adaptation to deleterious condition in accordance with the inducer (tissue injury or infection) that triggered the inflammatory response (Okin and Medzhitov, 2012).

The development of an appropriate inflammatory response is essential for the host. Indeed, the activation and recruitment of leukocytes are required for the processing and presentation of antigens by leukocytes, and effector function of any immune response (Teixeira et al., 2001). However, inflammatory processes have the potential to cause damage to host tissues. Indeed, the effector molecules produced in this process do not discriminate if their targets are a pathogen or a structure of the host, so the tissue damage is a potential side effect associated with any inflammatory response (Medzhitov, 2008; Nathan, 2006; Wink et al., 2011). Thus, this adaptive response is beneficial only if retained for a short duration. Chronic responses may lead to significant physiological changes. There is a wide range of human diseases associated with an inappropriate or uncontrolled inflammatory response that is triggered by known or unknown stimuli. These include rheumatoid arthritis, asthma, multiple sclerosis, chronic obstructive pulmonary disease and atherosclerosis (Libby, 2002; Vilcek and Feldmann, 2004; Weiner and Selkoe, 2002). Under these conditions, it is clear that tissue inflammation is deleterious. Therefore, an adequate control of inflammation is of fundamental importance for the restoration of the physiological conditions of the organism.

The current paradigm is that inflammation resolves in a highly coordinated, active process dictated by the spatial–temporal generation of pro-resolving mediators that act on specific receptors to modulate cell and tissue reactivity, in a process known as resolution of inflammation (Serhan et al., 2007). Recognizing the proactive nature of resolution of inflammation implicates that chronic, non-resolving inflammation is associated not only with excessive production of pro-inflammatory mediators but also attributed to a defect in endogenous anti-inflammatory mediators and pathways (Bonnans et al., 2002; Claria et al., 2012). A variety of different classes of pro-resolving mediators have now been identified including annexins, lipoxins, E-series resolvins, D-series resolvins, protectins/neuroprotectins, and maresins (reviewed by Perretti and D'Acquisto (2009), Serhan and Chiang (2008), Chiang et al. (2005), Serhan et al. (2009) and Serhan (2014)). These mediators display a multitude of protective actions, such as blocking neutrophil recruitment, promoting the recruitment and activation of monocytes, and mediating the nonphlogistic phagocytosis and lymphatic clearance of apoptotic neutrophils by activated macrophages (Fig. 1). It is therefore evident that pro-resolution mediators are not merely anti-inflammatory, for example, by blocking the binding of a cytokine to a receptor (*e.g.* interleukin 1 receptor (IL-1R), Allen et al. (1993)), but promote tissue restoration and return to homeostasis.

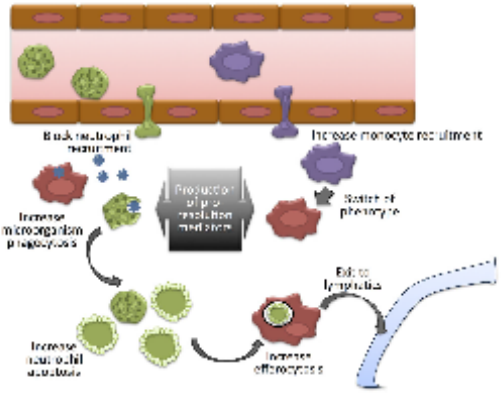

Fig. 1. Key steps in the resolution of inflammation initiated via pro-resolving mediators. After eliminating the inciting stimuli, by for example phagocytosis of microorganisms, the recruitment of neutrophils to the site of the inflammation must be discontinued, as neutrophils produce many mediators that could increase tissue damage. Remaining neutrophils must undergo apoptosis, and then be cleared by the monocytes that arrive later in the process and differentiate locally to macrophages. Different resolution mediators such as resolvins and annexin-A1 produced by the cells at the inflammatory site; as well as cell–cell interactions promotes a switch from pro-inflammatory to pro-resolution cell phenotypes and mediators. The inflammatory process will then end with either the incorporation of myeloid cells into the local population or their recirculation via lymphatic or blood vessels. Adapted from Norling and Perretti (2013).

2.1. Identification and generation of omega-3 derived resolvins

The initial identification, discovery and structural elucidation of resolvins was made by Serhan and his group at the turn of the 21st century. Firstly, they reported that inflammatory exudates collected from mice treated with omega-3 polyunsaturated fatty acids together with low dose aspirin contained a novel array of bioactive lipids. They also demonstrated the production of these lipids from human endothelial cells and polymorphonuclear leukocytes *in vitro* (Serhan et al., 2000). These new compounds were shown to be potent inhibitors of human polymorphonuclear leukocytes transendothelial migration and leukocyte infiltration *in vivo* (Serhan et al., 2000). During stress, cellular pathways utilize omega-3 fatty acids to biosynthesize these specialised bioactive lipid mediators that serve in anti-inflammation and resolution (Serhan et al., 2000, 2002). These new compounds were named Resolvins (resolution-phase interaction products) because they are (i) generated during the resolution phase and (ii) chemically redundant signals that play protective roles in dampening inflammation to promote a pro-resolution status (Serhan et al., 2002). The generation of resolvins derived from DHA, denoted D series resolvins (RvD) involves two iterative lipoxygenation steps. Initially DHA is converted to 17S-hydroperoxydocosahexaenoic acid by 15-lipoxygenase type I in humans and 12/15-lipoxygenase in mice, followed by a second enzymatic transformation *via* 5-lipoxygenase. This new intermediate can undergo hydrolysis or reduction, generating several chemically distinct bioactive compounds, including RvD1 to RvD6 (Fig. 2). Importantly, physiologically active levels of the D-series resolvin precursor 17S-hydroxy-4Z,7Z,10Z,13Z,15E,19Z-docosahexaenoic acid together with RvD1 and RvD2 were detected in plasma of healthy individuals following 3 weeks of dietary omega-3 supplementation (Mas et al., 2012). Resolvins can also be derived from EPA, denoted E series resolvins (RvE), which involves oxygenation of EPA *via* cytochrome P450 to produce an intermediate that will then be reduced into 18*R*-hydroxyeicosapentaenoic acid, followed by enzymatic transformation by 5-lipoxygenase, generating RvE1 or RvE2 (Fig. 2). The widely used anti-inflammatory drug, aspirin can also enhance generation of resolvins, some examples includes aspirin-triggered

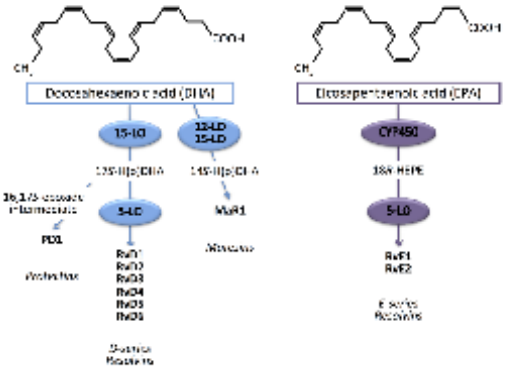

Fig. 2. Biosynthetic cascades of EPA- and DHA-derived pro-resolving mediators. The lipid mediators, termed resolvins, protectins and maresins are enzymatically biosynthesized *in vivo* from omega-3 PUFAs docosahexaenoic acid (DHA) and eicosapentaenoic acid (EPA). DHA is enzymatically converted to 17S-hydroperoxydocosahexaenoic acid (17S-H(p)DHA) by 15-LO (15-lipoxygenase type I). The 17S-H(p)DHA intermediate is further transformed by 5-LO *via* single cell or transcellular biosynthesis to resolvins of the D-series (RvD), or enzymatically hydrolyzed to protectin D1 (PD1). E-series resolvins are biosynthesized *via* conversion of EPA by the sequential actions of cytochrome P450 enzymes (CYP450) and 5-LO.

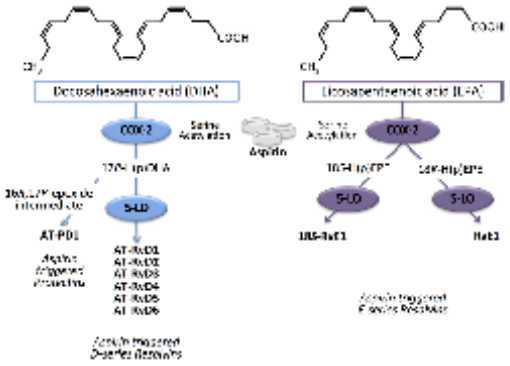

Fig. 3. Enhanced of formation of pro-resolvin mediators by aspirin. Aspirin can promote the generation of 17*R*-hydroperoxydocosahexaenoic acid (17*R*-H(p)DHA) from docosahexaenoic acid (DHA) *via* the acetylation of cyclooxygenase-2 (COX-2). 17*R*-H(p)DHA is further converted to aspirin triggered D-series resolvins (AT-RvD1-6) by 5-lipoxygenase (5-LO) or to aspirin triggered protectins (AT-PD1). The other omega-3 PUFAs, eicosapentaenoic acid (EPA), is also substrate for aspirin acetylated COX-2, that can result in to intermediates, 18S-H(p)EPE or 18R-H(p)EPE. Both intermediates can be converted to 18S-RvE1 or RvE1 respectively by 5-LO.

D-series resolvins (AT-RvD1-6), which are enzymatically generated *via* a pathway initiated by aspirin-acetylated cyclooxygenase 2 (Serhan and Petasis, 2011) (Fig. 3). Notably, bioactive concentrations of RvE1 could be measured in plasma of healthy volunteers 4 h after fish oil supplementation (1 g EPA and 0.7 g DHA) followed by low dose (160 mg) aspirin (Arita et al., 2005). Additionally, statins, widely used for the treatment of cardiovascular diseases for cholesterol lowering in cardiovascular disease, promote the biosynthesis of arachidonic acid-derived aspirin-triggered lipoxins *via* S-nitrosylation of cyclooxygenase 2 (Birnbaum et al., 2006). The steps for resolvin generation can occur within a single cell type (if all the ezymes required for the production are expressed) or *via* transcellular biosynthesis (where one cell type biosynthesizes and releases a component of the biosynthetic cascade that is used by a second cell to generate the final products). This process can occur, in myeloid cells, like neutrophils and macrophages (Dalli and Serhan, 2012; Serhan et al., 2000, 2002; Spite et al., 2009), but also in other cell types. For example, Herrera and colleagues demonstrated that osteoclasts incubated with EPA and acetylsalicylic acid, generate the precursor 18-hydroxyeicosapentaenoic acid, and when neutrophils were co-cultured, RvE1 production was produced (Herrera et al., 2008).

Resolvins act *via* specific G-protein-coupled receptors (GPCRs) to mediate their biological actions. To date, the receptors for RvD1, RvD3, RvD5, and RvE1 have been identified. Using a G-protein-coupled receptors β-arrestin coupled system, two G-protein-coupled receptors (GPCRs) were discovered for RvD1, the lipoxin A_4/annexin-A1 receptor (ALX/FPR2), and GPR32 (Krishnamoorthy et al., 2010). RvD3 and RvD5 also can activate recombinant GPR32 (Chiang et al., 2012; Dalli et al., 2013). GPR32 is expressed by human leukocytes, yet there is no known orthologue in mice, limiting some of the experimental studies on this receptor. On the other hand, the ALX/FPR2 receptor is identified in humans and N-formyl peptide receptor 2/3 (FPR2/3) identified in mice (Claria et al., 2012; Eickmeier et al., 2013; Nelson et al., 2014; Norling et al., 2012; Dufton et al., 2010). Specific binding sites for RvE1 were identified on monocytes (Arita et al., 2005); this receptor was identified as the human chemokine-like receptor 1 (ChemR23), which also serves as a receptor for chemerin (Wittamer et al., 2003). ChemR23 is expressed in the cardiovascular system, kidney, brain, gastrointestinal tissues, and bone marrow. RvE1 also acts as

a partial agonist on the leukotriene B_4 receptor (BLT1), thus competing with leukotriene B_4 for binding. The receptors for other resolvins are yet to be identified, but are predicted to be high-affinity G-protein-coupled receptors (GPCRs) as specific actions can be blocked with pertussis toxin, they exhibit stereoselectivity and are highly potent both in *in vitro* assays and experimental models.

In the next sections we will expand on the characteristics involved in the pathogenesis of rheumatoid arthritis and discuss the beneficial effects of DHA- and EPA-resolvins. To date, there is only limited data directly investigating the actions of DHA- and EPA-derived resolvins in animal models of arthritis. So for a general understanding of the capacity of these important mediators, we will also discus the actions of resolvins in other related diseases.

3. Disease progression of rheumatoid arthritis

Rheumatoid arthritis is a chronic inflammatory autoimmune disease, characterized by inflammation of the joints, which manifests as swelling, pain, functional impairment, and morning stiffness. This condition can also lead to muscle wasting and increased risk of osteoporosis. Most commonly affected joints are within the feet, knees and hands, but any peripheral joint could be affected. The etiological agent responsible for triggering the onset of rheumatoid arthritis is unknown, however, it is hypothesized that infection or traumatic insult may induce the initial inflammatory response in the synovial lining of the affected joints (Klareskog et al., 2009; McInnes and Schett, 2007). It is important to underline that rheumatoid arthritis is regarded as an autoimmune disease. In particular, there is a strong association between rheumatoid arthritis and several types of autoantibodies; the longest known and most important is rheumatoid factor, which is directed against the Fc fragment of immunoglobulin G. Aside from rheumatoid factor, responses to other autoantigens occur very commonly, both at the B- and T-cell level. Indeed, in experimental arthritis, a lack of Fcγ-receptors abrogates the induction of disease (Smolen and Steiner, 2003).

The inflammatory response of rheumatoid arthritis is characterized by infiltration of neutrophils, B and T lymphocytes and monocyte-derived macrophages in the arthritic joints. But the exact role of each cell type during rheumatoid arthritis pathogenesis is not completely understood. Neutrophils are the first immune cell to arrive at the site of inflammation. Within the synovial fluid, neutrophils phagocytose immune complexes and release powerful proteases and inflammatory mediators, which in turn recruit monocytes, T and B cells to the synovium. These cells then form discrete lymphoid aggregates, sometimes with ectopic germinal centers, while macrophage-like and fibroblast-like synoviocytes accumulate in the intima causing hyperplasia and secreting degradative enzymes. Among the proteases and inflammatory mediators produced by neutrophils, tumor necrosis factor-α is associated with activation of other cell types and induction of chemotactic factors, while reactive oxygen species are associated with tissue damage. Neutrophils also undergo apoptosis, a crucial process for neutrophil turnover and also for the resolution of inflammation. However, if there is an impairment of neutrophil clearance, apoptotic neutrophils undergo secondary necrosis. Ingestion of this cellular debris by macrophages induces production of pro-inflammatory cytokines, thus amplifying the inflammatory scenario (reviewed in Cascao et al. (2010)).

In association with the increased infiltration of inflammatory cells to the joints, patients with arthritis have increased levels of adhesion molecules including E-selectin, vascular cell adhesion molecule 1, and intercellular adhesion molecule-1, in the synovial endothelium and macrophage synovial tissue (Adams and Shaw, 1994; Bevilacqua et al., 1994). As the disease develops, the cells of the synovial lining proliferate, forming an invasive pannus. Together these processes can ultimately result in loss of cartilage, bone destruction and dramatic joint deformation with loss of function if uncontrolled. High concentrations of different cytokines and chemokines, including interleukin-1β, interleukin-6, interleukin-8, and tumor necrosis factor-α are found in synovial biopsies from patients with rheumatoid arthritis, which have been implicated in the development of the disease (Feldmann and Maini, 1999). In addition, prostaglandin-E_2, leukotriene-B_4, 5-hydroxyeicosatretraenic acid and platelet-activation factor are also found in the synovial fluid of patients with active rheumatoid arthritis (Sperling, 1995).

In the next sub-sections, we will present the known bioactions of DHA- and EPA-resolvins in the context of arthritis related symptoms such as inflammation and pain, and co-morbidities such as bone loss in periodontal disease.

3.1. Resolvins dampen immune cell activation

A massive infiltration of inflammatory cells is visualized in rheumatoid arthritic joints. In fact, up to a billion polymorphonuclear leukocytes per day can be detected within human synovial fluid, and are thought to impact the synovial lining by releasing reactive oxygen species and proteolytic enzymes (Wright et al., 2010). With this in mind, mediators that can prevent or reduce recruitment of polymorphonuclear leukocytes can be a potential strategy to counter-regulate the pathogenesis of the rheumatoid arthritis. One of the major shared characteristics of resolvins is their capacity to decrease polymorphonuclear leukocytes transmigration (Serhan et al., 2002). We have shown that RvD1 reduces human polymorphonuclear leukocytes recruitment to endothelial cells under shear conditions *via* both G-protein-coupled receptor 32 (GPR32) and the ALX/FPR2 receptor *in vitro* (Norling et al., 2012). The inhibition of granulocyte recruitment has also been shown for other mediators of the D-series and E-series family of resolvins (Arita et al., 2006; Spite et al., 2009).

A range of inflammatory mediators are involved in activation and recruitment of leukocytes to the site of inflammation. Complement 5a is a potent chemoattractant mediator, which is detected at high levels in synovial fluid of rheumatoid arthritis patients, and known to induce leukocyte activation and recruitment to the joint, being a key component involved in the pathogenesis of rheumatoid arthritis. We have shown that RvD2 at concentrations as low as 1 and 10 nM can drastically reduce complement 5a-induced superoxide release from human polymorphonuclear leukocytes, as well as complement 5a-induced polymorphonuclear leukocytes recruitment to endothelial monolayers (Spite et al., 2009).

Immunoglobulin G immune complex-induced lung injury is a model where intra-alveolar deposition of immunoglobulin G immune complexes stimulates alveolar macrophages *via* cross-linking of Fc-γ receptors, which results in robust formation of proinflammatory cytokines such as tumor necrosis factor-α and interleukin-6 (Gao et al., 2006; Guo and Ward, 2002), very similar to that visualized in rheumatoid arthritis. The formation of immunoglobulin G immune complexes in lung also results in *in situ* generation of the complement activation product complement 5a, resulting in the recruitment of inflammatory cells (Gao et al., 2006; Guo and Ward, 2002). In a recent study, AT-RvD1 was shown to have the ability to regulate the Fc-γ receptor-mediated induction of inflammatory cytokines and chemokines in both macrophages and neutrophils, and also reduced complement 5a levels in the bronchoalveolar lavage fluid in an immunoglobulin G immune complex-induced lung injury model (Tang et al., 2014).

Circulating monocytes in patients with rheumatoid arthritis are

known to be activated (Kawanaka et al., 2002; Kinne et al., 2007; Stuhlmuller et al., 2000; Torsteinsdottir et al., 1999), and the number of macrophages in the synovium correlates with joint damage (Mulherin et al., 1996) and clinical response to therapy (Haringman et al., 2005). Recently, Misharin et al. (2014) demonstrated that circulating monocytes are recruited to the joint during the effector phase of arthritis and differentiate into classically activated macrophages, which drive the development of the joint pathology. However as the arthritis progresses, these same classically activated macrophages change to an alternatively activated phenotype, which is necessary for the resolution of joint inflammation (Misharin et al., 2014). The actions of RvD1 also include promoting macrophage skewing from M1 (pro-inflammatory phenotype) to M2 (pro-resolving phenotype) macrophages (Titos et al., 2011; Zhang et al., 2013). Thus, locally generated RvD1 could be important in switching macrophage phenotype within the arthritic joint.

3.2. Counter-regulation of inflammatory mediators

Chronic inflammation is characterized by the production of inflammatory cytokines, arachidonic acid-derived eicosanoids (prostaglandins, thromboxanes, leukotrienes, and other oxidative derivatives), reactive oxygen species, and adhesion molecules. Rheumatoid arthritis, a chronic inflammatory disease, is not an exception. Indeed, high concentrations of different cytokines and chemokines are found in synovial biopsies from patients with rheumatoid arthritis. We have shown that RvD1 treatment in a model of peritonitis *in vivo* significantly reduces the levels of a number of pro-inflammatory mediators after zymozan administration, including prostaglandins and leukotriene B_4 (Norling et al., 2012). In addition, AT-RvD1 dramatically mitigates immunoglobulin G immune complex-induced nuclear factor-κB and CCAAT/enhancer binding protein activity in alveolar macrophages, and secretion of tumor necrosis factor-α, interleukin-6, and macrophage inflammatory protein 1α from immunoglobulin G immune complex-stimulated alveolar macrophages or neutrophils (Tang et al., 2014). RvD2 treatment also alters the cytokine and eicosanoid profiles, reducing interleukin-17, interleukin-10, prostaglandin E_2 and leukotriene B_4 in a murine polymicrobial sepsis model (Spite et al., 2009). RvE1 also displays potent counter-regulatory and tissue-protective actions *in vitro* and *in vivo*. In a model of periodontitis induced by ligature and application of *Porphyromonas gingivalis* in rabbits, topical treatment with RvE1 (4 μg/tooth – 3 times a week) resulted in reduced levels of interleukin-1β and C-reactive protein in serum (Hasturk et al., 2007).

3.3. Bone sparing properties of resolvins

Periodontal disease and rheumatoid arthritis are amongst the most prevalent chronic inflammatory diseases that affect soft and bone structures in humans (Albandar, 2005; Firestein, 2005). Although the agents triggering these diseases are different, periodontitis is triggered by infection while rheumatoid arthritis is an auto-immune disorder, both conditions present similar pathological features, including bone resorption, cell infiltration and release of inflammatory mediators, such as tumor necrosis factor-α (de Pablo et al., 2009). There is epidemiological evidence associating periodontal disease with incidence of rheumatoid arthritis (Scher and Abramson, 2013) and, conversely, there is a higher incidence of periodontitis in rheumatoid arthritis patients (Scher et al., 2012). In addition, animal models of rheumatoid arthritis present exacerbated periodontal bone damage (Montero-Melendez et al., 2014; Queiroz-Junior et al.,2012).

One of the first signals that resolvins could have an important role in preventing bone destruction was shown by Van Dyke's group in 2006. They showed that topical treatment with RvE1 (4 μg/tooth, 3 times a week) resulted in inhibition of tissue and bone damage by more than 95% (Hasturk et al., 2007, 2006). The reduction of bone loss was associated with lower numbers of tartrate-resistant acid phosphatase-positive cells, a marker for osteoclasts (Hasturk et al., 2006). But at that time, it was not known whether the bone-sparing action was a direct effect on osteoclasts or indirectly limiting tissue damage by reducing immune cell recruitment through the anti-inflammatory and pro-resolution actions of RvE1. It was later determined that osteoclast growth and resorption pit formation are markedly decreased in the presence of RvE1 (3 ng/ml) in bone marrow cells isolated from mice and cultured with murine colony-stimulating factor and receptor activator of nuclear factor-κB ligand (Herrera et al., 2008). The inhibition of osteoclast differentiation by RvE1 was demonstrated by a decreased number of multinuclear osteoclasts, delay in the time course of osteoclast development and attenuation of receptor activator of nuclear factor-κB ligand-induced nuclear translocation of the p50 subunit of nuclear factor-κB. Osteoclast survival and apoptosis rates were not altered by RvE1 treatment, showing that RvE1 only effects the maturation of osteoclasts and does not induce these cells to undergo apoptosis. Messenger RNA for both receptors of RvE1; ChemR23 and BLT1 receptors, are expressed in osteoclast cultures. Yet RvE1 binds only to BLT1 receptor *in vitro*. Indeed, the BLT1 receptor antagonist (U75302, 1 nM) prevents RvE1 inhibition of osteoclast growth, indicating that BLT1 receptor mediates RvE1 actions on osteoclasts (Herrera et al., 2008).

Further investigation of the actions of RvE1 treatment on specific stages of osteoclast maturation revealed that RvE1 targeted late stages of osteoclast maturation to decrease osteoclast formation by 32.8%. This occurred by inhibition of the fusion dendritic cell-specific transmembrane protein specifically targeted by RvE1 receptor binding (Zhu et al., 2013). RvE1 also enhances expression of osteoprotegerin in transgenic mice overexpressing ChemR23 on leukocytes, down-modulating osteoclast differentiation and increasing bone remodeling by direct actions on bone (Gao et al., 2013)

3.4. Analgesic actions of resolvins

Nowadays, treatment for inflammatory pain relies on the use of opioids and cyclooxygenase-2 inhibitors (some of which are associated with serious cardiovascular effects). The long-term use of these drugs is limited by their side effects, including respiratory depression, sedation, nausea, vomiting, constipation, dependence and tolerance. Newly discovery properties of resolvins show that these mediators may represent a new family of analgesics useful in treating inflammation-associated pain states such as arthritic and post-operative pain.

Using different inflammatory pain models (by intraplantar injection of formalin, carrageenan or complete Freund's adjuvant) it was observed that peripheral or spinal administration of RvE1 or RvD1 in mice potently reduces inflammatory pain, without affecting basal pain perception. This analgesic affect was induced by activation of ChemR23, a RvE1 receptor. Indeed, knockdown of ChemR23 with a specific siRNA abolished the antinociceptive actions of RvE1. ChemR23 is expressed in the dorsal root ganglion in neurons that express transient receptor potential vanilloid subtype-1 and in neurons of the spinal cord. ChemR23 is also expressed in axons of dorsal root ganglion neurons and primary afferent terminals in the spinal cord. Therefore, RvE1 might attenuate inflammatory pain *via* ChemR23 expressed in dorsal root ganglion and spinal cord neurons (Xu et al., 2010).

Analgesic effects were also observed after AT-RvD1 (100 or 300 ng/ip) treatment following an intraperitoneal injection of

complete Freund's adjuvant as a model of inflammatory arthritic pain. In addition, repeated treatment with AT-RvD1 (100 ng/ip, given 4 days, twice a day) was shown to have anti-hyperalgesic effects, reducing hind paw withdrawal frequency (Lima-Garcia et al., 2011).

Fibromyalgia is a complex painful syndrome, accompanied by a series of psychological and behavioral alterations (Busse et al., 2013), and characterized by chronic musculoskeletal pain (Wolfe et al., 2010). The hallmark symptom is chronic widespread pain, but patients also present fatigue, depression, cognitive dysfunctions, and sleep disturbances (Ceko et al., 2012; Wolfe et al., 2010). Many of these symptoms are also reported in patients with rheumatoid arthritis (Ryan, 2014). Importantly, AT-RvD1 as well as RvD2 modulates painful and depression-like symptoms in a mouse model of fibromyalgia induced by reserpine in mice (Klein et al., 2014).

3.5. Resolvins as therapeutic tools for rheumatic diseases

The importance of endogenous pro-resolving mediators and their counter-regulatory pathways is implicated in experimental arthritis. Null mice lacking either 12/15-lipoxigenase (a key enzyme involved in resolvin and lipoxin biosynthesis) or the ALX/FPR2 receptor, a high-affinity receptor for RvD1, lipoxin A_4 and annexin A1, display exacerbated disease severity and tissue damage in serum transfer induced inflammatory arthritis (Dufton et al., 2010; Kronke et al., 2009). Additionally, 5-lipoxygenase null mice display an exacerbated and prolonged duration of experimental infectious arthritis induced with *Borrelia burgdorferi* (Blaho et al., 2011). Furthermore, cyclooxygenase-2 and its metabolite, prostaglandin E_2, are present in the joints during resolution in a murine model of collagen-induced arthritis (Chan and Moore, 2010). Intriguingly, blocking cyclooxygenase-2 activity and prostaglandin E_2 production within the resolution phase perpetuated inflammation. Repletion with prostaglandin E_2 analogs restored homeostasis, which was found to be mediated by the pro-resolving lipoxygenase metabolite, lipoxin A_4, a potent stop signal (Chan and Moore, 2010). These findings may explain the enigma regarding why cyclooxygenase-2 inhibitors are palliative rather than curative in patients with rheumatoid arthritis, and also emphasizes the importance of endogenous pro-resolving mediators produced *via* cyclooxygenase-2 for the control of rheumatoid arthritis.

In synovial tissue of rheumatoid arthritis patients elevated levels of 5- and 15-Lipoxygenase as well as the ALX/FPR2 receptor expression are observed when compared to osteoarthritis patients (Gheorghe et al., 2009; Hashimoto et al., 2007). Thus it is known that elements of the resolvin pathway are expressed in the rheumatoid synovium. An initial study using mass-spectrometry based lipidomics analyses has identified the DHA-derived resolvin RvD5 and maresin-1, and also lipoxin A_4, within synovial fluid from a few rheumatoid arthritis patients (Giera et al., 2012). This preliminary investigation merits further attention to stratify patients according to disease severity, and taking into account arthritis therapies, and dietary intervention with omega-3 supplementation. We would anticipate that resolvin levels would negatively correlate with arthritis severity, and that omega-3 nutraceuticals would enhance endogenous levels of pro-resolving mediators and dampen inflammatory arthritis.

Only a few investigations have been performed to decipher the actions of resolvins in animal models of arthritis so far, yet these results are promising and show benefits for the use of DHA- and EPA-derived resolvins. Using a model of complete Freund's adjuvant-induced inflammation within the temporomandibular joint, we demonstrated that AT-RvD1 treatment administered (intravenously) within enriched nanoparticles could reduce neutrophil recruitment into the temporomandibular joint (Norling et al., 2011). Temporomandibular joint signs or symptoms can afflict up to 70% of rheumatoid arthritis patients depending on criteria for clinical assessment (Bessa-Nogueira et al., 2008). In some instances, the cartilage covering the condyle is completely replaced by fibrous tissue (Ueno et al., 2003) and inflammatory and degenerative changes can be seen within the synovium (Gynther et al., 1997). Protective effects of AT-RvD1 were also observed following an intraplantar injection of complete Freund's adjuvant as a model of inflammatory arthritic pain (Lima-Garcia et al., 2011). Is important to note that AT-RvD1 treatment (100 ng intraperitoneal injection twice daily) not only decreased inflammation (with reduced tumor necrosis factor-α and interleukin-1β within the paw), but also displayed anti-hyperalgesic effects, reducing hind paw withdrawal frequency (Lima-Garcia et al., 2011).

We tested the anti-arthritic potential of AT-RvD1 *in vivo* using an innate inflammatory model of arthritis. These mice were administered KBxN serum containing anti-glucose-6-phosphate isomerase antibodies that deposit on the joints initiating immune complex formation and complement mediated recruitment of neutrophils. Mice were treated with 100 ng AT-RvD1 daily either prophylactically (day 0) or therapeutically (ensuing overt signs of arthritis; day 4) and graded for arthritis severity, cachexia and hind paw edema daily. Prophylactic treatment with AT-RvD1 significantly attenuated arthritic score, weight loss, hind paw edema and reduced leukocyte infiltration within the paw. Importantly, therapeutic treatment decreased the peak in arthritis severity and shortened the resolution interval, suggesting AT-RvD1 offers a valuable therapeutic approach for inflammatory joint diseases (Norling et al., 2014).

Positive effects using DHA supplementation are observed in models of arthritis when very high doses are used. For instance, therapeutic chronic oral or intraarticular administration of DHA (10 mg/kg daily and 20 μg/knee) reduced pain-related behaviors and knee edema in arthritis induced by complete Freund's adjuvant (Torres-Guzman et al., 2014). In other work, using prophylactic DHA (1000 mg/kg and 25000 mg/kg daily for 4 weeks before induction of arthritis) treatment in complete Freund's adjuvant induced arthritis, proved to decrease clinical score and incidence. The higher dose of DHA (2500 mg/kg) had more marked and consistent effects on all arthritic parameters measured: clinical arthritis scores, disease incidence, histopathology, anti-collagen antibodies, and *ex vivo* cytokine production (Olson et al., 2013). Olson et al. (2013) suggested that doses of > 2 g/day of DHA may be required to reduce disease in humans. Which is in agreement with doses of fish oils used in human trials (1.6–7.1 g/day and averaged 3.5 g/day) that showed improvement in reducing duration of morning stiffness, number of tender or swollen joints, decreasing pain and time to fatigue, increasing grip strength, and decreasing use of non-steroidal anti-inflammatory drugs (reviewed in Calder (2008), and Miles and Calder (2012)). Until the necessary clinical trials are performed utilizing resolvins for inflammatory arthritis it is difficult to predict the dose required for beneficial outcome in humans, although based on their potency we would predict far lower amounts would be required in comparison to the parent compounds DHA or EPA.

Analogs of resolvins have been developed providing more stability *in vivo*. Resolvyx Pharmaceuticals (http://www.resolvyx.com) was the first company to take these resolution agonists to clinical trials. These include a resolvin E1 mimetic named RX-10045, which has performed well following topical application to treat dry-eye syndrome in phase I and II clinical trials and has now progressed to phase III trials.

4. Conclusion

Endogenous pro-resolving mediators including the resolvins give hope for the beginning of a new era for the treatment of inflammatory and pain-associated disorders, including rheumatoid arthritis. Current therapeutic approaches that target blockage of a single immune mediator, such as anti-tumor necrosis factor-α therapy, have been revolutionary, yet significant numbers of patients still fail to respond. The functional redundancy of the immune system limits the value of single pathway elimination to achieve meaningful and sustainable clinical responses for some chronic inflammatory diseases, such as rheumatoid arthritis. Resolvins, on other hand, can influence multiple different pathways, and as they activate resolution circuits and as resolvins are endogenous mediators, their use is believed to be associated with less collateral effects.

Acknowledgments

Our research is funded by the Arthritis Research UK (Career Development Fellowship 19909 to Lucy V. Norling). Patricia R Souza is a PhD student funded by the Brazilian Government (238277/2012-7)

References

Adams, D.H., Shaw, S., 1994. Leucocyte–endothelial interactions and regulation of leucocyte migration. Lancet 343, 831–836.
Albandar, J.M., 2005. Epidemiology and risk factors of periodontal diseases. Dent. Clin. North Am. 49, 517–532 (v–vi).
Allen, J.B., Wong, H.L., Costa, G.L., Bienkowski, M.J., Wahl, S.M., 1993. Suppression of monocyte function and differential regulation of IL-1 and IL-1ra by IL-4 contribute to resolution of experimental arthritis. J. Immunol. 151, 4344–4351.
Arita, M., Bianchini, F., Aliberti, J., Sher, A., Chiang, N., Hong, S., Yang, R., Petasis, N.A., Serhan, C.N., 2005. Stereochemical assignment, antiinflammatory properties, and receptor for the omega-3 lipid mediator resolvin E1. J. Exp. Med. 201, 713–722.
Arita, M., Oh, S.F., Chonan, T., Hong, S., Elangovan, S., Sun, Y.P., Uddin, J., Petasis, N.A., Serhan, C.N., 2006. Metabolic inactivation of resolvin E1 and stabilization of its anti-inflammatory actions. J. Biol. Chem. 281, 22847–22854.
Bessa-Nogueira, R.V., Vasconcelos, B.C., Duarte, A.P., Goes, P.S., Bezerra, T.P., 2008. Targeted assessment of the temporomandibular joint in patients with rheumatoid arthritis. J. Oral Maxillofac. Surg.: Off. J. Am. Assoc. Oral Maxillofac. Surg. 66, 1804–1811.
Bevilacqua, M.P., Nelson, R.M., Mannori, G., Cecconi, O., 1994. Endothelial-leukocyte adhesion molecules in human disease. Annu. Rev. Med. 45, 361–378.
Birnbaum, Y., Ye, Y., Lin, Y., Freeberg, S.Y., Nishi, S.P., Martinez, J.D., Huang, M.H., Uretsky, B.F., Perez-Polo, J.R., 2006. Augmentation of myocardial production of 15-epi-lipoxin-a4 by pioglitazone and atorvastatin in the rat. Circulation 114, 929–935.
Blaho, V.A., Zhang, Y., Hughes-Hanks, J.M., Brown, C.R., 2011. 5-Lipoxygenase-deficient mice infected with Borrelia burgdorferi develop persistent arthritis. J. Immunol. 186, 3076–3084.
Bonnans, C., Vachier, I., Chavis, C., Godard, P., Bousquet, J., Chanez, P., 2002. Lipoxins are potential endogenous antiinflammatory mediators in asthma. Am. J. Respir. Crit. Care Med. 165, 1531–1535.
Bradberry, J.C., Hilleman, D.E., 2013. Overview of omega-3 fatty acid therapies. P & T: Peer-Rev. J. Formul. Manag. 38, 681–691.
Busse, J.W., Ebrahim, S., Connell, G., Coomes, E.A., Bruno, P., Malik, K., Torrance, D., Ngo, T., Kilmayr, K., Avrahami, D., Riva, J.J., Struijs, P., Brunarski, D., Burnie, S.J., LeBlanc, F., Stroenstra, I.A., Mahood, Q., Thorlund, K., Montori, V.M., Sharaiah, V., Alexander, P., Jankowski, M., Lesniak, W., Faulhaber, M., Bala, M.M., Schandelmaier, S., Guyatt, G.H., 2013. Systematic review and network meta-analysis of interventions for fibromyalgia: a protocol. Syst. Rev. 2, 18.
Calder, P.C., 2008. Session 3: Joint Nutrition Society and Irish Nutrition and Dietetic Institute Symposium on 'Nutrition and autoimmune disease' PUFA, inflammatory processes and rheumatoid arthritis. Proc. Nutr. Soc. 67, 409–418.
Calder, P.C., 2015. Marine omega-3 fatty acids and inflammatory processes: Effects, mechanisms and clinical relevance. Biochim. Biophys. Acta 1851, 469–484.
Cascao, R., Rosario, H.S., Souto-Carneiro, M.M., Fonseca, J.E., 2010. Neutrophils in rheumatoid arthritis: more than simple final effectors. Autoimmun. Rev. 9, 531–535.
Ceko, M., Bushnell, M.C., Gracely, R.H., 2012. Neurobiology underlying fibromyalgia symptoms. Pain Res. Treat. 2012, 585419.
Chan, M.M., Moore, A.R., 2010. Resolution of inflammation in murine autoimmune arthritis is disrupted by cyclooxygenase-2 inhibition and restored by prostaglandin E2-mediated lipoxin A4 production. J. Immunol. 184, 6418–6426.
Chiang, N., Arita, M., Serhan, C.N., 2005. Anti-inflammatory circuitry: lipoxin, aspirin-triggered lipoxins and their receptor ALX. Prostaglandins, Leukot. Essent. Fat. Acids 73, 163–177.
Chiang, N., Fredman, G., Backhed, F., Oh, S.F., Vickery, T., Schmidt, B.A., Serhan, C.N., 2012. Infection regulates pro-resolving mediators that lower antibiotic requirements. Nature 484, 524–528.
Claria, J., Dalli, J., Yacoubian, S., Gao, F., Serhan, C.N., 2012. Resolvin D1 and resolvin D2 govern local inflammatory tone in obese fat. J. Immunol. 189, 2597–2605.
Cleland, L.G., French, J.K., Betts, W.H., Murphy, G.A., Elliott, M.J., 1988. Clinical and biochemical effects of dietary fish oil supplements in rheumatoid arthritis. J. Rheumatol. 15, 1471–1475.
Dalli, J., Serhan, C.N., 2012. Specific lipid mediator signatures of human phagocytes: microparticles stimulate macrophage efferocytosis and pro-resolving mediators. Blood 120, e60–e72.
Dalli, J., Winkler, J.W., Colas, R.A., Arnardottir, H., Cheng, C.Y., Chiang, N., Petasis, N. A., Serhan, C.N., 2013. Resolvin D3 and aspirin-triggered resolvin D3 are potent immunoresolvents. Chem. Biol. 20, 188–201.
de Pablo, P., Chapple, I.L., Buckley, C.D., Dietrich, T., 2009. Periodontitis in systemic rheumatic diseases. Nat. Rev. Rheumatol. 5, 218–224.
Dufton, N., Hannon, R., Brancaleone, V., Dalli, J., Patel, H.B., Gray, M., D'Acquisto, F., Buckingham, J.C., Perretti, M., Flower, R.J., 2010. Anti-inflammatory role of the murine formyl-peptide receptor 2: ligand-specific effects on leukocyte responses and experimental inflammation. J. Immunol. 184, 2611–2619.
Eickmeier, O., Seki, H., Haworth, O., Hilberath, J.N., Gao, F., Uddin, M., Croze, R.H., Carlo, T., Pfeffer, M.A., Levy, B.D., 2013. Aspirin-triggered resolvin D1 reduces mucosal inflammation and promotes resolution in a murine model of acute lung injury. Mucosal Immunol. 6, 256–266.
Espersen, G.T., Grunnet, N., Lervang, H.H., Nielsen, G.L., Thomsen, B.S., Faarvang, K. L., Dyerberg, J., Ernst, E., 1992. Decreased interleukin-1 beta levels in plasma from rheumatoid arthritis patients after dietary supplementation with n-3 polyunsaturated fatty acids. Clin. Rheumatol. 11, 393–395.
Feldmann, M., Maini, R.N., 1999. The role of cytokines in the pathogenesis of rheumatoid arthritis. Rheumatology 38 (Suppl. 2), 53–57.
Firestein, G.S., 2005. Immunologic mechanisms in the pathogenesis of rheumatoid arthritis. J. Clin. Rheumatol.: Pract. Rep. Rheum. Musculoskelet. Dis. 11, 539–544.
Gao, H., Neff, T., Ward, P.A., 2006. Regulation of lung inflammation in the model of IgG immune-complex injury. Annu. Rev. Pathol. 1, 215–242.
Gao, L., Faibish, D., Fredman, G., Herrera, B.S., Chiang, N., Serhan, C.N., Van Dyke, T.E., Gyurko, R., 2013. Resolvin E1 and chemokine-like receptor 1 mediate bone preservation. J. Immunol. 190, 689–694.
Gheorghe, K.R., Korotkova, M., Catrina, A.I., Backman, L., af Klint, E., Claesson, H.E., Radmark, O., Jakobsson, P.J., 2009. Expression of 5-lipoxygenase and 15-lipoxygenase in rheumatoid arthritis synovium and effects of intraarticular glucocorticoids. Arthritis Res. Ther. 11, R83.
Giera, M., Ioan-Facsinay, A., Toes, R., Gao, F., Dalli, J., Deelder, A.M., Serhan, C.N., Mayboroda, O.A., 2012. Lipid and lipid mediator profiling of human synovial fluid in rheumatoid arthritis patients by means of LC-MS/MS. Biochim. Biophys. Acta 1821, 1415–1424.
Guo, R.F., Ward, P.A., 2002. Mediators and regulation of neutrophil accumulation in inflammatory responses in lung: insights from the IgG immune complex model. Free Radic. Biol. Med. 33, 303–310.
Gynther, G.W., Holmlund, A.B., Reinholt, F.P., Lindblad, S., 1997. Temporomandibular joint involvement in generalized osteoarthritis and rheumatoid arthritis: a clinical, arthroscopic, histologic, and immunohistochemical study. Int. J. Oral Maxillofac. Surg. 26, 10–16.
Haringman, J.J., Gerlag, D.M., Zwinderman, A.H., Smeets, T.J., Kraan, M.C., Baeten, D., McInnes, I.B., Bresnihan, B., Tak, P.P., 2005. Synovial tissue macrophages: a sensitive biomarker for response to treatment in patients with rheumatoid arthritis. Ann. Rheum. Dis. 64, 834–838.
Hashimoto, A., Hayashi, I., Murakami, Y., Sato, Y., Kitasato, H., Matsushita, R., Iizuka, N., Urabe, K., Itoman, M., Hirohata, S., Endo, H., 2007. Antiinflammatory mediator lipoxin A4 and its receptor in synovitis of patients with rheumatoid arthritis. J. Rheumatol. 34, 2144–2153.
Hasturk, H., Kantarci, A., Goguet-Surmenian, E., Blackwood, A., Andry, C., Serhan, C. N., Van Dyke, T.E., 2007. Resolvin E1 regulates inflammation at the cellular and tissue level and restores tissue homeostasis in vivo. J. Immunol. 179, 7021–7029.
Hasturk, H., Kantarci, A., Ohira, T., Arita, M., Ebrahimi, N., Chiang, N., Petasis, N.A., Levy, B.D., Serhan, C.N., Van Dyke, T.E., 2006. RvE1 protects from local inflammation and osteoclast- mediated bone destruction in periodontitis. FASEB J.: Off. Publ. Fed. Am. Soc. Exp. Biol. 20, 401–403.
Herrera, B.S., Ohira, T., Gao, L., Omori, K., Yang, R., Zhu, M., Muscara, M.N., Serhan, C. N., Van Dyke, T.E., Gyurko, R., 2008. An endogenous regulator of inflammation, resolvin E1, modulates osteoclast differentiation and bone resorption. Br. J. Pharmacol. 155, 1214–1223.
Kawanaka, N., Yamamura, M., Aita, T., Morita, Y., Okamoto, A., Kawashima, M., Iwahashi, M., Ueno, A., Ohmoto, Y., Makino, H., 2002. CD14+,CD16+ blood monocytes and joint inflammation in rheumatoid arthritis. Arthritis Rheum. 46, 2578–2586.
Kinne, R.W., Stuhlmuller, B., Burmester, G.R., 2007. Cells of the synovium in rheumatoid arthritis. Macrophages. Arthritis Res. Ther. 9, 224.
Klareskog, L., Catrina, A.I., Paget, S., 2009. Rheumatoid arthritis. Lancet 373, 659–672.

Klein, C.P., Sperotto, N.D., Maciel, I.S., Leite, C.E., Souza, A.H., Campos, M.M., 2014. Effects of D-series resolvins on behavioral and neurochemical changes in a fibromyalgia-like model in mice. Neuropharmacology 86, 57–66.
Kremer, J.M., Jubiz, W., Michalek, A., Rynes, R.I., Bartholomew, L.E., Bigaouette, J., Timchalk, M., Beeler, D., Lininger, L., 1987. Fish-oil fatty acid supplementation in active rheumatoid arthritis. A double-blinded, controlled, crossover study. Ann. Intern. Med. 106, 497–503.
Kremer, J.M., Lawrence, D.A., Jubiz, W., DiGiacomo, R., Rynes, R., Bartholomew, L.E., Sherman, M., 1990. Dietary fish oil and olive oil supplementation in patients with rheumatoid arthritis. Clinical and immunologic effects. Arthritis Rheum. 33, 810–820.
Kremer, J.M., Lawrence, D.A., Petrillo, G.F., Litts, L.L., Mullaly, P.M., Rynes, R.I., Stocker, R.P., Parhami, N., Greenstein, N.S., Fuchs, B.R., et al., 1995. Effects of high-dose fish oil on rheumatoid arthritis after stopping nonsteroidal antiinflammatory drugs. Clinical and immune correlates. Arthritis Rheum. 38, 1107–1114.
Krishnamoorthy, S., Recchiuti, A., Chiang, N., Yacoubian, S., Lee, C.H., Yang, R., Petasis, N.A., Serhan, C.N., 2010. Resolvin D1 binds human phagocytes with evidence for proresolving receptors. Proc. Natl. Acad. Sci. U. S. A. 107, 1660–1665.
Kromann, N., Green, A., 1980. Epidemiological studies in the Upernavik district, Greenland. Incidence of some chronic diseases 1950–1974. Acta Med. Scand. 208, 401–406.
Kronke, G., Katzenbeisser, J., Uderhardt, S., Zaiss, M.M., Scholtysek, C., Schabbauer, G., Zarbock, A., Koenders, M.I., Axmann, R., Zwerina, J., Baenckler, H.W., van den Berg, W., Voll, R.E., Kuhn, H., Joosten, L.A., Schett, G., 2009. 12/15-lipoxygenase counteracts inflammation and tissue damage in arthritis. J. Immunol. 183, 3383–3389.
Libby, P., 2002. Inflammation in atherosclerosis. Nature 420, 868–874.
Lima-Garcia, J.F., Dutra, R.C., da Silva, K., Motta, E.M., Campos, M.M., Calixto, J.B., 2011. The precursor of resolvin D series and aspirin-triggered resolvin D1 display anti-hyperalgesic properties in adjuvant-induced arthritis in rats. Br. J. Pharmacol. 164, 278–293.
Mas, E., Croft, K.D., Zahra, P., Barden, A., Mori, T.A., 2012. Resolvins D1, D2, and other mediators of self-limited resolution of inflammation in human blood following n-3 fatty acid supplementation. Clin. Chem. 58, 1476–1484.
McInnes, I.B., Schett, G., 2007. Cytokines in the pathogenesis of rheumatoid arthritis. Nat. Rev. Immunol. 7, 429–442.
Medzhitov, R., 2008. Origin and physiological roles of inflammation. Nature 454, 428–435.
Medzhitov, R., 2010. Inflammation 2010: new adventures of an old flame. Cell 140, 771–776.
Miles, E.A., Calder, P.C., 2012. Influence of marine n-3 polyunsaturated fatty acids on immune function and a systematic review of their effects on clinical outcomes in rheumatoid arthritis. Br. J. Nutr. 107 (Suppl. 2), S171–S184.
Mikhailn, A.V., Cuda, C.M., Saber, R., Turner, J.D., Gierut, A.K., Haines3rd, G.K., Berdnikovs, S., Filer, A., Clark, A.R., Buckley, C.D., Mutlu, G.M., Budinger, G.R., Perlman, H., 2014. Nonclassical ly6C(-) monocytes drive the development of inflammatory arthritis in mice. Cell Rep. 9, 591–604.
Montero-Melendez, T., Madeira, M.F., Norling, L.V., Alsam, A., Curtis, M.A., da Silva, T.A., Perretti, M., 2014. Association between periodontal disease and inflammatory arthritis reveals modulatory functions by melanocortin receptor type 3. Am. J. Pathol. 184, 2333–2341.
Mulherin, D., Fitzgerald, O., Bresnihan, B., 1996. Synovial tissue macrophage populations and articular damage in rheumatoid arthritis. Arthritis Rheum. 39, 115–124.
Nathan, C., 2006. Neutrophils and immunity: challenges and opportunities. Nat. Rev. Immunol. 6, 173–182.
Nelson, J.W., Leigh, N.J., Mellas, R.E., McCall, A.D., Aguirre, A., Baker, O.J., 2014. ALX/FPR2 receptor for RvD1 is expressed and functional in salivary glands. Am. J. Physiol. Cell Physiol. 306, C178–C185.
Norling, L.V., Dalli, J., Flower, R.J., Serhan, C.N., Perretti, M., 2012. Resolvin D1 limits polymorphonuclear leukocyte recruitment to inflammatory loci: receptor-dependent actions. Arterioscler. Thromb. Vasc. Biol. 32, 1970–1978.
Norling, L.V., Headland, S.E., Dalli, J., Serhan, C.N., Perretti, M., 2014. Resolvin D1 protects from neutrophil mediated joint destruction in inflammatory arthritis. FASEB J. 28 (Suppl. 1), S146.5.
Norling, L.V., Perretti, M., 2013. Control of myeloid cell trafficking in resolution. J. Innate Immun. 5, 367–376.
Norling, L.V., Spite, M., Yang, R., Flower, R.J., Perretti, M., Serhan, C.N., 2011. Cutting edge: humanized nano-proresolving medicines mimic inflammation-resolution and enhance wound healing. J. Immun. 186, 5543–5547.
Okin, D., Medzhitov, R., 2012. Evolution of inflammatory diseases. Curr. Biol.: CB 22, R733–R740.
Olson, M.V., Liu, Y.C., Dangi, B., Paul Zimmer, J., Salem Jr., N., Nauroth, J.M., 2013. Docosahexaenoic acid reduces inflammation and joint destruction in mice with collagen-induced arthritis. Inflamm. Res.: Off. J. Eur. Histamine Res. Soc. ... [et al.] 62, 1003–1013.
Perretti, M., D'Acquisto, F., 2009. Annexin A1 and glucocorticoids as effectors of the resolution of inflammation. Nat. Rev. Immunol. 9, 62–70.
Queiroz-Junior, C.M., Madeira, M.F., Coelho, F.M., de Oliveira, C.R., Candido, L.C., Garlet, G.P., Teixeira, M.M., de Souza Dda, G., Silva, T.A., 2012. Experimental arthritis exacerbates aggregatibacter actinomycetemcomitans-induced periodontitis in mice. J. Clin. Periodontol. 39, 608–616.
Ryan, S., 2014. Psychological effects of living with rheumatoid arthritis. Nurs. Stand. 29, 52–59.
Scher, J.U., Abramson, S.B., 2013. Periodontal disease, porphyromonas gingivalis, and rheumatoid arthritis: what triggers autoimmunity and clinical disease? Arthritis Res. Ther. 15, 122.
Scher, J.U., Ubeda, C., Equinda, M., Khanin, R., Buischi, Y., Viale, A., Lipuma, L., Attur, M., Pillinger, M.H., Weissmann, G., Littman, D.R., Pamer, E.G., Bretz, W.A., Abramson, S.B., 2012. Periodontal disease and the oral microbiota in new-onset rheumatoid arthritis. Arthritis Rheum. 64, 3083–3094.
Serhan, C.N., 2014. Pro-resolving lipid mediators are leads for resolution physiology. Nature 510, 92–101.
Serhan, C.N., Brain, S.D., Buckley, C.D., Gilroy, D.W., Haslett, C., O'Neill, L.A., Perretti, M., Rossi, A.G., Wallace, J.L., 2007. Resolution of inflammation: state of the art, definitions and terms. FASEB J.: Off. Publ. Fed. Am. Soc. Exp. Biol. 21, 325–332.
Serhan, C.N., Chiang, N., 2008. Endogenous pro-resolving and anti-inflammatory lipid mediators: a new pharmacologic genus. Br. J. Pharmacol. 153 (Suppl. 1), S200–S215.
Serhan, C.N., Clish, C.B., Brannon, J., Colgan, S.P., Chiang, N., Gronert, K., 2000. Novel functional sets of lipid-derived mediators with antiinflammatory actions generated from omega-3 fatty acids via cyclooxygenase 2-nonsteroidal antiinflammatory drugs and transcellular processing. J. Exp. Med. 192, 1197–1204.
Serhan, C.N., Hong, S., Gronert, K., Colgan, S.P., Devchand, P.R., Mirick, G., Moussignac, R.L., 2002. Resolvins: a family of bioactive products of omega-3 fatty acid transformation circuits initiated by aspirin treatment that counter proinflammation signals. J. Exp. Med. 196, 1025–1037.
Serhan, C.N., Petasis, N.A., 2011. Resolvins and protectins in inflammation resolution. Chem. Rev. 111, 5922–5943.
Serhan, C.N., Yang, R., Martinod, K., Kasuga, K., Pillai, P.S., Porter, T.F., Oh, S.F., Spite, M., 2009. Maresins: novel macrophage mediators with potent antiinflammatory and proresolving actions. J. Exp. Med. 206, 15–23.
Smolen, J.S., Steiner, G., 2003. Therapeutic strategies for rheumatoid arthritis. Nat. Rev. Drug Discov. 2, 473–488.
Sperling, R.I., 1995. Eicosanoids in rheumatoid arthritis. Rheum. Dis. Clin. North Am. 21, 741–758.
Sperling, R.I., Weinblatt, M., Robin, J.L., Ravalese3rd, J., Hoover, R.L., House, F., Cobbyn, J.S., Fraser, P.A., Spur, B.W., Robinson, D.R., et al., 1987. Effects of dietary supplementation with marine fish oil on leukocyte lipid mediator generation and function in rheumatoid arthritis. Arthritis Rheum. 30, 988–997.
Spite, M., Norling, L.V., Summers, L., Yang, R., Cooper, D., Petasis, N.A., Flower, R.J., Perretti, M., Serhan, C.N., 2009. Resolvin D2 is a potent regulator of leukocytes and controls microbial sepsis. Nature 461, 1287–1291.
Stuhlmuller, B., Ungethum, U., Scholze, S., Martinez, L., Backhaus, M., Kraetsch, H.G., Kinne, R.W., Burmester, G.R., 2000. Identification of known and novel genes in activated monocytes from patients with rheumatoid arthritis. Arthritis Rheum. 43, 775–790.
Tang, H., Liu, Y., Yan, C., Petasis, N.A., Serhan, C.N., Gao, H., 2014. Protective actions of aspirin-triggered (17R) resolvin D1 and its analogue, 17R-hydroxy-19-para-fluorophenoxy-resolvin D1 methyl ester, in C5a-dependent IgG immune complex-induced inflammation and lung injury. J. Immunol. 193, 3769–3778.
Teixeira, M.M., Cunha, F.Q., Ferreira, S.H., 2001. Response to an infectious insult (e.g. bacterial or fungal infection). Braz. J. Med. Biol. Res.: Rev. Bras. Pesqui. Med. Biol./Soc. Bras. Biofisica ... [et al.] 34, 1 (preceding 555).
Titos, E., Rius, B., Gonzalez-Periz, A., Lopez-Vicario, C., Moran-Salvador, E., Martinez-Clemente, M., Arroyo, V., Claria, J., 2011. Resolvin D1 and its precursor docosahexaenoic acid promote resolution of adipose tissue inflammation by eliciting macrophage polarization toward an M2-like phenotype. J. Immunol. 187, 5408–5418.
Torres-Guzman, A.M., Morado-Urbina, C.E., Alvarado-Vazquez, P.A., Acosta-Gonzalez, R.I., Chavez-Pina, A.E., Montiel-Ruiz, R.M., Jimenez-Andrade, J.M., 2014. Chronic oral or intraarticular administration of docosahexaenoic acid reduces nociception and knee edema and improves functional outcomes in a mouse model of complete freund's adjuvant-induced knee arthritis. Arthritis Res. Ther. 16, R64.
Torsteindottir, I., Arvidson, N.G., Hallgren, R., Hakansson, L., 1999. Monocyte activation in rheumatoid arthritis (RA): increased integrin, Fc gamma and complement receptor expression and the effect of glucocorticoids. Clin. Exp. Immunol. 115, 554–560.
Ueno, T., Kagawa, T., Kanou, M., Ishida, N., Fujii, T., Fukunaga, J., Mizukawa, N., Sugahara, T., 2003. Pathology of the temporomandibular joint of patients with rheumatoid arthritis – case reports of secondary amyloidosis and macrophage populations. J. Cranio-Maxillo-Facial Surg.: Off. Publ. Eur. Assoc. Cranio-Maxillo-Facial Surg. 31, 252–256.
Vilcek, J., Feldmann, M., 2004. Historical review: cytokines as therapeutics and targets of therapeutics. Trends Pharmacol. Sci. 25, 201–209.
Weiner, H.L., Selkoe, D.J., 2002. Inflammation and therapeutic vaccination in CNS diseases. Nature 420, 879–884.
Wink, D.A., Hines, H.B., Cheng, R.Y., Switzer, C.H., Flores-Santana, W., Vitek, M.P., Ridnour, L.A., Colton, C.A., 2011. Nitric oxide and redox mechanisms in the immune response. J. Leukoc. Biol. 89, 873–891.
Wittamer, V., Franssen, J.D., Vulcano, M., Mirjolet, J.F., Le Poul, E., Migeotte, I., Brezillon, S., Tyldesley, R., Blanpain, C., Detheux, M., Mantovani, A., Sozzani, S., Vassart, G., Parmentier, M., Communi, D., 2003. Specific recruitment of antigen-presenting cells by chemerin, a novel processed ligand from human inflammatory fluids. J. Exp. Med. 198, 977–985.
Wolfe, F., Clauw, D.J., Fitzcharles, M.A., Goldenberg, D.L., Katz, R.S., Mease, P., Russell, A.S., Russell, I.J., Winfield, J.B., Yunus, M.B., 2010. The american college of rheumatology preliminary diagnostic criteria for fibromyalgia and measurement of symptom severity. Arthritis Care Res. 62, 600–610.
Wright, H.L., Moots, R.J., Bucknall, R.C., Edwards, S.W., 2010. Neutrophil function in

inflammation and inflammatory diseases. Rheumatology (Oxford) 49, 1618–1631.
Xu, Z.Z., Zhang, L., Liu, T., Park, J.Y., Berta, T., Yang, R., Serhan, C.N., Ji, R.R., 2010. Resolvins RvE1 and RvD1 attenuate inflammatory pain via central and peripheral actions. Nat. Med. 16, 592–597 (1p following 597).
Zhang, X., Qu, X., Sun, Y.B., Caruana, G., Bertram, J.F., Nikolic-Paterson, D.J., Li, J., 2013. Resolvin D1 protects podocytes in adriamycin-induced nephropathy through modulation of 14-3-3beta acetylation. PloS One 8, e57471.
Zhu, M., Van Dyke, T.E., Gyurko, R., 2013. Resolvin E1 regulates osteoclast fusion via DC-STAMP and NFATc1. FASEB J.: Off. Publ. Fed. Am. Soc. Exp. Biol. 27, 3344–3353.
http://www.resolvyx.com, (accessed 26.12.14).

7.2. Neutrophil-derived microvesicles enter cartilage and protect the joint in inflammatory arthritis

RESEARCH ARTICLE

RHEUMATOID ARTHRITIS

Neutrophil-derived microvesicles enter cartilage and protect the joint in inflammatory arthritis

Sarah E. Headland,[1] Hefin R. Jones,[1] Lucy V. Norling,[1] Andrew Kim,[2] Patricia R. Souza,[1] Elisa Corsiero,[1] Cristiane D. Gil,[3] Alessandra Nerviani,[1] Francesco Dell'Accio,[1,4] Costantino Pitzalis,[1,4] Sonia M. Oliani,[3] Lily Y. Jan,[2] Mauro Perretti[1]*

Microvesicles (MVs) are emerging as a new mechanism of intercellular communication by transferring cellular lipid and protein components to target cells, yet their function in disease is only now being explored. We found that neutrophil-derived MVs were increased in concentration in synovial fluid from rheumatoid arthritis patients compared to paired plasma. Synovial MVs overexpressed the proresolving, anti-inflammatory protein annexin A1 (AnxA1). Mice deficient in TMEM16F, a lipid scramblase required for microvesiculation, exhibited exacerbated cartilage damage when subjected to inflammatory arthritis. To determine the function of MVs in inflammatory arthritis, toward the possibility of MV-based therapeutics, we examined the role of immune cell–derived MVs in rodent models and in human primary chondrocytes. In vitro, exogenous neutrophil-derived AnxA1$^+$ MVs activated anabolic gene expression in chondrocytes, leading to extracellular matrix accumulation and cartilage protection through the reduction in stress-adaptive homeostatic mediators interleukin-8 and prostaglandin E_2. In vivo, intra-articular injection of AnxA1$^+$ MV lessened cartilage degradation caused by inflammatory arthritis. Arthritic mice receiving adoptive transfer of whole neutrophils displayed abundant MVs within cartilage matrix and revealed that MVs, but not neutrophils themselves, can penetrate cartilage. Mechanistic studies support a model whereby MV-associated AnxA1 interacts with its receptor FPR2 (formyl peptide receptor 2)/ALX, increasing transforming growth factor–β production by chondrocytes, ultimately leading to cartilage protection. We envisage that MVs, either directly or loaded with therapeutics, can be harnessed as a unique therapeutic strategy for protection in diseases associated with cartilage degeneration.

INTRODUCTION

In most rheumatoid arthritis (RA) patients, tumor necrosis factor–α (TNF-α) drives synovial inflammation, and in mice, TNF-α overexpression is sufficient to induce a severe form of inflammatory arthritis, culminating in cartilage and bone destruction (*1*). In a significant proportion of RA patients, TNF blockade arrests joint erosion; however, cartilage damage can progress despite the inflammatory process being well controlled, leading to secondary osteoarthritis and permanent disability. Arresting and, if possible, reversing the cartilage breakdown induced by the inflammatory environment of the arthritic joint is an unmet need.

Microvesicles (MVs; 0.05 to 1 μm), comprising both exosomes and microparticles, are emerging as novel determinants of paracellular communication. Released by most eukaryotic cells, MVs can transfer proteins, lipids, nucleic acids, and cytosolic material (*2*). MVs originating from different cells differ in composition and biological function; for instance, in human RA, MVs of leukocyte, platelet, and synovial fibroblast origin can be found in synovial fluids, with concentrations positively correlating with disease activity (*3*, *4*). Neutrophils accumulate in large numbers in the synovial space during acute and transient RA flares and contribute to ≥30% of total synovial fluid MVs during active phases of the disease. The "biological impact" of neutrophil MVs is intriguing because these microstructures express >300 proteins that vary in relation to the stimulus and microenvironment leading to their production. It is therefore plausible that neutrophil MV subtypes can elicit distinct downstream effects (*5*).

The concept that neutrophils are not just short-lived effectors of inflammation but have long-term homeostatic actions is gaining ground. For example, neutrophil apoptotic bodies reprogram M1 macrophages to an M2 phenotype via efferocytosis, and depletion of neutrophils in murine models of ulcerative colitis leads to disease exacerbation (*6*). Although neutrophil depletion in models of experimental arthritis attenuates inflammatory parameters (*7*), it also decreases cartilage proteoglycan synthesis (*8*). Because the interaction between these two cell types in vivo is undescribed, we investigated whether MVs could enable a novel mechanism for the proanabolic effects of neutrophils on cartilage synthesis.

Here, we found that human RA synovial fluids contain abundant neutrophil-derived MVs. Mice lacking TMEM16F (anoctamin 6) produced fewer neutrophil MVs and displayed higher cartilage erosion in experimental arthritis, compared with wild-type animals. When administered into mice with inflammatory arthritis (K/BxN model), MVs protected the cartilage from the loss of sulfated glycosaminoglycans (sGAGs). Building upon these observations that immune cells may interact indirectly with chondrocytes in mature cartilage, we envisage that this MV-chondrocyte interaction can be harnessed as a platform for innovative therapeutic strategies in arthritis and other cartilage degradation diseases.

[1]William Harvey Research Institute, Barts and The London School of Medicine, Queen Mary University of London, Charterhouse Square, London EC1M 6BQ, UK. [2]Department of Physiology, Howard Hughes Medical Institute, University of California, San Francisco, San Francisco, CA 94143, USA. [3]Department of Biology, Instituto de Biociências, Letras e Ciências Exatas, São Paulo State University (UNESP), São José do Rio Preto 15054-000, Brazil. [4]Department of Rheumatology, Barts Health Trust, Bancroft Road, London E1 4DG, UK. *Corresponding author. E-mail: m.perretti@qmul.ac.uk

RESULTS

Rheumatoid synovial fluid neutrophil MVs contain annexin A1

To characterize MVs in human disease, we quantified immune cell–derived MVs in synovial fluid and paired plasma samples of seven RA

patients (table S1). Significantly more neutrophil-derived ($CD66b^+$), monocyte-derived ($CD14^+$), and T cell–derived ($CD3^+$) MVs were in the synovial fluid compared with plasma for each patient (Fig. 1A). Synovial MVs were enriched in the proresolving/anti-inflammatory protein annexin A1 (AnxA1) compared to plasma MVs, with more $AnxA1^+$ MVs being of neutrophil origin ($CD66b^+$) (Fig. 1B). Further stratification of a second, larger cohort of RA synovial fluid samples (n = 22) revealed higher numbers of neutrophil MVs (Fig. 1C) compared to MVs of monocyte ($CD14^+$) or T cell origin ($CD3^+$) that also contained $AnxA1^+$ (Fig. 1D). Most MVs in human synovial fluids are therefore of neutrophil origin with the potential to elicit proresolving effects in the context of RA.

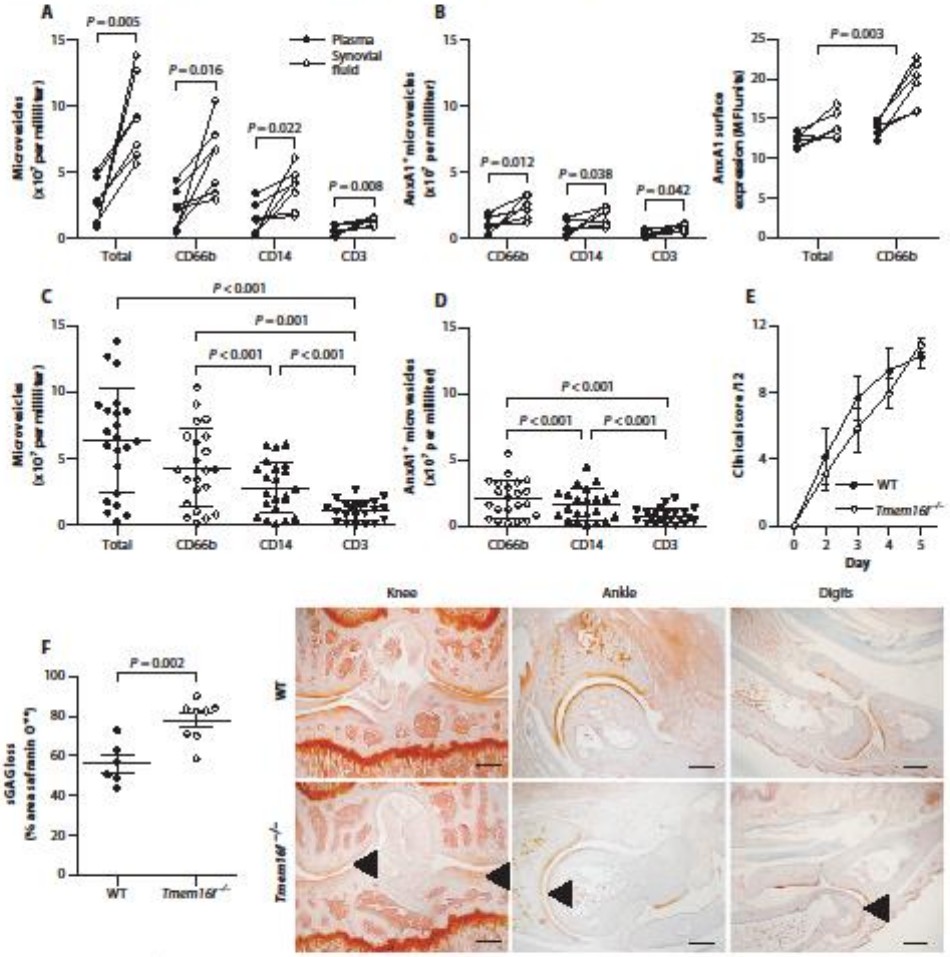

Fig. 1. Human RA synovial fluid is rich in AnxA1-positive neutrophil MVs that protect cartilage. (**A** and **B**) CD66b, CD14, and CD3 expression on MVs (A) and the presence and expression levels of AnxA1-positive MVs (B) from paired synovial fluid and plasma of RA patients (n = 7). P values were determined by paired, two-tailed Student's t test. MFI, mean fluorescence intensity. (**C** and **D**) Validation of synovial MV phenotype (C) and $AnxA1^+$ MVs (D) in additional RA patient synovial fluid samples (n = 22). Data are means ± SD. P values were determined by one-way analysis of variance (ANOVA) and Bonferroni multiple comparison test. (**E**) Mice deficient in the putative phospholipid scramblase TMEM16F ($Tmem16f^{-/-}$) and wild-type (WT) littermate controls were administered K/BxN serum to induce arthritis. Clinical scores are means of all joints ± SEM (n = 9 $Tmem16f^{-/-}$ and 6 WT mice). (**F**) Sections from digits, wrists, ankles, and knees at day 5 from mice in (E) were assessed for sGAG loss by safranin O staining. Data are means ± SEM (n = 6 to 9). P value was determined by unpaired two-tailed Student's t test. Arrowheads indicate sGAG loss. Scale bars, 250 μm.

Mice with impaired MV production exhibit exacerbated cartilage erosion during inflammatory arthritis

Neutrophil MVs can evoke anti-inflammatory effects (*9*–*11*), although their actions in disease are not defined. Thus, to determine whether neutrophil MVs affected joint pathophysiology, a model of neutrophilic arthritis (K/BxN serum transfer) was performed in mice lacking the lipid scramblase TMEM16F (*Tmem16f*$^{-/-}$). These mice display abnormal skeletal development, yet normal cartilage (*12*); their response to arthritic challenge has not been evaluated. The absence of TMEM16F affected neutrophil MV shedding, as evident in acute peritonitis (fig. S1, A to C). When subjected to inflammatory arthritis, *Tmem16f*$^{-/-}$ mice and wild-type littermates displayed similar clinical scores of inflammation and synovitis (Fig. 1E and fig. S1, D and E). However, an about twofold increase in sGAG loss, an index of cartilage integrity, was measured in *Tmem16f*$^{-/-}$ tissues (Fig. 1F and fig. S1F), suggesting that the loss of TMEM16F-dependent MV formation may exacerbate cartilage damage.

Neutrophil-derived MVs recapitulate physicochemical characteristics of those found in RA patient synovial fluids

Purified MVs from TNF-α–treated human neutrophils (fig. S2A) were used as a model of RA synovial fluid neutrophil-derived MV, with neutrophil activation confirmed by CD62L and CD11b expression (fig. S2, B and C). TNF-α stimulation led to a greater than twofold increase in MV shedding (referred to as MV_{TNF}) compared to vehicle-treated control cells (MV_{Ctrl}) (Fig. 2A). More than 75% of MVs were $CD66b^+$ and bound annexin V, indicating phosphatidylserine exposure, whereas about 60% were positive for phalloidin, confirming filamental actin in the vesicles (Fig. 2B) (*8*). MVs also expressed myeloid-related protein 8 (MRP8) (~80% positive) and its binding partner MRP14 (Fig. 2C). Flow cytometry (Fig. 2, D and E) and Western blotting (Fig. 2F) detected abundant AnxA1 expression, with larger positive percentages and higher intensities in the MV_{TNF} populations than MV_{Ctrl}. However, total protein concentration per MV remained unchanged with TNF-α stimulation (Fig. 2G), suggesting specific enrichment of AnxA1 in MV_{TNF}.

Nanoparticle tracking analysis (NTA) provided accurate measurements of pooled MV_{TNF} samples, where 90% of the vesides were <412 nm in diameter (dotted line) with mode frequency at 143 nm (Fig. 2H). Detection of small-diameter vesicles suggested the presence of exosomes, confirmed by the expression of the tetraspanin protein TSG101 (tumor susceptibility gene 101) in MVs from two healthy donors (fig. S3). Using imaging cytometry, we detected MVs with superior precision (Fig. 2I) and enumerated MV formation after stimulation of parent neutrophils with TNF-α, interleukin-8 (IL-8) (an unrelated cell activator), and phorbol myristate acetate (PMA) over 240 min (Fig. 2J). MVs were obtained within 20 min of stimulation, with a peak at 120 min. However, neutrophil extracellular trap (NET) formation was observed microscopically at the two later time points (Fig. 2K). On the basis of these data and previous kinetics data (*13*), we selected the 20-min time point to generate enriched MV preparations for further experimentation.

Neutrophil MVs enhance chondroprotection by inducing transforming growth factor–β generation

Because *Tmem16f*$^{-/-}$ mice exhibited exacerbated sGAG loss during arthritis, we modeled adult cartilage matrix turnover using high-density three-dimensional (3D) micromass cultures of the human chondrocyte cell line C28/I2 or primary adult human articular chondrocytes (AHACs) in vitro (*14*) and tested the effect of neutrophil MVs on extracellular matrix (ECM) metabolism. Treatment of chondrocytes with MV_{Ctrl} or MV_{TNF} (1×10^5) yielded no changes in ECM accumulation (Fig. 3A). However, when chondrocytes were first stimulated with IL-1β—a cytokine that induces destruction of articular cartilage (*15*)—or TNF-α, both MV_{Ctrl} and MV_{TNF} afforded protection from sGAG loss, showing an increase in ECM deposition versus vehicle controls (Fig. 3A and fig. S4A). Notably, the effects of neutrophil MVs were dependent on the degree of IL-1β stimulation: larger concentrations of MVs (>50,000) were required to induce an effect at 3 ng/ml IL-1β than at 30 ng/ml IL-1β (fig. S4B). Furthermore, cytokine sequestration was not responsible for increased ECM because MV_{TNF} did not express IL-1 receptor (IL-1R), although about 12 to 15% of isolated neutrophil MVs did express the TNF receptor (TNF-R1, fig. S4C).

Without evidence to support direct cytokine sequestration, we investigated whether neutrophil MVs might amplify ECM accumulation by inhibiting its degradation. To test this, we measured the amount of released (enzymatically cleaved) sGAG in the supernatant. As expected, IL-1β treatment induced more proteoglycan release compared to control, an effect abrogated by cotreatment with MVs (1×10^5; Fig. 3B), although no significant down-regulation of *MMP13* or *ADAMTS5* could be demonstrated at the mRNA level (fig. S5). However, IL-1β treatment of chondrocytes led to reduced expression of *ACAN* and *COL2A1* (the two most abundant cartilage matrix proteins) and *SOX9* (the transcription factor driving their expression)—effects partly reversed by cotreatments with either MV_{Ctrl} or MV_{TNF} (Fig. 3, C and D). Different molecular weight bands also appeared after MV coculture, yet their identities remain to be determined (Fig. 3D).

These chondrocyte responses to IL-1β were complemented by increased release of IL-8 and prostaglandin E_2 (PGE_2) (Fig. 3E), which in high levels are associated with cartilage degradation in RA (*16*). Both MV_{Ctrl} and MV_{TNF} significantly attenuated IL-8 (~30% reduction) and PGE_2 (>80% inhibition) release (Fig. 3E). Chondrocyte apoptosis is also associated with cartilage loss in animal models and in humans (*17*, *18*). Addition of high levels of IL-1β (50 ng/ml) increased C28/I2 chondrocyte apoptosis (Fig. 3F and fig. S6), but MV_{Ctrl} or MV_{TNF} prevented cell death (Fig. 3F).

Coculture of neutrophil MV with monocyte-derived macrophages (MDMs) or dendritic cells induces anti-inflammatory activity, partly via induction of transforming growth factor–β (TGF-β) (*10*, *11*). To determine whether chondroprotection resulted from increased TGF-β synthesis, we assessed the transcription of *TGFB1* in C28/I2 human chondrocyte micromasses. *TGFB1* mRNA was down-regulated about twofold by IL-1β treatment but significantly up-regulated after coculture with MV_{TNF}, with or without IL-1β (Fig. 3G). Blocking TGF-β resulted in significantly reduced (~50%) anabolic effects exerted by neutrophil MV_{TNF} in the coculture settings (Fig. 3H). These data suggest that chondroprotection results from MV-dependent TGF-β induction.

Collectively, these in vitro studies indicate that neutrophil-derived MVs protect against various sequelae involved in cartilage degradation (chondrocyte apoptosis, PGE_2 and IL-8 release, and ECM degradation) by significantly up-regulating the transcripts of genes key to cartilage anabolism after the induction of TGF-β.

MVs penetrate cartilage ex vivo and in vivo

To determine the mechanism behind MV-induced chondroprotection in a physiological setting where chondrocytes are surrounded by the dense, avascular, and cell-impenetrable cartilage matrix, fluorescent neutrophil MVs were cocultured for 18 hours with rat cartilage explants. The location of MVs was confirmed by immunostaining for anti-human

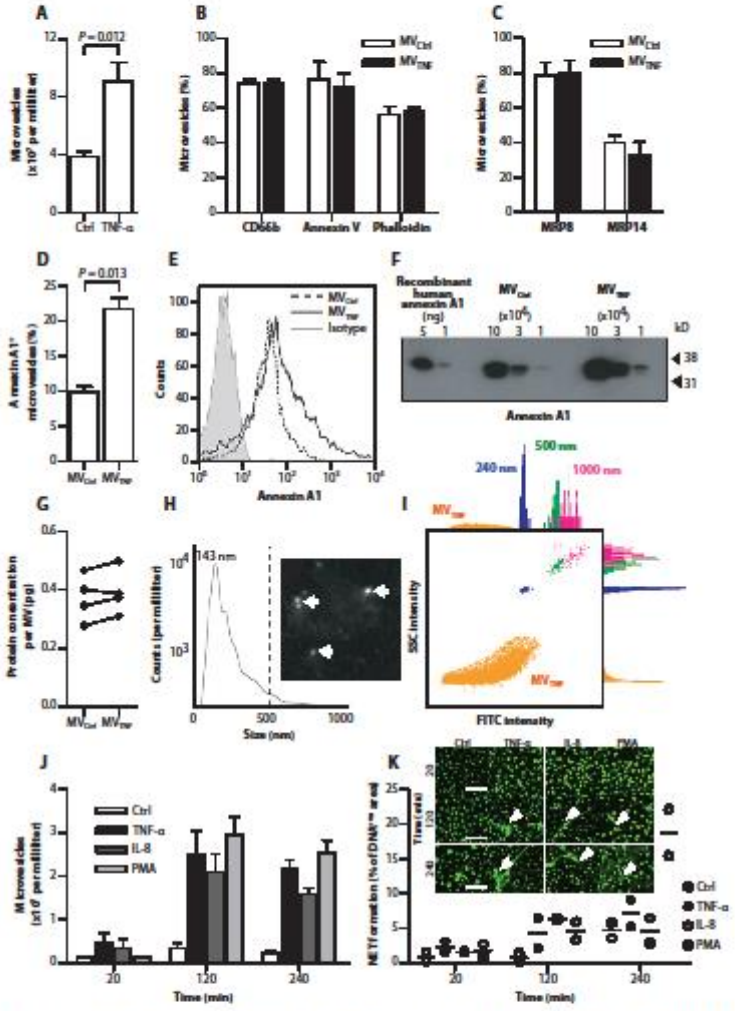

Fig. 2. Generation and characterization of AnxA1-rich MVs from healthy neutrophils. (**A**) Human circulating neutrophils (10^6) were stimulated with TNF-α (50 ng/ml) or vehicle (Control); resultant MV_{TNF} or MV_{Ctrl}, respectively, was enumerated. (**B**) Expression of CD66b, annexin V, and phalloidin. (**C**) Expression of MRP8 and MRP14. (**D** and **E**) The percentage of AnxA1$^+$ MVs (D) and comparative surface expression (E) of AnxA1. Data in (A) to (E) are means ± SEM ($n = 4$). *P* values were determined by two-tailed Student's *t* test. (**F**) AnxA1 content in MV_{TNF} by Western blotting. Human recombinant AnxA1 was the positive control. (**G**) Total protein concentration of paired MV_{Ctrl} and MV_{TNF} ($n = 4$ donors). (**H**) NTA for absolute MV size (six pooled MV_{TNF} donors). Dotted line indicates 90% of MVs below 412 nm; median was 143 nm. The representative image is a still from the NTA. White arrows indicate MVs. (**I**) Representative side scatter (SSC)/fluorescence plot from ImageStream^X showing MVs (orange) versus 240- (blue), 500- (green), and 1000-nm (pink) calibration beads, with related histograms. FITC, fluorescein isothiocyanate. (**J**) MVs quantified at 20 min, 2 hours, and 4 hours after stimulation of parent human neutrophils with TNF-α (50 ng/ml), IL-8 (50 ng/ml), or PMA (100 nM). Data are means ± SEM ($n = 3$). (**K**) NET formation ($n = 2$). Images are representative micrographs used for analysis; white arrowheads indicate NETs. Scale bars, 50 μm.

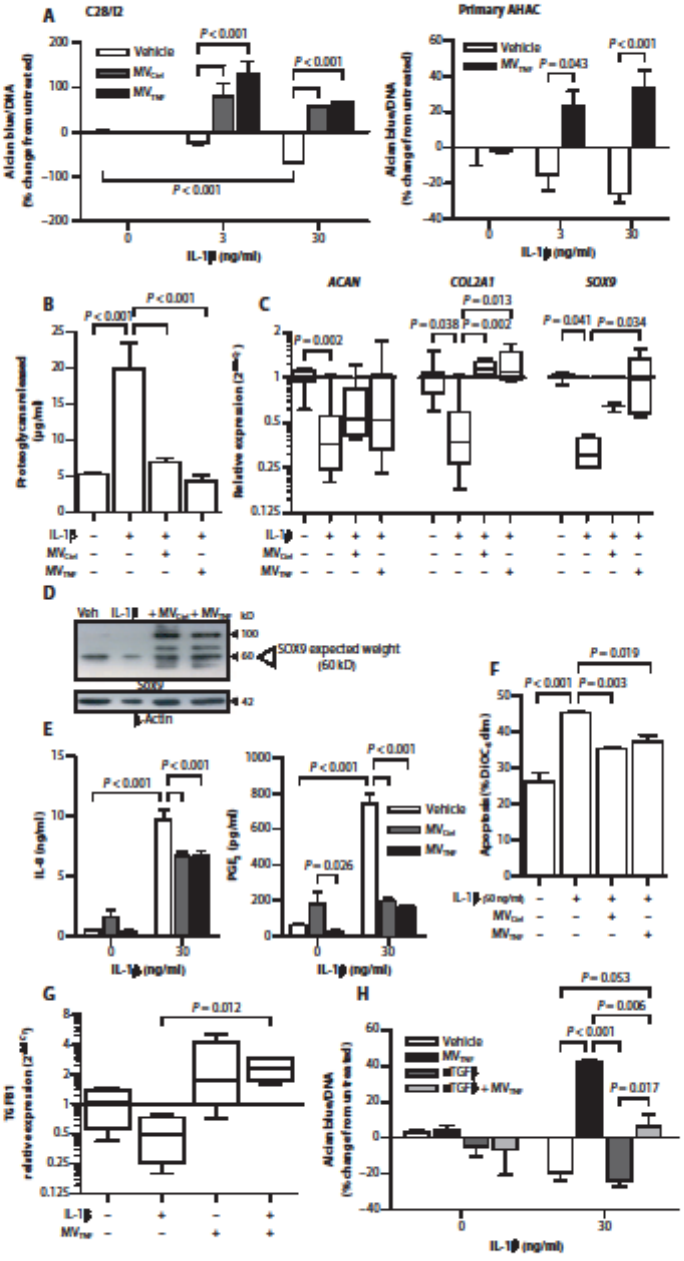

Fig. 3. Neutrophil MVs induce ECM accumulation and are chondroprotective in vitro in chondrocyte micromasses. Human C28/I2 chondrocyte and primary AHAC micromass cultures were stimulated with IL-1β (3 or 30 ng/ml) alone or with MV_{Ctrl} and MV_{TNF} (10^5). (**A**) ECM content normalized to DNA concentration. Data are means ± SEM (n = 6 separate MV and cell culture preparations). (**B**) ECM degradation in C28/I2 micromasses, quantified as amount of proteoglycans released. Data are means ± SEM (n = 10 separate MVs and 6 cell culture preparations). (**C**) Relative expression of *COL2A1*, *ACAN*, and *SOX9* mRNA in C28/I2 micromasses. Data are $2^{-\Delta\Delta C_T}$, median ± interquartile range [n = 3 or 4 separate MV and micromass preparations and relative to housekeeping gene (*rpl32*) and untreated]. (**D**) Representative Western blot for SOX9. (**E**) IL-8 and PGE_2 concentrations in C28/I2 micromass supernatants. Data are means ± SEM (n = 6). (**F**) C28/I2 chondrocyte apoptosis in micromasses treated as in (A) with IL-1β (50 ng/ml). Data are means ± SEM (n = 4). (**G**) *TGFB1* mRNA expression in C28/I2 micromasses stimulated as in (C). Data are $2^{-\Delta\Delta C_T}$, median ± interquartile range (n = 4) relative to housekeeping gene (*RPL32*) and untreated. (**H**) ECM production normalized to DNA content in C28/I2 micromass cultures stimulated as in (A) with or without TGF-β neutralizing antibodies (10 μg/ml; αTGFβ) for 24 hours. Data are means ± SEM (n = 3 separate MV donors). P values were determined by one- or two-way ANOVA and Bonferroni posttest (A, B, E, F, and H) or Kruskal-Wallis test and Dunn's multiple comparison posttest (C and G).

MRP8 (Fig. 4A), which was highly expressed in MV_{Ctrl} and MV_{TNF} (Fig. 2C). Migration of human MVs into cartilage was observed in both vehicle- and IL-1β–treated explants (Fig. 4A); however, the distance of penetration was significantly higher in IL-1β–stimulated explants (Fig. 4B). Synthetic fluorescent microcapsules of comparable size and AnxA1 content did not migrate into the cartilage, irrespective of cartilage treatment (Fig. 4A), suggesting that MV entry is not by passive diffusion. Coculture of sonicated (ruptured) MV_{TNF} with IL-1β–stimulated rat femoral heads failed to reduce sGAG loss, in contrast to whole MV_{TNF} (Fig. 4C), indicating that the intact MV structures are required for chondroprotection.

Sections from rat cartilage explants treated with IL-1β and cocultured with MV_{TNF} were stained for AnxA1 (Fig. 4D). Neutrophil-derived MVs colocalized with human $AnxA1^+$ staining and accumulated preferentially within the chondrocyte lacunae. Congruently, diffuse staining of human AnxA1 was observed, suggesting delivery to the chondrocyte cytoplasm. Movie S1 shows serial z-stack images of cartilage-resident chondrocytes that have engulfed human neutrophil-derived $AnxA1^+$ MVs.

We next tested the cartilage penetration of other myeloid-derived vesicles, abundant in RA synovial fluid. Incubation of cartilage explants with MDM-derived ($CD14^+$) MVs indicated lack of cartilage penetration or even adhesion to the articular surface, whereas neutrophil-derived ($CD66b^+$) MVs were abundant within the matrix (Fig. 4E). Thus, it appears that the selective interaction between MVs and cartilage matrix may involve a directed chemotactic response. We measured the expression levels of the IL-8 receptor CXCR2 on MVs because chondrocytes up-regulate IL-8 upon insult (*19*). Neutrophil-derived MVs expressed CXCR2, CXCR1, and CXCR4 (fig. S7A). However, a neutralizing CXCR2 antibody did not affect the ability of MV_{TNF} to migrate into cartilage explants (fig. S7B). Congruently, MVs generated from $Cxcr2^{-/-}$ mice entered cartilage to the same extent as wild-type MVs (fig. S7B). Thus, chemoattractant receptor(s) other than CXCR2 (expressed by

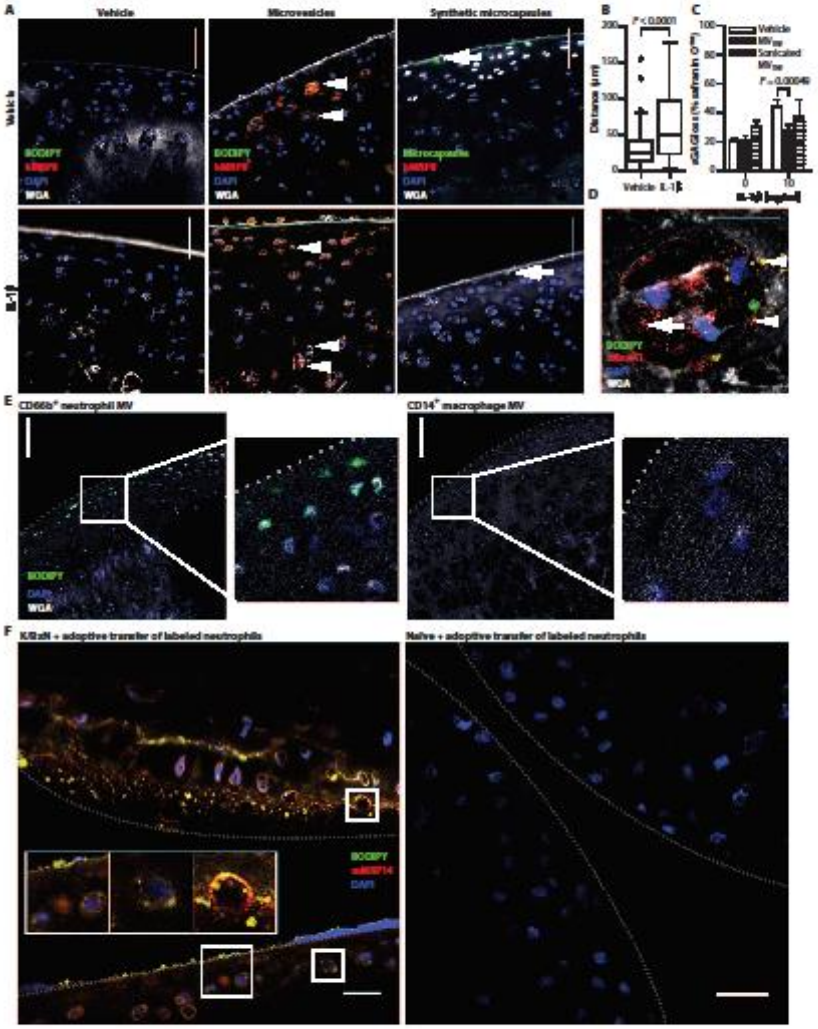

Fig. 4. MVs enter cartilage ex vivo and in vivo to deliver AnxA1. Rat femoral head cartilage explants were stimulated with IL-1β (10 ng/ml, 3 days incubation before the addition of MVs) or vehicle (Veh) [phosphate-buffered saline (PBS)] before coculture with fluorescently labeled MV_{TNF} (5×10^5) or synthetic fluorescent microcapsules (containing AnxA1). **(A)** Sections were stained for MRP8, 4′,6-diamidino-2-phenylindole (DAPI), and wheat germ agglutinin (WGA). Arrowheads indicate MV_{TNF}; arrows indicate microcapsules. **(B)** The distance of MV migration was measured. Data are Tukey's box and whiskers showing outliers ($n = 140$ or 166 MVs measured over at >10 individual micrographs). *P* values were determined by Mann-Whitney *t* test. Scale bars, 50 μm. **(C)** Murine cartilage explants were stimulated with IL-1β as in (A) or vehicle (saline) before coculture with MV_{TNF} or sonicated MV_{TNF}. sGAG loss was quantified by staining with safranin O. Data are means ± SEM ($n = 3$ or 6). *P* values were determined by two-way ANOVA with Bonferroni posttest. **(D)** Rat cartilage explants treated as in (A) stained for human AnxA1. Arrowheads indicate intact MVs; arrow indicates AnxA1 staining that is no longer MV-associated. Scale bar, 10 μm. Movie S1 shows related z-stack images. **(E)** Murine cartilage explants stimulated with IL-1β as in (A) and treated with fluorescently labeled neutrophil- or macrophage-derived MVs (5×10^5). Sections were stained with DAPI and WGA. Scale bars, 100 μm; insets, higher magnification. Dotted line indicates articular surface. Images are representative of $n = 3$ separate MV preparations. **(F)** Representative wrists from K/BxN or naïve mice ($n = 3$ per group) receiving fluorescently labeled whole neutrophils (green) intravenously. Sections were stained for MRP14 and DAPI. Scale bars, 20 μm. Dotted lines indicate opposing articular surfaces.

neutrophils and their offspring MV, but not by MDM or MDM MV) may be required for cartilage-directed migration. Candidate adhesion molecules ICAM-1 (intercellular adhesion molecule–1) and PECAM (platelet/endothelial cell adhesion molecule) were not expressed on $CD66b^+$ MVs (fig. S7A). The specific mechanism of neutrophil-derived MV uptake into cartilage is not yet clear, but we can rule out CXCR2, ICAM-1, and PECAM.

To determine whether MVs enter cartilage in pathophysiological settings in vivo, we injected systemically (intravenously) intact fluorescent murine neutrophils into mice with active inflammatory arthritis (day 3 after K/BxN serum transfer). Wrists were collected after 24 hours and costained for murine MRP14. $MRP14^+$ MVs were detected within the cartilage of arthritic mice, yet no MVs or MRP14 staining was evident in the wrists of nonarthritic mice administered with exogenous labeled neutrophils (Fig. 4F). We posit that neutrophils migrate into inflamed joints to release MVs locally, which can penetrate the sGAG-depleted cartilage matrix.

A functional distinction between whole neutrophils and their offspring MVs was demonstrated using neutrophil-C28/I2 chondrocyte coculture with Transwell filters (fig. S8A). Direct neutrophil contact with chondrocytes inhibited anabolism and induced cell death (fig. S8B). In contrast, restricting neutrophil migration while still allowing MV contact with chondrocytes, by the use of membrane pore sizes 200 and 400 nm, yielded chondroprotection, as evidenced by ECM deposition in the presence of IL-1β, similar to our other in vitro studies (Fig. 3A and fig. S4B).

Cartilage protection by MVs requires AnxA1 and its receptor FPR2/ALX

Because AnxA1 is elevated in neutrophil-derived MVs in RA synovial fluid, a feature reproduced with MV_{TNF}, we questioned whether this protein played an essential role in the chondroprotective properties defined here. Indeed, MVs lacking AnxA1 lost >80% of their proanabolic effects when added to C28/I2 chondrocyte micromass culture (Fig. 5A and fig. S9). We next established whether the AnxA1 receptor formyl peptide receptor 2 (FPR2)/ALX is involved in

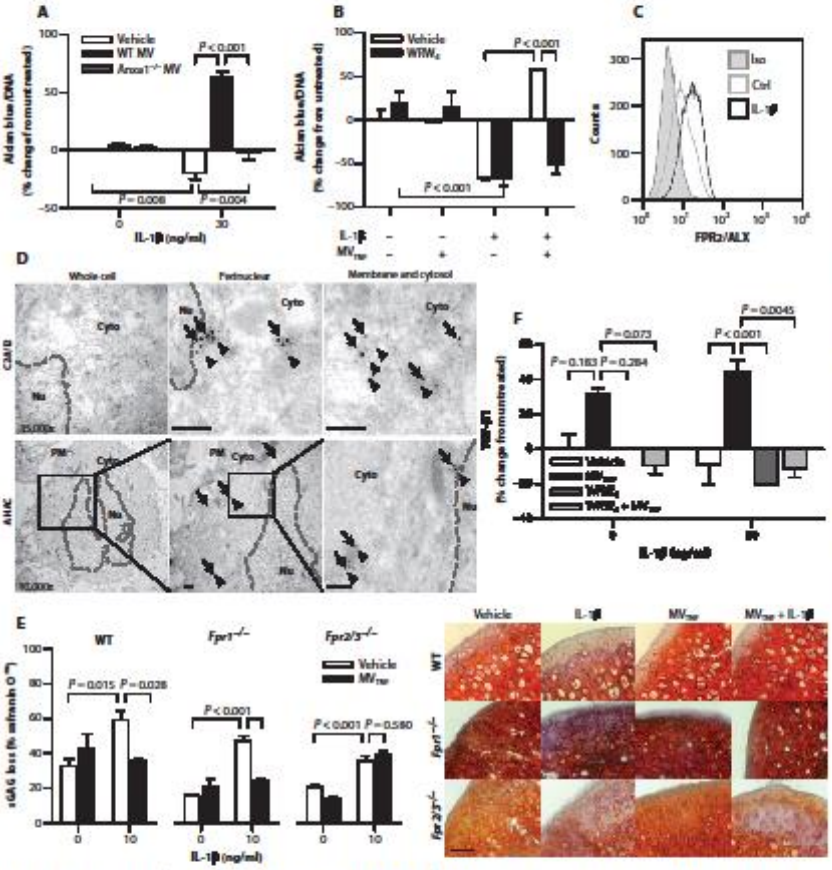

Fig. 5. Requirement of AnxA1 and its receptor FPR2/ALX for MV-induced chondroprotection. (**A**) ECM deposition normalized to DNA content in C28/I2 micromass cultures stimulated with IL-1β and cocultured with WT or *Anxa1*$^{-/-}$ mouse MV_{TNF} (10^5). (**B**) ECM deposition normalized to DNA content in C28/I2 micromass cultures stimulated with a combination of IL-1β (30 ng/ml), human neutrophil-derived MV_{TNF} (10^5), and WRW_4 (10 μM, 10 min before MV addition). Data in (A) and (B) are means ± SEM ($n = 4$ separate MV and cell culture preparations). (**C**) FPR2/ALX expression in C28/I2 micromasses [stimulated as in (A)]. Data are representative of $n = 3$. (**D**) Immunogold labeling of AnxA1 (arrows) and FPR2/ALX (arrowheads) in C28/I2 and AHAC micromasses. Black boxes indicate panel magnified to the right for AHAC. Dashed lines, nuclear envelope. PM, plasma membrane; Cyto, cytoplasm; Nu, nucleus. Scale bars, 100 nm. (**E**) Cartilage explants from WT, *Fpr1*$^{-/-}$, or *Fpr2/3*$^{-/-}$ mice were stimulated with IL-1β with or without 10^5 MV_{TNF}, every other day for 7 days. Sections were stained with safranin O. Representative images of micrographs used for analysis are shown. Scale bars, 200 μm. Data are means ± SEM ($n = 3$ to 6). (**F**) Total TGF-β1 content in supernatants of C28/I2 micromasses treated as in (B). Data are means ± SEM ($n = 8$ separate MV donors). *P* values were determined by two-way ANOVA and Bonferroni posttest (A, B, E, and F).

the protective properties of MVs. Application of the selective FPR2/ALX antagonist WRW_4 to C28/I2 chondrocytes in addition to MV_{TNF} abrogated the rescue of IL-1β–induced sGAG loss normally mediated by MV_{TNF}, without any direct biological actions (Fig. 5B). Chondrocytes expressed FPR2/ALX with a moderate increase after stimulation with IL-1β (Fig. 5C). The presence of endogenous FPR2/ALX and AnxA1 in chondrocytes (C28/I2 and primary AHAC), with frequent colocalization, was confirmed by electron microscopy (Fig. 5D). To further investigate the impact of the AnxA1 and FPR2/ALX on MV-induced chondroprotection, we incubated MVs with cartilage explants isolated from mice lacking FPR1 and FPR2/3 (the ortholog of human FPR2/ALX). The degradative effect of IL-1β was similar in cartilage explants from all animals; however, application of MV_{TNF} was effective only in wild-type and *Fpr1*$^{-/-}$ but not *Fpr2/3*$^{-/-}$ explants (Fig. 5E).

To determine whether chondroprotection resulted from the induction of TGF-β downstream of FPR2/ALX, we assayed C28/I2 culture supernatant after IL-1β and MV stimulation, with or without the FPR2/ALX antagonist. TGF-β levels were increased in C28/I2 chondrocyte micromasses after costimulation with IL-1β and MV_{TNF} (Fig. 5F). However, the addition of WRW_4 reduced TGF-β concentrations to levels comparable to IL-1β stimulation alone, suggesting FPR2/ALX engagement upstream of TGF-β production. Altogether, these data indicate that AnxA1 and FPR2/ALX are responsible for the protective properties of neutrophil MVs.

MVs protect from cartilage degradation in vivo in experimental inflammatory arthritis

To translate these findings, we administered MVs to a mouse model of K/BxN arthritis, in which the knee joint is markedly affected (*20*), providing a favorable site for intra-articular injection of MVs (*21*). MV_{TNFs} were injected into the right knee 3 days after arthritis induction, just before peak arthritis. Saline was administered to contralateral knees as a control. Cartilage integrity was determined on day 5. Nonarthritic mice retained sGAG, regardless of treatment, but arthritic mice experienced a marked reduction in sGAG content that was prevented in MV_{TNF}-treated joints (Fig. 6A). Confirming the nonredundant role of FPR2/ALX, MVs lost efficacy when coadministered with WRW_4 or injected into *Fpr2/3*$^{-/-}$ (Fig. 6, A and B). Similarly, in an adaptive immunity–dependent RA model, elicited by glucose-6-phosphate isomerase (GPI) immunization (*22*), MV_{TNF} injected into the right knee 21 days after arthritis induction (before peak arthritis) prevented sGAG content loss (~25%) compared with controls (saline, ~40%) (Fig. 6C).

DISCUSSION

We have uncovered chondroprotective properties of neutrophil-derived MVs, which directly interact with chondrocytes, revealing a potential new therapeutic approach for arthritis. Previous reports suggest pathogenic roles for MVs of platelet (*23*) and immune-cell origin (*24*) in the RA joint, focusing particularly on the synovial tissue as the target. However, MVs of neutrophil origin exert anti-inflammatory actions on macrophages and microvascular beds (*9*, *11*). We propose a model where neutrophils are recruited to the joint during the active flares of arthritis and release high numbers of MVs. These MVs enter the cartilage and bind the FPR2/ALX receptor, inducing TGF-β1 production and ECM deposition, while protecting chondrocytes from apoptosis.

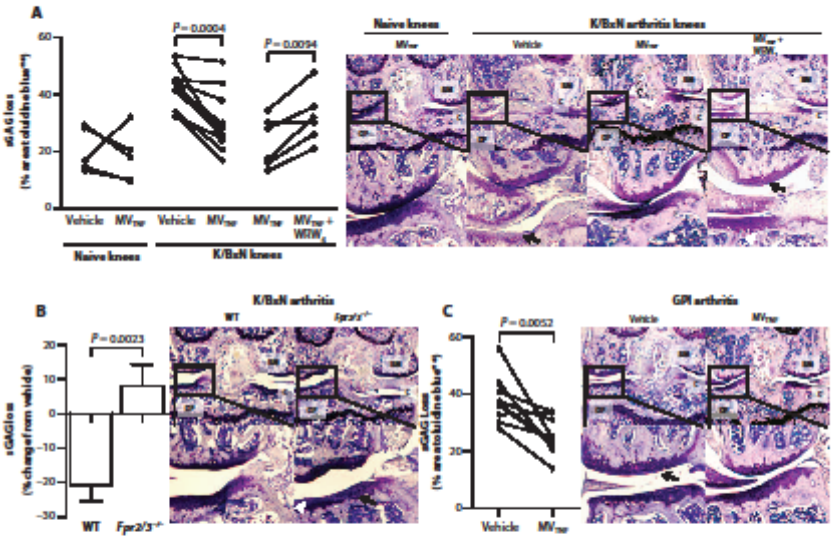

Fig. 6. Neutrophil MVs protect from cartilage degradation in models of inflammatory arthritis. (**A** and **B**) Mice received arthritogenic K/BxN serum (100 μl) on days 0 and 2; on day 3, vehicle (left knee; PBS, 5 μl) or MV_{TNF} (right knee; 3×10^4 in 5 μl) with or without WRW_4 (10 μM) was injected intra-articularly into WT (A) or *Fpr2/3*$^{-/-}$ mice (B). On day 5, knee joints were sectioned and stained with toluidine blue for sGAG content, and representative images are shown; black arrows in (A) indicate sGAG loss, and white arrowheads in (B) indicate cartilage surface fibrillations. Data are calculated from three sections per paired knees with three images per section ($n = 5$ to 9). *P* values were determined by two-way repeated-measures ANOVA and Bonferroni posttest. (**C**) DBA-1 female mice ($n = 9$) were immunized with GPI peptide on day 0 and administered vehicle intra-articularly in the left knee (PBS, 5 μl) or MV_{TNF} in the right knee (3×10^4 in 5 μl) intra-articularly on day 21. Knee joint sections were stained with toluidine blue, and representative images are shown; black arrows indicate sGAG loss. Data are from three sections per knee with three 20× images captured per section. *P* values were determined by paired, two-tailed Student's *t* test. In (A) to (C): BM, bone marrow; GP, growth plate; C, cartilage.

Furthermore, these MVs carry a complex cargo that includes the tissue-protective, proresolving protein AnxA1, opening up the possibility of modifying MVs to deliver other therapeutics.

Dogma dictates that cartilage is an immune cell–impenetrable, dense, avascular matrix through which metabolites from the synovial fluid must diffuse. Indeed, direct coculture of neutrophils with chondrocytes resulted in chondrocyte death. We provide evidence that neutrophil-derived MVs are instead able to cross this barrier to deliver AnxA1, a proresolving protein, and promote chondrocyte anabolism. Hence, cargo delivery via MVs through the impenetrable matrix may provide a mechanism of excluding damaging cell-cell contact while providing protection from cartilage degradation. MVs were active solely in inflammatory settings, likely through FPR2/ALX up-regulation, to promote anabolic gene transcription and accumulation of ECM in vitro and ex vivo in cartilage explants. These results were confirmed in vivo where selective presence of neutrophil MVs was observed in arthritic but not naïve joints after adoptive transfer of whole cells. Injection of MVs intra-articularly induced chondroprotection, whereas mice lacking TMEM16F, having inadequate production of endogenous MVs, experienced greater cartilage erosion, without differences in synovitis.

Human AnxA1 and MRP8 colocalized in part with an apparent vesicular form in rodent midzone cartilage, suggesting that a proportion of MVs may enter the chondrocyte in their entirety and release their content after fusion. Although studies determining the kinetics of endogenous human MV migration into cartilage are not feasible, there are reports that neutrophil-derived proteins are selectively present within human cartilage during arthritis. MRP8 protein, but not mRNA, is detected abundantly in human arthritic cartilage (*25*), and this protein is highly enriched in neutrophil MVs, as detected by proteomic analysis (*8*) and confirmed in this study. We speculate that the source of this myeloid-restricted protein within arthritic cartilage is neutrophil MVs; thus, although indirect, there is evidence that MV migration into cartilage may be a physiological process occurring in humans.

A higher degree of MV penetration was observed in inflammatory settings, which may result from the extent of cartilage damage and/or the presence of chemoattractant factors released by inflamed chondrocytes. Neutrophil-derived MVs contain several cytoskeletal proteins, a finding that may explain their ability to migrate in response to chemokine gradients (*8*). However, we could not identify the chemoattractant operative in our settings. A plausible candidate was IL-8 (or murine counterpart KC) because it is produced by human and rodent chondrocytes both in steady state and upon catabolism (*19*). However, we found that the IL-8 receptor CXCR2, albeit present on neutrophil MVs, was dispensable for matrix entry. Presently, the mechanism of MV migration is unclear, yet a degree of selectivity toward neutrophil MVs—rather than MDM-derived MVs—allows them to enter cartilage. Expression of some neutrophil-derived specific receptor, adhesion molecule, or matrix metalloproteinase may allow MV-matrix interactions, though any involvement of ICAM-1 and PECAM was excluded by this study.

Mediators of resolution regulate several phenomena, ultimately repairing injured tissue. An important effector of resolution is AnxA1, which activates tissue repair programs in the context of gut (*26*) and eye epithelia (*27*). AnxA1 lacks a signaling peptide (*28*) yet is found abundantly in inflammatory exudates, including RA synovial fluids (*29*), with its main mechanism of secretion likely to be via the release of MV. We found that neutrophil MVs in synovial fluid of RA patients were rich in AnxA1 compared to those circulating in plasma. This finding could reflect higher cell concentrations within the synovial fluid, but the context-specific activation of the cells leads to changes in their protein expression: AnxA1 gene promoter activation occurs in neutrophils during transmigration (*30*), explaining the AnxA1-enriched MV in RA exudates and the higher degree of expression at the single-vesicle level. Calcium (Ca^{2+}) chelation by AnxA1 promotes binding to phosphatidylserine and, subsequently, a conformational rearrangement with extrusion of the N-terminal region (*28*), enabling interaction with its receptor (*31*). Thus, Ca^{2+}-dependent MV generation (*13*, *32*), reliant on TMEM16F, provides the molecular requirements for externalization of active AnxA1. It is not clear from our data whether chondroprotection requires surface-expressed AnxA1 to bind FPR2/ALX or the engulfment of the entire particle. Certainly, surface-expressed AnxA1 would be in the correct orientation (with Ca^{2+} and bound to phospholipids) for FPR2/ALX binding; however, micrographs suggest engulfment and dismantling of the MVs; congruently, sonicated MVs do not evoke chondroprotective actions.

There is emerging evidence linking neutrophil MVs to the induction of TGF-β (*10*, *11*)—a key mediator of chondrocyte homeostasis that stimulates type II collagen and sGAG deposition (*33*) and down-regulates cartilage-degrading enzymes (*15*). We found that MV_{TNF} reversed TGF-β1 down-regulation by IL-1β, with levels higher than untreated chondrocytes. In support of a mechanism for production of TGF-β downstream of AnxA1-FPR2/ALX signaling, AnxA1 activates TGF-β production via FPRs in macrophages fed with apoptotic neutrophils (*34*). The augmentation of chondrocyte TGF-β production during MV coculture represents a protective mechanism against IL-1β–induced damage.

Using MVs as novel therapeutic tools in inflammatory diseases is a promising clinical approach because they can be enriched with proteins (*35*) or bioactive lipid mediators and their precursors (*36*). Relevantly, recent studies have used nanoparticle-based formulations to deliver peptide fragments of AnxA1 to resolve inflammation in murine models of atherosclerosis (*37*). Mesenchymal stem cells may be viable delivery vehicles for MVs because they naturally release exosomes that suppress hypoxia in mice (*38*). MVs are also amenable to targeting by incorporation of organ-specific homing peptides (*39*); moreover, because the sequence directing mRNAs to the pathway of MV secretion has been elucidated, MVs could be enriched for specific RNA species, enhancing their ability to deliver desired or therapeutic mRNA to target cells (*40*). Nevertheless, the future development of MV-based therapies requires the transition from mouse to human clinical studies. In support of advocating MV treatment in clinical trials, recent meta-analyses of platelet-rich plasma (PRP) administration into the joints of patients with mild degenerative chondral lesions demonstrated promising efficacy compared to hyaluronic acid treatment (*41*). We speculate that the MV component of PRP may be responsible for these effects, considering on average the presence of over 2×10^6 MVs per milliliter of plasma (*13*). Thus, a reasonable next step in ongoing PRP clinical studies would be to treat more advanced chondrodegenerative conditions, from trauma-induced damage to rheumatoid or osteoarthritis, to establish the translational potential of MVs.

In summary, the results presented indicate that neutrophil MVs, enriched in AnxA1, enter cartilage inducing FPR2/ALX signaling, which causes TGF-β production, matrix deposition, and chondrocyte homeostasis. These findings advocate the delivery of autologous MVs, either native or engineered to contain bioactive molecules, to chondrocytes

in situ. Our study sheds additional light on the functional and cellular associations between immune system and cartilage biology, delineating new strategies for innovative drug discovery with the goal of treating damaged cartilage of arthritic joints.

MATERIALS AND METHODS

Study design

The goal of this study was to investigate the role of neutrophil-derived MV during inflammatory arthritis and models of chondrocyte ECM turnover. We enumerated and performed phenotypic analyses on paired RA patient samples ($n = 7$) and a larger cohort of synovial fluid samples ($n = 22$). Because no previous data were available to estimate group variances, the entire biobank was analyzed to power the data as highly as possible. These human studies were approved by the Multicentre Research Ethics Committee (reference 07/Q0605/29) (table S1). Several in vitro and ex vivo approaches were used to determine the pro-anabolic function of human MV in chondrocyte coculture [prepared according to approved protocols: Research Ethics Committee [P/00/029 ELCHA (East London and The City Health Authority)]; volunteers gave written informed consent to blood collection, and procedures were approved by East London and The City Local Research Ethics Committee (REC Ref. 05/Q0603/34 ELCHA, London, UK)].

The chondroprotective effects of MV were examined in vivo in the K/BxN mouse model of arthritis by either knocking out *Tmem16f* or administering exogenous MVs. For one-way experiments, on the basis of the variance of pilot data (for 80% power and an α of 0.05), five mice per group were required to detect a mean difference of 25% sGAG loss between groups (considered a priori to be the minimal biologically significant effect; Cohen's d of ~1.5). For multifactorial experiments, at least six mice per group were required (for 80% power, α of 0.05 and smallest partial η^2 of ~0.3). All experiments were approved and performed under Home Office regulations (Scientific Procedures Act 1986). Mice were randomized to different groups, but the experimenter was not blinded to the group identities until after the administration of MVs. All samples were processed and analyzed in a blinded manner.

MV characterization and in vitro generation

Human RA synovial fluid MVs. Human RA synovial fluid (tables S1 to S3) was centrifuged at 3000*g* for 25 min at 4°C and treated with hyaluronidase (2 mg/ml; type I-S, 620 U/mg) for 30 min at room temperature. Samples were clarified by centrifugation at 10,000*g* for 10 min at room temperature. MVs were stained with antibodies directly in synovial fluid diluted 1:1 in double-sterile filtered (0.22-μm filter) PBS. Antibody targets (CD14, CD3, CD66b, and AnxA1) and preparations are described in Supplementary Materials and Methods.

Human neutrophil-derived MVs. Neutrophils were isolated from healthy human volunteers by density gradient centrifugation and then stimulated with recombinant TNF-α, IL-8, or phorbol myristate. MVs were then pelleted and stained for CD66b, AnxA1, TSG101, MRP8, MRP14, ICAM-1, PECAM, CXCR1, CXCR2, CXCR4, IL-1R1, TNF-R1, and annexin V and further characterized as described in Supplementary Materials and Methods.

Mouse MV generation. MV isolation from F_1 *Tmem16f*$^{-/-}$, C57BL/6 *Anxa1*$^{-/-}$, and *Cxcr2*$^{-/-}$ mice is described in Supplementary Materials and Methods.

Chondrocyte micromass culture and assays

Chondrocyte micromasses were formed from differentiated C28/I2 human chondrocytes and primary AHAC in culture. They were characterized by Alcian blue staining, proteoglycan, PGE_2, IL-8, and TGF-β release, gene expression, apoptosis, flow cytometry, electron microscopy, and Western blotting, as described in Supplementary Materials and Methods.

Ex vivo cartilage explants

Cartilage explants were collected from male Wistar rats or C57BL/6 mice (wild-type, *Fpr1*$^{-/-}$, or *Fpr2/3*$^{-/-}$) within 30 min of sacrifice, treated for 3 days with recombinant mouse IL-1β (10 ng/ml, 3 days), and cocultured with BODIPY-Maleimide–labeled human neutrophil MV or macrophage MV. Cryosections (6 μm) were stained with anti-MRP8, anti-AnxA1, DAPI, and WGA and visualized by confocal microscopy, or sGAG loss was quantified by safranin O staining.

In vivo arthritis

The induction of K/BxN arthritis and GPI-induced arthritis models is described in Supplementary Materials and Methods. *Tmem16f*$^{-/-}$ and wild-type littermate control mice (males) undergoing a 5-day K/BxN arthritis were scored daily, and ankle thickness was measured. Wild-type or *Fpr2/3*$^{-/-}$ mice (C57BL/6) undergoing a 5-day K/BxN arthritis were administered MV_{TNF} (3×10^6; 5-μl final volume) or PBS (5-μl final volume) intra-articularly on day 3, and joints were harvested for histological analysis on day 5. Wild-type female DBA-1 mice undergoing 25-day GPI arthritis were administered MV_{TNF} or PBS as above on day 21 before joint collection on day 25. Joints were decalcified in formic acid (10% v/v) and paraffin-embedded. Sections (10 μm; at least three per joint per mouse) were stained with toluidine blue stain or safranin O, and toluidine blue– or safranin O–positive percentage area was calculated from micrographs in a blinded manner using ImageJ.

A further cohort of mice undergoing K/BxN arthritis (as above) received adoptive transfer of BODIPY-Maleimide–labeled neutrophils intravenously on day 3. Joints were harvested for immunofluorescence staining on day 4 without decalcification.

Statistical analyses

Statistical comparisons were performed with mean ± SEM for continuous variables of experiments conducted at least three times, where n is the biological replicate (human donors or mice). Data were analyzed (two-tailed) using either paired or unpaired Student's t test, one-way ANOVA with Bonferroni posttest, Kruskal-Wallis followed by Dunn's multiple comparison, or two-way ANOVA with Bonferroni posttest where appropriate. In all cases, $P < 0.05$ was taken as significant. Analyses were performed using GraphPad Prism 5 or SPSS 22 software.

SUPPLEMENTARY MATERIALS

www.sciencetranslationalmedicine.org/cgi/content/full/7/315/315ra190/DC1
Materials and Methods
Fig. S1. *Tmem16f* knockout mice have reduced MV shedding and exacerbated sGAG loss in experimental arthritis.
Fig. S2. Characterization of parent neutrophils used to generate offspring MVs.
Fig. S3. Presence of tetraspanin TSG101 in neutrophil MVs.
Fig. S4. Concentration-dependent chondroprotection of MV against cytokine stimulation of chondrocytes.

Fig. S5. Selective effect of MV treatment on chondrocyte matrix degrading enzyme mRNA expression.
Fig. S6. MV treatment protects from chondrocyte apoptosis.
Fig. S7. MV chemokine receptor and adhesion molecule expression.
Fig. S8. Neutrophils induce ECM accumulation in chondrocytes only when prohibited from direct cell-to-cell contact.
Fig. S9. Generation of neutrophil MVs from $AnxA1^{-/-}$ mice.
Table S1. RA patient demographics.
Table S2. RA patient clinical profiles.
Table S3. RA patient treatment history.
Movie S1. MVs penetrate cartilage ex vivo to deliver AnxA1.

REFERENCES AND NOTES

1. J. Keffer, L. Probert, H. Cazlaris, S. Georgopoulos, E. Kaslaris, D. Kioussis, G. Kollias, Transgenic mice expressing human tumour necrosis factor: A predictive genetic model of arthritis. *EMBO J.* **10**, 4025–4031 (1991).
2. S. E. Headland, L. V. Norling, The resolution of inflammation: Principles and challenges. *Semin. Immunol.* **27**, 149–160 (2015).
3. R. J. Berckmans, R. Nieuwland, M. C. Kraan, M. C. Schaap, D. Pots, T. J. Smeets, A. Sturk, P. P. Tak, Synovial microparticles from arthritic patients modulate chemokine and cytokine release by synoviocytes. *Arthritis Res. Ther.* **7**, R536–R544 (2005).
4. N. Cloutier, S. Tan, L. H. Boudreau, C. Cramb, R. Subbaiah, L. Lahey, A. Albert, R. Shnayder, R. Gobezie, P. A. Nigrovic, R. W. Farndale, W. H. Robinson, A. Brisson, D. M. Lee, E. Boilard, The exposure of autoantigens by microparticles underlies the formation of potent inflammatory components: The microparticle-associated immune complexes. *EMBO Mol. Med.* **5**, 235–249 (2013).
5. J. Dalli, T. Montero-Melendez, L. V. Norling, X. Yin, C. Hinds, D. Haskard, M. Mayr, M. Perretti, Heterogeneity in neutrophil microparticles reveals distinct proteome and functional properties. *Mol. Cell. Proteomics* **12**, 2205–2219 (2013).
6. E. L. Campbell, W. J. Bruyninckx, C. J. Kelly, L. E. Glover, E. N. McNamee, B. E. Bowers, A. J. Bayless, M. Scully, B. J. Saeedi, L. Golden-Mason, S. F. Ehrentraut, V. F. Curtis, A. Burgess, J. F. Garvey, A. Sorensen, R. Nemenoff, P. Jedlicka, C. T. Taylor, D. J. Kominsky, S. P. Colgan, Transmigrating neutrophils shape the mucosal microenvironment through localized oxygen depletion to influence resolution of inflammation. *Immunity* **40**, 66–77 (2014).
7. J. L. Eyles, M. J. Hickey, M. U. Norman, B. A. Croker, A. W. Roberts, S. F. Drake, W. G. James, D. Metcalf, I. K. Campbell, I. P. Wicks, A key role for G-CSF-induced neutrophil production and trafficking during inflammatory arthritis. *Blood* **112**, 5193–5201 (2008).
8. M. S. Gresnigt, L. A. B. Joosten, I. Verschueren, J. W. M. van der Meer, M. G. Netea, C. A. Dinarello, F. L. van de Veerdonk, Neutrophil-mediated inhibition of proinflammatory cytokine responses. *J. Immunol.* **189**, 4806–4815 (2012).
9. J. Dalli, L. V. Norling, D. Renshaw, D. Cooper, K-Y. Leung, M. Perretti, Annexin 1 mediates the rapid anti-inflammatory effects of neutrophil-derived microparticles. *Blood* **112**, 2512–2519 (2008).
10. C. Eken, O. Gasser, G. Zenhausern, I. Oehri, C. Hess, J. A. Schifferli, Polymorphonuclear neutrophil-derived ectosomes interfere with the maturation of monocyte-derived dendritic cells. *J. Immunol.* **180**, 817–824 (2008).
11. O. Gasser, J. A. Schifferli, Activated polymorphonuclear neutrophils disseminate anti-inflammatory microparticles by ectocytosis. *Blood* **104**, 2543–2548 (2004).
12. H. W. A. Ehlen, M. Chinenkova, M. Moser, H-M. Munter, Y. Krause, S. Gross, B. Brachvogel, M. Wuelling, U. Kornak, A. Vortkamp, Inactivation of anoctamin-6/Tmem16f, a regulator of phosphatidylserine scrambling in osteoblasts, leads to decreased mineral deposition in skeletal tissues. *J. Bone Miner. Res.* **28**, 246–259 (2013).
13. S. E. Headland, H. R. Jones, A. S. V. D'Sa, M. Perretti, L. V. Norling, Cutting-edge analysis of extracellular microparticles using ImageStream^{X} imaging flow cytometry. *Sci. Rep.* **4**, 5237 (2014).
14. K. V. Greco, A. J. Iqbal, L. Rattazzi, G. Nalesso, N. Moradi-Bidhendi, A. R. Moore, M. B. Goldring, F. Dell'Accio, M. Perretti, High density micromass cultures of a human chondrocyte cell line: A reliable assay system to reveal the modulatory functions of pharmacological agents. *Biochem. Pharmacol.* **82**, 1919–1929 (2011).
15. H. M. van Beuningen, P. M. van der Kraan, O. J. Arntz, W. B. van den Berg, Protection from interleukin 1 induced destruction of articular cartilage by transforming growth factor β: Studies in anatomically intact cartilage in vitro and in vivo. *Ann. Rheum. Dis.* **52**, 185–191 (1993).
16. S-S. Nah, I-Y. Choi, C. K. Lee, J. S. Oh, Y. G. Kim, H-B. Moon, B. Yoo, Effects of advanced glycation end products on the expression of COX-2, PGE_2 and NO in human osteoarthritic chondrocytes. *Rheumatology* **47**, 425–431 (2008).
17. N. M. Elsaid, C. De Bari, P. Achan, C. Pitzalis, F. Dell'Accio, A novel in vivo murine model of cartilage regeneration. Age and strain-dependent outcome after joint surface injury. *Osteoarthritis Cartilage* **17**, 695–704 (2009).
18. O. Alvarez-Garcia, N. H. Rogers, R. G. Smith, M. K. Lotz, Palmitate has proapoptotic and proinflammatory effects on articular cartilage and synergizes with interleukin-1. *Arthritis Rheum.* **66**, 1779–1788 (2014).
19. J. Sherwood, J. Bertrand, G. Nalesso, B. Poulet, A. Pitsillides, L. Brandolini, A. Karystinou, C. De Bari, F. P. Luyten, C. Pitzalis, T. Pap, F. Dell'Accio, A homeostatic function of CXCR2 signalling in articular cartilage. *Ann. Rheum. Dis.* **74**, 2207–2215 (2014).
20. H. B. Patel, K. N. Kornerup, A. L. F. Sampaio, F. D'Acquisto, M. P. Seed, A. P. Girol, M. Gray, C. Pitzalis, S. M. Oliani, M. Perretti, The impact of endogenous annexin A1 on glucocorticoid control of inflammatory arthritis. *Ann. Rheum. Dis.* **71**, 1872–1880 (2012).
21. S. M. Ryan, J. McMorrow, A. Umerska, H. B. Patel, K. N. Kornerup, L. Tajber, E. P. Murphy, M. Perretti, O. I. Corrigan, D. J. Brayden, An intra-articular salmon calcitonin-based nanocomplex reduces experimental inflammatory arthritis. *J. Control. Release* **167**, 120–129 (2013).
22. R. Bockermann, D. Schubert, T. Kamradt, R. Holmdahl, Induction of a B-cell-dependent chronic arthritis with glucose-6-phosphate isomerase. *Arthritis Res. Ther.* **7**, R1316–R1324 (2005).
23. E. Boilard, P. A. Nigrovic, K. Larabee, G. F. M. Watts, J. S. Coblyn, M. E. Weinblatt, E. M. Massarotti, E. Remold-O'Donnell, R. W. Farndale, J. Ware, D. M. Lee, Platelets amplify inflammation in arthritis via collagen-dependent microparticle production. *Science* **327**, 580–583 (2010).
24. J. H. W. Distler, A. Jüngel, L. C. Huber, C. A. Seemayer, C. F. Reich III, R. E. Gay, B. A. Michel, A. Fontana, S. Gay, D. S. Pisetsky, O. Distler, The induction of matrix metalloproteinase and cytokine expression in synovial fibroblasts stimulated with immune cell microparticles. *Proc. Natl. Acad. Sci. U.S.A.* **102**, 2892–2897 (2005).
25. R. F. P. Schelbergen, A. B. Blom, M. H. J. van den Bosch, A. Slöetjes, S. Abdollahi-Roodsaz, B. W. Schreurs, J. S. Mort, T. Vogl, J. Roth, W. B. van den Berg, P. L. E. M. van Lent, Alarmins S100A8 and S100A9 elicit a catabolic effect in human osteoarthritic chondrocytes that is dependent on Toll-like receptor 4. *Arthritis Rheum.* **64**, 1477–1487 (2012).
26. G. Leoni, P-A. Neumann, N. Kamaly, M. Quiros, H. Nishio, H. R. Jones, R. Sumagin, R. S. Hilgarth, A. Alam, G. Fredman, I. Argyris, E. Rijcken, D. Kusters, C. Reutelingsperger, M. Perretti, C. A. Parkos, O. C. Farokhzad, A. S. Reiss, A. Nusrat, Annexin A1–containing extracellular vesicles and polymeric nanoparticles promote epithelial wound repair. *J. Clin. Invest.* **125**, 1215–1227 (2015).
27. A. P. Girol, K. K. O. Mimura, C. C. Drewes, S. M. Bolonheis, E. Solito, S. H. P. Farsky, C. D. Gil, S. M. Oliani, Anti-inflammatory mechanisms of the annexin A1 protein and its mimetic peptide Ac2-26 in models of ocular inflammation in vivo and in vitro. *J. Immunol.* **190**, 5689–5701 (2013).
28. V. Gerke, C. E. Creutz, S. E. Moss, Annexins: Linking Ca^{2+} signalling to membrane dynamics. *Nat. Rev. Mol. Cell Biol.* **6**, 449–461 (2005).
29. N. J. Goulding, J. Doxey, E. F. Morand, R. A. Dodds, L. S. Wilkinson, A. A. Pitsillides, J. C. Edwards, Differential distribution of annexins-I, -II, -IV, and -VI in synovium. *Ann. Rheum. Dis.* **54**, 841–845 (1995).
30. A. S. Damazo, S. Yona, R. J. Flower, M. Perretti, S. M. Oliani, Spatial and temporal profiles for anti-inflammatory gene expression in leukocytes during a resolving model of peritonitis. *J. Immunol.* **176**, 4410–4418 (2006).
31. S. Bena, V. Brancaleone, J. M. Wang, M. Perretti, R. J. Flower, Annexin A1 interaction with the FPR2/ALX receptor: Identification of distinct domains and downstream associated signaling. *J. Biol. Chem.* **287**, 24690–24697 (2012).
32. E. M. Bevers, T. Wiedmer, P. Comfurius, S. J. Shattil, H. J. Weiss, R. F. Zwaal, P. J. Sims, Defective Ca^{2+}-induced microvesiculation and deficient expression of procoagulant activity in erythrocytes from a patient with a bleeding disorder: A study of the red blood cells of Scott syndrome. *Blood* **79**, 380–388 (1992).
33. F. Redini, P. Galera, A. Mauviel, G. Loyau, J-P. Pujol, Transforming growth factor β stimulates collagen and glycosaminoglycan biosynthesis in cultured rabbit articular chondrocytes. *FEBS Lett.* **234**, 172–175 (1988).
34. M. Scannell, M. B. Flanagan, A. deStefani, K. J. Wynne, G. Cagney, C. Godson, P. Maderna, Annexin-1 and peptide derivatives are released by apoptotic cells and stimulate phagocytosis of apoptotic neutrophils by macrophages. *J. Immunol.* **178**, 4595–4605 (2007).
35. J. Dalli, L. V. Norling, T. Montero-Melendez, D. Federici Canova, H. Lashin, A. M. Pavlov, G. B. Sukhorukov, C. J. Hinds, M. Perretti, Microparticle alpha-2-macroglobulin enhances pro-resolving responses and promotes survival in sepsis. *EMBO Mol. Med.* **6**, 27–42 (2014).
36. L. V. Norling, M. Spite, R. Yang, R. J. Flower, M. Perretti, C. N. Serhan, Cutting edge: Humanized nano-proresolving medicines mimic inflammation-resolution and enhance wound healing. *J. Immunol.* **186**, 5543–5547 (2011).
37. G. Fredman, N. Kamaly, S. Spolitu, J. Milton, D. Ghorpade, R. Chiasson, G. Kuriakose, M. Perretti, O. Farokhzad, I. Tabas, Targeted nanoparticles containing the proresolving peptide Ac2-26 protect against advanced atherosclerosis in hypercholesterolemic mice. *Sci. Transl. Med.* **7**, 275ra20 (2015).
38. C. Lee, S. A. Mitsialis, M. Aslam, S. H. Vitali, E. Vergadi, G. Konstantinou, K. Sdrimas, A. Fernandez-Gonzalez, S. Kourembanas, Exosomes mediate the cytoprotective action of

mesenchymal stromal cells on hypoxia-induced pulmonary hypertension. *Circulation* **126**, 2601–2611 (2012).
39. S. EL Andaloussi, I. Mäger, X. O. Breakefield, M. J. A. Wood, Extracellular vesicles: Biology and emerging therapeutic opportunities. *Nat. Rev. Drug Discov.* **12**, 347–357 (2013).
40. M. F. Bolukbasi, A. Mizrak, G. B. Ozdener, S. Madlener, T. Ströbel, E. P. Erkan, J.-B. Fan, X. O. Breakefield, O. Saydam, miR-1289 and "Zipcode"-like sequence enrich mRNAs in microvesicles. *Mol. Ther. Nucleic Acids* **1**, e10 (2012).
41. K.-V. Chang, C.-Y. Hung, F. Aliwarga, T.-G. Wang, D.-S. Han, W.-S. Chen, Comparative effectiveness of platelet-rich plasma injections for treating knee joint cartilage degenerative pathology: A systematic review and meta-analysis. *Arch. Phys. Med. Rehabil.* **95**, 562–575 (2014).

Acknowledgments: We thank H.B. Patel and R. Jones (William Harvey Research Institute) for help with arthritis models, J. Dalli for conceptual insight, and G. Sukhorukov (Queen Mary University of London) for providing microcapsules. **Funding:** This work was supported by The Wellcome Trust (program 086867/Z/08 and 101604/Z/13/Z), FAPESP (Fundação de Amparo à Pesquisa do Estado de São Paulo; 2012/21603-2), and CNPq (Conselho Nacional de Desenvolvimento Científico e Tecnológico; 308144/2014-7) (to S.M.O.), and The Nuffield Foundation (Oliver Bird Studentship to S.E.H.). L.V.N. is supported by an Arthritis Research UK Career Development Fellowship (19909), and S.E.H. is supported by an Arthritis Research UK Foundation Fellowship (20842). L.Y.J. is an Investigator of the Howard Hughes Medical Institute. The Medical Research Council and Arthritis Research UK provided support for the development of the biobank that provided the samples for these studies.

Author contributions: S.E.H. designed and performed in vitro, ex vivo, and in vivo experiments and wrote the manuscript. H.R.J. performed MV expression analyses, in vitro experiments, and statistical analyses, and contributed to the manuscript. L.V.N. designed and performed in vivo experiments and contributed to the manuscript. C.D.G. and S.M.O. performed electron microscopy analyses. A.N. and C.P. provided clinical samples and data. E.C. and P.R.S. performed NET experiments. F.D. and C.P. provided conceptual expertise and edited the manuscript. A.K. and L.Y.J. provided mice and data and edited the manuscript. M.P. provided mice, coordinated the project, and wrote the manuscript. **Competing interests:** The authors declare that they have no competing interests. **Data and materials availability:** The data for this study have been deposited in the database dbGAP (database of Genotypes and Phenotypes).

Submitted 12 May 2015
Accepted 22 September 2015
Published 25 November 2015
10.1126/scitranslmed.aac9608

Citation: S. E. Headland, H. R. Jones, L. V. Norling, A. Kim, P. R. Souza, E. Corsiero, C. D. Gil, A. Nerviani, F. Dell'Accio, C. Pitzalis, S. M. Oliani, L. Y. Jan, M. Perretti, Neutrophil-derived microvesicles enter cartilage and protect the joint in inflammatory arthritis. *Sci. Transl. Med.* **7**, 315ra190 (2015).

Science Translational Medicine
AAAS

Neutrophil-derived microvesicles enter cartilage and protect the joint in inflammatory arthritis

Sarah E. Headland, Hefin R. Jones, Lucy V. Norling, Andrew Kim, Patricia R. Souza, Elisa Corsiero, Cristiane D. Gil, Alessandra Nerviani, Francesco Dell'Accio, Costantino Pitzalis, Sonia M. Oliani, Lily Y. Jan and Mauro Perretti (November 25, 2015)
Science Translational Medicine **7** (315), 315ra190. [doi: 10.1126/scitranslmed.aac5608]

Editor's Summary

Microparticles provide protection

Neutrophils play an active role in protecting cartilage from damage by dispatching microvesicles (MVs) to do their bidding in this tissue they otherwise can't access. Headland and colleagues found MVs present in the synovial fluid of patients with rheumatoid arthritis—an autoimmune disease that degrades cartilage in the joints. Cartilage is normally thought of as impenetrable to cells, so neutrophils send MVs, which easily enter the tissue and prevent damage induced by disease through a complex mechanism that involves the proresolving protein annexin A1 and its receptor. In two different mouse models of rheumatoid arthritis, MVs delivered locally entered the cartilage, prevented the loss of proteoglycans, and maintained cartilage integrity. This study suggests that immune cells can provide protection against tissue degradation in inflammatory arthritis and that the MVs may be manipulated to deliver therapeutics to diseased joints.

7.3. Galectin-3-null mice display defective neutrophil clearance during acute inflammation

Epub ahead of print October 12, 2016 - doi:10.1189/jlb.3A0116-026RR

JLB

Article

Galectin-3–null mice display defective neutrophil clearance during acute inflammation

Rachael D Wright, Patricia R. Souza, Magdalena B. Flak, Prasheetha Thedchanamoorthy, Lucy V. Norling, and Dianne Cooper[1]

William Harvey Research Institute, Barts and the London School of Medicine and Dentistry, London, United Kingdom

RECEIVED JANUARY 14, 2016; REVISED SEPTEMBER 6, 2016; ACCEPTED SEPTEMBER 15, 2016. DOI: 10.1189/jlb.3A0116-026RR

ABSTRACT

Galectin-3 has been associated with a plethora of proinflammatory functions because of its ability, among others, to promote neutrophil activation and because of the reduction in neutrophil recruitment in models of infection in Gal-3-null mice. Conversely, it has also been linked to resolution of inflammation through its actions as an opsonin and its ability to promote efferocytosis of apoptotic neutrophils. Using a self-resolving model of peritonitis, we have addressed the modulation and role of Gal-3 in acute inflammation. We have shown that Gal-3 expression is increased in neutrophils that travel to the inflamed peritoneum and that cellular localization of this lectin is modulated during the course of the inflammatory response. Furthermore, neutrophil recruitment to the inflamed peritoneum is increased in Gal-3–null mice during the course of the response, and that correlates with reduced numbers of monocytes/macrophages in the cavities of those mice, as well as reduced apoptosis and efferocytosis of Gal-3–null neutrophils. These data indicate a role for endogenous Gal-3 in neutrophil clearance during acute inflammation.
***J. Leukoc. Biol.* 101: 000–000; 2017.**

Introduction

Galectins are a family of β-galactoside–binding proteins that elicit their effects by binding to exposed *N*-acetyllactosamine residues on cells [1]. Several galectins have been designated with key immunomodulatory roles in a range of pathologic settings; of these, Gal-3 has been identified as a proinflammatory molecule that functions to drive the inflammatory response through the activation of innate immune cells and its chemoattractant actions [2–5]. During infections with pathogens such as *Streptococcus pneumoniae*, Gal-3 appears to be beneficial for the host, with enhanced pathogenicity observed in Gal-3–null mice and reduced infection in mice treated with recombinant Gal-3 [6, 7]. Such effects are thought to be due to Gal-3 enhancing the recruitment/activation of neutrophils as well as having direct bactericidal actions [6]. Administration of recombinant Gal-3 to human neutrophils results in degranulation, release of reactive oxygen species, and an increase in phagocytic capability [3, 5, 8]. Decreased neutrophil recruitment is seen in the lungs of Gal-3–null mice infected with *S. pneumoniae*, and that can be rescued by administration of the recombinant protein [9]; Gal-3 can also act directly as an adhesion molecule, and it promotes adhesion of neutrophils to endothelial cells in vitro [7]. The effects of Gal-3 on neutrophil trafficking appear to be specific to particular pathogens because no differences were observed in neutrophil trafficking to the lungs in Gal-3–null mice infected with *Escherichia coli* or to air pouches inoculated with the *Leishmania major* substrain Friedlin when compared with substrain LV39 [10]. Interestingly, both *S. pneumoniae* and LV39 induced release of Gal-3 into the inflammatory exudate, whereas *E. coli* and Friedlin did not, suggesting that it is the presence of Gal-3 in inflammatory exudates that functions to drive neutrophil recruitment. This hypothesis is supported by the finding that administration of recombinant Gal-3 into the murine air pouch results in neutrophil recruitment [10]. Whether endogenous Gal-3 is released and has a role in neutrophil trafficking to other sites of inflammation, such as an inflamed peritoneal cavity, is not clear. Colnot et al. [11] observed reduced recruitment of granulocytes in a model of thioglycollate-induced peritonitis in Gal-3–null mice on d 4 only, whereas Hsu et al. [12] observed reduced numbers of neutrophils on d 1 only. Furthermore, it is not clear how Gal-3 promotes neutrophil transmigration when it is released into inflammatory exudates or injected into a cavity such as the air pouch because it is not chemotactic for neutrophils [9], and it does not appear to modulate the levels of major chemokines/cytokines within inflammatory exudates [10].

As well as the aforementioned studies supporting a role for Gal-3 in driving innate immunity, there is evidence to suggest that it may facilitate resolution of inflammation through its actions as an opsonin [13]; furthermore, Gal-3–deficient macrophages are less efficient at phagocytosing apoptotic

Abbreviations: Gal-3 = galectin-3, KO = knockout, WT = wild-type

The online version of this paper, found at www.jleukbio.org, includes supplemental information.

1. Correspondence: William Harvey Research Institute, Barts and the London School of Medicine and Dentistry, London, EC1M 6BQ, United Kingdom. E-mail: d.cooper@qmul.ac.uk

JLB

neutrophils than WT cells are [6]. Binding of Gal-3 to human neutrophils promotes the exposure of phosphatidylserine without inducing apoptosis, a process known to act as an "eat-me" signal for phagocytes, suggesting a role for Gal-3 in the clearance of neutrophils [14]. However, evidence that treatment of human neutrophils with recombinant Gal-3 delays their spontaneous apoptosis and that the rate of neutrophil apoptosis from Gal-3–null mice does not differ from that of WT cells is at odds with a proresolving function [6, 11].

Although the studies mentioned provided evidence that Gal-3 is an important regulator of the innate immune system, the modulation of the endogenous protein in innate immune cells during the course of an inflammatory response has not, to our knowledge, been studied systematically. The expression of Gal-3 is reportedly negligible basally in both human and murine neutrophils, and whether levels are modulated during inflammation is not clear because, again, contrasting reports exist. Gil et al. [15] demonstrated an increase in Gal-3 expression in recruited neutrophils after Carrageenan-induced peritonitis in the rat, whereas Sato et al. [7] showed no increase in lectin expression in murine neutrophils that had been recruited to *S. pneumoniae*-infected alveoli. Human neutrophils express Gal-3, and levels are not modulated upon migration through an endothelial monolayer in an in vitro transmigration assay in response to IL-8 [16].

In this study, we characterized the regulation and function of Gal-3 in neutrophils during the course of a self-resolving inflammatory response. Our findings demonstrate that Gal-3 expression is increased in neutrophils that have migrated into the inflamed peritoneal cavity and that neutrophil numbers are increased in the peritoneal cavities of Gal-3–null mice. This is likely due to reduced clearance rather than increased trafficking, as evidenced by reduced levels of apoptosis in Gal-3–null neutrophils coupled with their reduced efferocytosis.

MATERIALS AND METHODS

Reagents

All Abs were purchased from eBioscience (San Diego, CA, USA). The Annexin V^{FITC} apoptosis detection kit was purchased from BD Biosciences (Franklin Lakes, NJ, USA). CellTrace carboxyfluorescein succinimidyl ester was purchased from Thermo Fisher Scientific (Waltham, MA, USA). Histopaque 1077 and Zymosan were purchased from Sigma-Aldrich (St. Louis, MO, USA).

Ethics

All animal studies were conducted with ethical approval from the Queen Mary University of London Local Ethical Review Committee and in accordance with the United Kingdom Home Office regulations (Guidance on the Operation of Animals, Scientific Procedures Act, 1986).

Mice

Male C57BL/6 mice were obtained from Charles River (Wilmington, MA, USA). Breeding pairs of Gal-3–null mice (B6.Cg-Lgals3tm1Po1/J) were provided by the Consortium for Functional Glycomics (http://functionalglycomics.org), and a colony was established in Margate, United Kingdom, at the Charles River Laboratories (Wilmington, MA, USA). These mice were on a C57BL/6 background, and age- and sex-matched controls were used for all experimental work. All animals were fed standard laboratory chow and water ad libitum and were maintained on a 12-h light–dark cycle under specific pathogen-free conditions. All experiments were performed with mice 6–7 wk old.

Peritonitis

Briefly, mice were injected with 1 mg zymosan (Sigma-Aldrich) i.p. in 1 ml sterile PBS, as previously described by Ajuebor et al. [17] in 1999; 0-h mice received no treatment. At 4, 24, 48, 72, and 96 h after injection, the mice were anesthetized, along with the 0 h controls, with isoflurane, and a cardiac puncture was performed to obtain peripheral blood. The mice were then sacrificed by cervical dislocation, and peritoneal lavages were performed with 4 ml ice-cold PBS to collect peritoneal exudates. Tibias and femurs were collected, cleaned, and flushed with sterile PBS using a 25-guage needle to extract bone marrow. Bone marrow cells were then filtered through a 70-μm filter and washed before staining for analysis by flow cytometry.

In some experiments peritonitis was induced using 1 mg lyophilized *E. coli* (strain K12; Sigma-Aldrich) i.p. in 1 ml sterile PBS. Peritoneal cavities were lavaged, as described above, at 4 h postinjection.

Flow cytometry

Murine cells were incubated with Abs for Ly6G (eBioscience, clone 1A8) to identify neutrophils or a combination of F4/80 and Gr-1 (eBioscience, clone BM8 and RB6-8C5, respectively) to identify classic and nonclassic monocyte/macrophages. Cells were then fixed and permeabilized with BD fixation and permeabilization buffer before the addition of the anti–Gal-3 Ab (eBioscience, clone M3/38) to assess intracellular Gal-3 levels (some cells were incubated with Ly6G and Gal-3 without permeabilization to assess cell surface levels). To determine cytosolic expression of Gal-3, mean fluorescence intensities for surface expression were deducted from the mean fluorescence intensity values obtained for total expression. In all cases, Abs or relevant isotype controls were incubated at 4°C before flow cytometric analysis using FlowJo software (Tree Star, Ashland, OR, USA).

Confocal microscopy

Peritoneal lavage cells were seeded onto Ibidi 8-well chamber slides in RPMI 1640 and allowed to adhere. After fixation with 1% paraformaldehyde, cells were blocked with 5% FBS before permeabilization with 0.05% Triton X-100. Staining for intracellular Gal-3 was performed using anti–Gal-3–PE (eBioscience) for 1 h at room temperature. Cells were washed 3 times and then incubated with phalloidin 647 for 20 min at room temperature. Finally, cells were mounted with ProLong Gold Antifade Mountant containing DAPI (Thermo Fisher Scientific). Immunofluorescence was assessed using a Zeiss LSM 710 confocal microscope (Carl Zeiss Microscopy, Jena, Germany). Images were processed using Zen 2012 (Carl Zeiss Microscopy) and Adobe Photoshop CS6 (Adobe Systems, San Jose, CA, USA) software.

Adoptive transfer

WT mice were euthanized, and tibias and femurs were collected, cleaned, and flushed with RPMI 1640 (10% FCS; 2 mM EDTA) using a 25-guage needle, as described previously [18]. Following centrifugation, red blood cells were lysed with 0.2% hypotonic saline for 20 s. Bone marrow cells were then washed in RPMI 1640, and the yield of neutrophils was quantified using Turk's solution. To label cells for transfer fluorescently, neutrophils were resuspended in PBS at a concentration of 5×10^6/ml; 5 μM CFSE (Thermo Fisher Scientific) was added, and cells were incubated at 37°C for 8 min. An equal volume of FCS was then added to quench excess CFSE, and the cells were washed. After 2 additional washes with ice-cold RPMI 1640, the cells were resuspended in ice-cold PBS at a density of 25×10^6/ml. Then, 5×10^6 neutrophils were administered to each Gal-3–null recipient mouse via the lateral tail vein, and 1 mg zymosan was injected i.p. 4 h after zymosan administration; peritoneal lavages were collected, as described above, and cells were stained with anti-Ly6G to identify neutrophils and Gal-3. Some cells were also permeabilized after the surface stain with Ly-6G to assess intracellular expression of Gal-3.

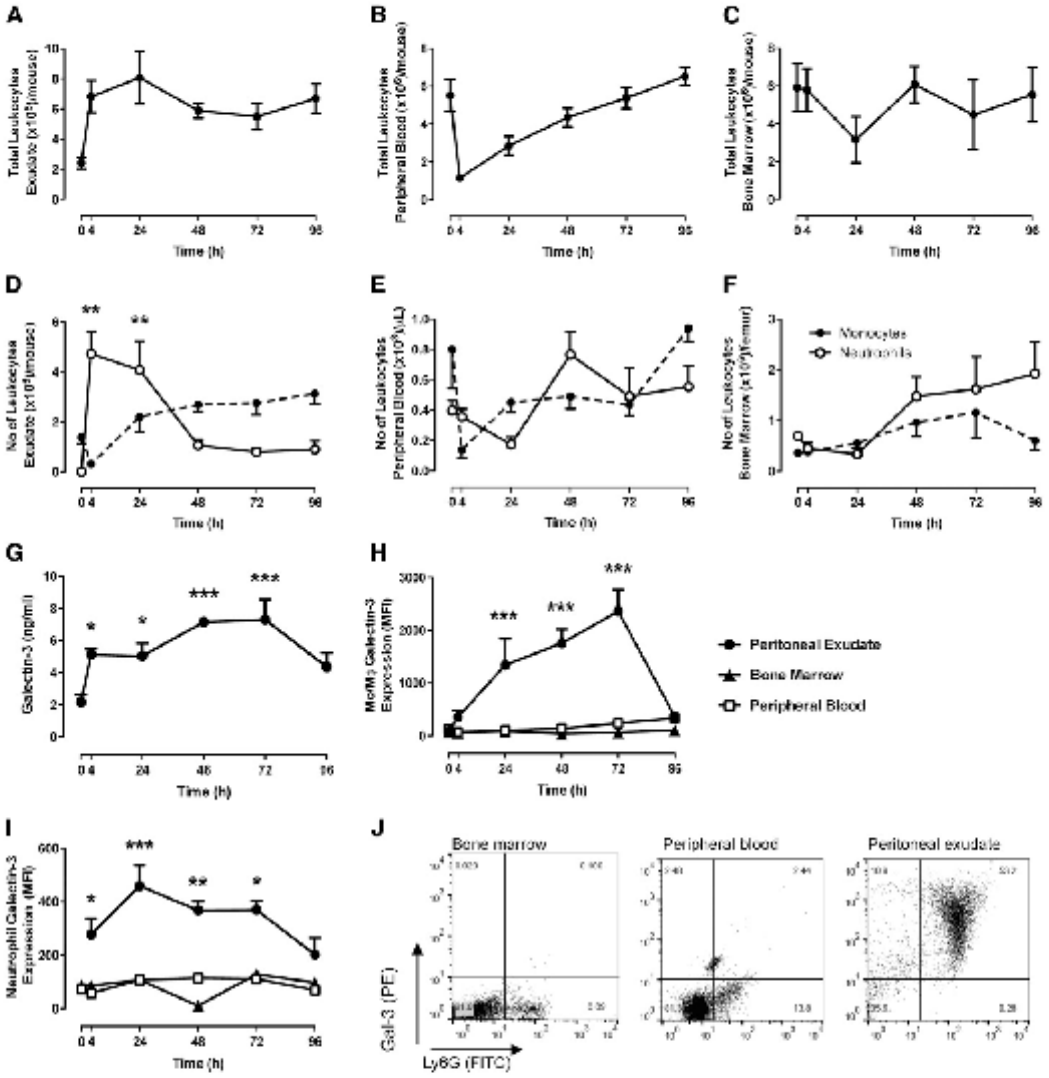

Figure 1. Expression of Gal-3 by murine neutrophils during a resolving inflammatory response. Total leukocyte counts in the peritoneal exudate (A), blood (B), and bone marrow (C) after zymosan (1 mg) challenge in the peritoneal cavity. Differential leukocyte counts in the peritoneal exudate (D), blood (E), and bone marrow (F) after zymosan (1 mg) challenge in the peritoneal cavity. (G) Gal-3 concentration in peritoneal exudate fluid after zymosan-induced peritonitis. Total Gal-3 expression in monocyte/macrophages (H) and neutrophils (I) after zymosan (1 mg) challenge in the peritoneal cavity. (J) Representative dot plot showing neutrophils double-stained for Ly6g and Gal-3 at 4 h after zymosan in the bone marrow, peripheral blood, and peritoneal cavity. $N = 12$/group for peritoneal exudate, 8/group for peripheral blood, and 4/group for bone marrow. MFI, mean fluorescence intensity; PE, peritoneal exudate. $^{*}P < 0.05$, $^{**}P < 0.01$, and $^{***}P < 0.001$ vs. peripheral blood and bone marrow at same time point or at 0-h control.

JLB

Gal-3 ELISA

Gal-3 levels were measured in peritoneal exudates using a commercial ELISA kit (R&D Systems, Minneapolis, MN, USA) according to manufacturer's instructions.

Apoptosis assay

Exudated neutrophils from WT and Gal3–null mice were collected after 4, 48, 72 and 96 h of zymosan-induced peritonitis and were labeled with Ly6G. Then, the cells were labeled with Annexin V and propidium iodide as per manufacturer's instructions (BD Biosciences) or Zombie NIR viability dye (1:400 dilution in PBS; BioLegend, San Diego, CA, USA) to assess apoptosis. In some experiments, 4-h exudated neutrophils were cultured overnight in RPMI 1640 and assessed the following day at 18 h for surface Gal-3 levels and apoptosis. Gal-3 staining was performed as described above, and apoptosis levels were assessed using Annexin V and Zombie NIR. Viable (Annexin V$^-$, Zombie$^-$) and late apoptotic (Annexin V–Zombie double positive) cells were gated, and Gal-3 expression assessed.

Efferocytosis assay

Biogel-elicited macrophages were collected from WT mice, as previously described [19], and were seeded into 24-well plates at 0.5×10^6 cells/well and allowed to adhere. Exudated neutrophils from WT and Gal-3–null mice were collected after 4 h zymosan-induced peritonitis and labeled with BODIPY-FL (Thermo Fisher Scientific) for 5 min at 37°C. After washing, neutrophils were resuspended in RPMI 1640 at 2×10^6/ml, and 0.5 ml was added to each well of macrophages and incubated for 1 h. After extensive washing efferocytosis was quantified using ImageJ software (U.S. National Institutes of Health, Bethesda, MD, USA). Images were split into their individual red/blue/green channels, and the same background threshold was applied to all images before quantification of fluorescence.

Statistical analysis

Statistical significance was assessed using SPSS computer software (SPSS Inc., Chicago, IL, USA). Data are expressed as means ± SEM of n experiments. All data were tested for normal distribution, and power calculations were performed using G*Power software (Heinrich Heine University of Düsseldorf, Düsseldorf, Germany) [20]. Statistical differences were analyzed by 1- or 2-tailed t test for 2 groups, 1-way ANOVA, followed by a Bonferroni or Dunnett's post hoc test (depending on whether all values or each value, respectively, was compared with a control) or 2-way ANOVA, followed by Bonferroni post hoc test. In all cases a P value < 0.05 was considered significant to reject the null hypothesis, and differences were considered significant.

RESULTS

Modulation of Gal-3 expression in murine neutrophils during inflammation

To investigate the endogenous levels of Gal-3 during the course of an acute inflammatory response, a zymosan-induced peritonitis was performed and monitored for 96 h; by which time, the inflammation had resolved. Because of the discrepancy among reports of Gal-3 expression in neutrophils, we fully investigated expression levels in 3 sources of neutrophils: those from the bone marrow, those from the peripheral blood, and those that had migrated into the inflamed peritoneal cavity. There was a rapid increase in the number of total leukocytes in the peritoneal cavity within 4–24 h after zymosan administration, and that number remained elevated during the course of the response, with increased leukocyte numbers still observed at 96 h compared with basal levels (**Fig. 1A**). The neutrophil number in the peritoneal cavity increased sharply for 4–24 h and then returned to basal levels within the 96-h time course. In contrast, the monocyte/macrophage numbers declined within the first 4 h of zymosan treatment and then repopulated the peritoneal cavity over the time course (Fig. 1D). The number of leukocytes within peripheral blood decreased rapidly after induction of peritonitis and then returned to basal levels during the course of the response (Fig. 1B). Monocytes account for the decrease in total cells seen at 4 h, which return to basal levels during the time course. Although there were no significant modulations in the numbers of neutrophils in the peripheral blood, a trend can be seen that mirrors the changes in the peritoneal cavity with a decrease as cells migrate from the peripheral blood to the peritoneal cavity and then an increase as the peripheral blood repopulates (Fig. 1E). Although no significant modulation of leukocyte number was observed within the bone marrow (Fig. 1C), a similar, yet delayed, trend followed the peripheral

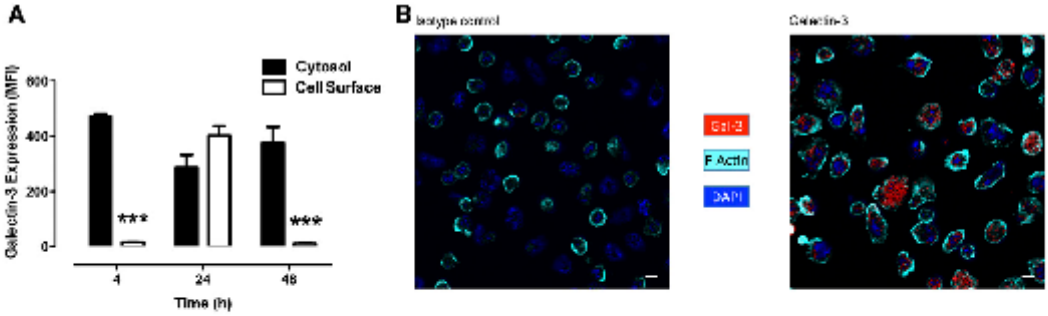

Figure 2. Cytosolic and cell surface expression of Gal-3 in murine neutrophils taken from the peritoneal exudate at 4, 24, and 48 h after zymosan ip. Surface Gal-3 expression was measured by flow cytometry on Ly6G$^+$ neutrophils, and total Gal-3 expression was measured after permeabilization. (A) Cytosolic expression was calculated by subtracting the cell surface expression from the total expression. (B) Gal-3 expression in neutrophils taken from the peritoneal exudate at 4 h after zymosan as detected by confocal microscopy. MFI, mean fluorescence intensity. Scale bar = 5 μm. N = 8–12/group. ***$P < 0.001$ vs. cytosol.

blood neutrophils with a decrease in cell numbers in the bone marrow approximately 24 h after that seen in the peripheral blood. This is likely to account for leukocyte mobilization to repopulate the peripheral circulation (Fig. 1F).

Analysis of peritoneal lavage fluid by ELISA revealed baseline levels of 2.155 ± 0.450 ng/ml Gal-3 within the cavity. These levels increased significantly during the peritonitis time course, with peak levels at 72 h (7.293 ± 1.239 ng/ml) (Fig. 1G). Endogenous expression of Gal-3 was minimal in monocyte/macrophages within the bone marrow and peripheral blood, but levels significantly increased in exudate peritoneal cells, with peak expression observed at 72 h (Fig. 1H). As expected, low levels of Gal-3 were detected in both peripheral blood [7, 9] and bone marrow–derived neutrophils; however, total levels were significantly increased in permeabilized, exudated neutrophils for 72 h, with peak expression observed at 24 h (Fig. 1I and J).

Cellular localization of Gal-3 is modulated in neutrophils during inflammation

To determine the cellular localization of Gal-3, flow cytometry was performed on nonpermeabilized vs. permeabilized neutrophils (**Fig. 2A**). At 4 h after zymosan, the Gal-3 expressed by murine neutrophils was predominantly intracellular; however, at 24 h, the protein was readily detected on the cell surface, and by 48 h, Gal-3 was again expressed predominantly in the intracellular compartment of the cell. Confocal analysis of the peritoneal neutrophils taken at the 4-h time point confirmed the intracellular localization of Gal-3 within the migrated neutrophils (Fig. 2B).

To determine whether the intracellular Gal-3 detected was derived from the extracellular environment, that is, being taken up from the inflammatory exudate or being produced by the neutrophils themselves, an adoptive transfer experiment was performed. CFSE-labeled bone marrow neutrophils isolated from WT mice were injected i.v. into Gal-3–null mice, and a zymosan-induced peritonitis performed. Neutrophils within lavage fluid were identified based on their characteristic forward/side light scatter and following doublet exclusion, Ly6G+ neutrophils were identified (**Fig. 3A-C**). CFSE-labeled Ly6G$^+$ neutrophils were clearly detectable within peritoneal lavages, as shown in Fig. 3D. Negligible levels of Gal-3 were detectable on the neutrophil surface (Fig. 3E), whereas Gal-3 was readily detectable in permeabilized cells (Fig. 3F), indicating the presence of intracellular Gal-3 as shown in Fig. 1J.

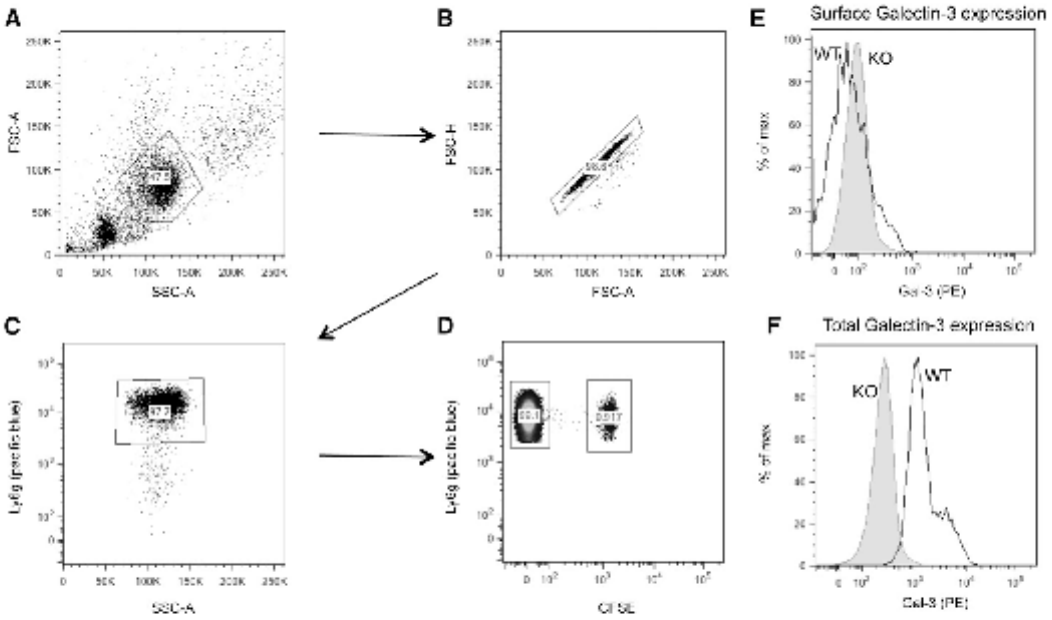

Figure 3. WT neutrophils exhibit increased Gal-3 expression upon transmigration to the peritoneal cavities of Gal-3–null mice. Bone marrow neutrophils were isolated from WT mice, labeled with CFSE, and administered i.v. to Gal-3–null mice, which subsequently underwent a zymosan (1 mg)–induced peritonitis. Peritoneal cavities were lavaged at 4 h and analyzed by flow cytometry. (A) Neutrophils were identifiable by their characteristic forward/side light scatter (FSC/SSC) profile. Following doublet exclusion (B), Ly6G$^+$ neutrophils were identified (C). (D) WT Ly6G$^+$ neutrophils were identified by their positive CFSE staining. Surface (E) and total (F) Gal-3 expression was measured on CFSE$^-$ (neutrophils from Gal-3–null mice) and CFSE$^+$ cells (neutrophils from WT mice) by flow cytometry, and representative histograms are shown. Max, maximum; PE, peritoneal exudate.

JLB

The role of Gal-3 in neutrophil clearance

To further investigate the role of neutrophil-derived Gal-3, the zymosan-induced peritonitis was repeated in Gal-3–null mice, initially at the 4 h point. That time point was chosen because it represents the peak of neutrophil infiltration into the cavity, which corresponds with low monocyte/macrophage numbers. Surprisingly, significantly higher numbers of leukocytes were observed in the cavities of Gal-3–null mice (**Fig. 4A**). Upon further examination, the percentage of neutrophils within the cavity was significantly higher in KO mice (Fig. 4B), whereas the percentage of macrophages was significantly lower (Fig. 4C). As shown in Fig. 2, surface expression of Gal-3 by peritoneal neutrophils was negligible (Fig. 4D), whereas it was readily detected in permeabilized cells by flow cytometry (Fig. 4E).

Neutrophil recruitment in Gal-3–null mice appears to vary in its magnitude depending on the inciting stimuli and the site of the inflammation. We, therefore, performed a peritonitis experiment in which we used *E. coli* instead of zymosan. The magnitude of the response was lower overall in neutrophil recruitment, and there were no differences between the 2 genotypes of mice in numbers of neutrophils recruited to the peritoneal cavity (data not shown). Again, Gal-3 was readily detectable within the cytosol of neutrophils that had traveled to the peritoneum in response to both *E. coli* and zymosan (Supplementary Fig. 1), whereas levels were low on the surface of zymosan-elicited neutrophils as well as on those elicited by *E. coli*. To investigate whether neutrophils lacking Gal-3 undergo apoptosis at a different rate than cells from WT animals, neutrophils collected from the peritoneal cavity were cultured overnight, and levels of apoptosis were assessed by flow cytometry. Upon removal from the cavity, most neutrophils were viable in both genotypes (**Fig. 5A**). However, after overnight culture, significantly fewer neutrophils from the Gal-3–null mice had undergone apoptosis (Fig. 5B–E). Because Gal-3 has been implicated in the clearance of neutrophils, experiments were conducted to investigate the role of neutrophil-derived Gal-3 on efferocytosis, and significantly reduced efferocytosis of Gal-3–null neutrophils was observed compared with WT neutrophils (Fig. 5F and G). Interestingly surface expression of Gal-3 was found to be increased on apoptotic neutrophils (Annexin V/Zombie double-positive cells), when compared with viable cells (Annexin V/Zombie double-negative cells) (Fig. 5 H and I).

Role of Gal-3 during the resolving phase of the peritonitis model

Because there is evidence in the literature that Gal-3 is involved in neutrophil clearance, a key facet of the resolution process, leukocyte trafficking was compared in Gal-3–null mice and their WT counterparts at 48–96 h after zymosan. At 48 h after zymosan, total leukocyte counts were comparable for WT and Gal-3–null mice; however, at 72 h, there was a trend toward more leukocytes in the peritoneal cavities of Gal-3–null mice, although that increase did not reach statistical significance, and levels had declined to those observed in WT mice by 96 h (**Fig. 6A**).

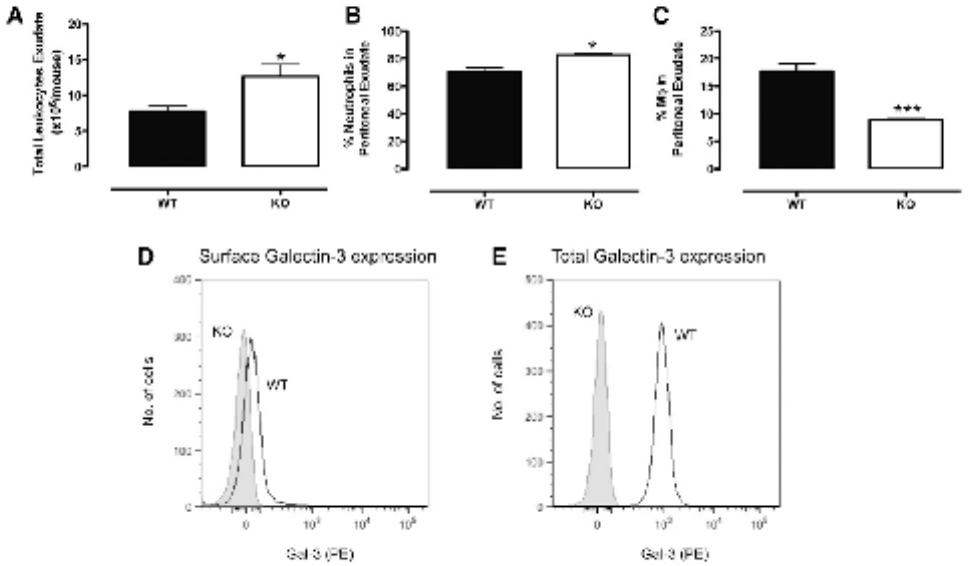

Figure 4. Gal-3–null mice demonstrate altered leukocyte trafficking. Total leukocyte counts (A), percentage of neutrophils (B), and percentage of macrophages (C) in the peritoneal exudate at 4 h after zymosan (1 mg) challenge. Surface (D) and total (E) Gal-3 expression was measured on $Ly6G^+$ neutrophils by flow cytometry and representative histograms are shown. $N = 4–7$/group; $^*P < 0.05$, $^{***}P < 0.0001$.>

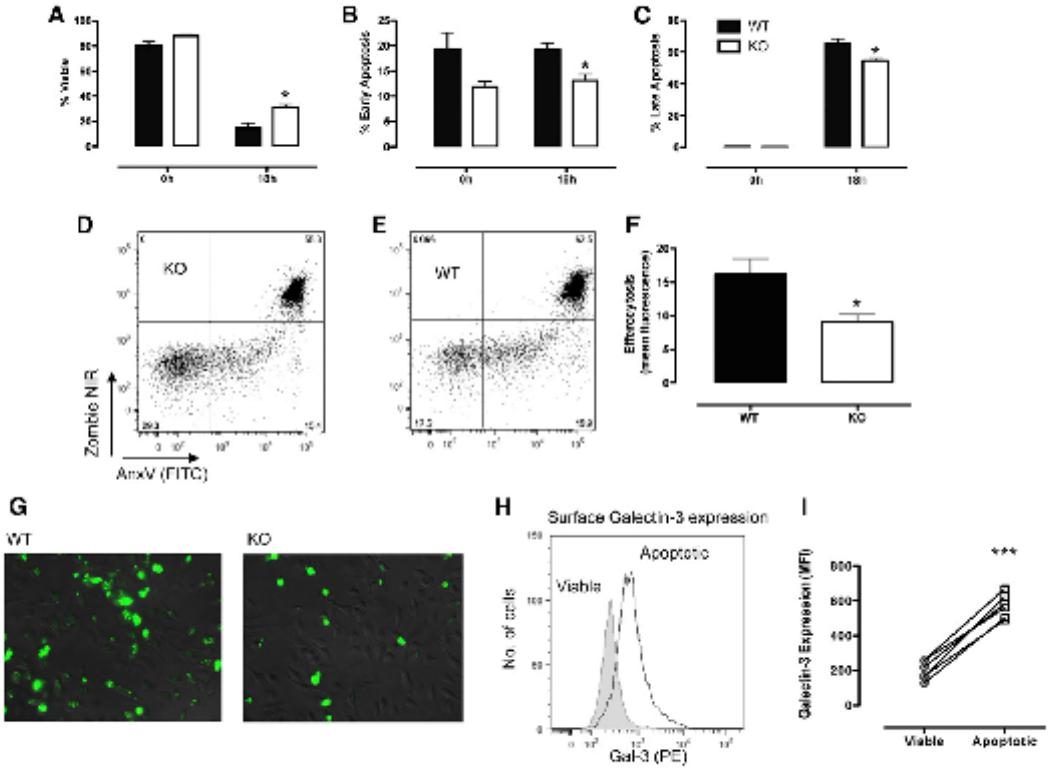

Figure 5. Gal-3–null mice demonstrate reduced levels of apoptosis. Percentage of viable cells (A), early apoptotic cells (B), and late apoptotic cells (C) after overnight culture of peritoneal exudate cells. Representative dot-plots after overnight culture of peritoneal exudate cells (taken 4 h after zymosan) showing cell viability (Zombie NIR) and phosphatidylserine exposure (Annexin V [AnxV]) in KO (D) and WT (E) mice exudated leukocytes. WT biogel-elicited macrophages were incubated with BODIPY-FL-labeled peritoneal exudate cells after overnight culture. (F) Efferocytosis was quantified using ImageJ software. (G) Representative images used for the data analysis are shown. Gal-3 levels were assessed on the surface of viable ($AnxV^-/Zombie^-$) and late apoptotic ($AnxV^+/zombie^+$) cells by flow cytometry (H and I). $N = 4–7$/group; $^*P < 0.05$, $^{***}P < 0.0001$.

Interestingly, the percentage of exudated neutrophils was significantly higher in Gal-3–null mice at the 72 and 96 h points (Fig. 6B), indicating a potential defect in neutrophil clearance in these mice. Assessment of apoptosis by Annexin V/propidium iodide staining revealed no differences between the 2 genotypes of mice in the levels of apoptotic cells at these later times (**Table 1**). Because monocytes, particularly nonclassic monocytes, are important in the resolution of inflammation, the numbers of both subsets were compared between the strains of mice. Approximately 40% of cells recovered were nonclassic monocytes in both genotypes at 48 h, and that 40% remained stable in Gal-3–null mice up to 96 h. This was in contrast to WT mice in which the number of nonclassic monocytes significantly increased at 96 h (Fig. 6C). In contrast, 20% of the cells recovered from the peritoneum were classic monocytes in both genotypes, and that was not significantly altered at 72 h, although a trend toward fewer classic monocytes was seen in the WT mice, with approximately 15% of total leukocytes being classic monocytes. By 96 h, the number of classic monocytes was negligible in both genotypes of mice (Fig. 6D).

DISCUSSION

The modulation of the inflammatory process, through effects on immune cell biology, by members of the galectin family is an ever-growing area of research. The focus has, however, been largely on the T cell–driven models of autoimmune disease and, in the case of Gal-3, in cancer. There are several reports describing the effects of Gal-3 on neutrophil activation and its

JLB

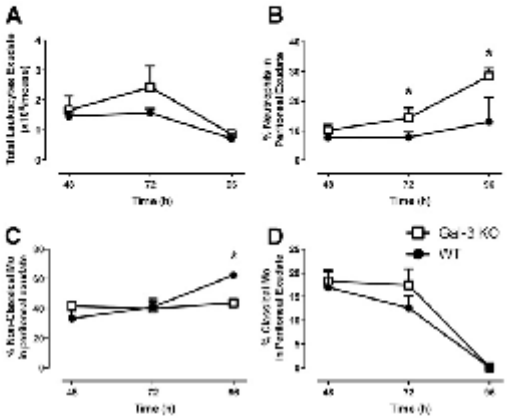

Figure 6. Gal-3–null mice demonstrate dysregulated resolution of inflammation compared with WT controls. Gal-3–null mice and age- and sex-matched WT controls were injected with 1 mg zymosan i.p., and peritoneal exudates were collected during the resolution period (48–96 h). Total leukocyte counts (A), percentage of neutrophils (B), percentage of nonclassic monocytes (Mo) (C), and percentage of classic monocytes (D) in peritoneal exudates after zymosan (1 mg) administration. $N = 5$/group; $^*P < 0.05$.

importance in models of infection, in which it might function as an alarmin by augmenting the inflammatory response [21]. With this study, we expanded current knowledge of the role of Gal-3 in acute inflammation, identifying a role for the endogenous protein in neutrophil apoptosis and clearance.

Previous studies have failed to detect expression of Gal-3 intracellularly in murine neutrophils, although it is readily detectable on the cell surface [7, 11]. This has led to the assumption that the effects on neutrophil recruitment in Gal-3–null mice are due to a lack of extracellular Gal-3, likely released from cells such as inflammatory macrophages. We have confirmed that bone marrow and murine neutrophils from naïve, peripheral blood express low levels of Gal-3. However, in contrast to previous findings, we have shown that upon migration to the inflamed peritoneal cavity, intracellular Gal-3 levels are significantly increased in neutrophils.

Struck by this significant increase in Gal-3 expression upon migration to the inflammatory site, we have sought to address the role of neutrophil Gal-3 through investigation of the profile of neutrophil recruitment, apoptosis, and clearance in the zymosan peritonitis model. Increased levels of neutrophil recruitment into the peritoneal cavity of Gal-3–null mice were observed at 4, 72, and 96 h. This is in contrast to the reported response to thioglycollate in previous studies, as well as in models of pneumonia, in which neutrophil migration to the peritoneal cavity and lungs, respectively, was reduced in Gal-3–null mice [6, 9, 11, 12]. Such discrepancies may be due to the inducing inflammatory stimuli because, similar to zymosan, *E. coli* infection also resulted in a significant enhancement of neutrophil trafficking to the lungs of Gal-3–null mice [9]. The finding that *E. coli* increases neutrophil migration to the lungs in Gal-3–null mice is in contrast to our findings in the peritoneal cavity. This highlights the differences among distinct anatomic sites and might be due to the effects of Gal-3 on stromal cells at different sites. A different strain of mice was used in this study, which may also account for the observed differences. Further similarities exist between these inciting stimuli, which may account for the differing responses seen. *Streptococcus pneumoniae* infection increases Gal-3 levels in bronchoalveolar lavage fluid as high as 50 μg/ml; likewise, cutaneous infection with *L. major* LV39 results in increased levels of extracellular Gal-3 and is associated with enhanced neutrophil recruitment. In contrast, infection with *E. coli* or the *L. major* substrain Friedlin failed to significantly induce Gal-3 release, and a role for Gal-3–dependent neutrophil recruitment was not observed. Although we observed Gal-3 within the peritoneal exudate and levels were significantly increased during the course of the response, the amount detectable was in the low nanograms per milliliter range, and similar to what was observed after *E. coli* infection, neutrophil recruitment was increased, rather than decreased, in Gal-3–null mice. Another important factor might be the mechanism by which neutrophils travel to the inflammatory site. Migration in response to zymosan and *E. coli* is known to be dependent on β2 integrins [22], which function to allow neutrophils to adhere to and crawl on the endothelium [23]. In contrast, neutrophil trafficking to the lungs in response to *S. pneumoniae* is independent of β2 integrins, and it is thought that, under these circumstances, Gal-3 is able to act as an adhesion molecule to facilitate neutrophil trafficking, which likely explains the requirement for high levels of the protein extracellularly in these models. Our data suggest that the observed enhancement in neutrophil numbers within the peritoneal cavity of Gal-3–null mice is due to alterations in neutrophil clearance, rather than a direct role on neutrophil trafficking per se, although a direct role cannot be ruled out.

It is important to consider the cellular localization of galectins when studying their actions. Published reports on the effects of Gal-3 have shown cellular localization affects its function in the induction of apoptosis in T cells. Extracellular Gal-3 induces T cell apoptosis [24], whereas intracellular Gal-3 inhibits apoptosis [25]. For neutrophils, extracellular Gal-3 delays spontaneous apoptosis, although no role has been identified for the intracellular protein in murine neutrophils with similar rates

TABLE 1. Levels of apoptosis in neutrophils recruited to the peritoneal cavity of mice after zymosan administration

	Early apoptotic ($AnxV^+/PI^-$)		Late apoptotic ($AnxV^+/PI^+$)	
Time (h)	WT	Gal-3–null	WT	Gal-3–null
48	15.9 ± 1.5	18.8 ± 2.0	71.1 ± 3.2	67.9 ± 2.2
72	15.6 ± 1.2	17.1 ± 1.7	73.8 ± 1.8	69.4 ± 2.6
96	3.6 ± 0.9	2.5 ± 0.4	8.6 ± 2.1	7.3 ± 1.8

Data are expressed as percentage of early or late apoptosis (means ± SEM). AnxV, Annexin V; PI, propidium iodide. $N = 3$–4 mice/group.

of apoptosis observed between WT and Gal-3–null cells [6]. This study demonstrated intracellular expression of Gal-3 at 4 h after zymosan administration, and importantly, our data show an increased surface expression of Gal-3 on apoptotic neutrophils. These findings, together with the delayed apoptosis observed in Gal-3–null neutrophils recovered from the peritoneal cavity, lead us to hypothesize that Gal-3 is externalized by neutrophils and acts as an "eat-me" signal. Because efferocytosis peaks in this model at 6 h after zymosan administration [26], it would be expected that more neutrophils would be retained in the peritoneal cavity of Gal-3–null mice at the 4 h time point. The role of Gal-3 as an "eat-me" signal also explains why there are fewer cells in the peritoneal cavity with surface Gal-3 at later times (48 h onward) because these cells will have been cleared from the peritoneal cavity. Our findings are in contrast to the aforementioned study by Farnworth et al. [6] and the study of Colnot et al. [11], in which no defect in apoptosis was observed in neutrophils from Gal-3–null mice. There are, however, differences among the studies; importantly, in our study, apoptosis was assessed after incubation of neutrophils that had emigrated to the inflamed peritoneal cavity, whereas bone marrow neutrophils were used in the study of Farnworth et al. [6]. Although Colnot et al. [11] assessed levels of apoptosis in neutrophils taken from the peritoneal cavity, this was in a model of thioglycollate-induced peritonitis, and cells were taken 24 h after administration, whereas we observed reduced levels of apoptosis in cells taken at 4 h. Similar to the findings of Colnot et al. [11], we did not observe differences in the levels of apoptosis in cells collected from the peritoneum at later times (48–96 h). During the course of the inflammatory response, we found that the cellular localization of Gal-3 was altered. As mentioned above, Gal-3 levels were increased in the cytosol of neutrophils present within the peritoneal cavity at the 4-h point. Our data from the adoptive transfer experiment indicate that the neutrophils themselves are a source of Gal-3, although that does not rule out the possibility that neutrophils can bind Gal-3 present within the extracellular environment. In fact Karlsson et al. [13] showed that apoptotic neutrophils readily bound recombinant Gal-3. At 24 h, Gal-3 was detectable on both the cell surface and intracellularly; we hypothesize that satiated neutrophils might translocate Gal-3 to the cell surface to signal to incoming phagocytes that they need to be cleared. This is supported by the observed reduction in efferocytosis of Gal-3–null neutrophils by WT biogel-elicited macrophages and the lack of neutrophils with surface Gal-3 detectable at 48 h after zymosan.

Macrophages are crucial to the resolution process, with essential roles in the clearance of apoptotic neutrophils [27]. Previous studies have demonstrated defective resolution processes in Gal-3–null mice, with reduced alternative monocyte activation and, consequently, reduced phagocytic capabilities of these cells [28, 29], which correlates with our data showing reduced numbers of nonclassic monocytes within the peritoneal cavity of Gal-3–null mice during the resolution phase.

Together, our data highlight a role for endogenous Gal-3 in the host phagocyte function, enhancing neutrophil apoptosis and clearance. Failure to eliminate dying neutrophils leads to tissue damage and dissemination of cellular contents, which can have major pathologic consequences, particularly in infection.

AUTHORSHIP

R.D.W performed experiments, analyzed data, and wrote the manuscript. P.R.S., P.T., and M.B.F. performed experiments and analyzed data. L.V.N. performed experiments, analyzed data, and wrote the manuscript, and D.C. designed and performed experiments, analyzed data, and wrote the manuscript.

ACKNOWLEDGMENTS

Funding to the authors' laboratory for the study of galectin biology in inflammation came from the Arthritis Research UK (Career Progression Fellowship 20387 [D.C.]; Career Development Fellowship 19909 [L.V.N.]) and the Medical Research Council.

DISCLOSURES

The authors declare no conflicts of interest.

REFERENCES

1. Barondes, S. H., Castronovo, V., Cooper, D. N., Cummings, R. D., Drickamer, K., Feizi, T., Gitt, M. A., Hirabayashi, J., Hughes, C., Kasai, K., Leffler, H., Liu, F. T., Lotan, R., Mercurio, A. M., Monsigny, M., Pillai, S., Poirier, F., Raz, A., Rigby, P. W. J., Rini, J. M., Wang, J. L. (1994) Galectins: a family of animal β-galactoside-binding lectins. *Cell* **76**, 597–598.
2. Frigeri, L. G., Zuberi, R. I., Liu, F. T. (1993) εBP, a β-galactoside-binding animal lectin, recognizes IgE receptor (FcεRI) and activates mast cells. *Biochemistry* **32**, 7644–7649.
3. Kuwabara, I., Liu, F. T. (1996) Galectin-3 promotes adhesion of human neutrophils to laminin. *J. Immunol.* **156**, 3939–3944.
4. Sano, H., Hsu, D. K., Yu, L., Apgar, J. R., Kuwabara, I., Yamanaka, T., Hirashima, M., Liu, F. T. (2000) Human galectin-3 is a novel chemoattractant for monocytes and macrophages. *J. Immunol.* **165**, 2156–2164.
5. Yamaoka, A., Kuwabara, I., Frigeri, L. G., Liu, F. T. (1995) A human lectin, galectin-3 (epsilon bp/Mac-2), stimulates superoxide production by neutrophils. *J. Immunol.* **154**, 3479–3487.
6. Farnworth, S. L., Henderson, N. C., Mackinnon, A. C., Atkinson, K. M., Wilkinson, T., Dhaliwal, K., Hayashi, K., Simpson, A. J., Rossi, A. G., Haslett, C., Sethi, T. (2008) Galectin-3 reduces the severity of pneumococcal pneumonia by augmenting neutrophil function. *Am. J. Pathol.* **172**, 395–405.
7. Sato, S., Ouellet, N., Pelletier, I., Simard, M., Rancourt, A., Bergeron, M. G. (2002) Role of galectin-3 as an adhesion molecule for neutrophil extravasation during streptococcal pneumonia. *J. Immunol.* **168**, 1813–1822.
8. Fernández, G. C., Barregui, J. M., Rubel, C. J., Toscano, M. A., Gómez, S. A., Beigier Bompadre, M., Isturiz, M. A., Rabinovich, G. A., Palermo, M. S. (2005) Galectin-3 and soluble fibrinogen act in concert to modulate neutrophil activation and survival: involvement of alternative MAPK pathways. *Glycobiology* **15**, 519–527.
9. Nieminen, J., St-Pierre, C., Bhaumik, P., Poirier, F., Sato, S. (2008) Role of galectin-3 in leukocyte recruitment in a murine model of lung infection by Streptococcus pneumoniae. *J. Immunol.* **180**, 2466–2473.
10. Bhaumik, P., St-Pierre, G., Milot, V., St-Pierre, C., Sato, S. (2013) Galectin-3 facilitates neutrophil recruitment as an innate immune response to a parasitic protozoa cutaneous infection. *J. Immunol.* **190**, 630–640.
11. Colnot, C., Ripoche, M. A., Milon, G., Montagutelli, X., Crocker, P. R., Poirier, F. (1998) Maintenance of granulocyte numbers during acute peritonitis is defective in galectin-3-null mutant mice. *Immunology* **94**, 290–296.
12. Hsu, D. K., Yang, R. Y., Pan, Z., Yu, L., Salomon, D. R., Fung-Leung, W. P., Liu, F. T. (2000) Targeted disruption of the galectin-3 gene results in attenuated peritoneal inflammatory responses. *Am. J. Pathol.* **156**, 1073–1083.
13. Karlsson, A., Christenson, K., Matlak, M., Björstad, A., Brown, K. L., Telemo, E., Salomonsson, E., Leffler, H., Bylund, J. (2009) Galectin-3 functions as an opsonin and enhances the macrophage clearance of apoptotic neutrophils. *Glycobiology* **19**, 16–20.

JLB

14. Stowell, S. R., Qian, Y., Karmakar, S., Koyama, N. S., Dias-Baruffi, M., Leffler, H., McEver, R. P., Cummings, R. D. (2008) Differential roles of galectin-1 and galectin-3 in regulating leukocyte viability and cytokine secretion. *J. Immunol.* **180**, 3091–3102.
15. Gil, C. D., Cooper, D., Rosignoli, G., Perretti, M., Oliani, S. M. (2006) Inflammation-induced modulation of cellular galectin-1 and -3 expression in a model of rat peritonitis. *Inflamm. Res.* **55**, 99–107.
16. Gil, C. D., La, M., Perretti, M., Oliani, S. M. (2006) Interaction of human neutrophils with endothelial cells regulates the expression of endogenous proteins annexin 1, galectin-1 and galectin-3. *Cell Biol. Int.* **30**, 338–344.
17. Ajuebor, M. N., Das, A. M., Virág, L., Flower, R. J., Szabó, C., Perretti, M. (1999) Role of resident peritoneal macrophages and mast cells in chemokine production and neutrophil migration in acute inflammation: evidence for an inhibitory loop involving endogenous IL-10. *J. Immunol.* **162**, 1685–1691.
18. Swamydas, M., Lionakis, M. S. (2013) Isolation, purification and labeling of mouse bone marrow neutrophils for functional studies and adoptive transfer experiments. *J. Vis. Exp.* 77:, e50586.
19. Dufton, N., Hannon, R., Brancaleone, V., Dalli, J., Patel, H. B., Gray, M., D'Acquisto, F., Buckingham, J. C., Perretti, M., Flower, R. J. (2010) Anti-inflammatory role of the murine formyl-peptide receptor 2: ligand-specific effects on leukocyte responses and experimental inflammation. *J. Immunol.* **184**, 2611–2619.
20. Faul, F., Erdfelder, E., Buchner, A., Lang, A. G. (2009) Statistical power analyses using G*Power 3.1: tests for correlation and regression analyses. *Behav. Res. Methods* **41**, 1149–1160.
21. Mishra, B. B., Li, Q., Steichen, A. L., Binstock, B. J., Metzger, D. W., Teale, J. M., Sharma, J. (2013) Galectin-3 functions as an alarmin: pathogenic role for sepsis development in murine respiratory tularemia. *PLoS One* **8**, e59616.
22. Perretti, M., Ahluwalia, A., Harris, J. G., Goulding, N. J., Flower, R. J. (1993) Lipocortin-1 fragments inhibit neutrophil accumulation and neutrophil-dependent edema in the mouse. A qualitative comparison with an anti-CD11b monoclonal antibody. *J. Immunol.* **151**, 4306–4314.
23. Ley, K., Laudanna, C., Cybulsky, M. I., Nourshargh, S. (2007) Getting to the site of inflammation: the leukocyte adhesion cascade updated. *Nat. Rev. Immunol.* **7**, 678–689.
24. Fukumori, T., Takenaka, Y., Yoshii, T., Kim, H. R., Hogan, V., Inohara, H., Kagawa, S., Raz, A. (2003) CD29 and CD7 mediate galectin-3-induced type II T-cell apoptosis. *Cancer Res.* **63**, 8902–8911.
25. Yang, R. Y., Hsu, D. K., Liu, F. T. (1996) Expression of galectin-3 modulates T-cell growth and apoptosis. *Proc. Natl. Acad. Sci. USA.* **93**, 6737–6742.
26. Kolaczkowska, E., Kozisl, A., Plytycz, B., Arnold, B. (2010) Inflammatory macrophages, and not only neutrophils, die by apoptosis during acute peritonitis. *Immunobiology* **215**, 492–504.
27. Korns, D., Frasch, S. C., Fernandez-Boyanapalli, R., Henson, P. M., Bratton, D. L. (2011) Modulation of macrophage efferocytosis in inflammation. *Front. Immunol.* **2**, 57.
28. MacKinnon, A. C., Farnworth, S. L., Hodkinson, P. S., Henderson, N. C., Atkinson, K. M., Leffler, H., Nilsson, U. J., Haslett, C., Forbes, S. J., Sethi, T. (2008) Regulation of alternative macrophage activation by galectin-3. *J. Immunol.* **180**, 2650–2658.
29. Sano, H., Hsu, D. K., Apgar, J. R., Yu, L., Sharma, B. B., Kuwabara, I., Izui, S., Liu, F. T. (2003) Critical role of galectin-3 in phagocytosis by macrophages. *J. Clin. Invest.* **112**, 389–397.

KEY WORDS:
lectin · efferocytosis · apoptosis · peritonitis

JLB JOURNAL OF LEUKOCYTE BIOLOGY

Galectin-3–null mice display defective neutrophil clearance during acute inflammation

Rachael D Wright, Patricia R. Souza, Magdalena B. Flak, et al.

J Leukoc Biol published online October 12, 2016
Access the most recent version at doi:10.1189/jlb.3A0116-026RR